Late Glacial and Holocene Palaeoecology of the Lake St Clair Region, Tasmania

Felicitas Hopf

A thesis submitted for the degree of Doctor of Philosophy

of The Australian National University.

March 2018

Declaration

I declare that this thesis was composed by myself, that the work contained herein is my own except where explicitly stated otherwise in the text, and that this work has not been submitted for any other degree or professional qualification except as specified.

Word count: 64, 505 words

Acknowledgements

Firstly, I'd like to thank my supervisory panel, chaired by Prof Simon Haberle and including Em Prof Geoffrey Hope, Dr Michael Macphail and Dr Janelle Stevenson. I have been very lucky to have so much great expertise at hand resulting in engaging discussions and valuable feedback. A big thank you to Simon for his support, guidance and encouragement over the years. I will be forever grateful for the support in making this last push to submission happen! Thank you to Geoff for involving me on the Skullbone Plains Bog project leading to the inclusion of the pollen record in this thesis. The Department of Archaeology and Natural History has been such a friendly and supportive working environment and I would also like to extend my thanks to all of my fellow students and other staff for their support and friendship over the years. In particular, the other pollen enthusiasts with whom I've shared many hours at the microscope: Ben, Ulli, Sue, Rebecca, Mat, Iona, Alexa and Jay. Thank you also to Larissa and Anna for your friendship as well as Rani for many years of shared office, home and friendship!

I'd like to thank Patrick De Deckker for the use of the MD03-2611 ocean core data, which provided interesting comparisons with the sediment cores from the Lake St Clair region, as well as his feedback on the discussion chapter and fruitful discussions about the data. Thank you also to Michael-Shawn Fletcher for many interesting discussions over the years and his generous sharing of his skillset in dataset analysis and presentation. This has taken a few years and I am very grateful for the many opportunities I've had to work on other projects both within Tasmania and beyond which has allowed me to grow within this wonderful field. Thanks again to Simon, Geoff, Janelle and Michael for these opportunities.

I'd also like to acknowledge the early origins of this project at the University of Newcastle. Thankyou to Eric Colhoun for introducing me to research in Tasmania and starting me off on a fantastic Honours project. I'd like to thank Eric for his support and guidance and opportunity to work on the Lake St Clair cores, retrieved from the great depths of Lake St Clair by Dr Charlie Barton, formerly at Geoscience Australia, with the help of Tony Fowler. I'd also like to thank the many people that helped in the field: Simon Richards, Peter Shimeld, Stuart Pearson, Paula Jones, Warwick Dyson, Glenn Behnke and Christian Thun. Thank you also to Stuart for his inspiring lectures and early support on the project and Peter Shimeld for his guidance on my entry into the world of pollen, his immense enthusiasm, knowledge and great friendship.

Special thanks also to the rangers at Lake St Clair for their help, support, interest and provision of accommodation during fieldwork. I will never forget the feeling of awe and excitement when I first stepped onto the shores of Cynthia Bay and looked out into the amazing landscape that I would have the privilege to explore. Thank you to Sib Corbett for providing vegetation maps and interesting discussions on Tasmania's vegetation. Thank you to Kevin Kiernan and

Tim Barrows for helpful discussions on the glaciation of the region. I have spent countless hours in Kevin's PhD thesis on the glacial geomorphology of the Lake St Clair region.

And finally, a big thank you to my family and friends for being there for me on this lengthy journey and their unquestionable support! Thank you to Simon Richards and Christian Reepmeyer for sharing a part of the journey. Thank you to Naroa and Janay for all the good times, support and laughter. Naroa's perfectly timed, surprise deliveries of ice cream played a critical role in reaching this point of thesis submission… not to mention the amazing friendship that is linked to this.

And how could I forget, thank you to the Bearded Ladies!

Abstract

This thesis presents a history of regional and local changes in vegetation in the Lake St Clair region, supported by modern vegetation and pollen analyses. The records span into oxygen isotope stage 3, with a focus on the last Glacial Holocene transition and fill a gap in the poorly studied region of Central Tasmania.

The vegetation during the last glaciation prior to the Last Glacial Maximum was characterised by widespread *Pherosphaera hookeriana* dominated alpine coniferous heath growing together with a mosaic of alpine grasslands, herbfields, heathland and sedgeland. The lakes at Clarence Lagoon and Excalibur Bog are inferred to have dried up under the cold and dry climate during the Last Glacial Maximum. The legacy of *Pherosphaera hookeriana* dominated vegetation extends to the early deglacial sediments in Lake St Clair, declining to only trace representation through the remainder of the late Glacial and Holocene in the wider Lake St Clair region.

Deglaciation of Lake St Clair was complete by c. 18.3 cal kyr BP and subsequent replacement of an early mosaic of alpine vegetation types, by subalpine *Athrotaxis cupressoides* and *Diselma archeri* dominated rainforest and/or woodland in response to rapidly rising temperatures and precipitation, is in sync with postglacial Antarctic warming and rising sea surface temperatures. A 900-year period of renewed grassland expansion is inferred to represent slightly cooler/drier conditions leading into the Antarctic Cold Reversal, abruptly ended by strong increases in rainforest mid-way through the Antarctic Cold Reversal suggesting a shift to a wetter and warmer climate leading to the establishment of *Phyllocladus aspleniifolius-Nothofagus cunninghamii* rainforest. The abrupt decline in *Phyllocladus aspleniifolius* at c. 12.4 cal kyr BP marks the expansion of *Nothofagus cunninghamii-Atherosperma moschatum* callidendrous rainforest growing under optimal conditions during the Early Holocene, which becomes more complex between c. 10-8 cal kyr when *Phyllocladus aspleniifolius* returns to high values, together with a secondary peak of *Athrotaxis*/*Diselma* under an inferred wetter and warm climate. At c. 8 cal kyr BP, the rainforest taxon *Anodopetalum*/*Eucryphia* becomes important and the remainder of the Holocene sees an overall decline in rainforest taxa and increase in sclerophyll and herbaceous taxa and fire activity, which intensifies during the late Holocene. The observed changes in the record are consistent with the onset of ENSO and a more variable climate from c. 8 cal kyr BP and an intensification and cooling temperatures from c. 5 cal kyr BP.

Table of Contents

List of Figures

List of Tables

List of Plates

Chapter 1 Introduction

1.1 Introduction

Future climate and environmental change continues to be a significant topic of global concern. During the last decade we have experienced the warmest temperatures on record and the rapid rate at which climate has changed over the past few decades as a consequence of increased anthropogenic greenhouse gas emissions has resulted in significant impacts on biological and physical systems across the globe (Cook et al., 2013; Rosenzweig et al., 2008; Oreskes, 2004). The continued trajectory of rapid climate change into the future creates an urgent need to better understand the mechanisms and consequences of abrupt climate change.

The development of models that simulate future climate change has been important to explore questions about the nature and degree of change that can be expected in the future as a result of climate change. Although models have developed greatly since the first purely atmosphere based climate model produced by Phillips (1956), through the development of the first coupled atmosphere-ocean general circulation models (AOGCM) in the late 1960s (Manabe et al., 1975; Bryan et al., 1975), to the incorporation of increasingly complex components involving biosphere-atmosphere feedbacks in Earth System Models in the 2000s (Cox et al., 2000; Friedlingstein et al., 2001; Friedlingstein et al., 2006), there is still a lack of agreement in future predictions and a continuing challenge for models to even accurately replicate present (or past) conditions due to the complexity of the feedback processes involved.

The incorporation of vegetation response in models has been important due to the role of vegetation in the carbon-climate feedback cycle (Cox et al., 2000; Cramer et al., 2001; Sitch et al., 2008). Models have produced a variety of predicted vegetation responses which can not be fully evaluated through direct observation alone due to the narrow temporal space covered by ecological monitoring records (Sitch et al., 2008). Palaeoecology, the study of past ecosystems through the analysis of fossil plant and animal remains, allows the observational basis to be greatly extended into the deeper past through the reconstruction of past ecological systems. The synthesis of palaeodata from terrestrial, marine and ice-core archives is key to improving the understanding of how ecosystems have responded to disturbance and climatic variability in the past (Seddon et al., 2014; Harrison and Dodson 1993) and thereby improving predictions of future responses to changes in climate and environment to be made. It is also important to understand how change is expressed geographically across the globe (heterogeneity) and whether any precursors may be identified to warn of imminent change.

Periods of abrupt climate change in the past are of particular interest and (Seddon et al., 2014) identified the question "What can palaeoecology reveal about early warning signals of abrupt change?" as one of the 50 priority research questions currently being addressed by palaeoecology.

Understanding the geographical variation across the globe in responses to abrupt climate change in the past not only will give us an idea of what kind of responses to expect in the future, but also gives us valuable information about understanding the underlying mechanisms involved that trigger abrupt climate change and the processes involved in transferring the abrupt climate signal to different parts of the globe.

1.2 Context

1.2.1 Periods of abrupt climate change in the past

The last glacial period in the North Atlantic area was punctuated by a series of large, abrupt, millennial scale changes in climate called Dansgaard-Oeschger (DO) events (Dansgaard et al., 1984; Johnsen et al., 1992; Dansgaard et al., 1993; Grootes et al., 1993). During these events, the climate in the North Atlantic warms abruptly by 5-16 °C within a time frame of a few years to several decades which results in an abrupt shift from stadial to interstadial conditions. The climate then cools gradually during the initial phases of the event and finishes with an abrupt cooling returning to stadial conditions over a period varying between a century up to several millenia (Petersen et al., 2013; Rasmussen et al., 2014). DO events have a recurrence interval of approximately 1-2 ka, however, evidence for a single periodicity or even a cyclical nature to the events has not been established (Thomas et al., 2011; Long and Stoy, 2013). The sequence of DO events are preserved most comprehensively in Greenland ice cores in the form of alternating Greenland stadials (GS) and Greenland interstadials (GI), but have also been observed in a wide variety of marine and terrestrial records with a bias towards the Northern Hemisphere overall, and to the North Atlantic in particular in the case of marine records (Rasmussen et al., 2014; Voelker, 2002).

Heinrich events are another type of abrupt climate change event during which large amounts of ice-rafted debris (IRD) were deposited in the North Atlantic in association with cold periods (Heinrich, 1988; Bond et al. 1992). These events were initially thought to be a possible trigger for DO events (Hemming, 2004; Margari et al., 2010), however, there are fewer Heinrich events than DO events and there is increasing evidence that Heinrich events do not precede DO events but in fact occur after a DO event is already underway (Gutjahr and Lippold, 2011; Marcott et al., 2011; Barker et al., 2015). What has been found is that stadials containing a

Heinrich event are longer in duration than those without (WAIS Divide Project Members, 2015).

In contrast with Greenland ice core records, Antarctic ice core records exhibit trends of gradual warming and cooling cycles in the form of Antarctic Isotopic Maxima (AIM) events (Barbante et al., 2006) which occur in anti-phase with the abrupt events recorded in the north (Blunier et al., 1998). This phenomenon, known as the bipolar see-saw effect (Broecker, 1998), is thought to be caused by changes in the Atlantic Meridional Overturning Circulation (AMOC) which transports heat from the Southern Hemisphere to the Northern Hemisphere through the northward flow of warm, near surface waters which descend in the North Atlantic and return southwards as cold North Atlantic deep water (Crowley, 1992; Stocker and Johnsen, 2003; Buizert and Schmittner, 2015). The AMOC is thought to operate in two main modes: a "stadial mode" where the AMOC is weak and the North Atlantic cold and an "interstadial mode" where the AMOC is strong and the North Atlantic warm. Stadials containing Heinrich events present as a third "glacial mode" where the AMOC is thought to be particularly weak and the North Atlantic experiences extreme cold (Buizert and Schmittner, 2015).

The bipolar seesaw phenomenon is typically described as a seesaw between the hemispheres, however, Rasmussen et al., (2016) found that the open North Atlantic experienced gradual warmings and coolings during DO events which were synchronous with Antarctic climate events and out-of-phase with the abrupt Greenland DO oscillations. They suggest if the system were a see-saw, the hinge would need to be close to the Greenland-Scotland ridge (geographic asymmetry). They put forward that the marine system appears to be operating as a 'push and pull' system rather than a seesaw system; 'pull' when the AMOC was strong during interstadials and 'push' when the AMOC was weak during stadials. They suggest that only marine areas in direct influence of Northern icesheets, including the Nordic seas, the belt of ice-rafter debris (IRD) in the North Atlantic and areas close to land in the far northeast and northwest, record the abrupt Greenland type climate signal. According to their survey of marine records, all other records from the North Atlantic tended to exhibit an Antarctic signal.

A recent review of the bipolar see-saw model by Landais et al., (2015) also suggests that the processes involved appear to be more complex than explained by the basic bipolar see-saw mechanism. Their high resolution analysis of Antarctic ice core data reveals that, although the large scale pattern of variations of Antarctic $\delta^{18}O$ indicate anti-phase warming/cooling during Greenland cold/warm periods as explained by the bipolar see saw model, at a submillenial scale the Antarctic records reveal regional differences (e.g. two step warming phases of AIM 8 and AIM 12) best explained by fast, atmospheric teleconnections with the low latitudes (Landais et al., 2015).

Although there is general agreement on the broad mechanism involved in abrupt climate change by means of the changes in the AMOC described above, to date there is no consensus on what actually triggers these shifts in the AMOC to take place (Rasmussen et al., 2016). There has been much debate on whether the Northern Hemisphere is forcing the Southern Hemisphere or vice versa and the types of processes which might trigger the events. Buizert and Schmittner (2015) put forward a Southern Ocean control on the AMOC where warming in the Southern Ocean and strengthening of the southern westerly winds results in a shift towards higher freshwater values in the AMOC causing the circulation to weaken. Other ideas also revolve around freshwater-driven changes to the AMOC, however, with Northern Hemisphere icesheets as a source through icesheet calving and freshwater discharges into the North Atlantic Ocean (e.g. Menviel et al. 2011).

Concerted efforts to tighten the timing of the opposing climate transitions observed in Greenland and Antarctica have resulted in a better understanding of how climate signals are propagated across the globe. Using a new and more robust composite Antarctic climate record, Pedro et al., (2011) found that there is little to no time lag (with a ca. 200 yr uncertainty) between the hemispheres and conclude that the inter-hemispheric coupling mechanisms involved are likely to be fast acting bipolar atmospheric and/or ocean teleconnections.

The analysis of a new, high accumulation Antarctic ice core, the West Antarctic Ice Sheet (WAIS) Divide ice core (WDC) has produced the most precise constraints on the interhemispheric phasing of climate variations to date (WAIS Divide Project Members, 2015). The findings indicate that the opposing climate transitions observed in Greenland and Antarctica are not synchronous, but the Northern Hemisphere has led the Southern Hemisphere by approximately 200 years (Greenland warming leads the onset of cooling in Antarctica by 218±92 years (2δ) and similarly Greenland cooling leads onset of Antarctic warming by 208±96 years) in both cooling and warming events. The significance of these findings includes not only that the directionality of the abrupt climate signal is demonstrated to be north to south, but also that the transmission of the signal can not be by fast atmospheric and/or oceanic mechanisms as suggested by the findings of Pedro et al. (2011) but by slower oceanic propagation. This still does not tell us that the trigger for the climate events was necessarily in the Northern Hemisphere (WAIS Divide Project Members, 2015; Landais et al., 2015). Such high precision on the timing has not previously been possibly as the resolution of the Antarctic records has not been high enough due to lower rates of accumulation compared with the WAIS WDC record.

1.2.2 The last glacial interglacial transition and teleconnections of climate signals

The last glacial interglacial transition is an example of a large scale, naturally forced, change in global climate (Pedro et al. 2011) and is the focus of this thesis. The period makes an excellent case study to study the effects of such a major climate change, where research efforts to date have focussed on understanding the nature and timing of climate events during this period in the polar regions as well as possible teleconnections in marine and terrestrial environments distal from the poles in the mid to low latitudes. The analysis of high resolution records with sound chronologies across the globe is essential to moving closer to elucidating the process(es) involved in triggering such abrupt climate change.

After the Last Glacial Maximum (LGM), most Northern Hemisphere ice sheets had begun to retreat by 20-19 cal kyr BP (Clark et al., 2009) after an initial rise in Northern Hemisphere summer insolation (Carlson and Winsor, 2012). Despite an increase in Northern Hemisphere CO_2 levels in step with Antarctic warming from around 18 cal kyr BP, Greenland temperatures according to ice core water isotope ($\delta^{18}O$) records remain low during Heinrich Stadial 1 until their abrupt rise at the start of the Bølling-Allerød period (14.7- 12.8 cal kyr BP). This suggests a late post LGM warming response in the Northern Hemisphere relative to the Southern Hemisphere and the superimposition of this anti-phased hemispheric bipolar see saw mechanism, causing the disparity in temperature response to changes in ocean circulation, on the overall global increase in CO_2 concentrations which drove in-phase warming at the Last Termination (Shakun et al., 2012). The Bølling-Allerød period is followed by an abrupt return to cold conditions in Greenland during the Younger Dryas period (12.8-11.7 cal kyr BP) after which warming resumes into the Holocene (Buizert et al., 2014; Sime, 2014). In Antarctica, the post LGM warming trend is interrupted by a gradual phase of cooling or pause in warming between 14.7-12.5 cal kyr BP known as the Antarctic Cold Reversal (ACR) (Blunier et al., 1997; Barker et al., 2009; Pedro et al., 2011; Shakun et al., 2012) concurrent with the Bølling-Allerød period in the Northern Hemisphere.

The puzzle over the delay in warming of Northern Hemisphere temperatures between 17.5-14.5 cal kyr BP led (Denton et al., 2006) to coin the term “Mystery Interval” (MI) for this period during Heinrich Stadial 1 (Oldest Dryas). He et al. (2013) demonstrate that the absence of warming in the Northern Hemisphere during this period when the Southern Hemisphere was warming can be adequately explained by the bipolar seesaw effect triggered by meltwater injection into the ocean from the melting Northern Hemisphere ice sheets resulting in warming in the Southern Hemisphere. Buizert et al. (2014) propose that $\delta_{18}O$ alone does not provide reliable, quantitative temperature reconstructions and instead use independent temperature reconstructions based on $\delta^{15}N$ from three ice cores in conjunction with coupled

ocean-atmosphere climate model simulations to demonstrate that a small increase in temperature occurred in Greenland during the mystery interval. Their reconstructions provide new information suggesting that the Younger Dryas period was actually around 4.5°C warmer than Heinrich Stadial 1 / Older Dryas Period which they ascribe to increased summer insolation and carbon dioxide forcing. Buizert et al. (2014) suggest the same approach could be applied to Antarctic ice core records to improve temperature reconstructions. Traditionally, the Younger Dryas period was thought to have been colder than the Heinrich Stadial 1 (the Oldest Dryas period) and, until recently, the was thought to be an outlier event separate from the other abrupt DO events registered in the NH. Favoured causes for the YD included catastrophic events such as the draining of Lake Agassis or even a comet impact, but in the meantime it has been found through evidence from Chinese stalagmites that the YD was an integral part of the sequence of deglaciation resulting in the global termination to the last glaciation (Broecker et al., 2010). The abrupt signal was not uniformly transmitted across Europe, however, with some records in Western Europe not showing a strong DO response highlighting variability in the translation of abrupt events according to location, environment and the type of proxy employed (Ampel et al., 2010).

The abrupt climate events associated with DO events in the North Atlantic region have been found to have been expressed widely across the Northern Hemisphere (Voelker, 2002; Clement and Peterson, 2008; Sánchez Goñi et al., 2008) as far as Asia (Wang et al., 2001) and into the tropics (Peterson et al., 2000; González et al., 2008) in both terrestrial and marine records, most likely through fast atmospheric transport of the climate signals. Teleconnection of the abrupt DO events in Antarctica has been shown to have followed slower, oceanic transport routes of the climate signal, as indicated by the lag in timing of AIM events by 200 years on average, and the more gradual, less pronounced millennial scale oscillations in cold and warm periods recorded in Antarctica (WAIS Divide Project Members, 2015).

Much research effort has been focussed on identifying the nature and degree of teleconnection between the low to mid latitudes of the Southern Hemisphere with the high latitudes of both hemispheres (Newnham et al., 2012). There has been much contention over evidence supporting Greenland vs Antarctic vs ambiguous climate signal linkages. The complexity of the observed changes in climate and environment in this region have made interpretations difficult, in particular due to the paucity of high resolution records with sound chronology which are required to address these questions (Turney et al., 2006; Tibby, 2012; Reeves et al. 2013a). The information from climate records from the low to mid latitudes of the Southern Hemisphere are vital to understanding the processes at large which ultimately

trigger climate change such as seen during the Last Termination/last glacial-interglacial transition.

The INTIMATE (integrating ice core, marine and terrestrial records) initiative has been successful in creating a precise event stratigraphy of climate events for the Last Interglacial-Glacial cycle in the North Atlantic region based on Greenland ice core records (Rasmussen et al., 2014). The AUS-INTIMATE (Australasian INTIMATE) initiative set out to create a similar event stratigraphy for the Australasian region between 30-8 cal kyr BP, however, the Australian sub group found few climatic events that were representative of such a broad region covering such an expanse of different climate zones. Instead they identified four key regions and collated syntheses of climate change in each: 1. The Southern Ocean (Bostock et al., 2013) 2. temperate Australia (Petherick et al., 2013) 3. The Australian drylands (Fitzsimmons et al., 2013) 4. Tropical Australasia (Reeves et al., 2013b) (Reeves et al., 2013a). The NZ sub group of the AUS-INTIMATE initiative was successful in creating a climate event stratigraphy for New Zealand (Barrell et al., 2005; Alloway et al., 2007; Barrell et al. 2013), however, identified significant challenges in resolving the nature, timing and amplitude of lateglacial reversal due to regional contrasts between marine and terrestrial records, and between biological or glaciological proxies versus speleothem isotopic signatures (Barrell et al. 2013).

Pedro et al., (2016) undertook the first non-subjective analysis of the spatial pattern of teleconnection of climate events during the LGIT using the case study of the Antarctic Cold Reversal. The following section, using the period of the Antarctic Cold Reversal/ Bølling-Allerød as a case study, explores the degree and nature of teleconnection in the Southern Hemisphere.

1.2.3 The Antarctic Cold Reversal

In Antarctic ice core records, the onset of warming after the Last Glacial Maximum occurs around 18 cal kyr BP and is interrupted by a gradual return to cooler conditions or pause in warming during the Antarctic Cold Reversal (ACR) between 14.7-13.0 cal kyr BP (Blunier et al., 1997; Barker et al., 2009; Pedro et al., 2011; Shakun et al., 2012). The gradual cooling is in contrast with the abrupt warming experienced at approximately the same time in the North Atlantic during the Bølling-Allerød period. Antarctic ice cores register the ACR through water stable isotope ratios ($\delta^{18}O$ and δD) as proxies for temperature to varying degrees, where inland ice cores exhibit the strongest ACR signals and near-coastal ice cores showing weaker ACR signals most likely due to stronger influence of regional anomalies in circulation and sea ice concentration on the climate signal at these sites (Pedro et al., 2016)

In a recent examination of the dynamics and spatial extent of the ACR in the Southern Hemisphere based on a synthesis and statistical analysis of 84 palaeoclimate records, Pedro et al. (2016) found that evidence for cooling during this time period is strongest in records from regions south of 40°S and the South Atlantic, whereas terrestrial regions in the Southern Hemisphere tropics and subtropics north of 20°S appear to have responded to Greenland-like climate signals instead expressed in the form of abrupt hyrdologic variations. The regions between 20°S and 40°S are mostly characterised by unclear climate signals (Pedro et al., 2016)

Through model simulations, Pedro et al. (2016) suggest that increased northward ocean heat transport in the Atlantic Ocean in combination with expanded sea ice in the Southern Ocean can explain the reversal in cooling observed in the SH during the ACR. They suggest that the abrupt hydrological signals in the tropics and subtropics, on the other hand, can be explained by a different process of atmospheric heat transport to the south via the Hadley circulation demonstrating that multiple processes are operating together to explain the spatial pattern of climate change (Pedro et al., 2016).

The strongest ACR signals outside of Antarctica are shown by marine records polewards of 40°S in the South Atlantic (Lamy et al., 2007) and southeast Pacific near Chile (Barker et al., 2009) with the addition of Southern Ocean marine cores south of Australia at 37° S also exhibiting an ACR signal (Calvo et al., 2007; De Deckker et al., 2012; Lopes dos Santos et al., 2012; Lopes dos Santos et al., 2013). Although ACR signals in marine cores near the east coast of New Zealand are weak, a stack of 26 marine records from >40°S in the Southern Ocean, including the two cores near South Australia at a slightly lower latitude, exhibits a clear ACR signal from the Southern Ocean (Pedro et al., 2016). Williams et al. (2015) suggest from evidence of weaker ACR signals in New Zealand that the bipolar see saw effect may diminish with distance from the poles.

There is also strong evidence for the presence of the ACR in terrestrial glacial records with glacial re-advances during the ACR recorded in both the South Island of New Zealand (Putnam et al., 2010; Kaplan et al., 2010; Doughty et al., 2013; Kaplan et al., 2013) and Patagonia (McCulloch et al., 2005; Moreno et al., 2009; Glasser et al., 2011; Strelin et al., 2011; García et al., 2012; Menounos et al., 2013; Pedro et al., 2016). Although approximately 1085 km^2 of Tasmania was glaciated during the LGM (Derbyshire, 1972), no evidence for any glacial readvances after the LGM have been found (Kiernan, 1992; Barrows et al., 2002; Colhoun et al., 2010; Colhoun et al., 2014).

Although previously some post LGM glacial re-advances in New Zealand and Patagonia were ascribed to the Younger Dryas, improved dating and new data have provided clear evidence

for glacier expansion in New Zealand (Putnam et al., 2010; Kaplan et al., 2013) and Patagonia (Moreno et al., 2009; García et al., 2012) at an earlier stage during the ACR (Pedro et al., 2016). Redating of moraines in the tropical Andes showed that even at lower latitudes, glaciers were responding to an Antarctic signal rather than a Greenland signal and expanded during the ACR rather than the YD (Jomelli et al., 2014).

Kaplan et al. (2013) estimate a reduction in temperature between 1.8°C and 2.6°C during the ACR based on numerical modelling experiments with precipitation remaining similar in New Zealand. Putnam et al. (2010) suggest that expansion of cold Southern Ocean waters as a result of northward migration of the southern Subtropical Front to have caused cooling during the ACR in New Zealand.

Although the consensus points towards the southern mid latitudes of the Southern Hemisphere picking up an Antarctic climate signal, Moreno et al. (2009) suggest that regional variation exists within Patagonia resulting in a blend of Antarctic (southwestern Patagonia, ~50°S) and Greenlandic (northern Patagonia, ~40°S) cold phases based on glacial and pollen records (Moreno et al., 2009). García et al. (2012) present the first clear evidence for the onset and duration of the ACR in southern Patagonia from glacial records in Torres del Paine and suggest that the southern westerly wind belt migrated north to the latitude of Torres del Paine at the start of the ACR in association with northward migration of the Antarctic Polar Front, bringing cold conditions and peak precipitation to the catchment of the glacier.

Evidence for the ACR from terrestrial palaeoecological records in the southern mid latitudes of the Southern Hemisphere is more limited, however, temperature reconstructions from pollen and chironomid records indicate cooling during the ACR in some areas of southern South America (Massaferro et al., 2009; Mansilla et al., 2016) , New Zealand (Vandergoes et al., 2008; Newnham et al., 2012) and Tasmania (Fletcher and Thomas, 2010a). A chironomid record from northwest Patagonia (42°S) exhibits an unclear ACR signal. Chironomid records from southern Tasmania (42°S) indicate continued warming through the ACR, however, the loss on ignition record from these sites pick up an ACR signal in the form of reduction of organic matter during the ACR which (Rees and Cwynar, 2010) suggest could reflect an increase in precipitation due to strengthening of the SWW during the ACR. In their reanalysis of pollen records from western Tasmania, Fletcher and Thomas (2010a) reconstruct temperatures for two sites and found that Tullabardine Dam (41°S) shows an ACR signal whereas Lake Selina (41°S) does not, however they note that the records are limited by low sample resolution and poor chronology.

Pedro et al. (2016) comment that, despite the presence of temperature trends which are consistent with an ACR, many terrestrial biological proxies from New Zealand fail under their automated statistical method to register an ACR signal. They suggest this is a result of the complexity of ecosystem data which can exhibit a high degree of variability and rapid or stepwise responses once ecological thresholds have been crossed in response to climate change (Smith, 1965; Tzedakis et al., 2004; Pedro et al., 2016).

1.3 Statement of Problem

Although significant advances have been made in determining the nature and timing of past abrupt climate events in the polar regions, there is still much contention about the degree to which these climate events are expressed globally and by what mechanisms the climate signals are transferred to the mid and low latitudes. In order to come closer to identifying the causative processes that ultimately trigger climate change, it is essential to gain a better understanding of these teleconnections. The biggest challenge in the endeavour to ascertain the degree of teleconnection in the Southern Hemisphere has been a paucity of suitable records of high resolution with robust chronology (Turney et al., 2006; Tibby, 2012; Reeves et al., 2013a).

Tasmania is an island state of Australia extending between latitudes 40º40'S and 44º40'S where it is positioned as one of the few landmasses in the vast Southern Ocean apart from New Zealand and southern South America. This position, within the strongest path of the Southern Westerly Wind Belt (The Roaring Forties), makes Tasmania sensitive to past movements in the Westerly Wind Belt and places it in an important transition zone between influences from the subtropics and Antarctica. Tasmania is separated from the mainland by Bass Straight, a shallow stretch of ocean which was mostly exposed during the periods of Pleistocene glaciation when sea levels were ~ 120 m lower (Thom and Chappell, 1975), creating a land bridge which connected Tasmania with mainland Australia and an increase in continentality due to the increase in landmass. Tasmania has a temperate marine climate characterised by mild winters and cool summers with a slight continental effect (Langford 1965). The climate of Tasmania is under strong influence from the prevailing westerly winds which, along with the mountainous topography which function to amplify climate signals, produce pronounced west-east environmental gradients sensitive to changes in both the atmosphere and ocean (Alloway et al., 2007). A strong precipitation gradient results in some regions in the west receiving over 3200 mm and areas lying in the rainshadow of the Central Plateau in the east receiving less than 600 mm of average annual rainfall (Hill et al 2009).

The pioneering pollen records of postglacial vegetation and climate history produced by Macphail (1975, 1979) demonstrated that Tasmania is well suited for palaeoecological studies.

Since then a high density of pollen records have been published for Tasmania, however, most are located in Western Tasmania with very few records extending back to the Last Glacial Maximum and beyond. Although numerous records cover the Last Glacial-Interglacial Transition, the limiting factor of these records is the low samples resolution and poor chronology.

Our knowledge of climate change during the Quaternary Period in Tasmania has seen rapid advances in the last 35 years as noted by Colhoun et al. (2010) in a recent review focusing on climate changes inferred from glacial, pollen and speleothem records from Tasmania. The advent of exposure dating in particular, in conjunction with more detailed field studies and examination of pollen sequences stratigraphically related to glacial deposits, has allowed correlation of Tasmanian glacial events with marine isotope stages (MIS) stages globally (Colhoun et al., 2010).

Colhoun and Shimeld (2012), in their review of Tasmanian pollen records from which they constructed maps of the major Tasmanian vegetation formations during different time slices during the Late Quaternary, conclude that vegetation changes were primarily driven by climate, but that Aboriginal use of fire impacted strongly on the vegetation after their arrival 35 000 years BP. Fletcher and Thomas (2010b) propose that the latter use of fire through the Late Glacial deflected interglacial vegetation development and that the present-day moorland-dominated landscape of western Tasmania represents an ancient cultural landscape.

With growing consensus that the mid latitudes of the Southern Hemisphere are impacted by an Antarctic signal during the last glacial interglacial transition, there is no strong evidence from Tasmania which links vegetation change to climate events in Antarctica apart from possible ACR signals at Tullabardine Dam (Fletcher and Thomas 2010) and Mt Field (Rees Cwynar 2010) mentioned in the previous section.

In order to link Tasmanian vegetation-climate changes to global climate events, more regional vegetation records studied at high resolution with robust chronology are needed. The likelihood for climate to be the main reason explaining the change in vegetation in a large lake representing a regional record is much higher than at a small site with a localised record. In order to pick up a regional signal that will be representative of the broad changes in vegetation and climate in Tasmania, a large lake in the less studied area of Central Tasmania is targeted which is located in a sensitive boundary zone mid-way along the strong west-east environmental gradient across Tasmania.

1.4 Research Aims

1.4.1 Primary Aim

The primary aim of this thesis is to reconstruct the palaeoenvironment of a site sensitive to regional environmental changes in central Tasmania, with particular focus on the last glacial interglacial transition, and from this to infer a climate history for central Tasmania and by extension the southern mid latitudes of the Southern Hemisphere.

Questions which will be addressed:

1. What was the nature of the last glacial interglacial transition in central Tasmania?

2. How do Tasmanian climate events during the last glacial interglacial transition correlate with global climate events during this period?

- What is the nature of teleconnection with climate events at the higher latitudes? Does Tasmania pick up an Antarctic signal, a Greenland signal or is it ambiguous and why?

More specific questions:

1. Is post LGM warming synchronous with increasing Antarctic temperatures?

Evidence from New Zealand and southern South America suggests that deglaciation and establishment of forests occurred in step with Antarctic warming (e.g. Vandergoes et al. 2013; Barrows et al, 2002; Moreno et al., 2015).

- When was deglaciation complete? A minimum date for deglaciation can be obtained by dating the basal sediments in the lake.
- When did forests first establish? Dating the transition from non-forest to forest vegetation will give an indication of the timing of onset of warming in Tasmania.

2. Is the Antarctic Cold Reversal observed in central Tasmania?

3. What is the timing and nature of the late Last Glacial/Holocene boundary in central Tasmania?

In order to address these questions, a high resolution, regional record in central Tasmania was targeted that would minimise noise from local signals recorded at smaller sites and to increase the likelihood of picking up broad, regional climate signals representative of Tasmania. Western central Tasmania lies in a climatically sensitive transition zone mid-way along the strong west-east environmental gradients across Tasmania. Lake St Clair was selected for further analysis as previous studies (Hopf, 1997; Hopf et al., 2000) demonstrated that this large glacial lake contains a late Last Glacial-Holocene record suitable for high resolution analysis of the last glacial interglacial transition.

Sub-aim 1 To reconstruct the vegetation history of central Tasmania

Sub-aim 2 To reconstruct the fire history of central Tasmania

Sub-aim 3 To infer a climate history for central Tasmania and explore links with global climate events during the last glacial interglacial transition

The above will be supported by modern pollen analysis, sedimentological analyses and radiocarbon dating.

1.4.2 Secondary Aim

The secondary aim of this thesis is to extend the palaeoenvironmental record for Central Tasmania beyond the late Last Glacial.

How does the full glacial vegetation compare with the postglacial vegetation associations and what can this tell us about the evolution of the modern subalpine vegetation?

There is a lack of sites covering the Last Glacial Maximum (LGM) and pre-dating the LGM in Central Tasmania and Tasmania as a whole (Colhoun and Shimeld, 2012). In order to find sites of this age, sites lying outside the ice limits of the LGM (Clarence Lagoon and Excalibur Bog, information about these sites will be detailed in Chapter 3) were targeted as these have potential to hold sediments predating and including the LGM.

1.5 Thesis plan

Chapter Two describes the modern environmental setting with particular emphasis on the vegetation and the factors that influence its distribution (climate, fire and other environmental conditions).

Chapter Three outlines the selection of sites and methods employed to address the research aims of this thesis. Pollen, macroscopic and microscopic charcoal analysis will be used to produce vegetation and fire histories and these will be supported by sediment analyses (stratigraphy, magnetic susceptibility and particle size analysis, carbon/nitrogen analysis) and radiocarbon chronology.

Chapter Four presents modern pollen analyses undertaken in the Lake St Clair region. A sound understanding of the modern pollen-vegetation relationship and ecology of the vegetation is essential as a foundation for interpretations of past vegetation associations. The ecology of key plant taxa that are important indicators of particular vegetation types or climatic conditions will be outlined. The chapter also includes analysis of the modern pollen rain and its representation of the modern vegetation to support interpretation of the fossil pollen record. Descriptions of key pollen taxa will be given to indicate those that are most useful as indicators of environmental change. The chapter will also review large lake pollen records and

the importance of fluvial transport of pollen to these lake in addition to aerial deposition of pollen.

Chapter Five presents the results for Core CG from Lake St Clair, a late Glacial-Holocene record. The last glacial-interglacial transition is analysed at high resolution to address the primary aim of this thesis.

Chapter Six describes the results of two pre-LGM sites, Clarence Lagoon and Excalibur Bog, to address the secondary aim of this thesis to extend the palaeoenvironmental record of Central Tasmania beyond the LGM. In addition, records from Skullbone Plains Bog and Clarence Bog are presented and provide detail of local changes within the Lake St Clair catchment, during the Holocene and Late Holocene respectively, to complement the predominantly regional record from Lake St Clair.

Chapter Seven presents the interpretation of the results and considers the implications for long term vegetation and fire dynamics, climate change and global teleconnections.

Chapter 8 presents the conclusions of the project and future research directions.

Chapter 2 The Modern Environment

2.1 Location and topographical setting

Tasmania is an island in the Southern Ocean extending between latitudes 40º40'S and 44º40'S. Tasmania is the sixth state of Australia and is separated from the mainland by Bass Strait, a shallow stretch of ocean most of which is only 60-80 m deep. Two north-south trending ridges extend from the northeastern and northwestern corners of Tasmania and contain a series of islands, notably the Furneaux Group and King Island. During the periods of Pleistocene glaciation when sea levels were ~ 120 m lower (Thom and Chappell, 1975), most of Bass Strait was exposed, creating a land bridge which connected Tasmania with mainland Australia. The remainder of Tasmania is surrounded by the vast Southern Ocean (Tasman Sea), the closest land masses to the east and west being New Zealand and South America respectively (Figure 2.1).

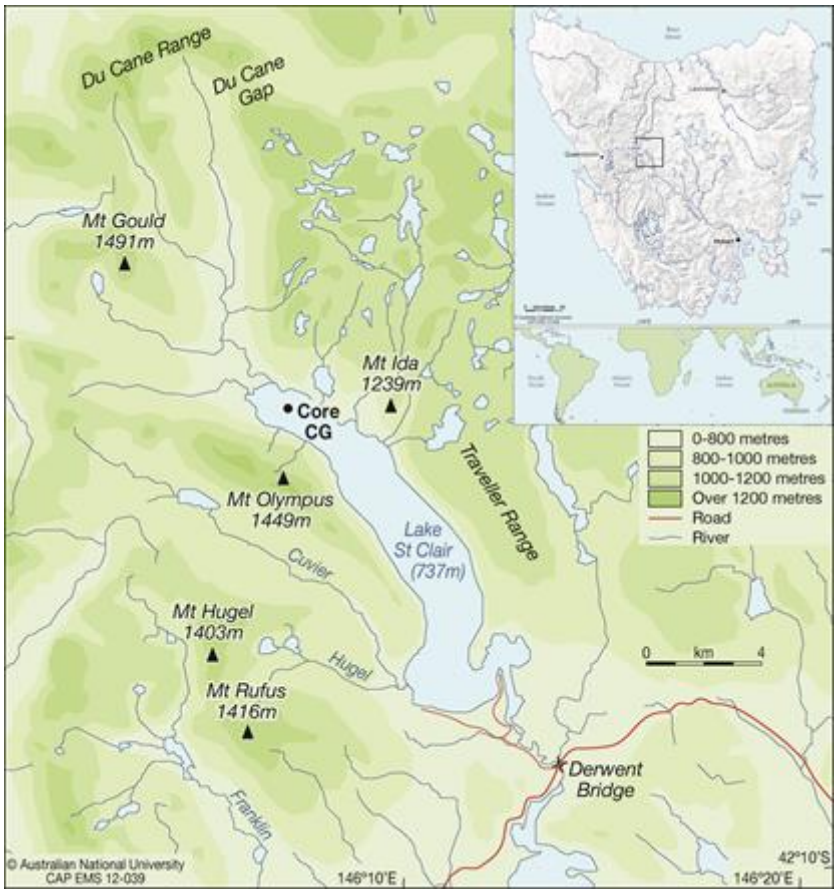

Figure 2-1 Location map of the study area

In contrast with mainland Australia, Tasmania is very mountainous. The mountains and hills more or less adjoin the coast, rising to Tasmania's highest peak, Mt. Ossa (1616 m) in the central highlands of Tasmania. The coast consists mostly of narrow emerged marine platforms

and only restricted depositional plains. The plain occupying the Midlands Graben between Launceston and Turnbridge is the only extensive inland plain (Davies, 1965).

The ridge-like mountains of western Tasmania contrast with the plateau-like mountains of central, eastern and southeastern Tasmania. In western Tasmania and northeastern Tasmania, folded pre-Carboniferous rocks are exposed. The ridge-like mountains are composed of hard, quartz metamorphics and conglomerates separated by valleys which have been eroded by river systems along the strike of the softer rocks. The trend of these mountain ranges follows the axis of tectonic folding, hence the area is referred to as the fold structure province (Davies, 1965). In central and eastern Tasmania, the mountains are more plateau-like in character. This is a direct reflection of the geology, which in this area consists of near horizontal post-Carboniferous sediments often capped by intrusions of Jurassic Dolerite producing plateaus and flat-topped mountains. The dominant tectonic structures of this region are a result of fault movements during the late Cretaceous and early Tertiary, hence it is referred to as the fault structure province by Davies (1965).

The research area, including Lake St. Clair (146º10'E 42º06'S; Figure 2.1), lies within the eastern fault structure province at the boundary with the western fold structure province. The geology of the area is characterised by three main rock types: a Precambrian basement of sediments and metasediments overlain by Permo-Triassic sedimentary rocks of the Parmeneer Supergroup which were intruded by and are overlain by Jurassic Dolerite. The Precambrian basement consists mostly of intensely folded quartz schists which are a common feature of western Tasmania where they typically carry shallow, acid and infertile soils. The only outcrop in the Lake St Clair area is at Mt Arrowsmith approximately 13.5 km to the southwest (Derbyshire 1963; Jackson 1999b).

The Jurassic dolerite is the most outstanding feature of the landscape forming the surface of the Central Plateau as well as the summits of most of the higher mountains. The valley sides and floors are comprised of Permian mudstones and Triassic sandstones (Derbyshire 1963; Banks 1973). Lake St. Clair exploits a north-northwest trending fault, which has displaced the boundary between the Jurassic dolerite and Permo-Triassic sediments which lies at approximately 1300 m on Mt Olympus on the western side of the lake. On the eastern side of the lake, the base of the dolerite lies below lake level (Derbyshire, 1971).

Quaternary deposits make up the shoreline and consist mostly of tills but also washed sands and gravels, talus and solifluctual debris (Kiernan, 1992). In contrast to the west, the alpine humus soils formed on the dolerite and glacial deposits tend to be more fertile and are characterised by a strong brown colour and medium to strong aciditity. The soils contain

boulders and fragments of dolerite set in an earthy matrix with sandy to clay texture and usually have a peaty surface horizon (Nicolls and Dimmock, 1965).

An outstanding feature of central Tasmania is the Central Plateau — a unique plateau covering an area of approximately 10,000 km^2 and scattered with thousands of lakes. The plateau gently slopes to the southeast and contains three main surfaces: the St. Clair surface (750 m – 825 m), the Lower Plateau Surface (900 m – 1050 m) and the Higher Plateau Surface (1200 m – 1420 m in the northwest). The Great Pine Tier forms the southwestern boundary between the Lower Plateau Surface and Higher Plateau surface (Davies 1959; Banks et al 1977).

Lake St. Clair lies at an altitude of 737 m and is Australia's deepest lake (182 m) (Derbyshire, 1971). The lake is large, spanning 14 km along its NNW – SSE striking length in alignment with two convergent faults with a broadly arcuate glacially sculptured form. The lake contains four distinct basins in addition to a lateral basin to the southeast – the Derwent Basin (Derbyshire, 1971). The eastern shores rise steeply to the edge of the Central Plateau described above. Mounts Rufus, Hugel and Olympus rise from the lake's western shores to altitudes over 1400 m and are separated by the Cuvier Valley (> 800 m altitude). This area is the source of the Cuvier and Hugel Rivers, which become confluent at Watersmeet shortly before entering Lake St. Clair on its southwestern shore. Mt. Gould (1491 m) and the Du Cane Range (Mt. Geryon, 1509 m) lie to the north of the lake and are the sources of the Narcissus River, which enters Lake St. Clair at its northern end at Narcissus Bay. To the south of the lake lie the Navarre Plains and the low peaks of the Bedlam Wall area (> 900 m). Lake St. Clair is the source of the Derwent River, which flows through Derwent Bridge and the artificial Lake King William to Hobart to the southeast.

Derbyshire (1971) describes Lake St Clair as a glacially over-deepened reach of the Derwent River valley. Derbyshire proposed that the over-deepening and development of the main Lake St Clair trench resulted from the convergence of three valley glaciers with critical input of ice from an ice cap covering the Central Plateau directly to the east of the lake. He argues that without such a reservoir of ice from the Plateau, it is unlikely that such a large rock basin would have been formed (Derbyshire, 1971).

2.2 Climate

2.2.1 Overview

Tasmania has a temperate marine climate characterised by mild winters and cool summers with a slight continental effect (Langford 1965). Most of Tasmania receives winter dominant rainfall apart from the southeast where rainfall is uniform throughout the seasons (Bureau of Meterology, 2018a). The climate of Tasmania is under strong influence from the prevailing

westerly winds which, along with the mountainous topography, produce a strong precipitation gradient from west to east resulting in some regions in the west receiving over 3200 mm and areas lying in the rain-shadow of the Central Plateau in the east receiving less than 600 mm of average annual rainfall (Hill et al 2009) (see figure: Average Annual Rainfall). Temperatures are coldest in central and inland western Tasmania, mostly as a result of higher altitudes, but also due to increased orographic cloud cover which contrast with the higher temperatures and decreased cloud cover experience by eastern Tasmania as a result of the Föhn effect (Jackson, 1999b).

Lake St Clair lies mid-way along the strong west-east environmental gradient and receives 1885 mm of annual rainfall. Rainfall displays a clear winter/spring maximum which contrasts with a 50% reduction in rainfall during the summer months of January and February as well as March. Mean annual temperatures range between 2.8°C and 13.1°C. The highest mean daily maximum temperatures occur in January and February and the lowest mean daily minimum temperatures in July and August. Although the mean daily minimum temperatures in summer are above 5.0°C, frost, snow and hail can occur at any time of the year (Bureau of Meterology, 2018c).

2.2.2 Tasmanian Climate Drivers

2.2.2.1 Southern Annular Mode and the Southern Westerly Winds

The Southern Annular Mode (SAM), also known as the Antarctic Oscillation (AAO), is the most important mode of atmospheric variability in the mid to high latitudes of the Southern Hemisphere on synoptic to multi-decadal timescales (Lim et al., 2013; Pohl et al., 2010; Hill et al. 2009; Thompson and Wallace 2000). Gong and Wang (1999) define the zonal mean pressure difference between 40°S and 65°S as the Antarctic Oscilllation Index and it is this seesaw in atmospheric pressure between the Antarctic region and the mid latitudes of the Southern Hemisphere which is the foundation of SAM. SAM is forced by the strong gradient of meridional temperature between high and low latitudes and is persistent for most of the year becoming slightly weaker during the austral summer (Hill et al. 2009 and references therein).

SAM most strongly affects rainfall in southwest Tasmania, with little correlation between SAM and rainfall characteristic of eastern and north-eastern Tasmania (Mariani and Fletcher, 2016). During positive SAM events, anomalously low pressure occurs over Antarctica whilst higher than normal pressure occurs in the southern mid latitudes. This is accompanied by a southward shift in the southern westerly wind belt (SWW) which is associated with west to east moving storm tracks and cold fronts. Hence positive SAM results in reduced rainfall, particularly over the west, due to less frontal and extratropical cyclone activity over Tasmania. During negative SAM events, the southern westerly wind belt moves north towards the

equator resulting in lower pressure and more storm systems moving over southern Australia which, in Tasmania, usually leads to more rainfall over western Tasmania in combination with drier conditions in the east as a result of orographic effects. SAM exhibits a general pattern of being in its most positive/negative phase during the austral summer/winter (Hill et al. 2009 and references therein; Pohl et al. 2010; Bureau of Meteorology, 2018a).

Although monthly to seasonal variations in SAM occur due to variability of internal atmospheric dynamics, a strong teleconnection between SAM and the El Niño-Southern Oscillation (ENSO) has been observed during the austral summer season at the interannual time scale where El Niño tends to correspond with negative SAM events and La Niña with positive SAM events (Carvalho et al. 2005; Pohl et al. 2010; Lim et al. 2013).

2.2.2.2 The Southern Westerly Winds (SWW)

The southern westerly winds are responsible for the majority of Tasmania's rainfall which, together with the strong orographic influence of high mountains in the west and relatively flat topography in the east, results in the large west-east gradient of mean rainfall and variability. Rainfall seasonality is stronger in western Tasmania which displays high winter rainfall, but although a gradient of high rainfall variability in the west towards weaker variability in the east exists, the dominant mode of rainfall variability is island-wide. (Hill, et al 2009)

The occurrence of blocking high events is important in all seasons. During a blocking high, western Tasmania in particular receives reduced rainfall as a result of weakened westerly flow due to the blocking effect of the event. During spring, ENSO and blocking highs account for over 50% of the variance in rainfall falling in the north and east of the state (Risbey et al., 2009)

2.2.2.3 El Niño-Southern Oscillation (ENSO)

Whereas SAM is the most important mode of atmospheric variability in the mid to high latitudes, the El Niño Southern Oscillation (ENSO) is the most important pattern of large scale variability in the tropics. The influence of ENSO has been found to decrease with latitude, however, extends along the extent of the East Coast of Australia as far as Tasmania (Nicholls and Wong, 1990).

The Southern Oscillation index (SOI) is one way in which ENSO is quantified and is based on the difference in sea level pressure between Darwin and Tahiti, where the fluctuation between positive (La Niña) and negative (El Niño) phases occurs with an irregular periodicity of around 3-7 years (Hill et al. 2009). ENSO is also thought to operate on longer timescales of variability from millennial to semi-precessional. The degree of variability on these timescales is poorly

known, however, an intensification of ENSO relative to modern conditions from the mid Holocene (c. 7-4 ka) has been observed (Petherick et al. 2013 and references therein).

El Niño years are characterised by above average pressure in the Indonesian-North Australian region and anomalously warm temperatures in the central and eastern Pacific Ocean resulting in lower than average rainfall and sometimes major drought episodes in northern and eastern Australia as far south as Tasmania. The converse applies during La Niña years (Petherick et al. 2013 and references therein). The ENSO signal has been found to project island-wide in Tasmania, but with a stronger influence in the north due to the weakening latitudinal effects of ENSO mentioned earlier (Hill et al. 2009).

ENSO also displays a seasonal cycle associated with the seasonal drift of the tropical convection zones resulting in a cold state during the austral winter and a warm state during the austral summer. McBride and Nicholls (1983) found that, overall, ENSO most strongly influences rainfall in Australia during the austral spring (Hill et al. 2009).

2.2.2.4 The Pacific-South American (PSA) modes

The Pacific-South American (PSA) modes include two modes of variability which link tropical and extratropical climates. PSA1 relates to decadal scale sea surface temperature anomalies over the central and eastern Pacific which are thought to be a response to ENSO variability on an interannual time scale. PSA2, on the other hand, is thought to be linked with the quasi-biennial component of ENSO, displaying the strongest connections during the austral spring with a periodicity of 22-28 months (Hill et al. 2009; Mo and Paegle 2001).

The PSA has a significant impact on Tasmanian climate and appears to have a similar influence on Tasmanian rainfall as the SAM, despite having a different origin, through its influence on the SWW combined with orographic effects. During positive PSA years, an island-wide increase in rainfall is observed which is strongest in the west. During negative PSA years rainfall is reduced and also shows the strongest anomalies in the west. The strongest correlation with rainfall is observed during the austral winter (Hill et al. 2009). It is thought that PSA and SAM interact with each other resulting in an enhancement (reduction) of the SWW during positive (negative) PSA phases (Hill et al. 2009).

2.2.2.5 Interactions between the key climate drivers: the SAM, ENSO and PSA

The Southern Annular Mode (SAM), El Niño - Southern Oscillation (ENSO) and Pacific-South American mode (PSA) each have been found to have clear influences on the interannual variability of rainfall over Tasmania, however, the interactions between these three climate modes and their seasonal variation is complex. The impact of ENSO tends to be concentrated in the north whereas that of both the PSA and SAM is more significant in the west. ENSO and

SAM have been found to be in phase during the austral summer but it is during winter when ENSO influences moisture availability and the strength and position of the westerlies is modified by SAM that the most coherent impacts are observed. The PSA displays weaker seasonality but the same projection as SAM during winter (Hill et al. 2009)

Two modes have been observed which explain rainfall variability of Tasmania to different degrees. The dominant mode, explaining 70% of rainfall variability, is an island-wide mode and mostly attributed to the PSA and ENSO and a lesser extent to SAM. The second mode, explaining 14% of rainfall variability, is the out of phase mode which produces conditions of high rainfall fluctuations in the west (and low variability in the east) caused by the passage of anomalous westerly winds over the western mountains producing orographic rainfall in the west. This mode is likened to the negative SAM phase and positive PSA phase (Hill et al. 2009).

2.2.3 Climate-Fire-Vegetation links

2.2.3.1 SAM and fire

An association between positive SAM phases and increased fire activity has been demonstrated in southern South America (Holz and Veblen, 2011) and western Tasmania (Mariani and Fletcher, 2016) lying in the latitudinal band of the Southern Hemisphere where SAM has the strongest influence over rainfall and has been found to be the main driver of interannual fire activity (Mariani and Fletcher, 2016). In southern South America, the association is attributed to teleconnection of SAM with spring drought (Holz and Veblen, 2011). In Tasmania, Mariani and Fletcher (2016) found that there is a 1 year lag between positive (negative) SAM phases associated with anomalously dry (wet) years and increased (decreased) fire activity during the fire season (December-March) in the following year. They attribute this lag to the high moisture content of fuels characteristic of western Tasmania requiring considerable time to precondition in order to burn, which contrasts with the much drier conditions typical of the Patagonian forest-steppe ecotone in southern South America that produce fuels which are more rapidly conditioned to burn (Mariani and Fletcher, 2016).

2.2.3.2 ENSO and fire

A positive SOI during winter and spring of the year preceding a fire season together with a strong relationship between precipitation and ENSO across south-eastern Australia as put forward by Mariani et al. (2016), results in a reduction of water availability and a net result of conditions conducive to successful ignition during the following fire season. The authors further demonstrate that an El Niño state during the fire season results in an amplified number of fires and area burnt. A La Niña state during winter and spring of the year preceding the fire

season and during summer and autumn of the year of the actual fire season is correlated with low fire years.

2.3 Vegetation

2.3.1 Introduction

The vegetation of Tasmania is strongly influenced by the pronounced precipitation gradient across the island and is characterised by two distinct elements. The vegetation of eastern Tasmania, where mean annual rainfall lies between 400 and 1000 mm, is predominantly Australian in character. This Australian element shares many similarities with mainland Australia, in particular the families Myrtaceae, Proteaceae, Ericaceae and Asteraceae. The vegetation of the western Tasmania, where mean annual rainfall largely exceeds 2000 mm with mountains receiving over 3000 mm, contains a strong Gondwanan or Southern Ocean element, which shows closer affinities with the floras of New Zealand and southern South America than with mainland Australia. Families typical of this Gondwanan element include the Cunoniaceae (*Anodopetalum biglandulosum, Bauera rubioides*), Eucryphiaceae (*Eucryphia lucida, E.milliganii*), Escalloniaceae (*Anopterus glandulosus, Tetracarpaea tasmanica*), Fagaceae (*Nothofagus cunninghamii, N.gunnii*), Podocarpaceae (Lagarostrobus franklinii, *Phyllocladus aspleniifolius, Podocarpus lawrencii*) and Winteraceae (*Tasmannia lanceolata*) (McKendrick, 1981; Jackson, 1999a).

Furthermore, Tasmania's vegetation can be broadly divided into three formations: austral montane, temperate rainforest and sclerophyll forest. A long history of fire disturbance along with edaphic and soil factors produce a large number of disclimax communities, particularly in western Tasmania where source rocks weather slowly and are nutritionally poor (Jackson, 1999a). Western Tasmania is covered by vast expanses of sedge moorland and scrub interspersed with rainforest and wet sclerophyll vegetation. This contrasts with eastern Tasmania which is covered mostly by dry sclerophyll eucalypt forest and cleared land, with only small pockets of rainforest and wet sclerophyll vegetation present. The Central Highlands lie in an interesting ecotonal zone where you find both wet and dry sclerophyll forest growing together along with rainforest, moorland and scrub and, at higher altitudes, alpine and subalpine vegetation. The boundary between dry sclerophyll and wet sclerophyll forests is not sharp, instead the medium shrub layer gradually increases to heights of 15 m with increasing rainfall until wet sclerophyll forests are produced which are more common in western Tasmania (Jackson, 1999a).

2.3.2 Vegetation Types

2.3.2.1 Alpine and Subalpine Vegetation

The location of the treeline is principally determined by mean summer maximum temperature but other geographic variables and local factors (such as aspect, frost pockets, soils and fire) can modify the effect of the thermal gradient (Crowden, 1999). Nunez & Colhoun (1986) determined the thermal gradient to be 0.65 °C per 100 m vertical rise in altitude. A feature of Tasmanian treelines is that there is no sharp transition from forest to shrubland due to a subtle environmental gradient. The treeline typically consists of the subalpine eucalypt species *Eucalyptus coccifera* and *E. vernicosa* or *Nothofagus cunninghamiil,* which gradually reduce in height and continue above the treeline as part of the alpine shrubbery (Crowden, 1999).

Where fire frequency is low, other rainforest elements also continue into the alpine zone and *Nothofagus cunninghamii* and *Nothofagus gunnii* can form thickets up to an altitude of 1400 m. In areas which are drier and more frequently disturbed by fire, ericaceous and proteaceous shrubs typically dominate and continue to grow from the montane vegetation below the treeline into the alpine zone as alpine shrub/heathland with a minimal herbaceous component. The grassland-herbland element typical of the Australian or New Zealand Alps is limited due to the reduced snow typical of Tasmania's maritime climate.

All Tasmanian vegetation above the treeline would be classified as subalpine according to altitudinal vegetation banding applied elsewhere in the world due to its woody, heath-like nature and the lack of dominance of herbaceous plants. Only ten of the > 300 species found in the treeless subalpine and alpine zones are restricted to above the climatic treeline (Kirkpatrick, 1986) and Kirkpatrick (1983) applies the term alpine to incorporate both vegetation types due to the lack of sharp treelines. Another feature of the Tasmanian alpine zone is the survival of the conifer element including *Athrotaxis* forests and *Diselma* and *Microstrobos* shrubberies which can grow up to 1400 m. These communities are very sensitive to fire. The alpine zone is otherwise typically a mosaic of different vegetation types with wet communities of bog, sedgeland and bolster moor being accentuated by fire (Crowden 1999; Jackson 1999a).

2.3.2.2 Rainforest

The rainforest in Tasmania is classified as cool temperate rainforest which, by the definition of Jarman and Brown (1983), are forests which can regenerate in the absence of large scale disturbances such as fire and are dominated by species of *Nothofagus*, *Atherosperma*, *Eucryphia*, *Athrotaxis*, *Lagarostrobos*, *Phyllocladus* or *Diselma* (Jarman et al. 1999). Rainforests are broadly limited to sites receiving at least c. 800 mm of annual rainfall with a minimum of c. 25 mm per month falling during the months of January, February and March (Jackson, 1983).

Where annual rainfall is high (>2000 mm) and uniformly distributed with at least 50 mm falling per month during summer months, Jackson (1968) put forward that neither soil, aspect nor edaphic situation should limit rainforest, yet currently a high proportion of area climatically suitable for rainforest growth (~ 47%) is occupied by sclerophyllous vegetation. Although the wider distribution of rainforest is clearly limited by rainfall, current rainforest boundaries are rarely controlled by water stress, rather the history of fire activity is the key factor explaining these boundaries (Read, 1999). Topography, through its link to fire activity, has been found to be most important in determining the location of rainforests which, on the nutrient poor substrates of southwest Tasmania, have been shown to be most commonly found in valleys and steep south-facing slopes. Fire activity in the same region is most likely to be focussed on ridges, flats and steep north-facing slopes supporting the hypothesis that fire sensitive rainforest tends to be located in topographic fire refugia (Wood et al 2011b). Several models have been put forward to explain the juxtaposition of fire sensitive and fire promoting vegetation observed in the Tasmanian landscape and will be discussed in a later section.

Two distinct rainforest alliances characterise Tasmania's rainforests (Jarman and Kantvillas, 1994). The Myrtle-beech alliance is dominated by *Nothofagus, Atherosperma, Eucryphia, Phyllocladus, Athrotaxis, Lagarostrobos* or *Diselma* and grows from sea level to approximately 1000 m, comprising the bulk of Tasmanian rainforest. The alliance consists of three types of rainforest which form an intergrading series from callidendrous, thamnic to implicate rainforest (Jarman et al 1999).

Callidendrous rainforest is found mostly in eastern, northwestern and central Tasmania on good quality sites with fertile soils developed on basalt, dolerite and nutrient-rich granites. They are typically dominated by *N. cunninghamii* and/or *Atherosperma* moschatum with *Leptospermum lanigerum* and *Acacia melanoxylon* often being important components and *Telopea truncata* and *Tasmannia lanceolata* common as undershrubs at higher altitudes although the understorey is typically open and park-like. Callidendrous forests are usually medium to tall forests with the height of the forest decreaseing with altitude (*N. cunnighamii* can be found growing as krumholz) (Jarman et al., 1999).

Thamnic rainforest occurs mostly in western and southwestern Tasmania and consists of medium height forests with a distinct shrub layer. The canopy may contain 2-5 species including *N. cunnighamii*, *N.gunnii*, *E. lucida*, *E. milliganii*, *A. moschatum*, *Phyllocladus*, *Lagarostrobos* and *A. selaginoides.* The following species may be common in the understorey: *Anodopetalum biglandulosum*, *Richea pandanifolia*, *Acradenia frankliniae*, *Anopertus glandulosus*, *Archeria ericarpa*/*A. hirtella*, *Trochocarpa gunnii*/*T. cunnighamii* and *Cenarrhenes*

nitida (Jarman et al., 1999). Thamnic rainforests tend to occur on site types intermediate between callidendrous and implicate types.

Like the thamnic rainforests, implicate rainforest also occurs mostly in western and southwestern Tasmania. Implicate rainforests are characterised by low, uneven, broken canopies with a tangled understorey which extending from ground level right through to the canopy. The canopy may be dominated by several species including typical rainforest species such as *N. cunnighamii*, *N.gunnii*, *E. lucida*, *E. milliganii*, *Phyllocladus*, *Lagarostrobos*, *A. selaginoides* and *Diselma archeri*, but also specis of *Leptospermum*, *Melaleuca* and *Acacia.* The following species may be common in the understorey: *Anodopetalum biglandulosum*, *Anopertus glandulosus, Cenarrhenes nitida*, *Agastachys* odorata, *Telopea* truncate, *Coprosma nitida*, *Olearia persoonioides*, *Archeria*, *Trochocarpa*, *Richea*, *Dracophyllum* and *Prionotes* (Jarman et al., 1999). They tend to grow on mineral soils developed on nutrient poor rock types (e.g. quartzites and siliceous conglomerates) or poorly drained ground.

The second, much smaller group of rainforest in Tasmania is the pencil pine alliance. This consists of open montane forest found mostly at altitudes > 800 m on the Central Plateau (small populations also occur on southern mountains) and is dominated by *Athrotaxis cuppressoides* (less commonly *A. selaginoides*). Fern diversity is typically low, woody species diversity high and there is a high level of species endemnism. The understorey is usually dominated by low shrubs, but sometimes also includes grasses and mosses. Common shrubs in the Pencil pine alliance include *N. cunninghamii* (growing as a shrub), *N. gunnii, Diselma archeri, Microstrobos niphophilus, Podocarpus lawrencei, Orites acicularis, O. revoluta, Leptospermum rupestre, Richea pandanifolia, R. scoparia, R. sprengelioides, Epacris serpyllifolia, Tasmannia lanceolata* and *Baeckea gunniana* (Jarman et al., 1999).

2.3.2.3 Wet sclerophyll

The term wet sclerophyll forest was defined by Beadle and Costin (1952) to describe tall, eucalypt dominated forests with an understorey of broad-leaved shrubs. Gilbert (1959) coined the term “Mixed Forest” for tall, open forests with a rainforest, rather than broad-leaved shrub understorey. In Tasmania, the term wet eucalypt forest was introduced by Kirkpatrick et al. (1988) which includes both wet sclerophyll and mixed forest (Wells and Hickey, 1999).

Wet sclerophyll forests occur in areas where more frequent fire disturbance restricts the growth of rainforest species and the forest instead consists of eucalypts with a tall understorey of typically *Acacia* and other mesophyll trees and shrubs (e.g. *Olearia, Bedfordia, Pomaderris and Phebalium).* Rainforest is usually the climax vegetation type in wet sclerophyll areas. If fire disturbance is decreased, a closed rainforest understorey may form under the eucalypts

preventing the regeneration of eucalypts due to lack of light (Jackson, 1999a). Climatic requirements for wet sclerophyll forest include mean annual rainfalls of over 1000 mm with at least 25 mm falling in the driest month, low temperatures not limiting to tree growth and shelter from dessicating fire-promoting winds (Wells and Hickey 1999 and references therein).

2.3.2.4 Dry Sclerophyll

Dry sclerophyll forests lack the tall shrub layer of the wet sclerophyll forests and instead typically contain a layer of low scattered trees such as *Banksia* and *Allocasuarina, Banksia, Exaocarpus and Bursaria* and a medium to low shrub layer including species of Asteraceae, Epacridaceae, Fabaceae and Myrtaceae. The boundary between dry sclerophyll and wet sclerophyll forests is not sharp, instead the medium shrub layer gradually increases to heights of 15 m with increasing rainfall until the typical wet sclerophyll forests develop (Jackson 1999a and references therein).

Most dry sclerophyll forests and woodlands in Tasmania are dominated by eucalypts which are adapted to survive (and possibly even promote) fire and are characterised by a multi-layered understorey of xeromorphic shrubs with a variable non-woody ground layer typically including grasses, sedges and bracken. In fire shadow sites, the relatively fire sensitive taxa *Callitris* and *Allocasuarina verticillata* can dominate (Duncan 1999).

2.3.2.5 Buttongrass Moorland

Moorland, sedgeland and scrub predominate in areas of Tasmania up to 900 m which are prone to continued firing where forest trees have been selectively removed and pyrogenic heaths and sedgelands thrive in conditions of low soil fertility and/or poor aeration of surface soils. These communities are usually dominated by *Gymnoschoenus sphaerocephalus* along with a diverse array of ericacous shrubs and other (Cyperaceae and Restionaceae), however, *Lepidosperma filiforme* may dominate on more skeletal soils. The greatest development of this vegetation type is in western Tasmania where it occupies 47% of the area regarded suitable for rainforest (Jackson, 1999a). Jarman et al. (1988) classified moorlands into two types: 1. Blanket moor which is extensive in western and southwestern Tasmania on pre-Carboniferous substrates, growing mostly on shallow peat in areas up to 1000 m altitude; 2. Eastern moor which predominates in eastern and northwestern Tasmania on seasonally waterlogged soils, especially on poorly drained dolerite substrate of Central Plateau (Brown, 1999).

2.3.3 Vegetation Models

On a broad scale, the distribution of vegetation types across Tasmania is controlled by climate and altitude (temperature) with strong contrasts between the wetter western Tasmania and

drier eastern portion of the island. However, at the smaller sub-regional scales, a juxtaposition of different vegetation types growing as mosaics is observed. The southwest of Tasmania is a prime example where fire sensitive rainforest is found growing in pockets amongst flammable moorland and other schlerophyllous vegetation types in an environment with a climate optimal for rainforest growth (Wood et al. 2011b). As mentioned earlier, in these high rainfall areas rainforest is not limited by moisture. This has led to several models being put forward to explain this phenomenon and it is arguably one of the most discussed features of the vegetation of Tasmania.

2.3.3.1 The 'ecologic drift' hypothesis of Jackson (1968)

The 'ecological drift' hypothesis of Jackson (1968) is one of the earliest examples of an alternative stable states model mediated by fire put forward to explain the mosaic of juxtaposing fire sensitive and fire promoting vegetation types observed in southwest Tasmania (Wood and Bowman 2012b). Jackson (1968) suggested that positive feedbacks between vegetation, fire frequency and soil fertility results in each vegetation community being resilient to change and in the process hindering or constraining other vegetation types from establishing (Wood et al. 2011a; Wood and Bowman 2012). He outlines the fire frequencies characteristic of each vegetation type. Chance disturbances causing a change in fire interval, although assumed to be improbable, may result in a shift to another vegetation community, the vegetation as result drifting between the two end states of highly flammable moorland and non-flammable rainforest, via intermediary stages of sclerophyll scrub and forest depending upon fire frequency (Jackson 1968; Wood et al. 2011b; Macphail 2010). In the scenario of a stable state transition from rainforest towards moorland, a vegetation community will initially resist the disturbance caused by fire and return to the original rainforest stable state, however if repeated stand replacing fires occur, the vegetation community will be pushed beyond its threshold and transition to its neighbouring stable state as a result of positive feedbacks from the latter (Wood and Bowman 2012).

2.3.3.2 The 'stable fire cyle' model of Mount (1979)

The 'stable fire cycle' model of Mount (1979) proposes that the underlying physical environmental characteristics of a site (such as geology, topography and drainage) initially determine the vegetation type which are then merely reinforced by fire. In this model, the vegetation determines the risk of fire. In contrast with the model of Jackson (1968) which permits the possibility of shifts between alternative stable states, Mount (1979) suggests that the resilience caused by vegetation-fire feedbacks is strong enough to eliminate any vegetation state transitions resulting in geographically stable vegetation patterns (Wood et al. 2011a; Wood and Bowman 2012a).

2.3.3.3 The edaphic model of Pemberton (1989)

The edaphic model of (Pemberton, 1989) puts forward an alternative model which suggests that edaphic factors are most important in affecting vegetation type rather than fire. Moorland is viewed as a natural edaphic disclimax developed on nutrient poor acidic soils which are frequently waterlogged (Thomas et al 2010).

2.3.3.4 The 'climate reinforcement' model of Macphail (1980)

The 'climate reinforcement model' of Macphail (1980) proposes that the postglacial succession of vegetation observed in pollen records from southern Tasmania (Macphail 1976, 1979, 1980, 1986) can be primarily explained by climate, although interactions between climate and both soil fertility and fire frequency as put forward by Jackson (1968) may have resulted in this climatic control to be indirect. The model emphasises that climate has modified the impact of fires during the postglacial period. During the Early Holocene, the warm and wet climate permitted cool temperate rainforest to expand at higher elevations despite concurrent fire pressure. During the middle and late Holocene, an increasingly variable and cooler climate favoured the expansion of sclerophyll vegetation culminating in a late Holocene revertance to more open vegetation types (Macphail 2010).

2.3.3.5 The 'Iversen glacial-interglacial cycle' model of Colhoun (1996)

The 'Iversen glacial-interglacial cycle' model of Colhoun (1996) applies the four stages (Cryocratic, Protocratic, Mesocratic and Telocratic) of postglacial vegetation change proposed by Iversen (1958) to those observed in pollen records from western Tasmania (Macphail, 1976, 1979, 1986; Macphail and Colhoun, 1985; Colhoun; 1985; Colhoun and van de Geer, 1986, 1987; Colhoun et al., 1991, 1992; van de Geer et al. 1989). The model recognises that the major change in vegetation across the last glacial interglacial boundary was driven by climate, however, based on the non-synchronous timing of the successional vegetation changes, put forward that biological and physical environmental factors other than climate were more important in explaining the vegetation change which followed. In contrast with the climate-forced Late Holocene revertance proposed by Macphail (1980), the author suggests that the vegetation changes should be viewed as local and caused by either Aboriginal burning or sedimentary processes resulting in the infilling of small lakes rather than climate (Colhoun, 1996).

2.3.3.6 The 'Last Glacial inheritance' hypothesis of Fletcher and Thomas (2007a)

The 'Last Glacial Inheritance' hypothesis of Fletcher and Thomas (2007) argues against widespread expansion and dominance of rainforest in the southwest of Tasmania during the mid Holocene. Fletcher and Thomas (2007) argue that moorland surrounding Lake Pedder has been present throughout the Holocene and that all other records from lowland moorland sites

(Colhoun et al. 1991, 1992, 1998; Colhoun 1992, 1996; Thomas, 1995; Macphail et al. 1999) likewise support the persistent domination of the landscape by moorlands since at least the Late Glacial. They suggest that the moorlands are an artefact of anthropogenic burning and that fire activity explains the persistence of moorlands in a climatic environment ideal for the development of rainforest (Fletcher and Thomas, 2007a).

Although historical ecology studies undertaken at decadal to millennial time scales suggest that vegetation patterns in the lowlands of southwest Tasmania have been predominantly stable, which supports the idea of vegetation community resilience common to both models, field studies demonstrating vegetation transitions at forest boundaries (e.g. Brown and Podger 1982, Podger et al. 1988, Brown et al. 2002) are more in support of the Jacksons (1968) 'ecological drift' model although the timing of transitions are much slower (Wood and Bowman 2012a).

2.3.3.7 Evidence from Northern Tasmania

The above models have all focused on the vegetation dynamics observed on the nutrient poor soils of southwestern Tasmania. A recent study of non-forest/forest boundaries, on the more fertile substrates and under the drier climate of northern Tasmania, shows that forest has been encroaching on grasslands since the 1950s at a much more rapid rate than the negligible encroachment observed during the same time period in the southwest (Bowman et al. 2013; Wood and Bowman 2012). This lends support to the Jackson (1968) model. In contrast with the nutrient poor soils of southwestern Tasmania, northern Tasmanian substrates were found to have higher soil nutrients, in particular phosphorous, which facilitate more rapid forest growth. However, despite the overall higher fertility, the contrast in phosphorous observed at moorland/rainforest boundaries by Wood and Bowman (2012b) in the southwest is not observed in the north. Bowman et al (2013) therefore suggest that edaphic controls can not explain the actual expansion of forest (although higher fertility increases the rate of expansion), but rather they suggest it is the reduction of burning as a result of the removal of Tasmanian Aborigines that likely is the key driver of forest expansion in these areas of northern Tasmania.

A palaeoecological record from the Gog Range in northern Tasmania demonstrates an unequivocal transition from forest to non-forest following a catastrophic fire event 7000 years ago. The authors suggest that the non-forest state was most likely maintained via eco-hydrological and eco-physical feedbacks despite observable fire activity following the event. This example lends clear support for the Jackson (1968) model as an example of a shift between two alternative stable states at longer time scales (Fletcher et al., 2013b).

Figure 2-2 A) Cushion plants growing on Mt Ossa B) Buttongrass moorlands and dry eucalypt forest south of Lake St Clair C) Steep rainforest slopes on Mt Olympus D) Dry eucalypt forest on the steep eastern slopes of Lake St Clair leading onto the Central Plateau E) *Nothofagus gunni* growing amongst dolerite scree on the southern slopes of Mt Olympus overlooking the Cuvier Valley F) *Athrotaxis cuppressoides-Nothofagus gunnii* short rainforest, alpine heathland and sedgeland growing on the Central Plateau G) Subalpine eucalypt forest on overlooking the Mt Gould Plateau and Lake St Clair in the distance H) Mosaic of alpine sedgeland and coniferous heath with *Astelia alpine*, *Gleichenia alpine* and *Richea pandaniifolia* in the foreground.

Chapter 3 Methods

The primary method used to address the aims of this thesis is the reconstruction of the vegetation history of the area by means of pollen analysis. This is supported by the construction of a fire history record by means of microscopic and macroscopic charcoal analysis. These records are complemented by robust chronology based on radiocarbon dating, other sediment analyses and relevant statistical analyses of the dataset. Modern pollen analysis forms the foundation for the interpretation of the fossil pollen analyses.

3.1 Site Selection and Previous Research

3.1.1 Site Selection

In order to address the primary aim of this thesis, a suitably large lake was required that would provide a regional record spanning the last glacial- interglacial transition with potential to analyse this period at high resolution. The Central Highlands of Tasmania were targeted for this purpose as they lie in an interesting transition zone mid-way along the west-east environmental gradients across Tasmania in an area where few pollen records have been produced.

Lake St Clair (146º10'E 42º06'S), which infills a large deep glacial hollow, was selected as the primary study site because previous studies at the site (Hopf 1997; Hopf et al. 2000) showed that the lake contains late Glacial and Holocene sediments which would be suitable for high resolution pollen and charcoal analysis.

3.1.2 Previous research in the area

In February 1996, three sediment cores (cores CA-CC) were extracted from the southern end of Lake St Clair by a team from Geoscience Australia and the University of Newcastle using a modified 6 m length Mackereth corer (Mackereth, 1958). Core CB, the longest core at 396 cm, was selected for palaeomagnetic and pollen analysis and the results for this Late Glacial – Holocene record reported by Hopf (1997) and Hopf et al (2000). A set of modern pollen samples from the five major vegetation types in the study area were also analysed to study the pollen-vegetation relationship (Hopf, 1997).

3.2 Fieldwork

3.2.1 Coring

In February 1998, the team from Geoscience Australia and the University of Newcastle returned to Lake St Clair and a further ten cores (cores CD-CN) were collected along the length of the lake. As the top 20-60 cm of sediment is often lost when using a Mackereth corer (C.

Barton pers. comm., 1998), short cores were collected from all Mackereth core locations using a Glew type gravity corer (Glew et al. 2001).

3.2.2 Vegetation survey and modern pollen analysis

A sound understanding of the relationship between the contemporary vegetation and modern pollen rain forms the foundation for the interpretation of fossil pollen records. The modern pollen rain can be captured by a variety of means including man made pollen traps (e.g. Tauber and Cundill), natural pollen traps such as moss polsters as well as the surface sediments of lakes which all function as natural traps of the modern pollen rain (Faegri and Iversen, 2000).

In a study comparing the modern pollen and spore assemblages found in three sample types: moss cushions, surface soils and surface lake sediments, Wilmshurst and McGlone (2005) concluded that moss cushions most accurately represented the surrounding vegetation. They found that surface soils are typically corroded and biased towards the most resistant pollen and spore types. Lake sediments were found to contain a mixture of pollen and spore types present in both the moss and soil samples, the influence of reworked grains from catchment soils being pronounced (Wilmshurst and McGlone 2005).

For the purpose of this study, primarily moss polsters and lake surface sediments were selected. Moss polsters were most widely available within the study area, however, lake mud-water interface samples were targeted wherever available. In most cases these consisted of small, shallow tarns which could be sampled by hand trowel. Deeper tarns and lakes were sampled using a Glew type gravity corer (Glew et al. 2001) where the top cm from the resulting short core was used for modern pollen analysis. Moss samples were collected by combining numerous "pinches" of moss within a 10 m^2 area of a particular vegetation type. The vegetation within the same area was recorded in the form of a plant list and relative abundance of each plant noted as: dominant, common or rare.

3.3 Laboratory Work

3.3.1 Core selection

The sediment cores were transported to and stored in the cool rooms at Geoscience Australia in Canberra. From previous work on core CB from the southern end of Lake St Clair, it was observed that the basal glacial sediments have high magnetic susceptibility which contrasts strongly with the very low magnetic susceptibility of the overlying more organic lake sediments (Hopf et al, 2000). Based on this information, whole core magnetic susceptibility measurements were run by Dr Charles Barton on all ten cores (Figures 4-5) collected using a Bartington Susceptibility Bridge and the most promising core, in terms of likelihood of full

recovery of a late Glacial/Holocene sequence, selected without having to cut the cores to assess the stratigraphy.

As the focus for this study would be the northern end of Lake St Clair, Core CG was selected because:

1. the core was of good length (548 cm),

2. appeared to include both glacial and lake sediments (unlike e.g. cores CE, CN and CK which most likely only include Holocene lake sediments or CI, CJ and CM which only appear to have captured glacial sediments) and, in contrast to core CB,

3. appeared likely to cover a more transitional phase between the high magnetic susceptibility glacial sediments and low magnetic susceptibility lake sediments (between 260cm and 450 cm) suggesting that there would be potential for higher resolution analysis of this transitional time period.

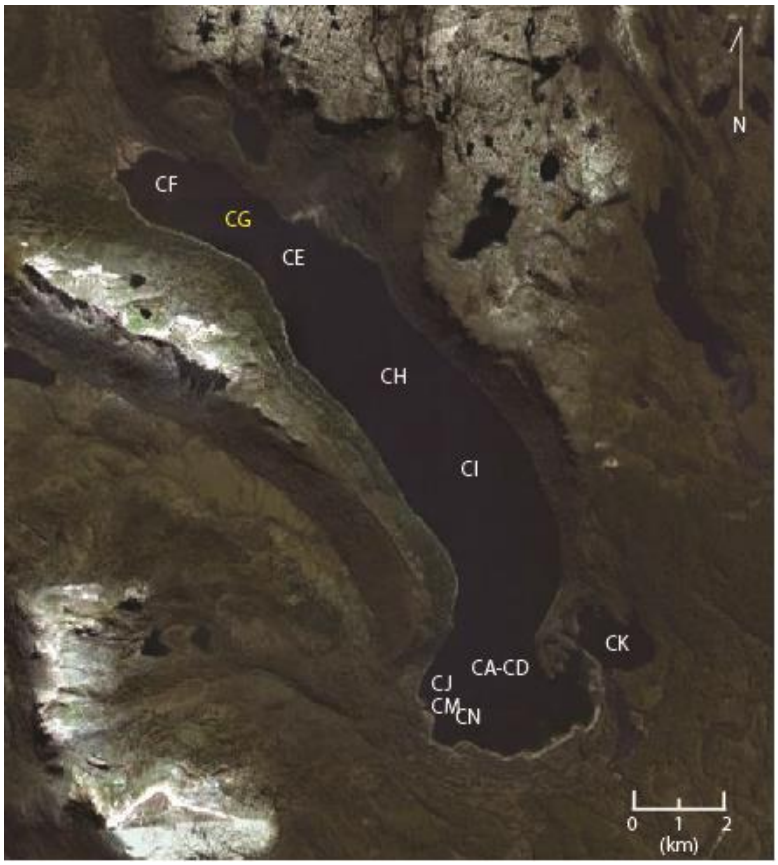

Figure 3-1 Mackereth core locations in Lake St Clair

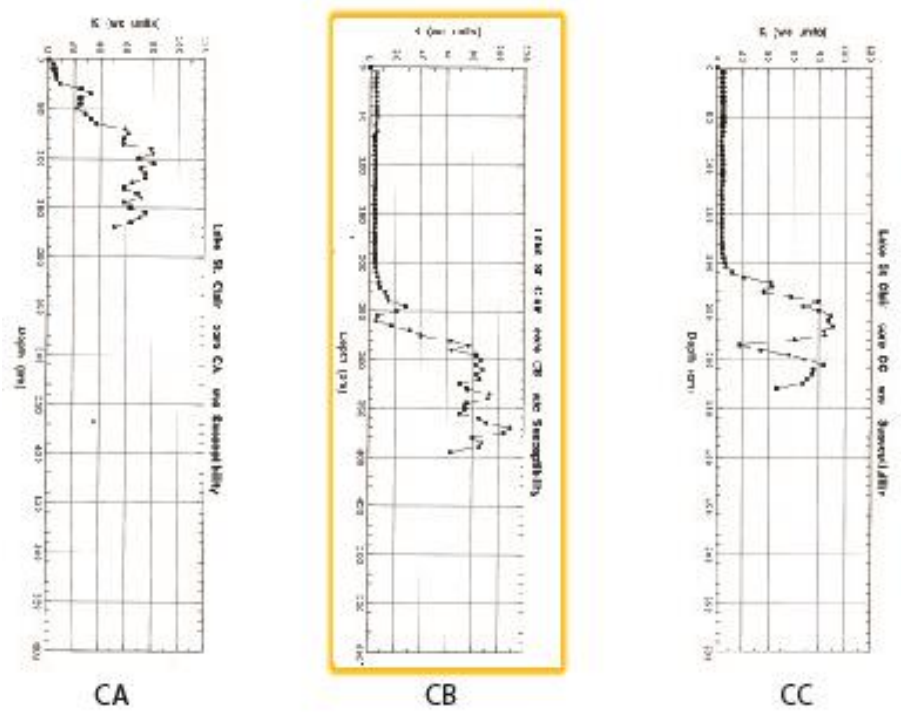

Figure 3-2 Magnetic susceptibility plots for cores CA-CC.

3.3.2 Description of the core

3.3.2.1 Stratigraphy and sub-sampling

Core CG was split, photographed and the stratigraphy described at Geoscience Australia. The core was sliced at 1 cm intervals, outer edges of sediment in contact with the core tube were discarded and the remaining sample bagged and returned to the ANH laboratories, ANU where they were stored for further analysis.

3.3.2.2 Particle Size Analysis

Particle size analysis of the Core CG sediments was carried out by laser diffraction using a Malvern Mastersizer 2000 with Hydro MU attachment housed at the Fenner School of Environment & Society, ANU. The samples were first treated with 10% HCl to remove carbonates and 30% H_2O_2 to remove organic matter. Calgon was added to disperse any aggregates in the sediment and 30 seconds of additional ultrasonic dispersal was applied just prior to measurement. Five repeat measurements were taken for each sample, the average results of which were then assigned to groups of the various size fractions of sand, silt and clay.

3.3.2.3 Loss on Ignition and Carbon/Nitrogen Analysis

Loss on ignition is a method that can be used to estimate the amount of organic matter in sediments. The procedure outlined by Dean (1974) was followed using dried 2.5 cc subsamples which were weighed before and after controlled heating to a temperature of

550°C to calculate the % of sample lost in the form of carbon dioxide which can be directly correlated with organic matter content.

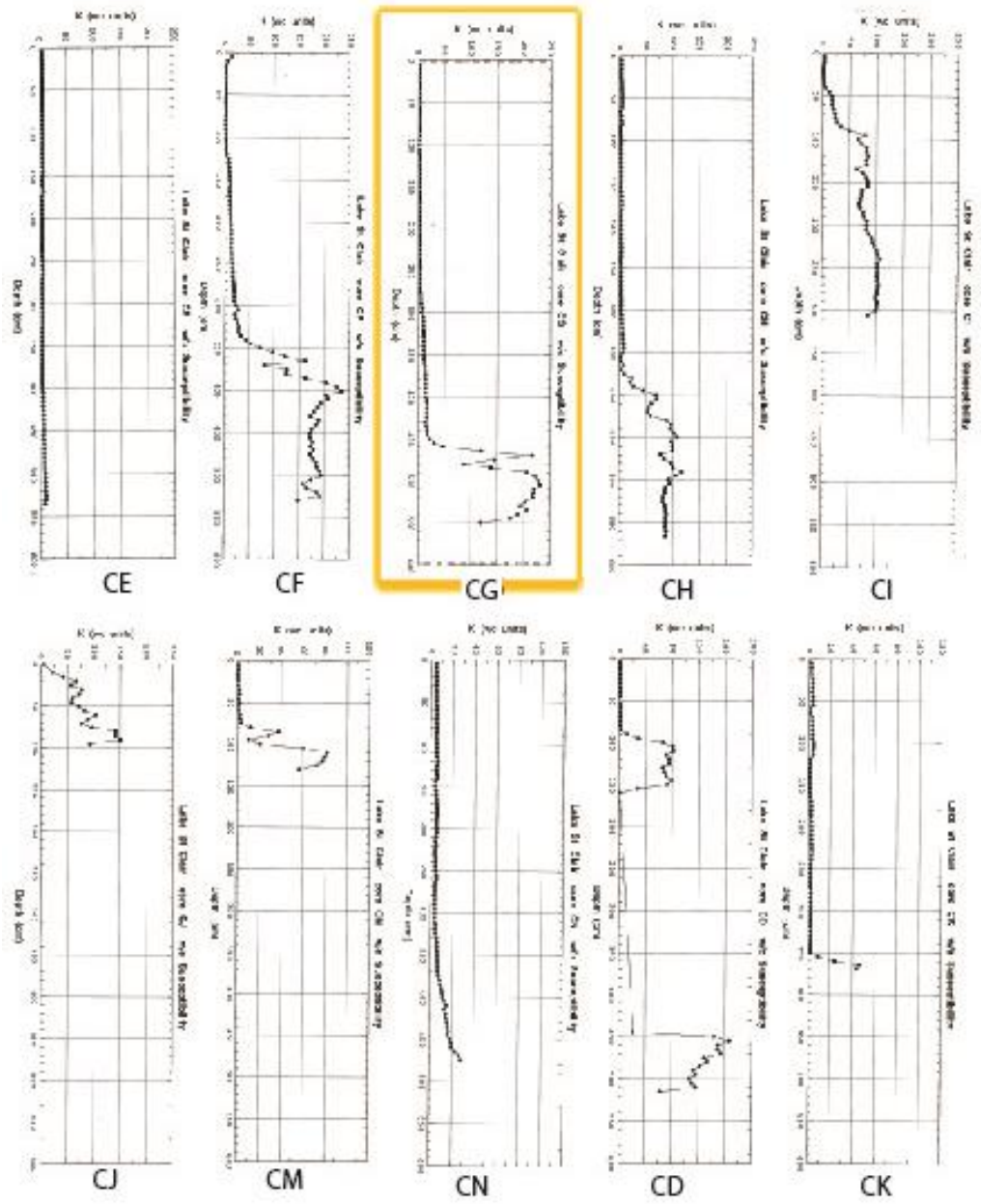

Figure 3-3 Magnetic susceptibility plots for cores CE-CN.

Total Carbon is another way in which the organic component in a sediment can be measured. An Elementar VarioMAX CNS elemental analyser was used at the Fenner School of Environment & Society, ANU to measure total carbon and nitrogen using small sub-samples of approximately 0.5 cc. more detail. Whereas total organic matter and total carbon can give a general indication of the productivity of a system, the ratio of carbon to nitrogen in a sample can further inform about the likely source of the sediment in the lake. Low ratios around 4-10 are indicative of sediment that was produced within the lake system itself whereas high ratios

of > 20 point towards sediment being transported from the surrounding catchment into the lake system (Meyers, 1994).

3.3.3 Radiocarbon Dating

Bulk sediment samples were taken from all cores and submitted for accelerator mass spectrometry (AMS) radiocarbon dating at the Australian Nuclear Science and Technology Organisation (ANSTO) and the Australian National University (ANU) Radiocarbon Dating Laboratory. No suitable terrestrial macrofossil remains were isolated for dating purposes. Initial samples received the standard alkali-acid pretreatment; those submitted to the ANU Radiocarbon Dating Laboratory from 2012 were first split into the humin and humic acid fractions and each fraction dated separately. Individual radiocarbon ages were calibrated using Clam v.2 (Blaauw, 2010) using the Southern Hemisphere calibration dataset SHCal13 (Hogg et al., 2013). A chronology was produced using Bacon v.2.2 (Blaauw and Christen, 2011) by age depth modelling based on Bayesian statistics.

3.3.4 Pollen Analysis

3.3.4.1 Pollen and Microscopic Charcoal Preparation

Pollen processing followed standard HCL, HF, KOH and acetolysis methods (Faegri & Iversen, 1989) using 1cc subsamples and included addition of *Lycopodium* marker grains to calculate concentrations of pollen, spores and microscopic charcoal (Stockmarr, 1971). Samples were processed at 2 cm intervals between 180-440 cm to cover the LGIT in detail and at 4 cm intervals for the remainder of the core. Pollen residues were mounted on slides in a medium of glycerol and sealed with nail polish.

3.3.4.2 Pollen and Microscopic Charcoal Counting

Pollen, spores and microscopic charcoal (> 10µm) were counted at 400 x magnification using a Zeiss Axiophot microscope and identifications made using the reference collection held at the Department of Archaeology & Natural History, Australian National University (ANU) and the Australian Pollen and Spore Atlas (APSA Members, 2007). At least 300 terrestrial pollen grains were counted in each sample wherever possible.

3.3.5 Macroscopic Charcoal Analysis

Contiguous, 1.25 cc sub-samples were taken from Core CG and processed for macroscopic charcoal analysis according to a modified technique developed by Stevenson and Haberle (2005) based on the method by Rhodes (1998). The samples were dispersed in calgon, bleached and then washed through 125 micron and 250 micron sieves to obtain the macroscopic charcoal fractions that are greater than 125 microns in size (macroscopic

charcoal). The total number of macroscopic charcoal pieces in each fraction were counted for each sample using a dissecting microscope.

3.4 Data Analysis

3.4.1 Pollen Analysis

3.4.1.1 Pollen diagram and zonation

Pollen diagrams were produced using Tilia v. 2.0.33 (Grimm, 2013) and amended with Adobe Illustrator CS2. Pollen and spores are presented as percentages of the total terrestrial pollen sum. Stratigraphically constrained cluster analysis (CONISS, Grimm 1987) was performed on the total terrestrial pollen dataset to identify pollen zones. Pollen and microscopic charcoal accumulation rates were calculated using the Bacon age depth model output of calibrated ages.

3.4.1.2 Ordination

Ordination is a statistical approach used to graphically summarise complex relationships in a dataset and through this process find and describe patterns. Gradient analysis is one application where ordination is used to identify patterns in species composition which changes according to underlying factors that vary constantly along environmental or historical gradients. The purpose of ordination is to identify the most important factors and patterns in the dataset from those that are less important. Principle component analysis, correspondence analysis and detrended correspondence analysis (DCA) are the most popular ordination techniques used in ecology (McCune and Grace, 2002).

PC-ORD (McCune and Metford, 1999) was used to undertake detrended correspondence analysis (DCA) (Hill and Gauch, 1980) based on the total terrestrial pollen subsets of both fossil and modern datasets and presented as DCA biplots to identify patterns. The data was square root transformed prior to analysis.

3.4.2 Macroscopic Charcoal Analysis

CharAnalysis (Higuera et al., 2009) was used to analyse the macroscopic charcoal counts in order to reconstruct the local fire history and identify significant charcoal peaks. The process involved the calculation of charcoal accumulation rates (CHAR; particles/cm/yr) using calibrated age output from the Bacon age model. A 500 yr lowess smoother which is robust to outliers was used to decompose BCHAR into noise and peaks. Kelly et al. (2011) suggest using a SNI cutoff of 3.0 to identify peaks representing significant fire episodes. As a result, only peaks with an SNI of 3.0 or greater were selected from the CharAnalysis output and plotted using the peak magnitude values which are interpreted to reflect fire size and/or intensity (Higuera et al. 2009; Higuera et al. 2010).

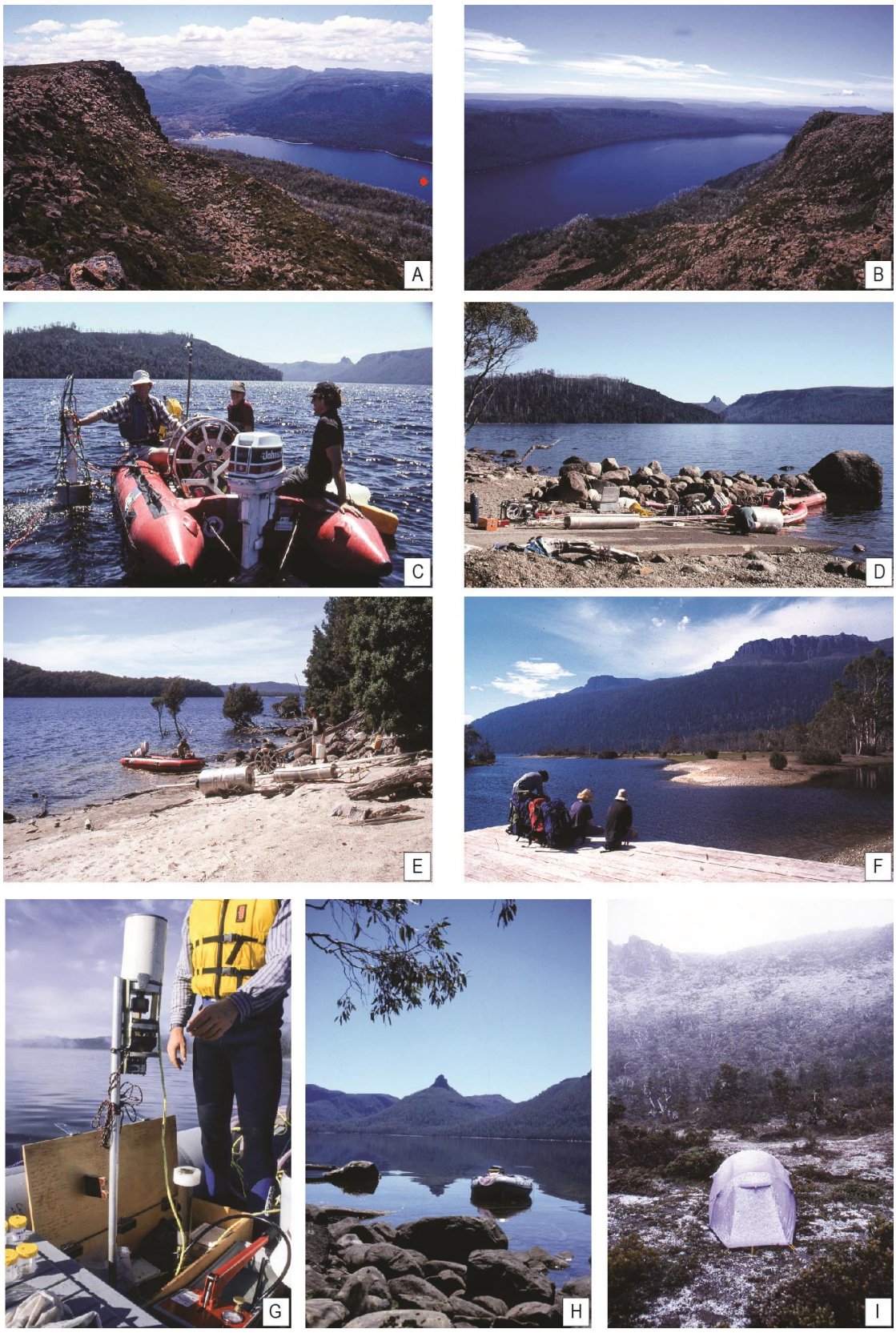

Plate 3-1 A) The northern end of Lake St Clair viewed from Mt Olympus; core CG location marked as red circle B) The Central basin of Lake St Clair viewed from Mt Olympus looking south C) Dr Charles Barton ready to send the Mackereth corer to the depths of Lake St Clair D) The Mackereth corer laid out at Cynthia Bay E) Beach on western edge of Lake St Clair F) Narcissus Bay with Mt Olympus in background G) Gravity corer used to collect short cores from Lake St Clair D) Looking towards the core CG site and Mt Ida I) Mid-summer snow storm

Chapter 4 Modern Pollen Deposition in Large Lakes

4.1 Introduction

Large lakes provide unique environments for pollen deposition which contrast with other types of palaeoenvironmental sites through their large aerial pollen source areas and in many cases the additional influence of significant fluvial pollen source areas. This chapter reviews the nature of aerial and fluvial pollen source areas in relation to large lakes which is then applied to analysis of a dataset of modern pollen samples from the Lake St Clair catchment with the goal of gaining a better understanding of how to interpret pollen records of this nature.

4.1.1 Modern pollen analysis

A thorough understanding of the relationships between pollen production, transport and deposition and the nature and area of its source vegetation lays the foundation for the interpretation of fossil pollen records. Although the use of modern pollen-vegetation relationships as an analogue for the past is a valuable basis for interpretion of the palaeovegetation (Overpeck et al., 1985; Jackson and Williams, 2004), it needs to be take into careful consideration that these relationships may have varied in the past under different climates and different environmental conditions. During glacial times, in particular, currently forested sites may have instead been surrounded by treeless vegetation with a significantly larger pollen source area resulting in the deposition of a higher proportion of long distance transported pollen (Felde et al., 2014). In addition, changing climates and other environmental factors may have produced new niches resulting in the establishment of non-analogue vegetation types (Huntley, 1990; Overpeck et al., 1992; Jackson and Williams, 2004; Williams et al., 2004; Veloz et al., 2012), an example being the *Phyllocladus-Eucalyptus* association recorded in many Tasmanian pollen records during the Last Glacial Interglacial Transition (Macphail, 1979; Colhoun, 1996a). Vegetation communities and climates without no modern analogues were also common across North America during the late Glacial when CO_2 levels were reduced, seasonality of insolation increased and ice extent increased (Jackson and Williams, 2004; Veloz et al., 2012). It has been established that plant taxa respond to environmental change as individuals rather than as communities as a whole with the effect that certain unique assemblages only occurred for relatively short periods of time as environmental conditions changed (Bennett, 1990; Birks, 1993). Nonetheless, modern pollen studies remain a valuable first step in the interpretation of palaeovegetation from fossil pollen records when combined with a sound understanding of plant ecology.

4.1.2 Modern pollen analysis in Tasmania

Macphail (1975, 1976, 1979) undertook the first modern pollen studies in Tasmania through analysis of a comprehensive, island-wide dataset comprising pollen trap and surface sample data from key Tasmanian vegetation types. The findings showed that the Tasmanian regional pollen rain, a group of reoccurring pollen and spore types which were present in samples regardless of whether the source plant was present in the local vegetation, included the following taxa: Poaceae, *Phyllocladus*, Chenopodiaceae, *Allocasuarina*, *Pomaderris apetala*-type, *Dicksonia*, *Nothofagus cunninghamii*, *Eucalyptus* and Asteraceae with *Athrotaxis* and *Pherosphaera* also being widely dispersed (Macphail, 1979). Macphail (1979) noted that important insect-pollinated species including *Atherosperma*, *Eucryphia-Anodopetalum*, Proteaceae, Ericaceae, Myrtaceae (except *Eucalyptus*) and Fabaceae but also some wind pollinated species including *Microcachyrs*, *Podocarpus*, *Nothofagus gunnii*, Restionaceae, Cyperaceae (including *Gymnoschoenus*) and ferns (except *Histiopteris* and *Phymatosaurus*) were rarely present in pollen trap samples yet were locally abundant in surface samples leading to the conclusion that these pollen types are predominantly transported by water and that even small percentages found in pollen records are likely to be significant indicators of specific environments (Macphail, 1979). Macphail also noted that alpine vegetation typically contains pollen from the lower slopes, resulting from upslope transport via wind vectors, providing representation of the forest growing at lower altitudes.

Hopf (1997) analysed moss samples from each of the key vegetation types in the Lake St Clair area and by comparing with abundances of each taxon in the vegetation from survey data, calculated R values (sensu Davis, 1963) to quantify the degree of pollen representation of each taxon finding that the degree of representation of the same taxon may vary between different vegetation types. Hopf (1997) also compiled relative pollen representation values using the categories from Dodson (1983) (under-, over-, well represented) for the taxa within the dataset comparing these with findings from other Australian pollen studies (Binder, 1978; Colhoun, 1980; Colhoun and Goede, 1979; Derrick, 1966; Derrick, 1962; Dodson and Myers, 1986; Dodson, 1983, 1977; Hope, 1974; Kodela, 1990a; Kodela, 1990b; Ladd, 1979a; Ladd, 1979b; Macphail, 1979; Phillips, 1941). As a whole, the relative pollen representation of the most important Tasmanian taxa is well understood. Hopf added two subcategories: 1. in the under-represented category, those taxa that are not represented at all by pollen and 2. in the over-represented category, those taxa which are not present in the actual vegetation surveyed but coming from outside the sample area.

Analysis of the modern pollen dataset from the Lake St Clair area for indicator taxa of the five different vegetation types addressed showed that the more poorly dispersed pollen types

were the strongest indicators differentiating the vegetation types, with the exception of rainforest which was differentiated by values above 50% of *Nothofagus cunninghamii*. *Leptospermum-Baeckea* type, *Hakea*, *Allocasuarina* were found to be good indicators of eucalypt heath*;* Cyperaceae and Restionaceae of sedgeland-heathland and *Microcachrys*, Proteaceae *Orites* type and *Podocarpus* of alpine vegetation (Hopf, 1997). *Atherosperma* and *Eucryphia* were found to be severely under-represented. Of special note is a modern pollen sample taken from callidendrous rainforest comprising almost exclusively of *Nothofagus cunninghamii* and *Atherosperma moschatum* as co-dominants, yet the pollen sample containined only 3% *Atherosperma moschatum.* This reinforces that presence of rare taxa such as *Atherosperma* in pollen records are likely to be a significant indicator of the presence of the taxon locally at the site.

Fletcher and Thomas (2007b) undertook a comprehensive descriptive and quantitative assessment of pollen-vegetation relationships using a dataset of 96 surface pollen samples from western Tasmania. They assessed the representation of pollen taxa by calculating fidelity and dispersability indices (sensu McGlone and Moar, 1997) and then assigned taxa to four categories (after Dodson, 1983 and Deng et al., 2006): over-represented, well-represented, under-represented and severely under-represented (other species).

They undertook ordination analysis of the entire dataset and found that vegetation types could be clearly distinguished irrespective of the surface sample type, further, separate ordination analysis of the moorland subset of samples showed that Eastern Moor could be distinguished from Blanket Moor. Fletcher and Thomas (2007a, b) reinforce the importance of *Gymnoschoenus sphaerocephalus* as an indicator of moorland vegetation, despite its under-representation in pollen records, re-iterating their belief that an absence of this pollen type from some Tasmanian pollen records is likely to be due to failure of ability to distinguish this pollen type.

As part of their ordination analysis, Fletcher and Thomas (2007b) compared the modern pollen data with environmental data representing the key environmental determinants of the vegetation in western Tasmania: altitude, fire and seasonality. They calculated fire interval scores based on Brown and Podger (1982) and fire susceptibility scores based on fire sensitivity info from Pyrke and Marsden-Smedley (2005). Fletcher et al (2007b) suggest that this allows the influence of fire on the palaeovegetation to be addressed independently of carbonised particle analysis. Overall, Fletcher and Thomas (2007b) presented valuable information on representation and relationship with fire for each of the key taxa present in Western Tasmania.

Quantitative reconstructions of vegetation using pollen-based models (Sugita, 2007b, 2007a) have been widely applied in Europe and North America where the vegetation is predominantly wind pollinated. The main challenge in applying this approach to Australia is that these models make the assumption that all pollen is airborne and the vegetation in Australia is largely animal and insect pollinated. Mariani et al. (2016) tested the suitability of two of the leading pollen dispersal models, the Gaussian Plume Model (GPM) and the Lagrangian Stochastic Model (LSM), for the first time in an Australian context.

Mariani et al. (2016) selected thirteen pollen taxa based on their ecological importance in the modern vegetation and their representation in fossil pollen records to calibrate modern pollen-vegetation relationships in western Tasmania. Twenty-seven sites were sampled from Cradle Mountain, Lake St Clair and the West Coast. They estimated pollen settling velocities (m/s) for the thirteen taxa using Stoke's Law and averaging measurements of at least 30 randomly chosen grains of each taxon from modern pollen samples. They assessed the modern pollen vegetation relationships using distance weighted plant abundances which were fed into the pollen-based models.

They found that the LSM gave more realistic estimates of pollen dispersal than the GPM which over-estimated pollen productivities for small grains with low fall speeds such as *Eucryphia lucida* and under estimated these for larger pollen grains with high fall speed such as *Gymnoschoenus sphaerocephalus*. They conclude that, although the results are promising for an application of a quantified approach to past vegetation cover estimation in Tasmania, the technique should only be applied to Holocene records due to potential variation in pollen production during glacial times, and that further work is required to assess the significant differences in pollen productivity estimates produced by the two different models.

Although aerial pollen transport is the key contributor to many pollen records and the quantification of this through pollen based models has been a major advance, in the case of pollen records from large lakes such as Lake St Clair, it is important to consider other processes that are significant in large lakes, notably the importance of fluvial pollen transport and the very large pollen source area, which create a different type of pollen record unique to large lakes.

4.1.3 Pollen deposition in large lakes

Whereas small lakes generally contain a record of vegetation change in the local environment large lakes collect regional pollen records with wide aerial pollen source areas (Janssen, 1973; Bradshaw and Webb, 1985; Jackson, 1990). Fluvial pollen inputs add a local pollen signature from vegetation within the lake's catchment. The relative importance of aerial versus fluvial

pollen input is disputed (e.g. Wang et al., 2014; Xu et al., 2012) and is likely to vary depending on the lake.

4.1.3.1 The aerial pollen source area

Models of the relationship between pollen and vegetation have developed from the basic R-value model (Davis, 1963) which calculates a simple pollen/vegetation ratio through to the incorporation of background pollen into estimates (Anderson, 1970; Bradshaw and Webb, 1985; Jackson and Wong, 1994; Prentice, 1985), extended R-value models which correct for the Fagerlind effect (Parsons et al., 1980; Parsons and Prentice, 1981; Prentice and Parsons, 1983) and models which consider the size and extent of the pollen source area and relevant distance weightings (Prentice, 1985; Sugita, 1993, 1994; Jackson and Wong, 1994; Calcote, 1995; Jackson et al., 1995; Hjelle and Sugita, 2012)

The pollen source area increases as the basin size increases (Tauber, 1967, 1977; Berglund, 1973; Jacobson and Bradshaw, 1981; Davis, 2000), where small lakes generally contain a record of vegetation change of the local environment and large lakes collect regional pollen records with wide aerial pollen source areas (Janssen, 1973; Bradshaw and Webb, 1985; Jackson, 1990). Sugita (1994) defines the 'relevant source area of pollen' (RSAP) as the area beyond which the pollen does not considerably affect the local variations in vegetation recorded within this area. The REVEALS model (Sugita, 2007a) estimates the composition of the regional vegetation using pollen records from large lakes (≥ 100-500 ha) based on the theory that pollen assemblages from different large lakes within a regional landscape are not statistically different even when the vegetation is heterogeneous. The pollen records from these large lakes is thought to represent the regional vegetation composition within a 10^4–10^5 km^2 area of the lakes (Sugita, 2007a; Hellman et al., 2008).

The pollen-based models used for the reconstruction of past vegetation, including the REVEALS model are limited in that they only consider the aerial pollen input to lakes and do not consider the input of water-borne pollen. Other assumptions of the model include that the sedimentary basin is a circular opening in the canopy and that pollen dispersal is even from all directions (Hellman et al., 2008) Lakes with fluvial input can contain a significant component of fluvial transported pollen grains in their sediments, and vegetation types in the dominant wind directions from a basin should have a stronger influence on the pollen assemblage being deposited in the basin, however, models taking these factors into account are yet to be developed.

4.1.3.2 Fluvial transport of pollen

Early studies in the English Lake District (Peck 1973, 1974, Bonny 1976, 1978 and Pennington, 1979) and the North American Great Lakes (McAndrews and Power, 1973 and Crowder and Cuddy, 1973) found that fluvial transport and slope in-wash accounted for the majority (up to 97%) of pollen deposited in the lakes. Further studies (e.g. Brown, 1985; David and Roberts, 1990; Traverse, 1994, 1992) have resulted in a widespread acceptance of the dominance of fluvially transported pollen in medium to large sized lakes and near-shore marine sediments and that the key factors affecting the ratio of aerial to fluvial pollen input include the surface area of the lake and the size, topography and vegetation of the lake's catchment (Brown, 2007). Brown suggests that these factors could be modelled in a quantitative way similar to the airborne component with the potential outcome of further improving pollen-based vegetation reconstructions.

Further, it has been found that floods are responsible for transporting the vast majority of fluvial pollen and spores, the composition of resulting assemblages being controlled predominantly by the local catchment vegetation (Brown, 2007). Anomalous single-level peaks can occur in records as a result of seasonal flushes of pollen spores from vegetation types growing near-stream (Brown, 2007).

The predominance of fluvial pollen in large lakes is debated however, Wang et al (2014) argue that fluvial input is minimal when compared with aerial deposition on the arid, flat, treeless Tibetan plateau due to the flat topography being ideal for aeolian transport, small areas of upper catchments contributing little pollen load to the lakes and inflows typical of arid and semi-arid regions being insufficient in transporting large quantities of pollen to the lakes. In contrast, Xu et al. (2012) demonstrate through analysis of comparative pollen trap data from above and below the surface of Lake Baiyangdian (surface area = 366 km^2) in northern China that fluvial input is responsible for ~92% of non-aquatic pollen assemblages.

Luly (1995) found that fluvial transport and surface wash made no significant contributions to pollen input to Lake Tyrell, a large, shallow lake in semi-arid north-western Victoria. However, the unique environment means that most water in the lake is derived from rain with only occasional fluvial input to the lake by Tyrell Creek which feeds the lake approximately once every five years (Luly, 1995, Teller et al. 1982 (in Luly)).

Large variations in pollen deposition have been observed within large lakes as a result of variations in settling velocity, grain size and atmospheric dispersal patterns (Davis, 1963, 1967; Luly, 1997; Giesecke and Fontana, 2008; Wang et al., 2014). Selection deposition as a result of fluvial transport of pollen to lakes as well as hydrodynamics within lakes has also been

observed (DeBusk Jr., 1997; Zhu et al., 2002; Qinghai et al., 2005; Wang et al., 2014). Investigation of the variability in pollen deposition within Lake St Clair will be important.

4.1.4 Aims of modern pollen analysis in this study

The goals of this modern pollen analysis are to:

1. evaluate the pollen source area, both aerial and fluvial, of the large lake: Lake St Clair
2. disentangle the local from the regional signal in the lake to ascertain the nature of pollen record captured in the lake
3. to contribute to the wider knowledge of modern pollen deposition in Tasmania by means of surface sample analysis within the Lake St Clair catchment.

4.2 The Lake St Clair Pollen Source Area

4.2.1 Aerial pollen source area

The minimum aerial pollen source area for wind-dispersed pollen types to the Core CG site in Lake St Clair has been estimated to be 100 km based on the concept that pollen records from large lakes (≥ 100-500 ha) are thought to represent the regional vegetation composition within a 10^4–10^5 km^2 area of the lakes (Sugita, 2007a; Hellman et al., 2008). Figure 4.1 illustrates the hypothetical 100 km pollen source area and the vegetation types it includes. Realistically, the aerial pollen source area (APSA) is likely to include an even larger area likely encompassing the entire island of Tasmania with long distance transport from mainland Australia also likely. An example is the chenopod steppe of South Australia which has been suggested for elevated values of Amaranthaceae in glacial pollen records from Tasmania (Macphail 1975, 1979). The wide scope of the APSA needs to be considered for Lake St Clair, especially, considering the large size of the lake. It should be noted that pollen source area is not only dependent on the size of basin, but also dispersal and depositional characteristics of each pollen taxon (Tauber, 1965, 1977, Janssen, 1966, 1973; Anderson, 1970; Jacobson and Bradshaw, 1981; Parsons and Prentice, 1981; Prentice, 1985; Wang et al., 2014) and it follows that insect pollinated, predominantly wind transported pollen types will not be transported from beyond the local catchment even if widespread in the larger aerial pollen source area.

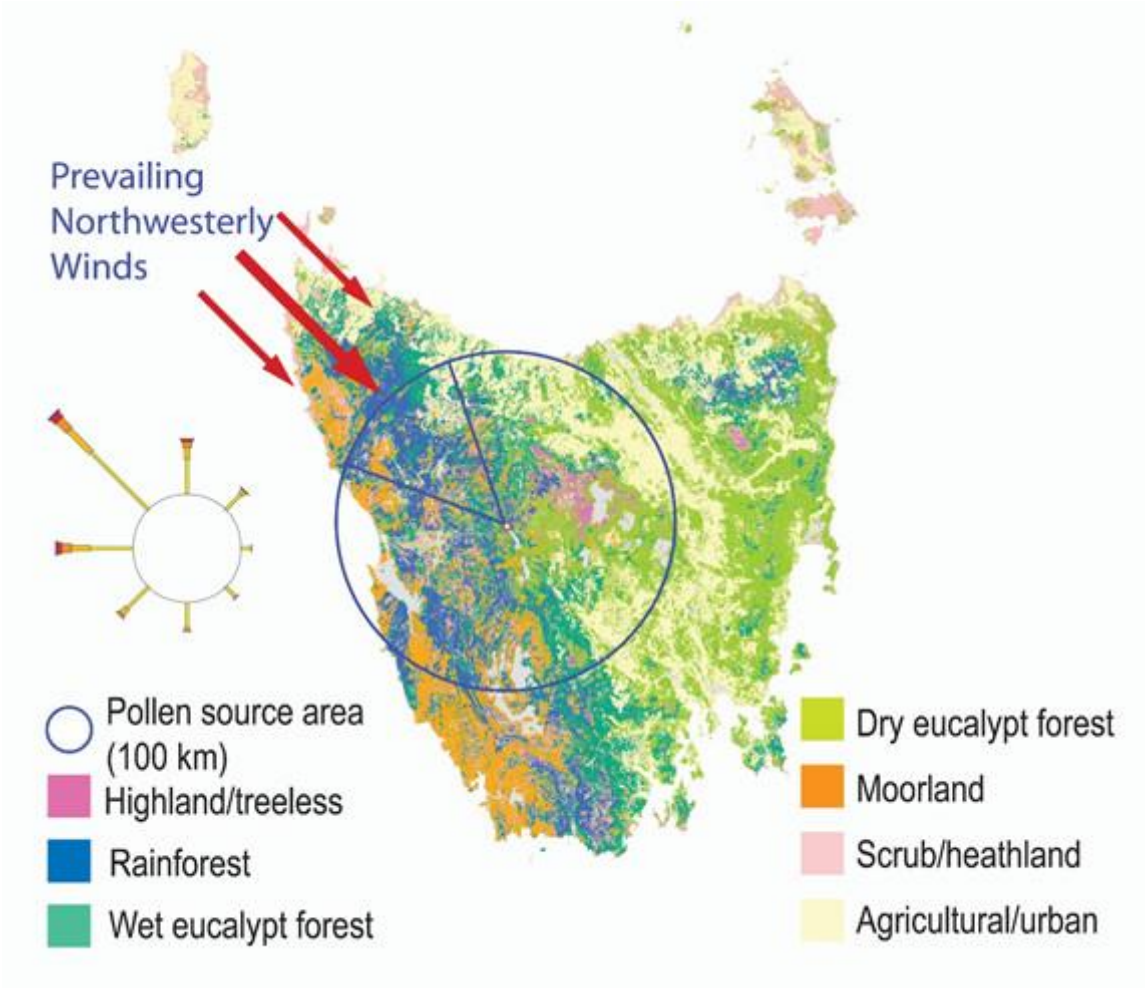

Figure 4-1 Estimated aerial pollen source area for Lake St Clair and simplified vegetation map of Tasmania. The predominant wind direction for Lake St Clair are marked and wind rose included as inset.

As can be seen from figure 4.1, all of the key Tasmanian vegetation types are represented within the APSA for Lake St Clair. The relative pollen source area model of Sugita assumes that the aerial pollen is uniformly delivered from all directions. However, the bias of a predominant wind direction should be taken into consideration as the pollen rain is likely to be preferentially sourced from certain vegetation types. Not only due to the wind direction, but also as a result of the varying degrees of pollen representation of different plants. The modern day prevailing north-westerly winds would result in a strong bias towards pollen sourced from rainforest and to a lesser extent wet eucalypt forest and moorland reaching Lake St Clair. We know from modern pollen studies that indicator pollen types of moorland vegetation are poorly dispersed by wind, so these are unlikely to contribute much to the pollen rain. In the past, the predominant wind direction may have varied from today, however, it is thought that the SWW predominated through to the last glacial period with the main factor of variation being the intensity of the SWW so we could assume that the regional pollen rain for Lake St Clair is dominated by pollen from the vegetation types mentioned to the northwest. The large

size of the aerial pollen source area for Lake St Clair make it ideal to pick up any broad scale changes in vegetation driven by climate.

4.2.2 Fluvial pollen source area

As discussed earlier, fluvial transport has been found to be an important contributor to pollen records for lakes with inflowing rivers. Three watersheds (figure 4.2) influence the core CG site (sample 7) which lies ~ 2km southeast of the Narcissus River mouth which descends ~ 14.5 km from the Du Cane Range to the north, passing from highland and treeless vegetation through wet eucalypt forest and rainforest as it descends to the lower altitudes covered mostly by dry eucalypt forest and moorland. The watershed of the Narcissus River to the north covers the largest area (~8000 ha), however several smaller creeks flowing into the lake from the Lake Laura (~815 ha) and Mt Olympus (~700 ha) watersheds also influence the core site.

The key vegetation types are illustrated as transects from the core site northwest to Mt Gould (figure 4.3) and west-east from Mt Olympus through the core site onto the Central Plateau (figure 4.4) as well as in the vegetation map in figure 4.5. As detailed in chapter 2, a mosaic of vegetation types occur, reflecting varying degrees of influence of fire ranging from rainforest to wet sclerophyll, dry eucalypt scrub/heath to moorland at lower altitudes with highland and treeless vegetation represented at higher altitudes.

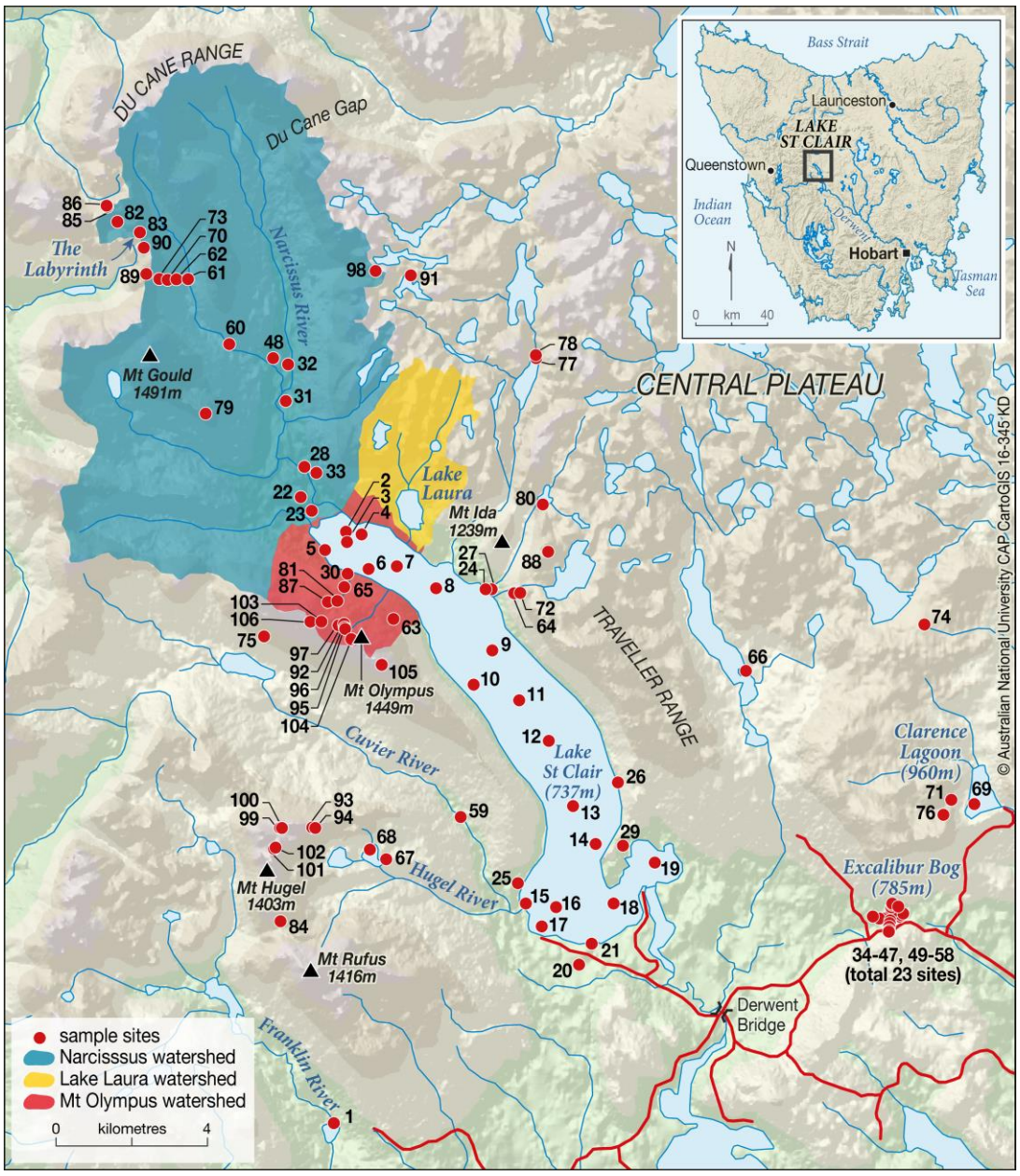

Figure 4-2 Fluvial pollen source areas for the core CG core site are indicated by the three main watersheds feedings the northern area of the lake. The map also illustrates all modern pollen sample locations included in the modern pollen Lake St Clair dataset.

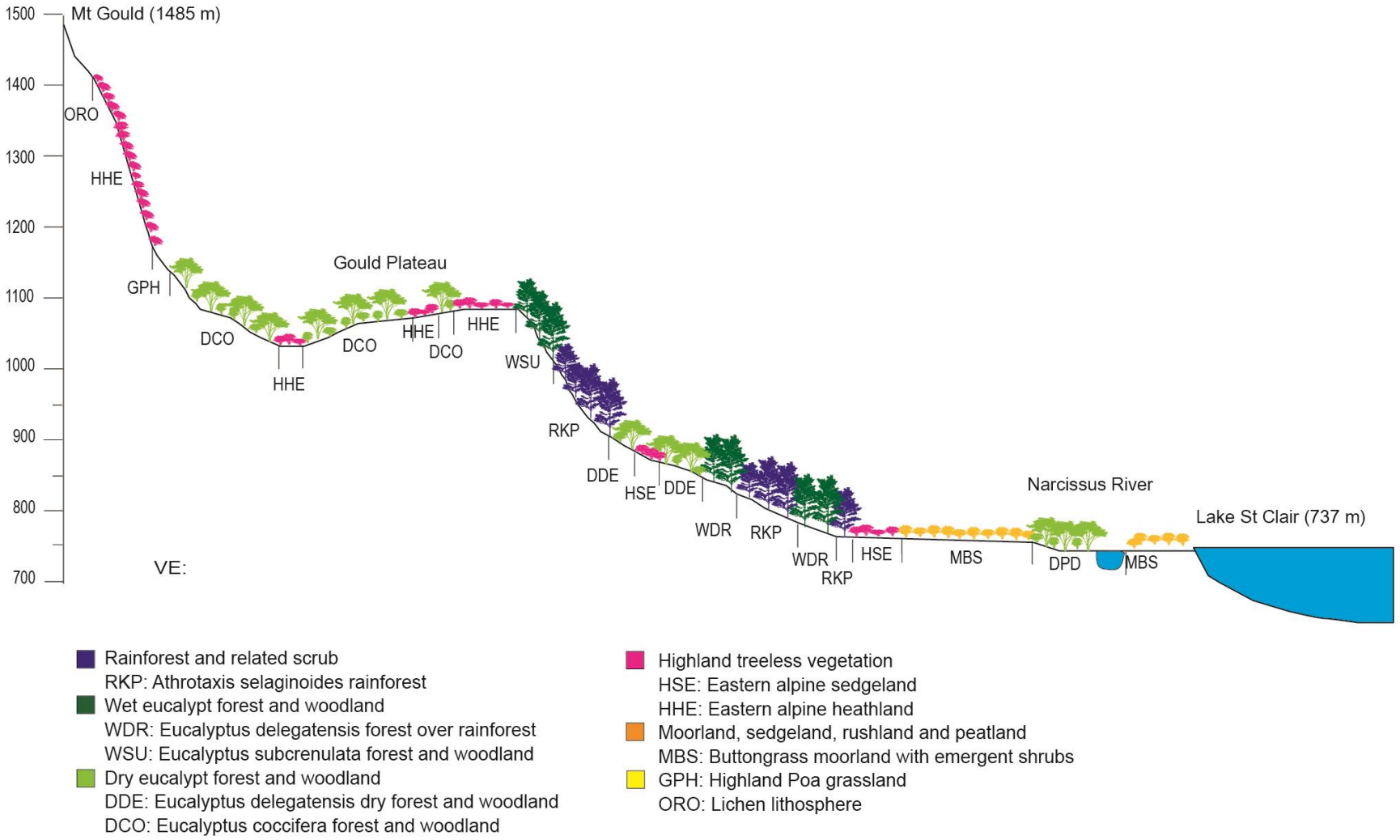

Figure 4-3 Cross section of vegetation from the core site northwest to Mt Gould

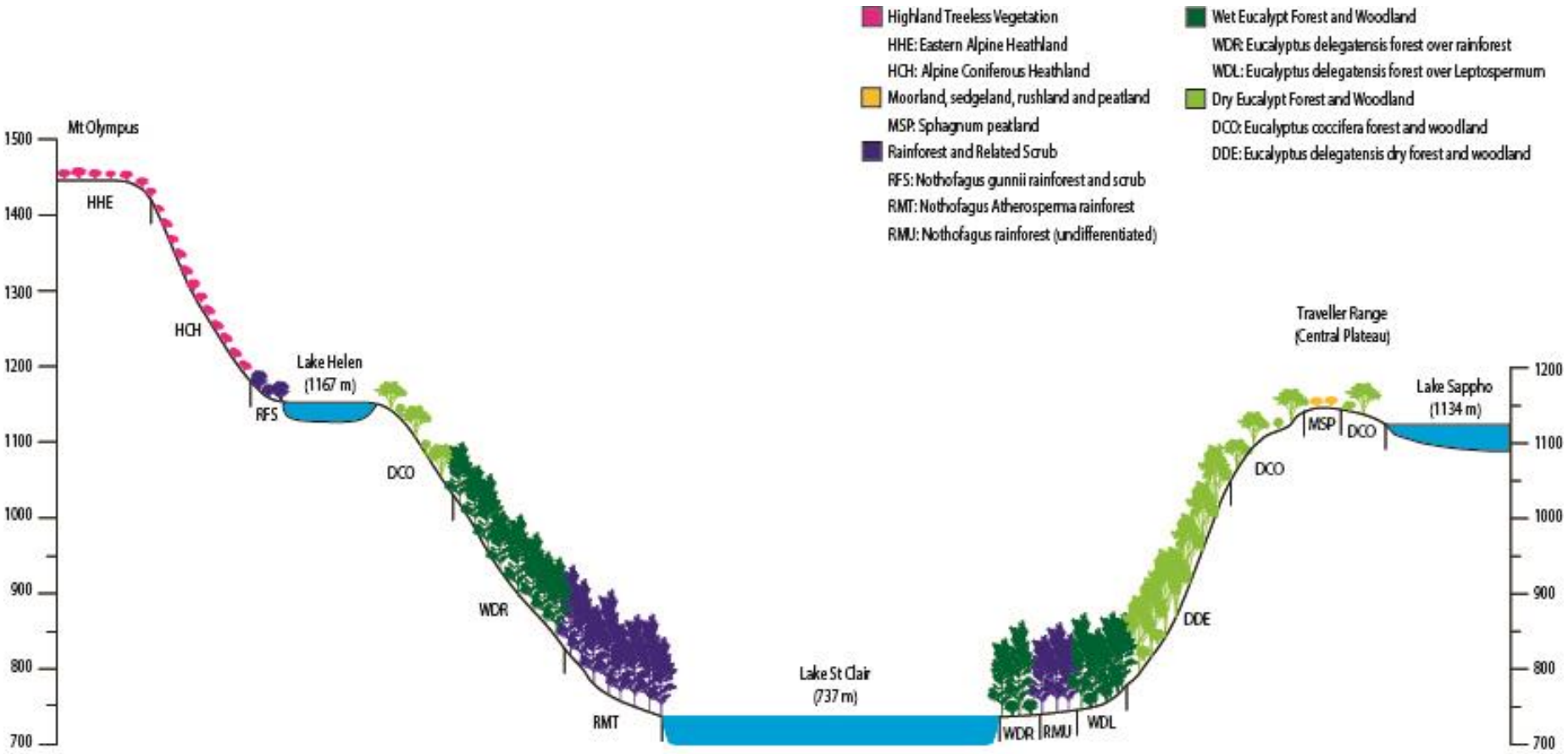

Figure 4-4 West-east cross section of vegetation from Mt Olympus through the core site and onto the Central Plateau

4.3 Modern Pollen Deposition in the Lake St Clair Region

4.3.1 Introduction

To investigate the nature of the pollen record captured by the large lake environment of Lake St Clair, 21 lake samples (18 mud-water interface samples from Lake St Clair) and 85 moss and tarn samples representing all key vegetation types in the Lake St Clair catchment were analysed to gain insights into the source areas of the pollen (figure 4.5). Large lakes like Lake St Clair have a large aerial pollen source area resulting in a mixture of local and regional wind dispersed pollen being deposited in the lake basin along with an additional pollen component contributed by inflowing rivers and creeks and slope-wash derived from the local catchment. The data was investigated by means of ordination analysis and box plots of key taxa together with comparisons with vegetation maps and indicator analysis with the goal of disentangling the main components of the pollen record of the lake.

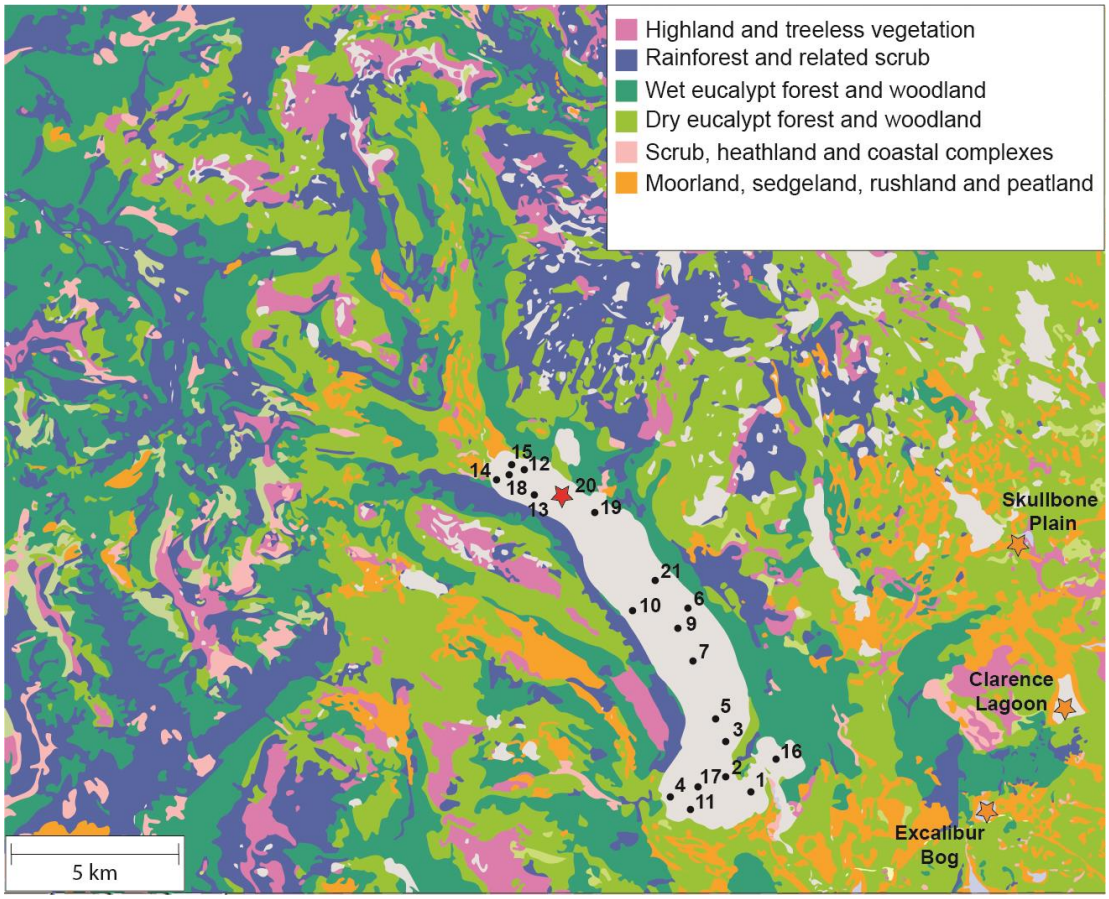

Figure 4-5 Vegetation map of the Lake St Clair area and lake sample locations included in the modern pollen dataset. Sample 20 is the mud-water interface sample for the core CG location.

4.3.2 Results

The percentage pollen data of the full dataset of modern pollen samples from the Lake St Clair area is presented in figures 4.6-4.8. Samples are grouped by vegetation type with lake samples grouped separately and all samples sorted by altitude within each vegetation type. Taxa

groupings are based on representation groups in Fletcher and Thomas (2007) with the addition of wetland, fern spores and other taxa included as well. It is clear from the diagram that certain taxa are present at elevated levels in the lake samples relative to those taken from the catchment and high values of some taxa are unique to certain vegetation types. These patterns are explored further in the following analyses and figures.

Detrended correspondence analysis with down weighting of rare taxa was performed on the full dataset of modern pollen samples from the Lake St Clair area (figure 4.9) to determine whether the different vegetation types can be distinguished by their pollen signature and to observe where the lake samples place in relation to the catchment samples. DCA axis 1 (r^2=0.403) is most strongly correlated with *Eucalyptus* (r^2 =0.573) and also correlates weakly with *Microcachrys* (r^2 =0.236), *Nothofagus gunnii* (r^2 =0.214) and *Athrotaxis*/*Diselma* (r^2 =0.182). DCA axis 2 (r^2 =0.172) is most strongly correlated with *Gymnoschoenus* (r^2 =0.430), with weaker correlations also shown with Ericaceae (r^2 =0.351), *Leptospermum*/*Baeckea* (r^2 =0.240) and *Nothofagus cunninghamii* (r^2 =0.193).

Axis 1 appears to reflect in part the variation caused by altitude with below treeline vegetation communities plotting towards the lower end of axis 1 (dry eucalypt forest, wet eucalypt forest, moorland and *Nothofagus cunninghamii-Atherosperma* rainforest) and vegetation communities above the treeline plotting high on the axis (eastern alpine heathland, eastern alpine sedgeland and *Athrotaxis cupressoides-Nothofagus gunnii* short rainforest). Axis 2 reflects the increasing influence of fire on the vegetation with *Nothofagus cunninghamii-Atherosperma* rainforest plotting lowest on the axis progressing through wet eucalypt forest, dry eucalypt forest and finally *Gymnoschoenus*-rich moorland below the treeline, and above the treeline the very fire sensitive *Athrotaxis cupressoides-Nothofagus gunnii* short rainforest and alpine coniferous heathland plotting lower on the axis than eastern alpine heathland.

The broad vegetation groups form distinct groups within the DCA ordination space with a small amount of overlap, notably by some higher altitude samples of dry and wet eucalypt forest plotting just within the highland treeless vegetation and *Athrotaxis cupressoides-Nothofagus gunnii* short rainforest groups. This is explained by proximity of these samples to the latter vegetation types resulting in pollen transport of some taxa between the communities. Some

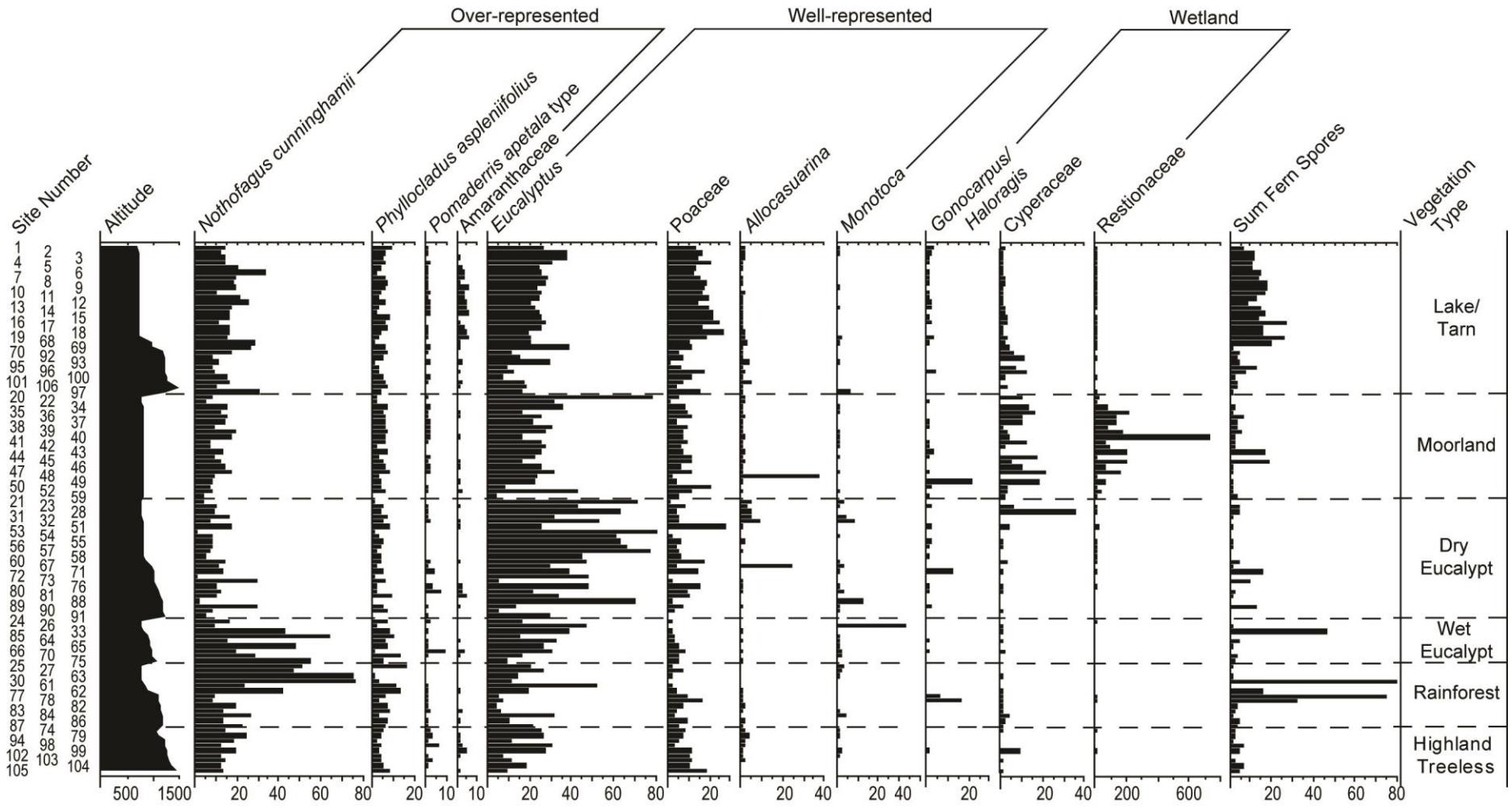

Figure 4-6 Percentage pollen diagram modern pollen dataset grouped by vegetation type and pollen representation (part 1)

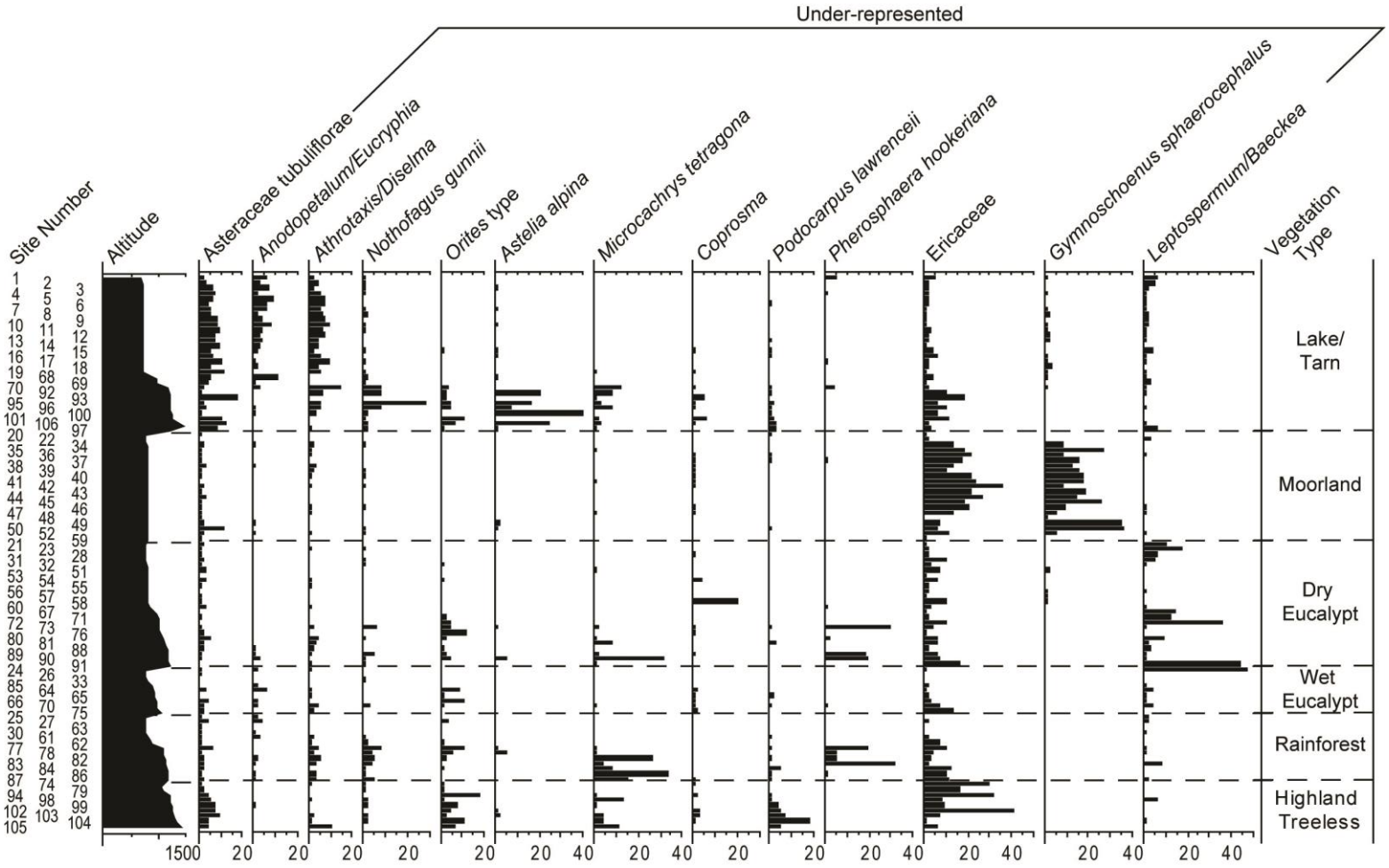

Figure 4-7 Percentage pollen diagram modern pollen dataset grouped by vegetation type and pollen representation (part 2)

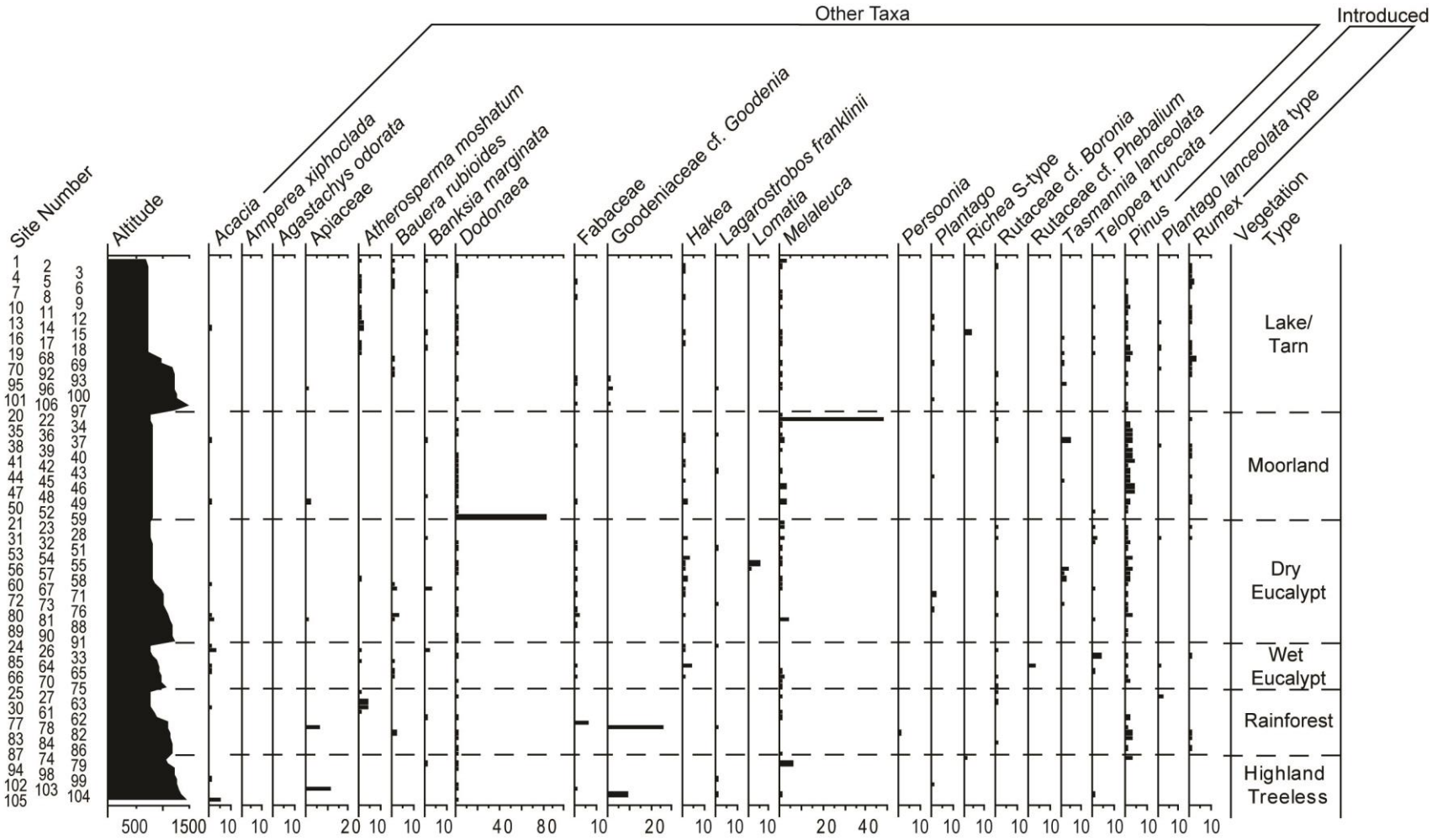

Figure 4-8 Percentage pollen diagram modern pollen dataset grouped by vegetation type and pollen representation (part 3)

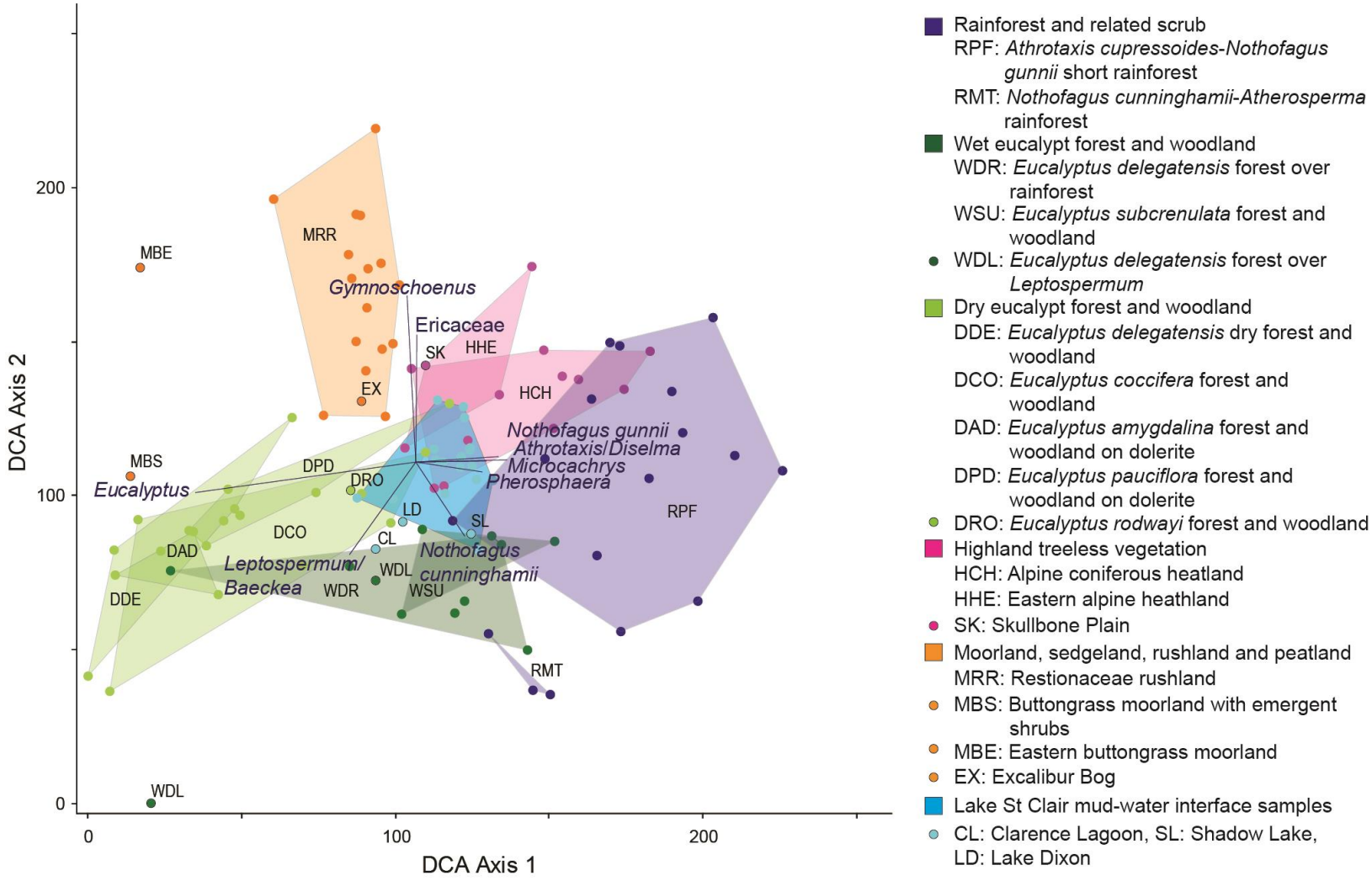

Figure 4-9 DCA biplot of the modern pollen dataset grouped by vegetation type

samples of the intermediate wet eucalypt forest also overlap with dry eucalypt and *Nothofagus cunninghamii-Atherosperma* rainforest depending on the relative proportions of rainforest versus sclerophyll components in the samples. The different types of dry eucalypt and wet eucalypt communities overlap consistent with their broader associations, whereas the highland rainforest (*Athrotaxis cupressoides-Nothofagus gunnii* short rainforest) is clearly separated from lower altitude rainforest (*Nothofagus cunninghamii-Atherosperma* rainforest).

The mud-water interface samples from Lake St Clair group in a central position in the DCA plot (figure 4.9), likely representing the regional pollen signal in common with the catchment samples which distinguish themselves by their more unique local pollen components. Within the Lake St Clair group, most samples overlap with highland treeless vegetation groups which can also be explained by the shared regional pollen signature. As mentioned earlier, treeless vegetation communities contain a higher proportion of regional pollen due to a lack of strong local pollen sources and processes such as the upslope transport of pollen of forest taxa.

To further investigate the degree to which certain pollen taxa are indicative of specific vegetation types, indicator species analysis was run on the dataset (table 4.1) and the median and ranges of key pollen taxa plotted as box plots for each vegetation type (figures 4.10-4.12). One group of taxa are present as a widespread component of samples from all vegetation types as part of the regional pollen rain: *Eucalyptus*, Poaceae, *Nothofagus cunninghamii*, *Phyllocladus aspleniifolius*, Asteraceae, Amaranthaceae, *Allocasuarina, Pomaderris* apetala type and possibly *Athrotaxis*/*Diselma.* In some cases, high values are indicative of local presence of specific vegetation types. A subset is markedly higher in the lake samples than background values observed in all vegetation types: *Eucalyptus*, Poaceae, *Athrotaxis-Diselma*, Amaranthaceae and Asteraceae which could be a result of the large pollen source areas of these taxa Tasmania-wide and/or increased water transport to the lake from within the catchment.

Another group of taxa have poorly dispersed pollen and even small values in the pollen record are strong indicators of local presence of specific vegetation types: *Eucryphia*/*Anodopetalum*, Ericaceae, *Leptospermum*/*Baeckea*, *Gymnoschoenus sphaerocephalus*, *Monotoca*, *Atherosperma moschatum*, *Orites*/*Bellendena*, *Pherosphaera hookeriana*, *Nothofagus gunnii*, *Astelia alpina*, *Microcachrys tetragona*, *Podocarpus lawrenceii*.

Table 4-1 Key indicator taxa and values for different vegetation types

VegCode	Pollen Taxon	IV	Vegetation Description
HCH	*Podocarpus* *Astelia* *Orites*	54.1 24 20.8	Alpine coniferous heathland
HHE	Ericaceae *Plantago*	28.9 21.4	Eastern alpine heathland
RMT	*Atherosperma* *Nothofagus cunninghamii*	90.5 27.1	*Nothofagus cunninghamii-Atherosperma* rainforest
RPF	*Nothofagus gunnii* *Pherosphaera* *Microcachrys* Apiaceae	71.4 70.7 60.5 8.9	*Athrotaxis cupressoides-Nothofagus gunnii* short rainforest
WDL	*Eucryphia/ Anodopetalum* *Hakea* *Leptospermum/ Baeckea* *Acacia*	49.6 49.1 40.1 22	*Eucalyptus delegatensis* forest over Leptospermum
WDR	*Monotoca* *Phyllocladus*	29.9 12.3	*Eucalyptus delegatensis* forest over rainforest
WSU	*Pomaderris*	14.5	*Eucalyptus subcrenulata* forest and woodland
DAD	*Melaleuca* *Allocasuarina* *Eucalyptus*	25 17.6 16.6	*Eucalyptus amygdalThe second Middle Atlas study site (MICH) is located in the Michliffen caldera at 33° 32′ N, 5° 6′ W (~2000 m a.* *s.l.)ina* forest and woodland on dolerite
DDE	*Coprosma*	25.1	*Eucalyptus delegatensis* dry forest and woodland
DPD	*Tasmannia*	29.7	*Eucalyptus pauciflora forest and woodland on dolerite*
MRR	*Gymnoschoenus*	94.6	Restionaceae rushland
Lake	Asteraceae Amaranthaceae Poaceae *Athrotaxis/ Diselma* *Banksia*	19.4 23.8 20.7 29.8 10.8	Lake St Clair

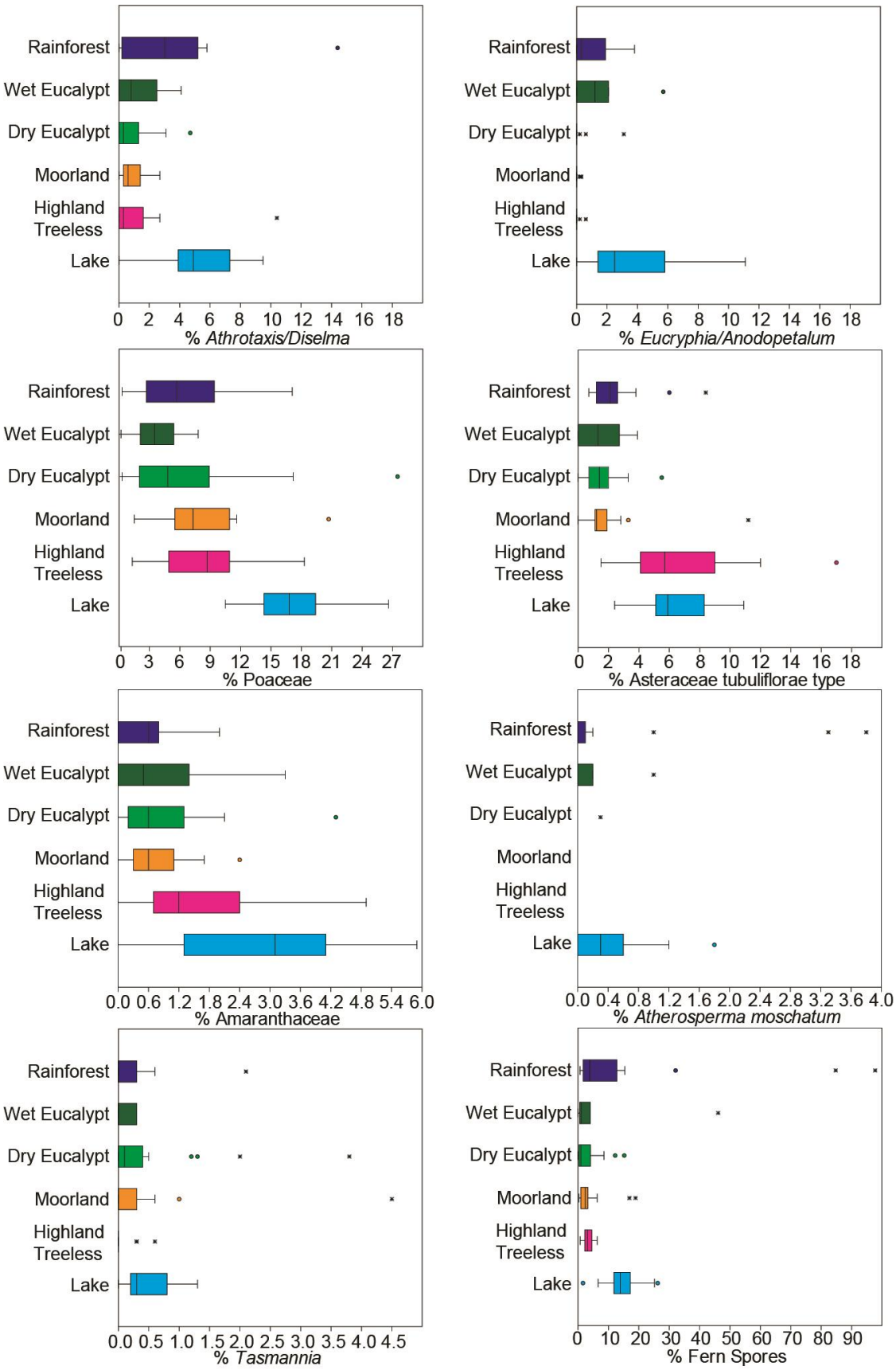

Figure 4-10 Boxplots of the range of median percentages of key taxa in different vegetation types (part 1)

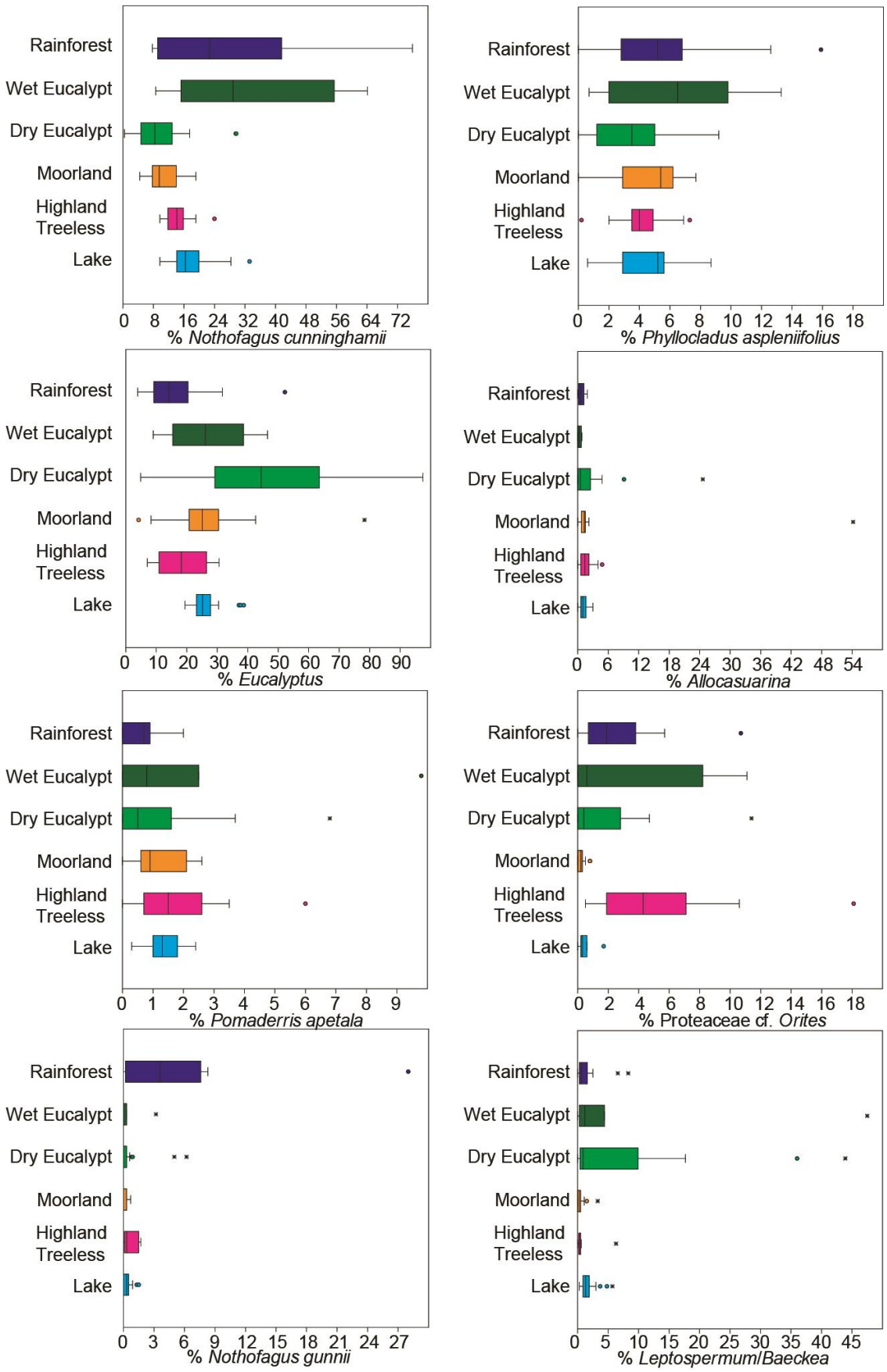

Figure 4-11 Boxplots of the range of median percentages of key taxa in different vegetation types (part 2)

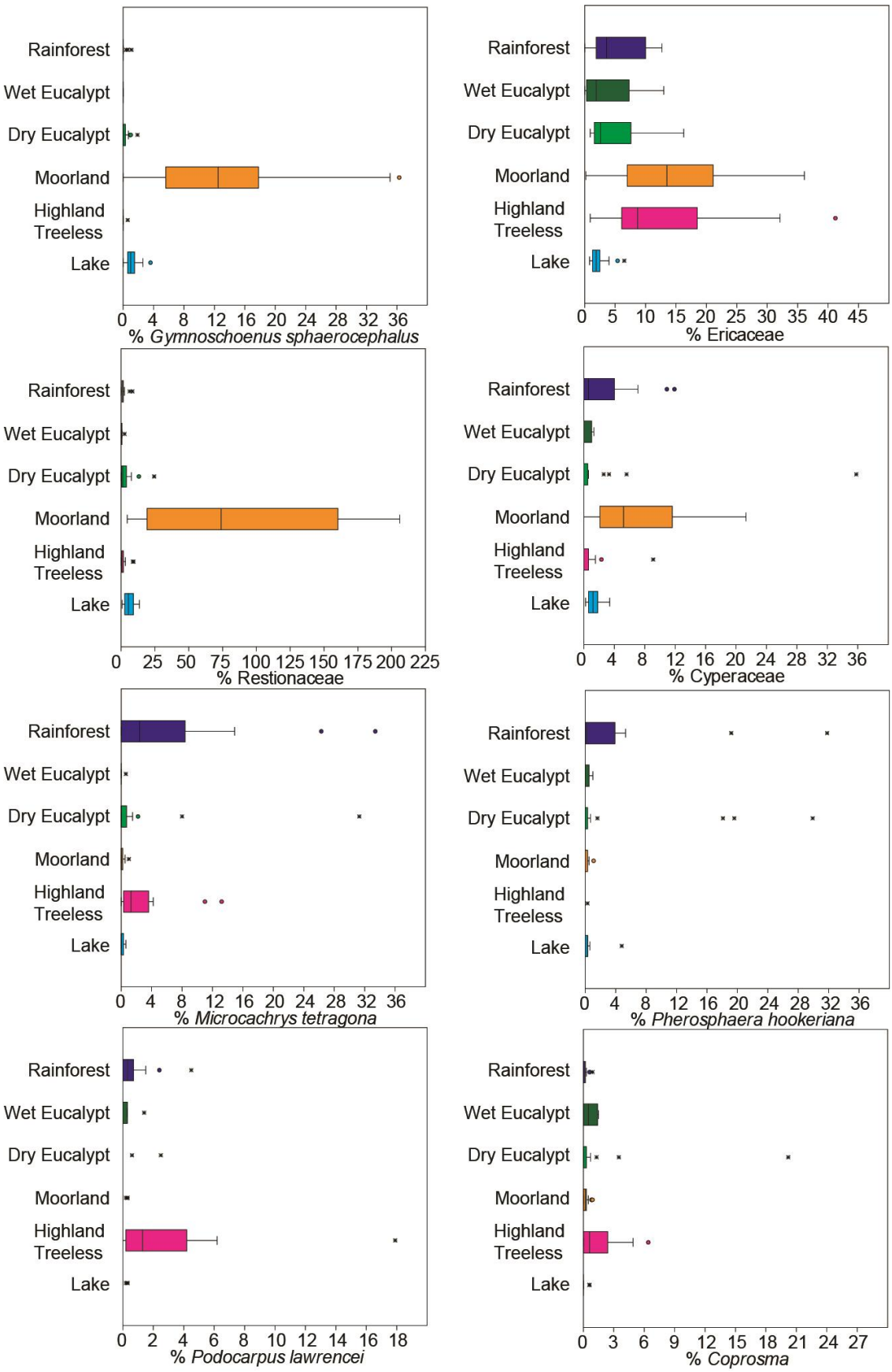

Figure 4-12 Boxplots of the range of median percentages of key taxa in different vegetation types (part 3)

Due to the large variations in pollen deposition which have been observed within large lakes (Davis, 1963, 1967; Luly, 1997; Giesecke and Fontana, 2008; Wang et al., 2014), the degree of variability in pollen deposition within Lake St Clair was investigated. DCA was performed on the Lake St Clair mud-water interface sample subset (figure 4.13), with samples placed in three broad groups according to their location within the lake: 1. northern basin, 2. central basin and 3. southern basin. DCA axis 1 (r^2=0.267) is significantly correlated with Amaranthaceae (r^2=0.542), *Phyllocladus* (r^2=0.431), Ericaceae (r^2=0.426) and *Nothofagus cunninghamii* (r^2=0.419). DCA axis 2 (r^2=0.242) is most strongly correlated with *Eucalyptus* (0.522), *Eucryphia-Anodopetalum* (r^2=0.508) and Poaceae (r^2=0.469). The total variability in the species data (inertia) is 0.1770.

The three location-based groups plot as distinct groups within the ordination space. There is a small degree of overlap between the northern and southern basin groups with the central basin samples being most similar to the northern basin samples. Two samples from the central basin overlap with the northern basin, which could be explained by their location at the northernmost end of the central basin group. The central basin samples also distinguish themselves by a higher mean water depth in this part of Lake St Clair (up to 115 m deep; see box plot for median water depth for each group in figure 4.14) which may affect processes of pollen transport and deposition.

To investigate the source of variability within the lake further, box plots of the most important pollen taxa grouped by location within the lake are presented in figure 4.14. Key vegetation communities in the Lake St Clair area are plotted in figures 4.15 and 4.16 to compare with the pollen data to determine potential sources accounting for the variability. Given that the wider regional pollen component is likely to be similar for the whole lake, the variability is likely a result of variations in pollen sources more proximal to the lake. The northern samples a characterised by higher proportions of forest taxa, *Eucryphia*/*Anodopetalum* and *Eucalyptus,* in contrast with the southern samples which have higher proportions of grass and shrub taxa, notably Poaceae, Asteraceae, Ericaceae and *Allocasuarina.* This pattern can be explained by the dominant vegetation communities observed bordering the lake with include predominantly rainforest and wet/dry eucalypt forest in the north and moorland and grassy vegetation communities proximal to the southern end of the lake (fig. 4.16 c,d). *Eucryphia*/*Anodopetalum* in particular is poorly transported and indicative of local presence of source vegetation and as a result is likely to be mostly transported to the northern lake samples location by slope-wash and fluvial transport.

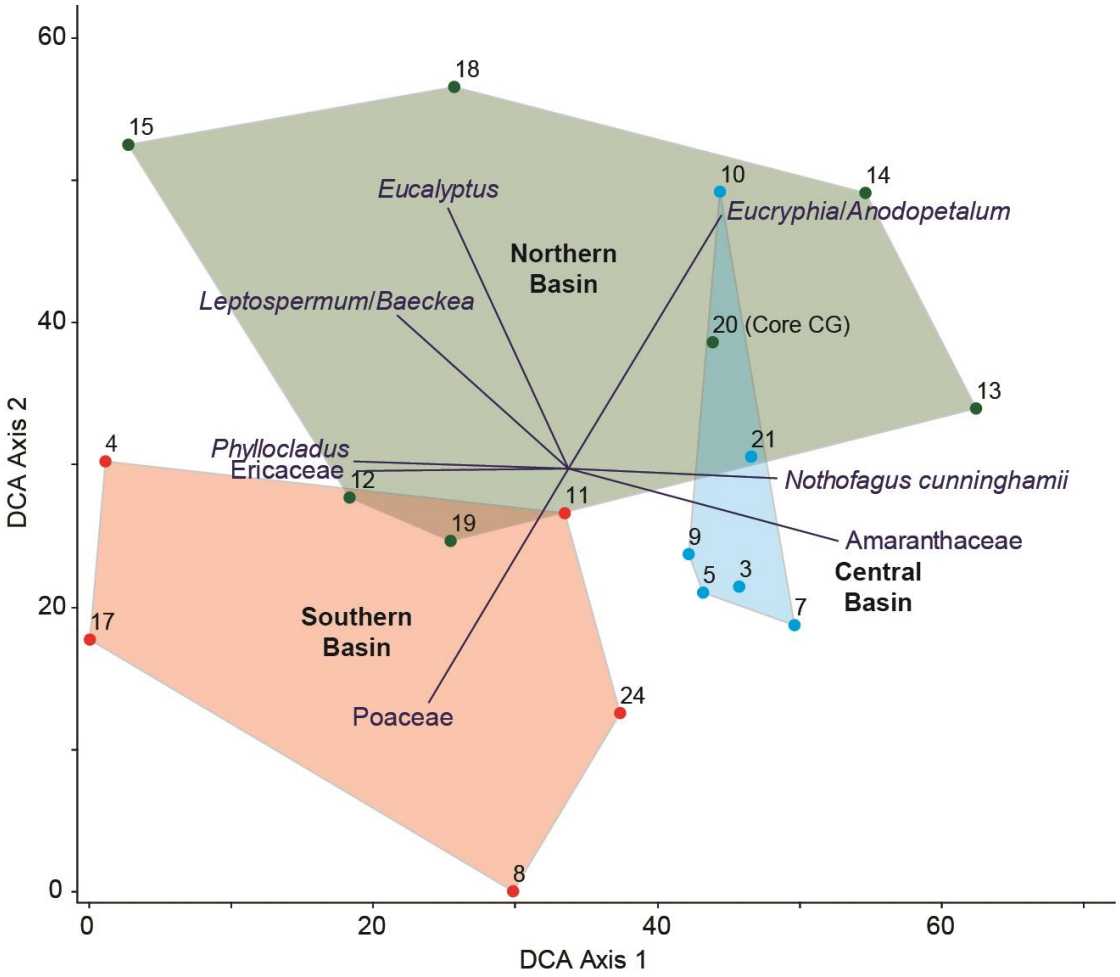

Figure 4-13 DCA biplot of variation of pollen samples within Lake St Clair

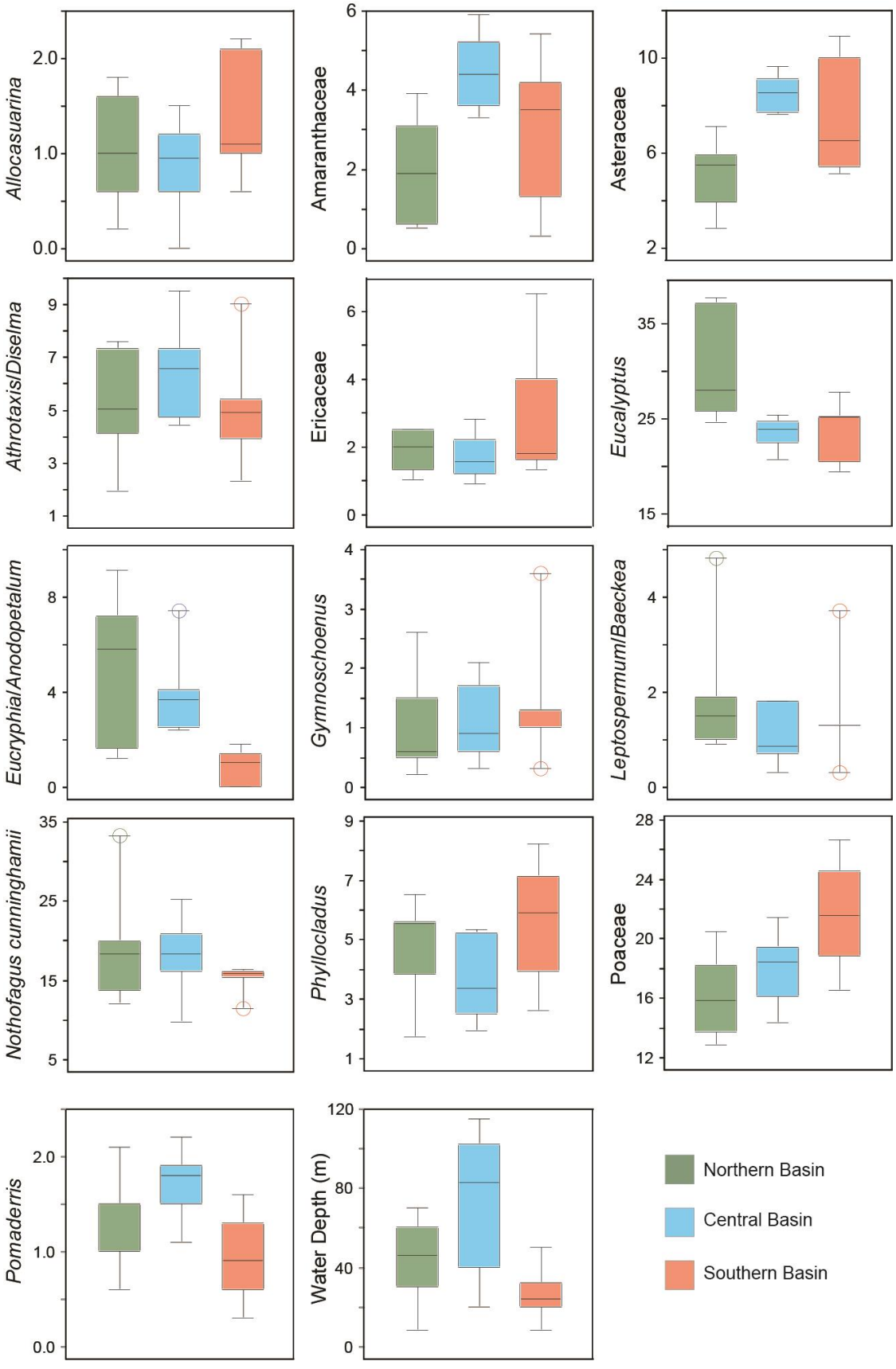

Figure 4-14 Box plots of median % range of key taxa within Lake St Clair

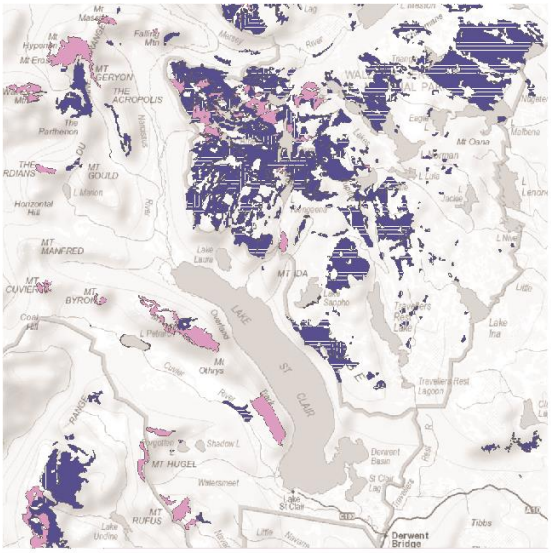

a) *Athrotaxis cupressoides* vegetation communities (blue; including *Athrotaxis cupressoides-Nothofagus gunnii* short rainforest, *Athrotaxis cupressoides* open woodland and *Athrotaxis cupressoides* rainforest) and alpine coniferous heathland (pink)

b) *Athrotaxis selaginoides* rainforest (blue)

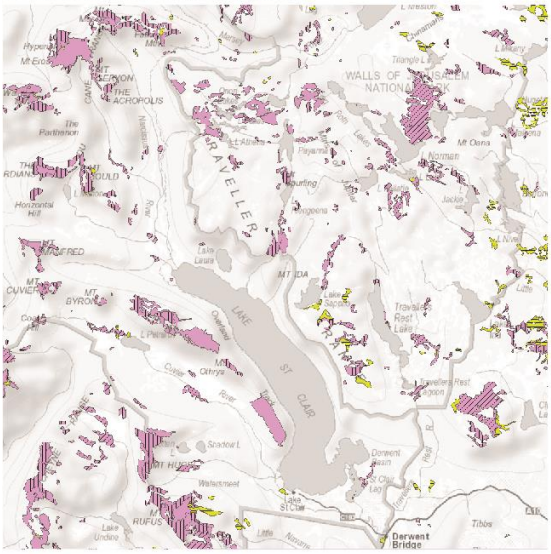

c) Highland treeless vegetation communities (pink; including alpine coniferous heathland, cushion moorland, eastern alpine heathland and eastern alpine sedgeland) and highland *Poa* grassland (yellow)

d) Grassy vegetation communities (yellow) including highland *Poa* grassland and highland grassy sedgeland

Figure 4-15 Maps showing ranges of key vegetation types within the Lake St Clair region. Data source:*(Department of Primary Industries, Parks, Water and Environment, 2013)*

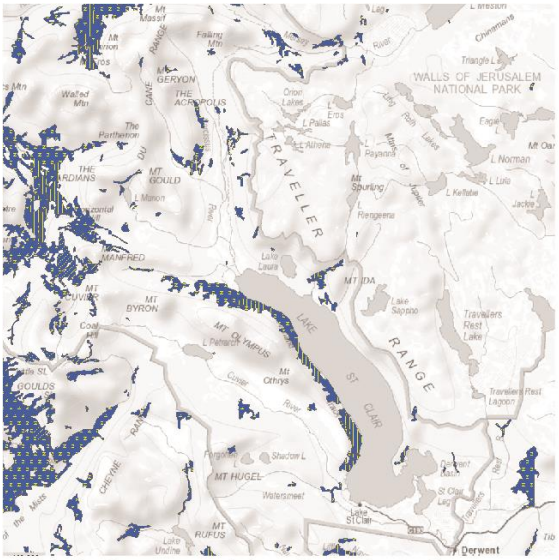

a) *Nothofagus cunnighamii* dominated communities including *Nothofagus-Atherosperma* rainforest and *Nothofagus* forest (undifferentiated)

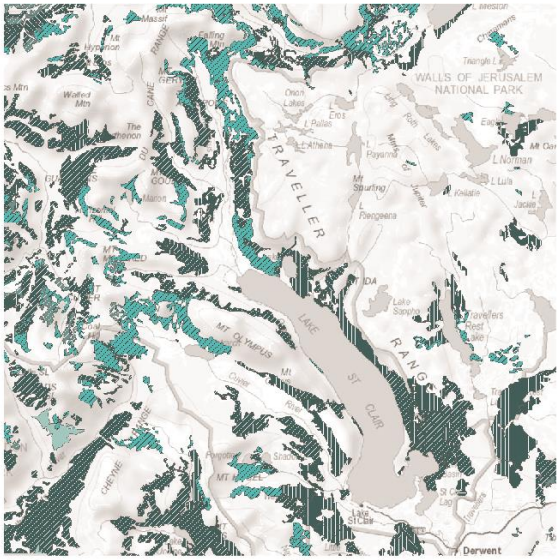

b) Wet eucalypt communities including *Eucalyptus delegatensis* forest over *Leptospermum*, *Eucalyptus delegatensis* forest over rainforest, *Eucalyptus delegatensis* forest with broad-leaf shrubs, *Eucalyptus delegatensis* wet forest (undifferentiated) and *Eucalyptus subcrenulata* forest and woodland

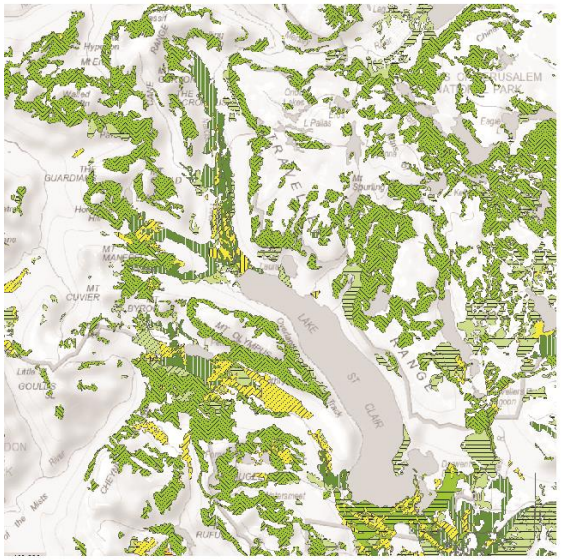

c) Dry eucalypt communities including *Eucalyptus amygdalina* forest and woodland on dolerite, *Eucalyptus coccifera* forest and woodland, *Eucalyptus delegatensis* dry forest and woodland, *Eucalyptus gunnii* woodland *Eucalyptus pauciflora* forest and woodland on dolerite and *Eucalyptus rodwayi* forest and woodland

d) Buttongrass moorland communities including buttongrass moorland (undifferentiated),buttongrass moorland with emergent shrubs, eastern buttongrass moorland and pure buttongrass moorland

Figure 4-16 Maps showing ranges of key vegetation types within the Lake St Clair region. Data source:(Department of Primary Industries, Parks, Water and Environment, 2013)

4.4 The Lake St Clair Pollen Signal

A summary of the key pollen taxa is presented in table 4.2 and discussed below:

4.4.1 Nothofagus cunninghamii

Nothofagus cunninghamii (fig. 4.10) is widespread as part of the regional pollen rain occurring in samples from all vegetation types. Median background values range between 12-15% in vegetation types where *Nothofagus cunninghamii* is absent and strong local pollen sources are absent, median values being slightly lower at 3-10% in dry eucalypt forest samples which are dominated by *Eucalyptus* spp. pollen. Values in Lake St Clair range between 14-19%* (median=16%). Although *Nothofagus cunninghamii* pollen is present in all vegetation types, high values are a clear indicator of local presence of *Nothofagus cunninghamii-Atherosperma* rainforest (51-76%; median=75%) and wet eucalypt forests (19-55%; median=42%) at lower altitudes. In the latter case, wet eucalypt forest with a *Leptospermum* understorey is an exception due to the strong representation of *Leptospermum*/*Baeckea* pollen in these samples. The pollen of *Nothofagus cunninghamii* is widely dispersed by wind and the pollen source area is large due to the widespread distribution of the taxon ranging from sea level through to c. 1200 m where it can be found growing in shrub form (Kirkpatrick et al., 1997; Read, 1999). The taxon is generally over-represented in all vegetation types (Hope, 1974; Colhoun and Goede, 1979; Macphail, 1979; Hopf, 1997; Fletcher and Thomas, 2007b) although has also been has been found to represent abundance in the vegetation well when growing locally (Fletcher and Thomas, 2007b).

4.4.2 Phyllocladus aspleniifolius

Phyllocladus aspleniifolius (fig. 4.10) is also a component of the regional pollen rain occurring in samples from all vegetation types. However, median background values are lower than for *Nothofagus cunninghamii,* with values generally between 2-6% and as low as 1% in dry eucalypt forest samples. Values in Lake St Clair range between 2-6% (median=5%). Where present in the vegetation, *Phyllocladus* often does not exceed typical median background values although the range is generally higher extending to 16% in rainforest and 13% in wet eucalypt forest at lower altitudes. *Phyllocladus aspleniifolius* also has a widespread distribution from sea level through to c. 1200 m where it performs better on poorer soils than *Nothofagus cunninghamii* (Read, 1999). It is generally over-represented by its pollen when not present in the vegetation (Colhoun and Goede, 1979; Macphail, 1979; Hopf, 1997; Fletcher and Thomas, 2007b) and its representation may vary from over- to under-represented when present in the vegetation (Hopf, 1997; Fletcher and Thomas, 2007b).

Table 4-2 Summary information for the key pollen taxa encounted in Lake St Clair samples

Pollen Taxon	Background (median)	Lake St Clair (median)	Regional Pollen Rain	Local	Indicator	Pollen Source Area
Eucalyptus spp.	10-26%	25%	✓	✓	High median values indicative of dry eucalypt forest (34-71%)	Widespread across Tasmania from sea level to alpine zone
Poaceae	1.5-8.9%	18%	✓	~		Limited proximal grassy vegetation, most abundant in drier east and northeast
Nothofagus cunninghamii	12-15%	16%	✓	✓	High median values indicative of rainforest (75%) and wet eucalypt forest (42%)	Widespread from sea level to alpine zone where not limited by precipitation
Phyllocladus aspleniifolius	1.5-6.4%	5.0%	✓	✓		Widespread from sea level to alpine zone where not limited by precipitation
Asteraceae	0.3-3.3%	6.8%	✓	✓		Widespread
Amaranthaceae	0.2-1.5%	3.4%	✓	×	LDT	Coastal areas and midlands, mainland
Allocasuarina spp.	0.0-3.1%	1.0%	✓	✓	LDT, slightly elevated dry eucalypt where present	Widespread, most abundant in drier east
***Pomaderris apetala* type**	0.2-2.6%	1.3%	✓	✓		Widespread
Athrotaxis /Diselma	0.0-1.3%	5.2%	~	✓	Higher values indicative of *A.cupressoides - N. gunnii* short rainforest (very fire sensitive)	Most proximal source areas include *A. cupressoides* communities and *Diselma* in alpine coniferous heath in Central Highlands and Plateau area, *A. selaginoides* more prominent in west but small pockets in catchment, *Callitris* abundant in drier east
Eucryphia /Anodopetalum		2.5%	×	✓	Rainforest and wet eucalypt forest	Local communities in the Lake St Clair catchment Limited aerial pollen transport Predominantly transported to lake by fluvial transport and slope-wash
Ericaceae		1.9%	×	✓	Higher values in alpine and moorland	
Leptospermum/Baeckea		1.3%	×	✓	Strong indicator of local presence	
Gymnoschoenus sphaerocephalus		1.0%	×	✓	Strong indicator of moorland	
Monotoca spp.		0.6%	×	✓	Widespread	
Atherosperma moschatum		0.3%	×	✓	Strong indicator of rainforest	
Orites/Bellendena		0.3%	×	✓	Higher values more frequent at higher altitudes but widespread	
Pherosphaera hookeriana		0.3%	~	✓	Alpine vegetation (very fire sensitive)	
Nothofagus gunnii		0.3%	×	✓	Alpine vegetation (very fire sensitive)	
Astelia alpina		0.3%	×	✓	Alpine vegetation	
Microcachrys tetragona		0.0%	×	✓	Alpine vegetation (very fire sensitive)	
Podocarpus lawrencei		0.0%	~	✓	Alpine vegetation (very fire sensitive)	

4.4.3 Eucalyptus

Eucalyptus (fig. 4.10) is occurs at median background values between 10-26% in vegetation types where it is not present, with values in Lake St Clair ranging between 23-28% (median=25%). High median values (34-71%) of *Eucalyptus* are an indicator of dry eucalypt forest, median values of wet eucalypt forest between 24-30% and ranging up to 47%.

Eucalyptus grows across a wide altitudinal range as a dominant component of the vegetation across Tasmania with 29 different species (de Salas and Baker, 2017; Jordan and Tng, 2017), the pollen of which unfortunately can not be distinguished. The pollen representation of *Eucalyptus* is variable with some studies finding it to be under- to well- (Colhoun and Goede, 1979; Derrick, 1962), well- (Phillips, 1941; Hope, 1974; Ladd, 1976), well- to over- (Dodson, 1977, 1983; Binder, 1978; Ladd, 1978, 1979a; Kodela, 1990a; Hopf, 1997; Fletcher and Thomas, 2007b) and well- (Ladd, 1979b; Macphail, 1979) represented.

Transect data from dry eucalypt forest/woodland to moorland at Excalibur Bog (see Chapter 6) and Liawenee Moor near Great Lake (Shimeld and Colhoun, 2001) indicate that *Eucalyptus* pollen values decrease abruptly within 6 m of the forest/woodland boundary onto moorland where they settle at median values of 25% at Excalibur Bog and values < 11% at Liawenee Moor (Shimeld and Colhoun, 2001).

4.4.4 Poaceae

Poaceae (fig. 4.10) is a pollen taxon which is markedly amplified in Lake St Clair with values ranging between 16-20% (median=18%), compared with median background values of 2-9% across all vegetation types.

The pollen representation varies of Poaceae in other parts of Tasmania and mainland Australia varies from well- (Binder, 1978; Colhoun, 1980), well- to over- (Derrick, 1962; Derrick, 1966; Dodson, 1977, 1983, Ladd, 1978, 1979b, 1979a; Kodela, 1990a) to over- (Sands, 1967; Hope, 1974; Ladd, 1976; Macphail, 1979; Smart et al., 1979; Hopf, 1997; Fletcher and Thomas, 2007b) and Dodson (1983) suggests the taxon requires further research.

There is very little grassland within the local Lake St Clair catchment. There are a few small patches of highland grassland (Highland *Poa* Grassland, found > 600 m) on the Traveller Range to the east near Lake Sappho, on Mt Gould to the northwest, near Lake Petrarch in the Cuvier Valley to the west and on Mt Rufus to the southwest (fig. 4.11c). Highland grassy sedgeland (see figure 4.11d) is a little more widespread, in particular towards the southeastern corner of Lake St Clair as mentioned previously as a possible source of the slightly higher values of Poaceae in the southern mud-water interface sample group from Lake St Clair (fig. 4.10).

The most expansive areas of highland *Poa* grassland are found on the upper Central Plateau approximately 30 km to northeast towards Great Lake and 55-70 km to the NNW-NW including the basalt plains just north of Cradle Mountain and the Vale of Belvoir (Kitchener and Harris, 2013). Below 600 m, native grassland grades into a variety of lowland grassland communities found predominantly in the drier regions of eastern Tasmania, in particular the Midlands, as well as fringing the Tasmanian coastline as part of Coastal Grass and Herbfield. This constitutes the bulk of the grasslands found in Tasmania, a proportion of which has been human-induced through the burning and clearing of trees in grassy woodlands (Kitchener and Harris, 2013). Pre-1800, grassy vegetation covered a large part of central and eastern Tasmania with an almost absence of grassy vegetation in the west, northwest and northeast of Tasmania (Kirkpatrick, 1999).

Fletcher and Thomas (2007) found Poaceae to be a potential indicator of Eastern Moor in Western Tasmania, samples from which contained between 1-49% Poaceae in their study. Poaceae does not stand out as an indicator of moorland in the Lake St Clair dataset, despite being a drier environment it is present in similar levels through all vegetation types apart from being markedly elevated in the lake samples.

4.4.5 Asteraceae

Asteraceae (fig. 4.10) is widespread across all vegetation types as part of the regional pollen rain (Macphail, 1979) with median values generally low (0.3-3.3%), higher median values of 5% being indicative of highland and treeless vegetation. Values are elevated in Lake St Clair ranging between 5-9% (median=7%).

Asteraceae has been found to be well- (Hope, 1974; Fletcher and Thomas, 2007b), well- to over- (Kodela, 1990a) to over- (Phillips, 1941; Derrick, 1962; Derrick, 1966; Dodson, 1977, 1983; Macphail, 1979; Colhoun, 1980; Hopf, 1997) represented by its pollen.

4.4.6 Amaranthaceae

Amaranthaceae (fig. 4.10) is a widely transported pollen grain as part of the Tasmanian regional pollen rain (Macphail, 1979), the source vegetation being mostly confined to coastal sand dunes and salt marshes (Hill and Orchard, 1999). Low median background values between 0.2-1.5% occur across all vegetation types, with slightly elevated values 2-4% (median=3%) in samples from Lake St Clair.

Amaranthaceae has been found to be under- (Derrick, 1962), well- (Phillips, 1941; Derrick, 1962; Dodson, 1983), well- to over- (Kodela, 1990a) to over- (Hope, 1974; Dodson, 1977, 1983; Binder, 1978; Macphail, 1979; Hopf, 1997; Fletcher and Thomas, 2007b) represented.

4.4.7 Cupressaceae

There are three genera within the Cupressaceae in Tasmania which have indistinguishable pollen: *Callitris* being restricted to the drier forests of eastern Tasmania and *Diselma* and *Athrotaxis* both growing in the wetter rainforests of central and western Tasmania extending and into the alpine zone (fig. 4.17). All are very fire sensitive. *Diselma archeri* has a similar distribution to *Microcachrys tetragona* and its habit ranges from forming a small tree in subalpine rainforests to shrub form in coniferous heath and alpine shrubberies (Kirkpatrick 1982; Hill & Orchard, 1999; Jackson & Brown, 1999). *Athrotaxis* contains two key species *A. cupressoides* and *A. selaginoides* and a third hybrid between the two *A. laxifolia*. *A. cupressoides* mostly grows as a small tree within open subalpine woodland and *A. selaginoides* mostly grows as a tall rainforest tree extending to lower altitudes, although individuals can also be found growing in shrub form up into the alpine zone. *A. cupressoides* is most widespread in the Lake St Clair area, growing extensively on the Central Plateau, The Labyrinth and other mountains below the treeline (figure 4.15 a). The most extensive area of *A. selaginoides* grows at lower altitude in Pine Valley just northwest of Narcissus Bay, otherwise mostly found as individual plants occasionally (small trees/shrubs) and other vegetation communities to the west of Lake St Clair (figure 4.15 b). *Diselma archeri* is also widespread in the Lake St Clair catchment and is often found growing together with *A. cupressoides.* Although a component of *Callitris* pollen could be transported as LDT pollen, the Cupressaceae pollen is most likely to be from the genera *Athrotaxis* and *Diselma* and is named as such.

Macphail (1979) found the pollen of *Athrotaxis* to be widely dispersed and a component of the regional pollen in southern Tasmania, whereas Fletcher and Thomas (2007) found the taxon to be under-represented in the regional pollen rain in Western Tasmania. Hopf (1997) found Athrotaxis-*Diselma* to vary from under- to well- represented in the local vegetation in the Lake St Clair region which is consistent with the wider dataset analysed in this study.

Elevated values in Lake St Clair (fig. 4.10) ranging between 4-7% (median=5%) relative to median background values of 0-1.3% in vegetation types where *Athrotaxis*/*Diselma* is absent suggests that Lake St Clair captures a mixed signal of local and regional *Athrotaxis*/*Diselma*. However, it is difficult to ascertain whether the amplified values in the lake are a consequence of wind transport of regional pollen or increased transport of the taxon by water, similar to the case of increased fern spores in lake/marine sediments. Due to the large potential source area of Cupressaceae pollen within the Lake St Clair catchment and the broader Tasmanian region, it is likely to be a combination of both.

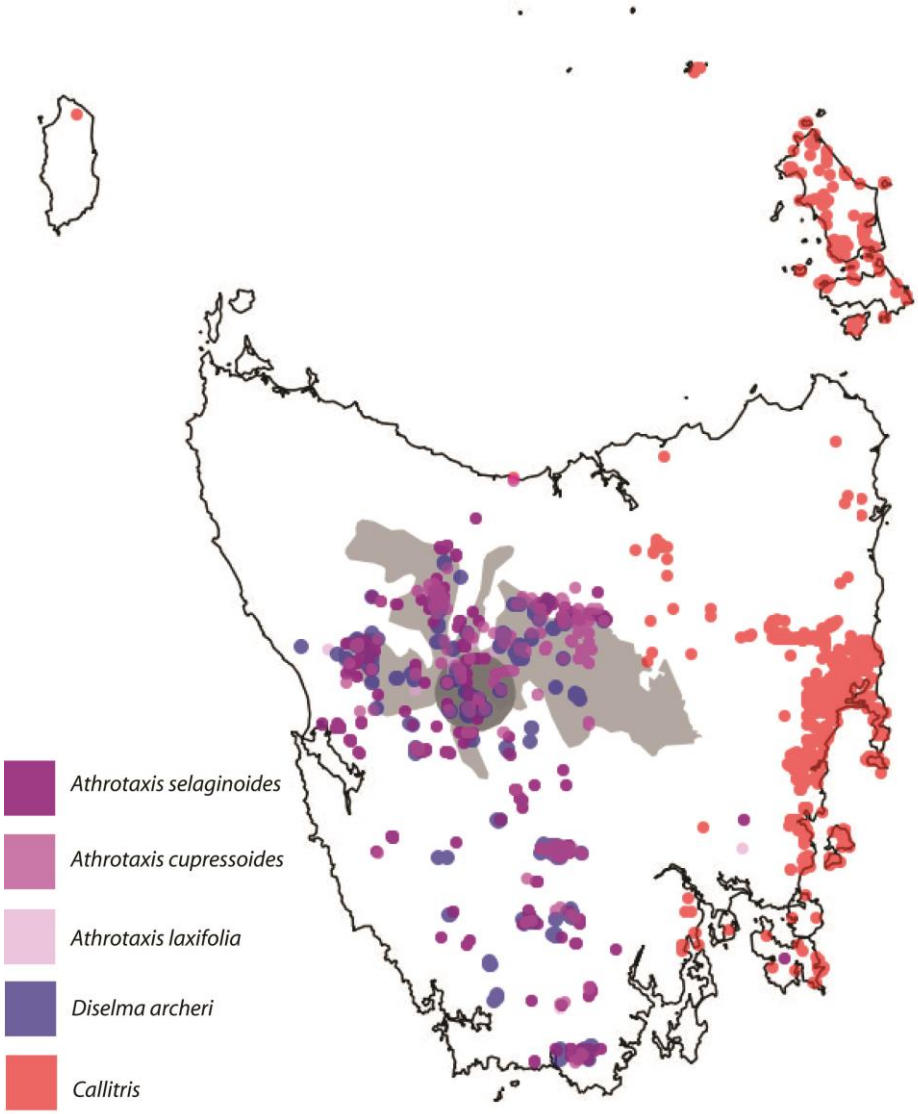

Figure 4-17 Distribution of the Cupressaceae family in Tasmania. *Data source: Atlas of Living Australia https://www.ala.org.au/*

4.4.8 Ericaceae

Ericaceae is widespread across all vegetation types with median values between 0-8%, with a median value of 1.85% recorded for Lake St Clair. Higher median values are indicative of eastern alpine heathland (8-23%) and moorland (19%). Fletcher and Thomas (2007) found Ericaceae to be the only other taxon other than *Gymnoschoenus sphaerocephalus* to be consistently present in all moorland samples.

Studies have found the taxon to be under- (Hope, 1974; Binder, 1978; Macphail, 1979; Hopf, 1997) and under- to well- (Ladd, 1979a; Fletcher and Thomas, 2007b) represented.

4.4.9 Eucryphia/Anodopetalum

The pollen of *Eucryphia* and *Anodopetalum* is difficult to reliably distinguish (Colhoun, 1980) and is grouped in pollen counts as *Eucryphia/Anodopetalum*. Both are a component of rainforest on poorer sites (Read, 1999), where *E. milliganii* can also be found as a component of alpine and coniferous heath in western and central Tasmania (Kirkpatrick et al., 1997)

Eucryphia/Anodopetalum (fig. 4.11) is a poorly dispersed, insect pollinated taxon which is under-represented (Macphail, 1979; Hopf, 1997; Fletcher and Thomas, 2007b). Values are highest for wet eucalypt forest (up to 5.7%) and rainforest (up to 3.1%) samples where part of the vegetation, the taxon is otherwise mostly absent from other vegetation types except as occasional trace values.

Lake St Clair samples record a median value of 2.5%, however, are variable and some samples recorded values up to 9.1%. This is likely a result of variable water transport from rainforest and wet eucalypt forest near the lake or rivers/creeks. Mud-water interface samples from Lake Dixon and Shadow Lake record values of 5.7% and 11.1% respectively, indicating water transport of this poorly dispersed, insect pollinated taxon is important.

4.4.10 Atherosperma moschatum

Atherosperma moschatum is severely under-represented in the pollen record (Ladd, 1979a; Macphail, 1979; Hopf, 1997; Fletcher and Thomas, 2007b). It is a clear indicator of *Nothofagus cunninghamii-Atherosperma* rainforest (fig. 4.11, table 4.1) in this dataset with a median value of 3.3%. The pollen is virtually absent in samples from other vegetation types and often times may be absent even if the source plant is present in the vegetation (Hopf, 1997; Fletcher and Thomas, 2007). An example includes a sample of *Nothofagus cunninghamii-Atherosperma* rainforest where *Atherosperma* is co-dominant with *Nothofagus cunninghamii* (approximately 45% cover each) and the pollen sample contains only 3% *Atherosperma* with *Nothofagus cunninghamii* strongly over-represented at 77%. In another rainforest sample, *Atherosperma* present at 45% in the vegetation and completely absent from the pollen sample in which *Nothofagus cunninghamii* is over-represented and *Phyllocladus* well-represented.

Even small values of *Atherosperma* in the pollen record should be interpreted as significant presence in the local vegetation. The median value of *Atherosperma* is low (0.3%) in Lake St Clair although values up to 1.8% are recorded in some mud-water interface samples indicating that the pollen is transported to the lake, most likely by slope-wash and fluvial transport from rainforests near the lake.

4.4.11 Gymnoschoenus sphaerocephalus

Gymnoschoenus sphaerocephalus (fig. 4.11) is poorly dispersed and as a result under-represented in the pollen record (Macphail, 1979; Hopf, 1997; Fletcher and Thomas, 2007b). It is a clear indicator of moorland vegetation, but, like *Atherosperma* may be absent from samples even if present in vegetation. A median value of 15.3% and values up to 36% were recorded for the taxon from the Excalibur Bog moorland, however, only traces were recorded in other samples.

4.4.12 Orites/Bellendena

Four species of *Orites* grow in Tasmania, *O. revoluta* and *O. acicularis* being most widespread in the Lake St Clair area where they are most common as dominant components of alpine and subalpine heath (Kirkpatrick et al., 1997; Jordan and Tng, 2017). The pollen is difficult to distinguish from *Bellendena montana* which is also widespread in alpine and subalpine heaths. The pollen of both genera are grouped as *Orites*/*Bellendena* and, although widespread in samples from all vegetation types, is more prevailent at higher altitudes and thus a suggested indicator of subalpine/alpine vegetation. In the pollen diagram (fig. 4.7) it can be observed that higher percentages of *Orites*/*Bellendena* occur at higher altitudes (generally above 900 m) in dry eucalypt forest, wet eucalypt forest, rainforest, highland and treeless vegetation and tarns within these vegetation types.

Values of *Orites*/*Bellendena* range up to 18% when present in the vegetation, although median values are generally below 5% and the taxon only occurs as traces in other samples when not present in the vegetation. Values are low in Lake St Clair (median=0.3%, ranging up to 1.7%) and the pollen is likely transported by water to the lake.

4.4.13 Alpine Taxa

Unlike other alpine areas in the world, the Tasmanian alpine zone lacks a pronounced grass-herbaceous component and instead is dominated by woody shrubs which lack a strong pollen signal resulting a large component of pollen in samples being derived from the regional pollen rain.

Most key alpine taxa, when present in the record, are strong indicators of the alpine source vegetation (Table 4.1) growing locally and include *Pherosphaera hookeriana*, *Microstrobos tetragona*, *Podocarpus lawrenceii* and *Nothofagus gunnii* (fig. 4.11). These taxa have all been found to be under-represented in various studies (Binder, 1978; Ladd, 1979a; Macphail, 1979; Hopf, 1997; Fletcher and Thomas, 2007b) and only occur as traces in some lake samples and in other vegetation types where source plants are not growing. The taxa are also united, like *Athrotaxis* and *Diselma*, by being very sensitive to fire and their distributions are strongly

restricted to locations which have been protected from fire. Macphail suggests that *Pherosphaera hookeriana* is also a possible component of the regional pollen rain in southern Tasmania (Macphail, 1975, 1979) and this could explain the value of 4.8% *Pherosphaera* in a mud-water interface sample from Lake Dixon which lies to the southwest of Lake St Clair at an elevation of 661 m well below the alpine zone. The lake is surrounded by a mosaic of moorland, dry and wet eucalypt forest and rainforest.

4.4.14 Astelia alpina

Astelia alpina pollen is poorly dispersed and as a result under-represented (Hopf, 1997; Fletcher and Thomas, 2007), in some cases even absent from samples even if present in the vegetation (Hopf, 1997). Values up to 20-40% in the dataset are exclusively derived from tarn samples in highland and treeless vegetation where *Astelia* pollen has been washed into the tarns. Fletcher and Thomas (2007) also found it to be a good indicator of alpine wetland sites in Western Tasmania.

Astelia alpina (Liliaceae) is an endemic, mat-forming plant common on almost all Tasmanian mountains where it is found in most vegetation types. In the central and eastern mountains, it dominates tall alpine sedgeland with the alpine coral fern *Gleichenia alpina* (Gleicheniaceae) and the sedges *Empodisma minus* (Restionaceae), *Restio australis* (Restionaceae) and *Carpha alpina* (Cyperaceae). This type of alpine sedgeland occurs on fairly poorly drained, peaty soils and typically forms after fire resulting in the death of shrubs (Kirkpatrick, 1997).

4.4.15 Other regional taxa

Species of *Allocasuarina* occur across Tasmania being most widespread in drier eastern Tasmania, in particular through the midlands and towards the coast (fig. 4.18). *A. monilifera* and *A. zephyrea* are most common at higher altitudes in Central Tasmania, where they generally occur as shrubs in dry eucalypt forests. *Allocasuarina* constitutes part of the Tasmanian regional pollen rain Macphail (1979) and its representation has been found to vary from under- to well- (DERRICK, 1962), well- to over- (Kodela, 1990a) and over- (Phillips, 1941; Hope, 1974; Dodson, 1977, 1983; Binder, 1978; Macphail, 1979; Hopf, 1997). *Allocasuarina* (fig. 4.12) is present at low median background values between 0-3.1% across all vegetation types unless locally present in dry eucalypt forest where values up to 25% were recorded. The median value for Lake St Clair is 1%.

Pomaderris apetala type (fig. 4.8c) is also part of regional pollen rain (Macphail, 1979; Fletcher and Thomas, 2007) and the taxon has been widely found to be over-represented (Hope, 1974; Binder, 1978; Ladd, 1978; Colhoun and Goede, 1979; Macphail, 1979; Kodela, 1990a; Hopf, 1997; Fletcher and Thomas, 2007b). Median background values between 0-2.6% are recorded

across all vegetation types and 1.3% in Lake St Clair. The taxon is an indicator of wet eucalypt forest at Lake St Clair where values up to 10% are recorded.

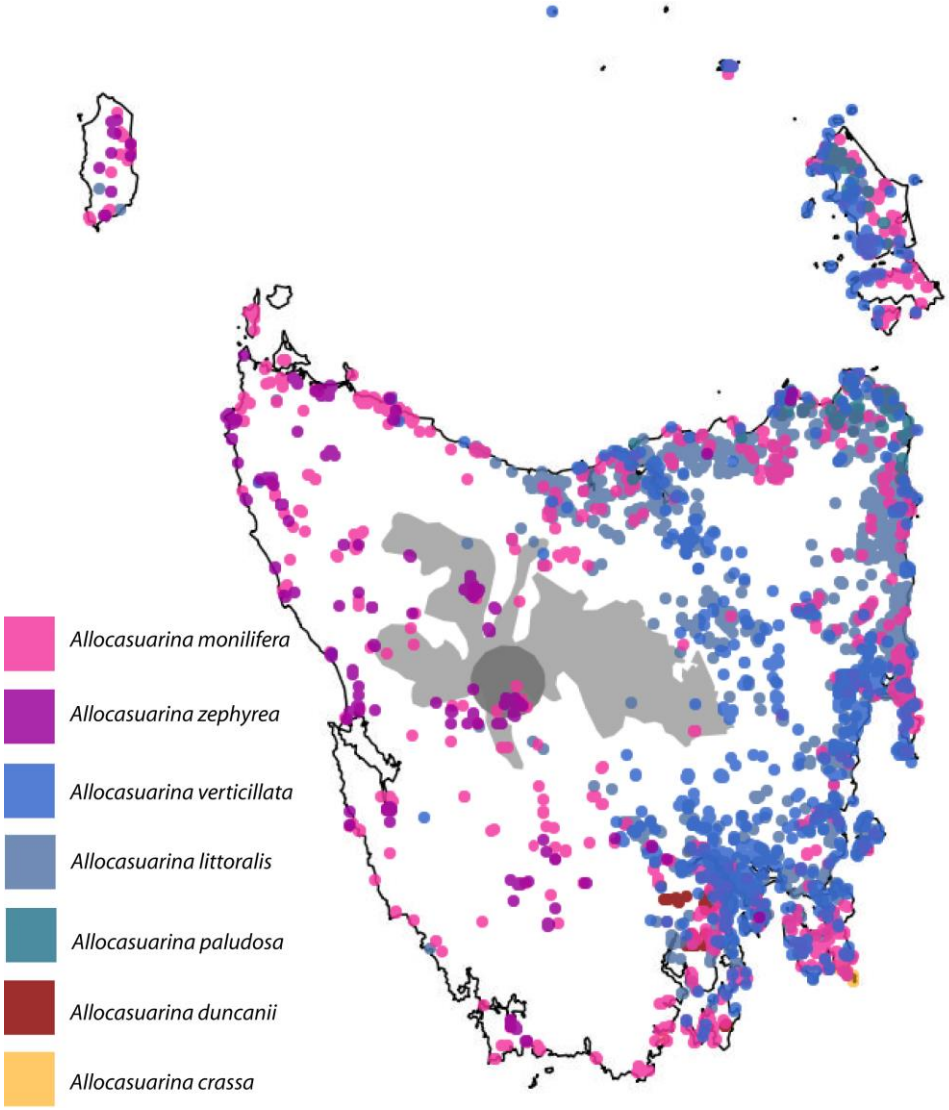

Figure 4-18 The distribution of the different species of Allocasuarina within Tasmania. Data source: Atlas of Living Australia https://www.ala.org.au/

4.4.16 Other taxa also common in pollen diagrams

The pollen of *Leptospermum* and *Baeckea* is difficult to distinguish and has been grouped in pollen counts as *Leptospermum*/*Baeckea*. Species of *Leptospermum* are common across all vegetation types with *L. rupestre* common as an alpine/subalpine shrub. *Baeckea gunniana* is likewise a common alpine/subalpine shrub.

Leptospermum/*Baeckea* (fig. 4.12) is generally well-represented when growing in the vegetation (Hope, 1974; Dodson, 1977, 1983, Ladd, 1978, 1979a). In the Lake St Clair dataset, high median values of 26% indicative of wet eucalypt forest where *Leptospermum* forms the understorey and median values up to 10% in some types of dry eucalypt forest.

Lake St Clair samples have a median value of 1.3%, but some samples record up to 4.8%, the variation likely attributed to water transport from source vegetation proximal to the sample site.

Monotoca (fig. 4.12) is widespread at low values in all vegetation types except moorland. Occasional higher values occur when samples taken close to source plants (up to 33% in wet eucalypt forest and 8-10% in dry eucalypt forest), however median values are typically between 0.2-1.2% with Lake St Clair recording a median of 0.6%.

The representation has been found to variable with studies finding *Monotoca* to be well- (Fletcher and Thomas, 2007), over- (Hopf, 1997) and under- to over- (Kodela, 1990) represented. Fletcher and Thomas (2007) also found *Monotoca* with values ranging between 1-50% common in many rainforest sites (1-50%), low to moderate values between 1-9% in blanket moor and an absence from samples from eastern moor which is similar to the findings of this study.

4.5 Conclusions

Regional pollen types indicated in table 4.2 with variably large pollen source areas across Tasmania are likely to represent broad scale changes in vegetation driven by climate in pollen record. Although not analysed, the pollen record is likely to be biased by the dominant wind direction from the NW. The Tasmanian pollen record is already biased towards certain vegetation types, rainforest and wet/dry eucalypt forest. Alpine vegetation and moorland are under-represented due to a lack of strong pollen sources. Similarly, an important, often "invisible" pollen taxon, is *Atherosperma moschatum*, an important co-dominant of callidendrous rainforest. Small values and changes in values of indicator taxa in the record need to be taken as significant, notably *Gymnoschoenus* (moorland), *Atherosperma* (callidendrous rainforest) and alpine taxa (*Microcachrys*, *Pherosphaera*, *Podocarpus*, *N. gunnii*, *Orites*).

Local pollen types are indicative of more specific vegetation within the catchment. Being predominantly transported to the lake by water, they will be most influenced by changes in climate that cause changes in precipitation, in particular variations to storm events resulting in flood events/increased river flow, which may result in spikes of local taxa (Brown, 1985). *Eucryphia* clearly displays this variability in the modern mud-water interface samples from Lake St Clair. In addition, water transported pollen assemblages derived from catchment soils can be biased towards more resistant pollen and spore types (Wilmshurst and McGlone, 2005; Qin et al., 2015).

Fletcher and Thomas (2007) analysed the modern pollen-vegetation relationships in Western Tasmanian rainforest, moorland and alpine/subalpine vegetation. This study adds a dataset from Central Tasmania with the addition of two additional vegetation types analysed: wet and dry eucalypt forests and woodlands.

Chapter 5 Results: Lake St Clair

5.1 Sediments and Dating

5.1.1 Particle Size Analysis

Core CG (CG-LC) consists of 116 cm of glacial sands, silts and clays overlain by 432 cm of lacustrine sediments. The short core (CG-SC) collected from the Mackereth Core CG location consists of 22 cm of lacustrine sediments. Particle size analysis (PSA) was carried out at 10 cm intervals on core CG-LC and the results are presented in Figure 4. Stratigraphically constrained cluster analysis (CONISS) of the PSA data identified 3 key zones:

Zone PSA 1 incorporates the basal glacial sands, silts and clays. Visually, these sediments consist of many alternating layers of coarse silts and sands with finer clays and silts which are not picked up in detail in the PSA results due to the coarse resolution of the analysis. The section between 480 cm and 460 cm was analysed at 2 cm intervals to explore the secondary magnetic susceptibility peak observed during the whole core magnetic susceptibility measurements. The PSA revealed that the secondary magnetic susceptibility peak occurs during a band of coarser sandy sediment.

Zone PSA 2 consists of a period of relatively uniform sediments, mostly silts, with very little variation in the proportion of the different size fractions.

Zone PSA 3 begins with a period of considerably coarser sediment deposition, mainly coarse silts and sands, between 231 cm and 201 cm followed by medium silts between 211 cm and 181 cm. The remainder of the zone reverts to more uniform deposition with two smaller pulses of coarser sediment at 141 cm and 121 cm.

5.1.2 Total Organic Matter and Carbon/Nitrogen Analysis

The total organic matter (%) was estimated by loss on ignition at 10 cm resolution (see Figures 4 and 5). Total carbon and nitrogen were also determined using a Vario Max CNS element analyser at 4 cm resolution and the results are presented in Figure 5. The total organic matter (%) and total carbon curves follow the same trend of a progressive increase from the base of the core until around 270 cm where levels increase more steeply leading into elevated values between ~ 236 cm and 171 cm. After 180 cm, total organic matter (%) exhibits a slightly increasing trend, whereas total carbon values exhibit a notable decrease between 180 cm and 127 cm. After another peak at 127 cm, total carbon values mostly remain between 8 and 10 to the top of the core.

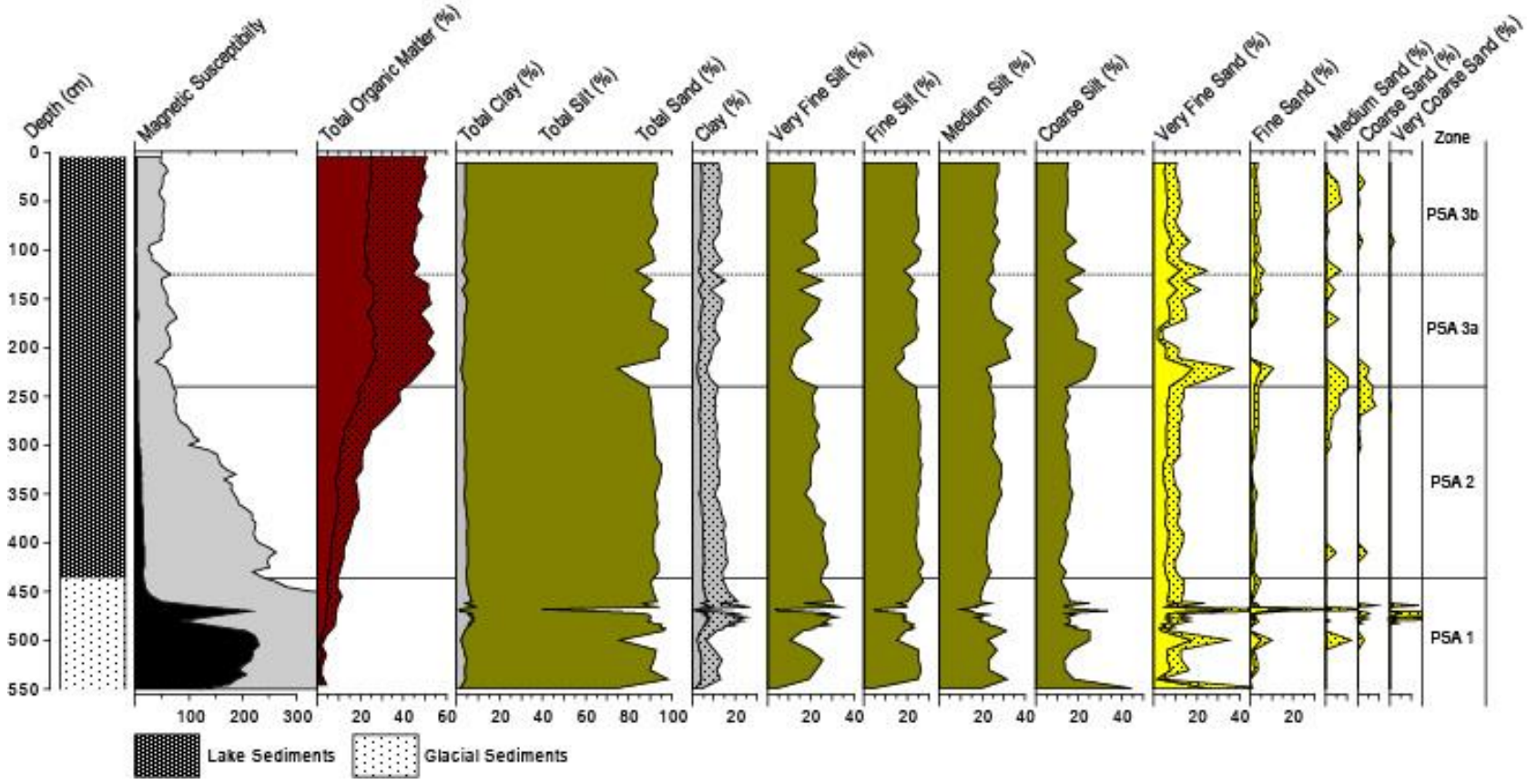

Figure 5-1 Core CG-LC sediment properties: magnetic susceptibility, total organic matter (%) and particle size analysis.

The C/N ratio is mostly very high in the glacial sediments indicating that there was a strong input of terrestrial plant matter along with the glacial sediments. C/N ratios are much reduced for the overlying lake sediments. Initially values are lower and range mostly between 10 and 14 until 288 cm after which ratios remain mostly above 15 ranging as high as 27 at 220 cm and 180 cm. This suggests there was a higher, yet variable, input of terrestrial plant matter after 288 cm compared with the previous period, the ratios of which are more intermediate between those of terrestrial plant matter (generally over 17) and fresh algal material (generally between 4 and 10) (Meyers & Teranes, 2001).

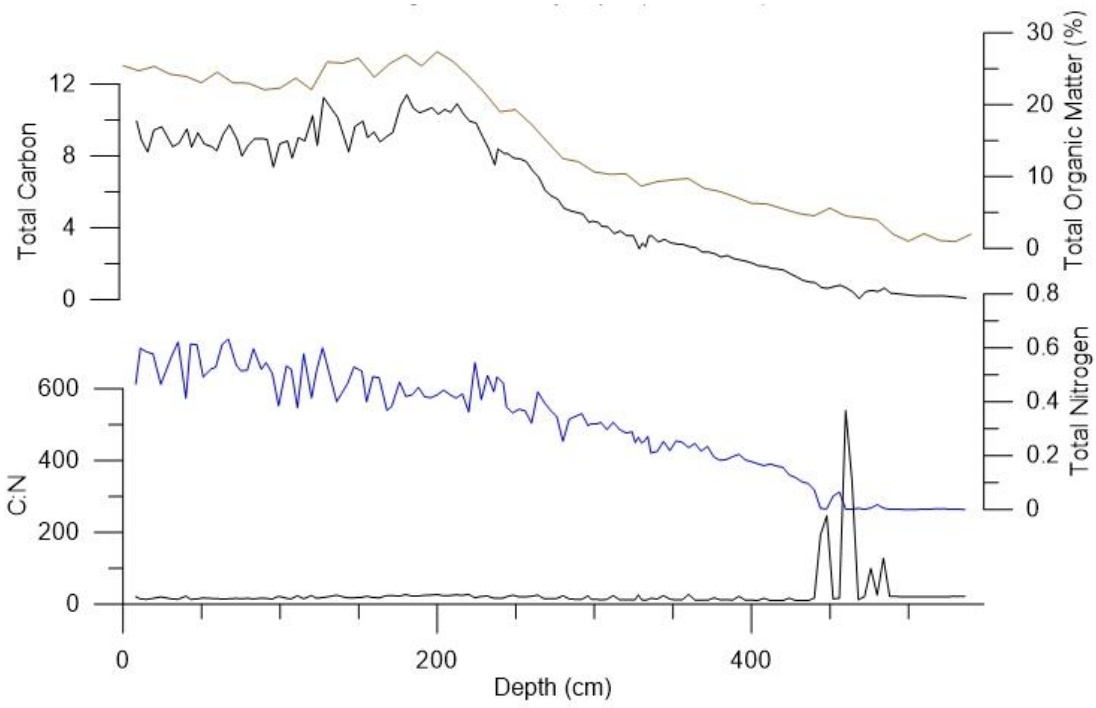

Figure 5-2 Carbon nitrogen results by depth for core CG-LC.

5.1.3 Radiocarbon Dating

Twenty-seven ^{14}C radiocarbon dates were obtained for the CG core location: 23 for the long core CG-LC and four for the short core CG-SC. The results are shown in Table 5.1. An age depth model produced with BACON is presented in Figure 5.3. For those samples where the humin and humic acid fractions were dated separately, the humin fractions fell as outliers (see BACON output in Figure 6). Only small amounts of carbon were retrieved from these samples resulting in large uncertainties on the ages. BACON also identified the ages obtained for 302 cm, 304 cm and 324 cm as outliers. The age model suggests a relatively uniform deposition rate (41 yr/cm; 2.4 mm/yr) for the lake sediments from near the boundary at 432 cm / ca. 18.5-18.0 cal kyr BP until present apart from the topmost samples where deposition according to the age model slows which can be explained by loss of sediment at the top at the sediment

water interface. The ages of the basal sediments (432-548 cm) are considerably older and the age model suggests a basal date of 35.2 cal kyr BP for core CG-LC. The basal age of core CG-SC (1717-1878 (95%) cal kyr BP at 20-21 cm) overlaps with the topmost age obtained for core CG-LC (1303-1488 (92.3%) at 12-13cm), suggesting that there is no time gap between the two cores. The uppermost age obtained for the short core of 612 (668-560) cal yr BP at 2-3 cm suggests that there could be a reservoir effect in the order of 500 years in the lake. Applying the deposition rate of 1 cm in 65 years between 2-3cm and 20-21cm to extrapolate age of the mud water interface produces an age of 482 cal yr BP. Alternative, slowing of sedimentation rate unlikely, or loss of surface sediment/mixing.

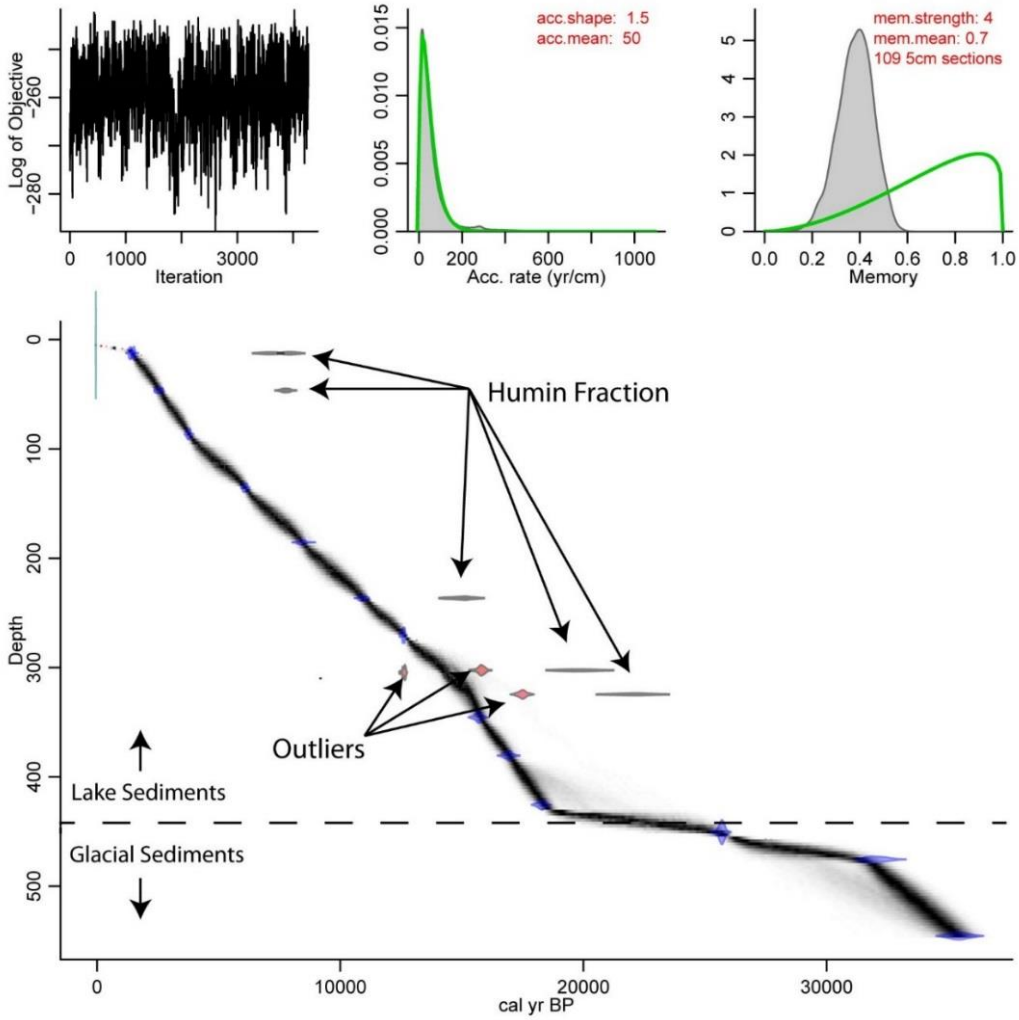

Figure 5-3 BACON age model for Core CG-LC.

Table 5-1 Table of radiocarbon dates obtained for cores CG-LC and CG-SC.

Depth (cm)	Lab Code	Material Dated	Radiocarbon Age (^{14}C yr BP)	Error (^{14}C yr BP)	□^{13}C	Calibrated Age (cal yr BP) [mean (range)]
1-2	ANU 32035	Humin fraction	5130	60	-22.94	5821 (5981-5661)
2-3	ANU 34429	Humic acid fraction	705	25	-29.42	612 (668-560)
20-21	ANU 32033	Humin fraction	6220	120	-10.80	7064 (7410-6750)
20-21	ANU 31027	Humic acid fraction	1900	35	-26.50	1793 (1880-1715)
12-13	ANU 32029	Humin fraction	6270	270	50.14	7087 (7610-6496)
12-13	ANU 31029	Humic acid fraction	1650	35	-27.33	1493 (1579-1411)
12-13 (duplicate)	ANU 32019	Humin fraction	7150	250	19.10	7958 (8410-7508)
12-13 (duplicate)	ANU 31035	Humic acid fraction	1535	50	-26.06	1387 (1511-1303)
46-47	ANU 32027	Humin fraction	6950	180	4.87	7768 (8151-7435)
46-47	ANU 31030	Humic acid fraction	2505	35	-21.71	2551 (2711-2365)
86-87	ANU 9909	Bulk sediment	3540	30	-28.81	3768 (3871-3646)
135-136	ANU 9910	Bulk sediment	5350	30	-28.08	6088 (6201-5950)
185-186	ANU 9911	Bulk sediment	7660	120	-29.34	8428 (8700-8170)
236-237	ANU 32026	Humin fraction	12740	190	-26.55	15013 (15697-14241)
236-237	ANU 31031	Humic acid fraction	9605	50	-22.39	10918 (11126-10711)
270-271	ANU 9912	Bulk sediment	10660	30	-27.38	12603 (12675-12451)
302-303	ANU 32025	Humin fraction	16420	540	-5.40	19857 (21221-18622)
302-303	ANU 31037	Humic acid fraction	13200	60	-27.88	15804 (16050-15568)
304-305	ANU 34538	Humic acid fraction	10705	50	-29.36	12627 (12714-12455)

324-325	ANU 32021	Humin fraction	18310	580	-12.69	22109 (23530-20703)
324-325	ANU 34525	Humic acid fraction	14400	90	-32.30	17491 (17788-17186)
345-346	ANU 9913	Bulk sediment	13120	40	-26.96	15676 (15895-15415)
380-381	ANU 9914	Bulk sediment	14000	50	-28.68	16924 (17157-16655)
425-426	OZD 286	Bulk sediment	15090	80		18278 (18521-18026)
450-451	ANU 9916	Bulk sediment	21390	80	-30.47	25686 (25880-25489)
475-476	OZD 287	Bulk sediment	28200	250		32057 (32795-31394)
545-546	OZD 288	Bulk sediment	31600	300		35459 (36110-34836)

5.2 Charcoal Analysis

The results of the macroscopic charcoal peak detection using CharAnalysis (Higuera et al., 2009) are presented in Table 5.2 and Figure 5.5. Peaks with a signal to noise ratio (SNI) greater than 3.0 were selected (Kelly et al., 2011) to represent significant fire episodes. These are highlighted in grey in Table 5.2 and in red in Figure 5.4.

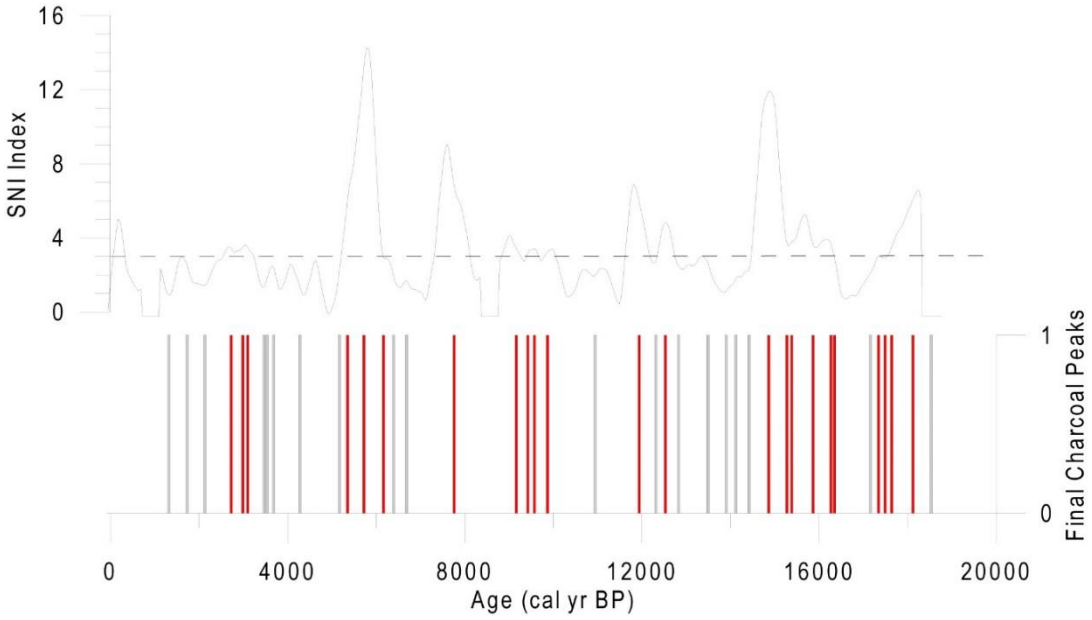

Figure 5-4 Macroscopic charcoal peaks and SNI detected by CharAnalysis. The peaks with an SNI over 3 are coloured red and those less than 3 in grey.

Both macroscopic and microscopic charcoal accumulation rates along with these fire events against time in figure 8 to give an overview of local and regional fire history recorded in Lake St Clair. was used to calculate charcoal accumulation rates (CHAR; particles/cm/yr) from the macroscopic charcoal counts which were then analysed to extract significant charcoal peaks.

5.2.1 Zone 1: > LGM – 18.2 cal kyr BP

The glacial sediments are low in both microscopic and macroscopic charcoal. No significant peaks were identified by CharAnalysis.

5.2.2 Zone 2: 18.2 – 14.9 cal kyr BP

Both microscopic and macroscopic charcoal increase and peak at the start of the zone and then exhibit a decreasing trend. CharAnalysis identified 10 charcoal peaks during this period with an SNI over 3.0, however, most of these peaks have an SNI of 4.0 or less apart from the peaks at 18.1 and at 14.9 cal kyr BP at the boundary to Zone 3.

5.2.3 Zone 3: 14.9-7.9 cal kyr BP

During this period, both microscopic charcoal and macroscopic charcoal accumulation rates are reduced. CharAnalysis identified 6 charcoal peaks during this period, however, the average peak magnitude is lower than for Zone 2.

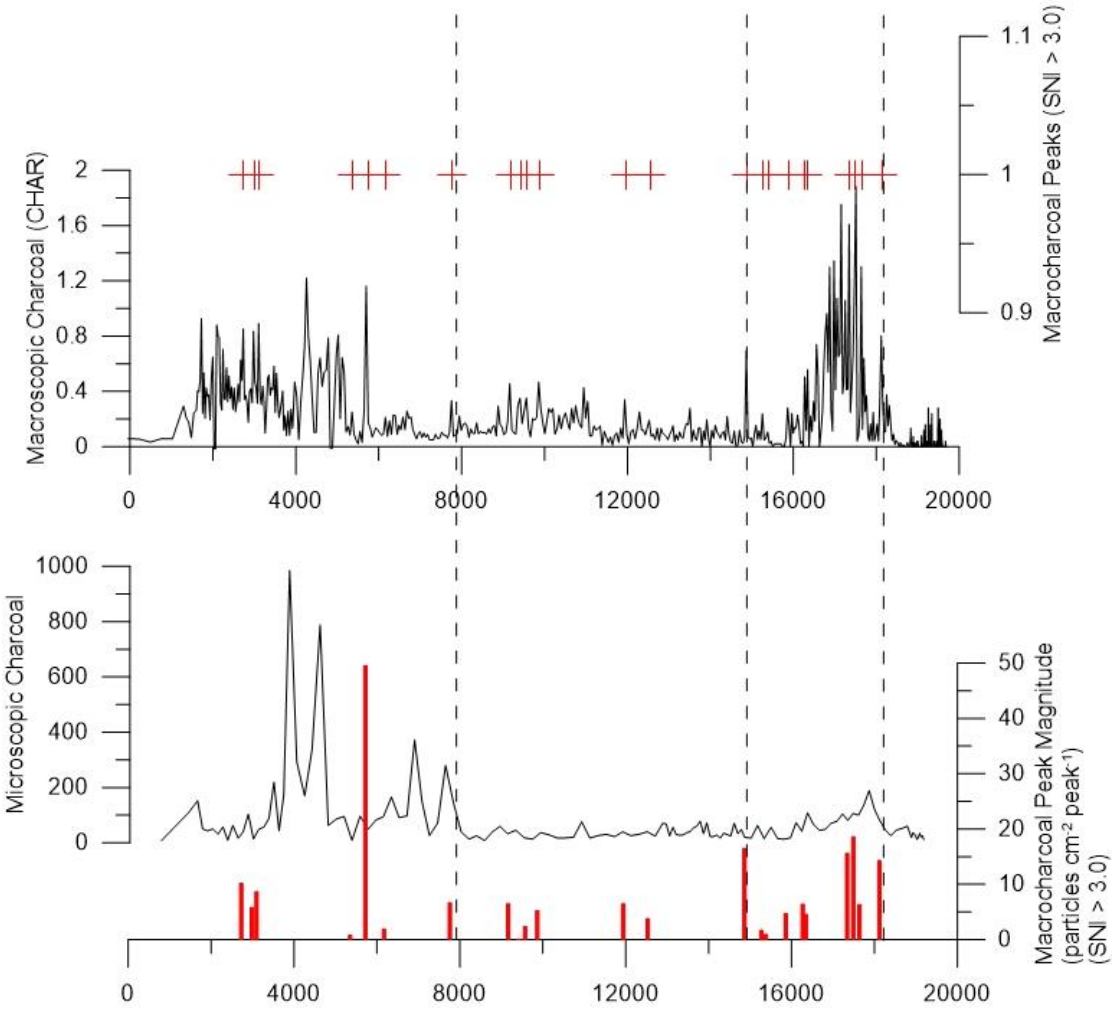

Figure 5-5 Macroscopic and microscopic charcoal accumulation rates along with the number and magnitude of macroscopic charcoal peaks with an SNI > 3.0. The CONISS derived pollen zones are indicated on the graphs as dashed lines.

5.2.4 Zone 4: 7.9-0.8 cal kyr BP

Microscopic charcoal accumulation rates increase at the start of this zone and exhibit two peaks at 7.6 and 6.9 cal kyr BP, followed by a period of lower levels of microscopic charcoal and then two large peaks at 4.6 and 3.9 cal kyr BP. Microscopic charcoal levels are mostly reduced levels towards the top of the core, but on average higher and more variable than during zone 2. Macroscopic charcoal accumulation rates, in contrast, remain low until about 5.7 cal kyr BP after which levels are elevated until almost the top of the core. CharAnalysis identified 17 peaks during this period, however, only 7 of these have an SNI over 3.0.

Table 5-2 Macroscopic charcoal peak magnitudes and SNI detected by CharAnalysis.

	Depth (cm)	**Age (cal yr BP)**	**SNI** (index)	**Peak Magnitude** (particles/cm^2/peak)
Pollen Zone 4	10.5	1321	1.13	0.6062
7.9-0.8 cal kyr BP	19.2	1728	2.81	6.8454
	32.4	2135	1.66	2.5941
	51.8	2727	3.65	10.1790
	60.2	2986	3.68	5.7608
	63.7	3097	3.73	8.6406
	75.8	3467	1.56	0.7118
	78.2	3541	2.00	0.5543
	83.3	3689	2.62	0.6956
	97.5	4281	1.59	12.2364
	116.1	5169	2.32	2.2194
	120.0	5354	6.15	0.7584
	127.5	5724	13.34	49.5330
	137.1	6168	3.13	1.8868
	141.8	6390	2.27	2.1411
	148.1	6686	1.90	0.9976
	171.1	7759	7.12	6.6271
Pollen Zone 3	201.1	9165	3.65	6.4758
14.9-7.9 cal kyr BP	206.3	9424	3.37	0.0934
	209.2	9572	3.62	2.3131
	215.2	9868	3.43	5.2293
	237.0	10941	2.18	1.9448
	257.1	11940	6.22	6.4517
	264.5	12310	2.90	2.0129
	269.2	12532	5.04	3.7636
	275.4	12828	2.71	0.1220
	291.7	13494	2.88	2.0861
	301.7	13901	1.31	0.1844
	307.2	14123	1.99	0.3985
	314.4	14419	2.45	1.4630
	324.9	14863	12.09	16.4928
Pollen Zone 2	335.4	15270	4.01	1.6893
18.2-14.9 cal kyr BP	338.1	15381	3.99	0.9100
	350.0	15862	3.90	4.6733
	361.9	16269	3.93	6.3943
	364.1	16343	3.27	4.5618
	387.1	17157	2.28	10.1621
	392.9	17342	3.23	15.5304
	397.5	17490	3.15	18.5838
	402.0	17638	3.67	6.3396
	417.0	18119	6.28	14.2728
Pollen Zone 1	429.32	18526	0.00	184.6477

The peak at 5.7 cal kyr BP has the highest for the record and is followed by a period of elevated macroscopic charcoal accumulation rates. The magnitude of the other peaks is mostly not much higher than those in the preceding zone. No significant macroscopic charcoal peaks were detected around the time of the two largest microscopic charcoal peaks although CHAR is elevated during this period relative to earlier periods.

5.3 Pollen Analysis

5.3.1 Percentage Pollen Diagram and CONISS

The pollen and spore record for Core CG is presented as a percentage pollen diagram in Figures 5.6-5.9. Four major pollen zones were selected after running CONISS on the terrestrial pollen dataset. Some zones are split into subzones, also based on CONISS, to facilitate descriptions of key changes within each zone. CONISS results indicate a boundary between zones 4 and 3 at 419 cm based on the terrestrial pollen dataset, however, if aquatics are included in the analysis, the boundary is placed at 432 cm which is the stratigraphic boundary between the glacial and lake sediments. For the purposes of the following descriptions, the zones based only on the terrestrial pollen dataset are used. The short core CG-SC is presented in Figures 5.10 and 5.11

5.3.2 Detrended Correspondence Analysis (DCA)

A DCA biplot for the terrestrial pollen dataset with the data categorised by the eight subzones selected based on CONISS results is presented in figure 5.12. A r-sqared cutoff value of 0.4 was used to plot the most significant taxon response vectors. Axis 1 explains 31% of variation in the dataset and is most strongly correlated with Poaceae and *Nothofagus cunninghamii* along with Amaranthaceae, Asteraceae and *Plantago*. Axis 2 explains 7.6% of variation in dataset and is most strongly correlated with *Phyllocladus* and Cupressaceae. The samples belonging to Zone 1 (<LGM – 18.2 cal kyr BP) form a distinctly separate group and are characterised by a Poaceae-Amaranthaceae-Asteraceae pollen assemblage. The remaining three zones also form distinct groups with a small amount of overlap. Zone 2 (18.2-14.9 cal kyr BP) encompasses a period of peak development of Cupressaceae. Zone 3 (14.9-9.7 cal kyr BP) *Phyllocladus-Eucalyptus-Nothofagus*. Subzone 3b covers the period of the Antarctic Cold Reversal and notably the samples from this time period form a distinct group both according to CONISS as well as DCA, which sit higher on Axis 2 than adjoining subzones 3a and 3c. Zone 4 (7.9-0.8 cal kyr BP) is marked by increasing importance of *Eucryphia*, *Eucalyptus* and herbs & forbs. The dataset of mud-water interface samples from St Clair is plotted to compare present variability within the lake with that observed in the past within the short and long core. The modern samples overlap with approximately half of the short core and a section of Zone 4b, the short core also overlapping with the section of subzone 4b highest on axis 1.

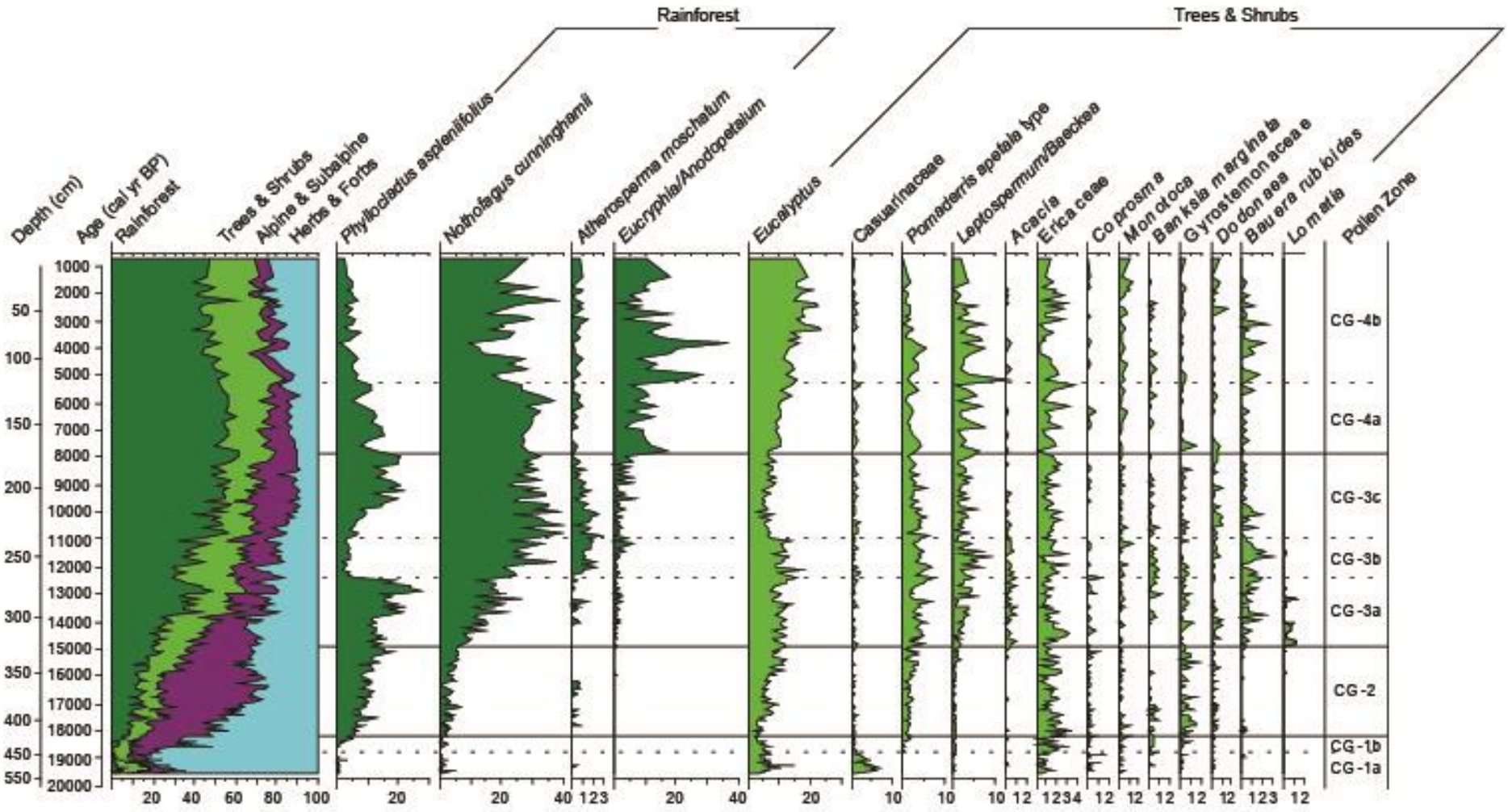

Figure 5-6 Core CG percentage pollen diagram (part 1). Note individual scaling of axes.

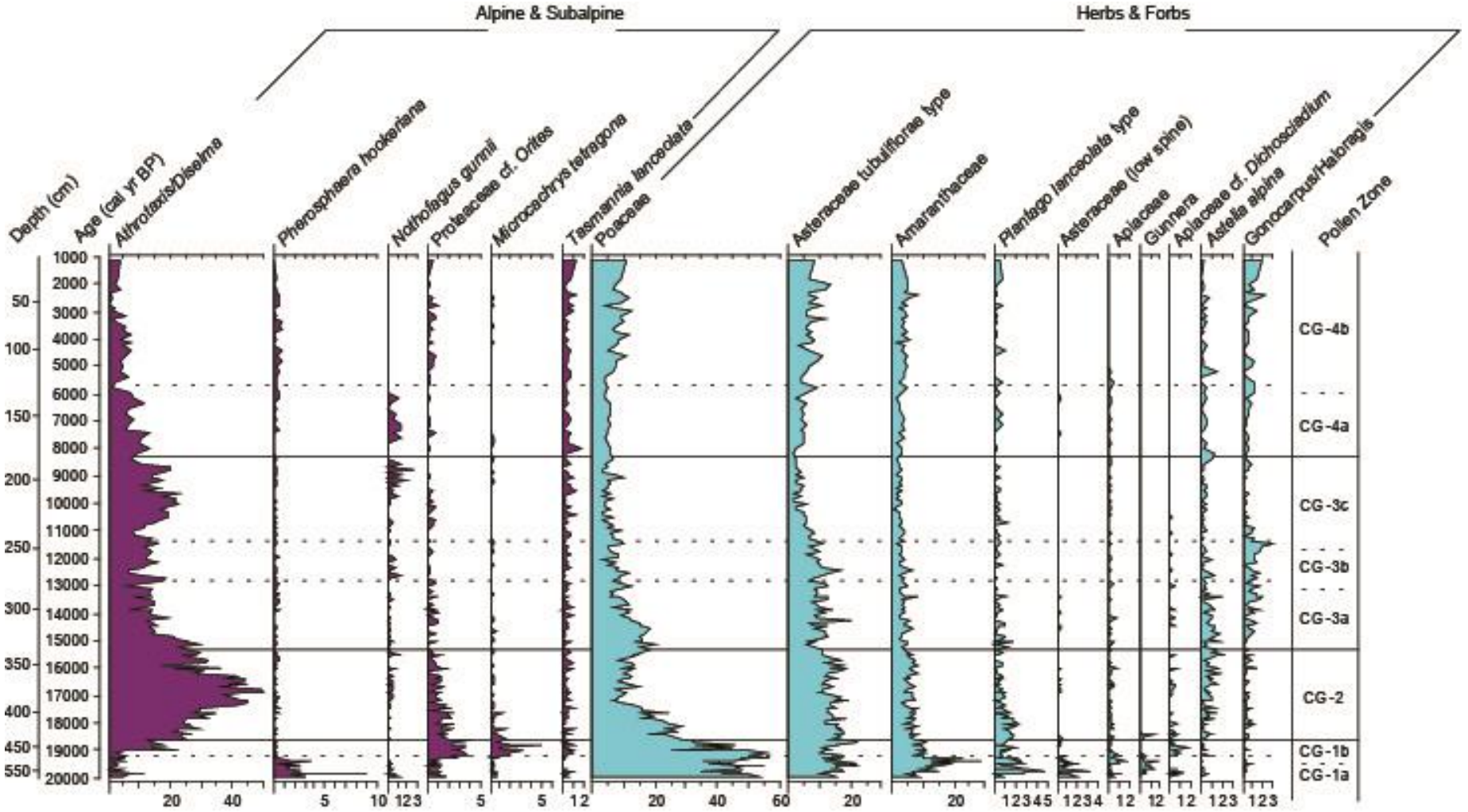

Figure 5-7 Core CG percentage pollen diagram (part 2). Note individual scaling of axes.

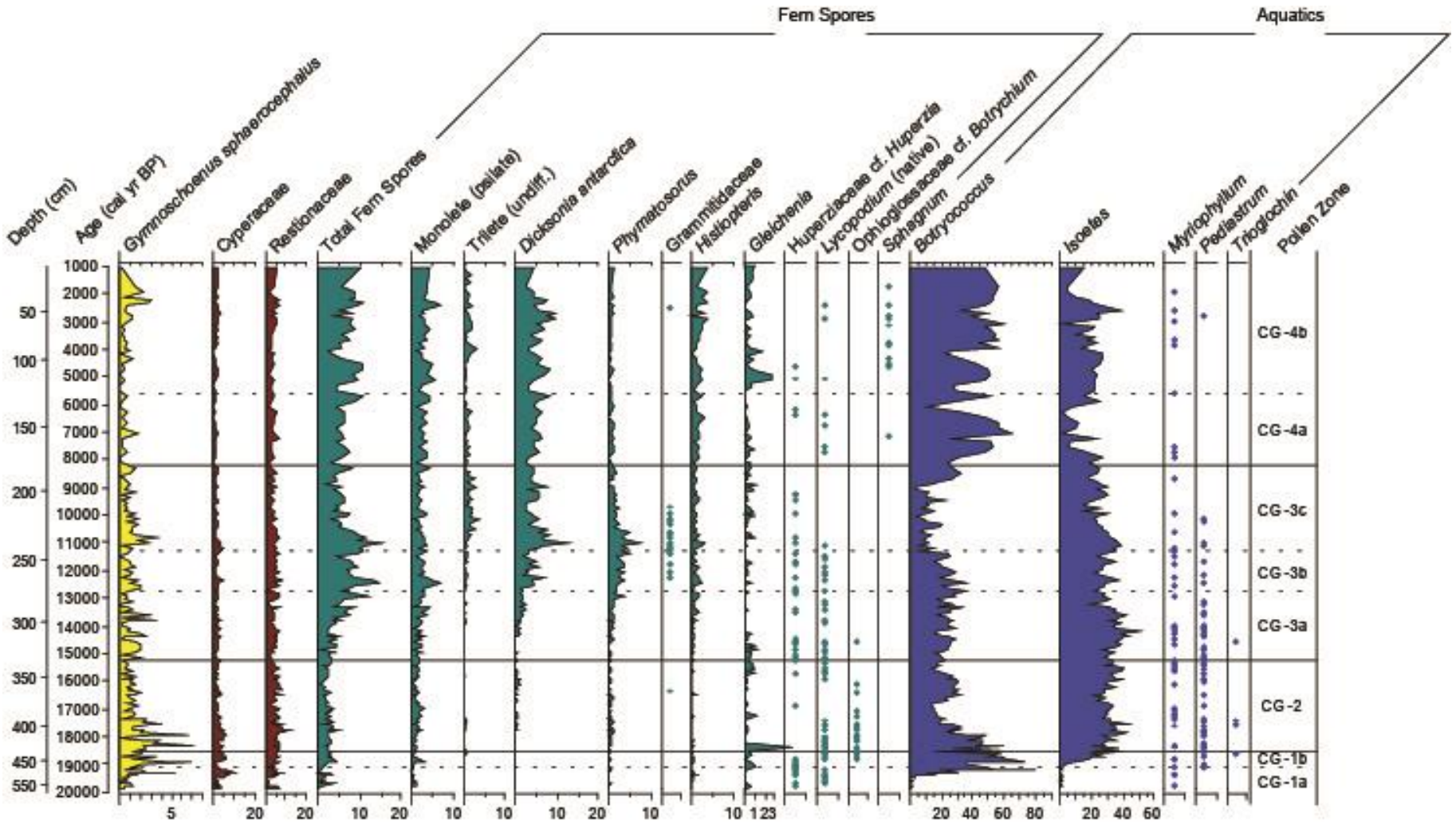

Figure 5-8 Core CG percentage pollen diagram (part 3). Note individual scaling of axes.

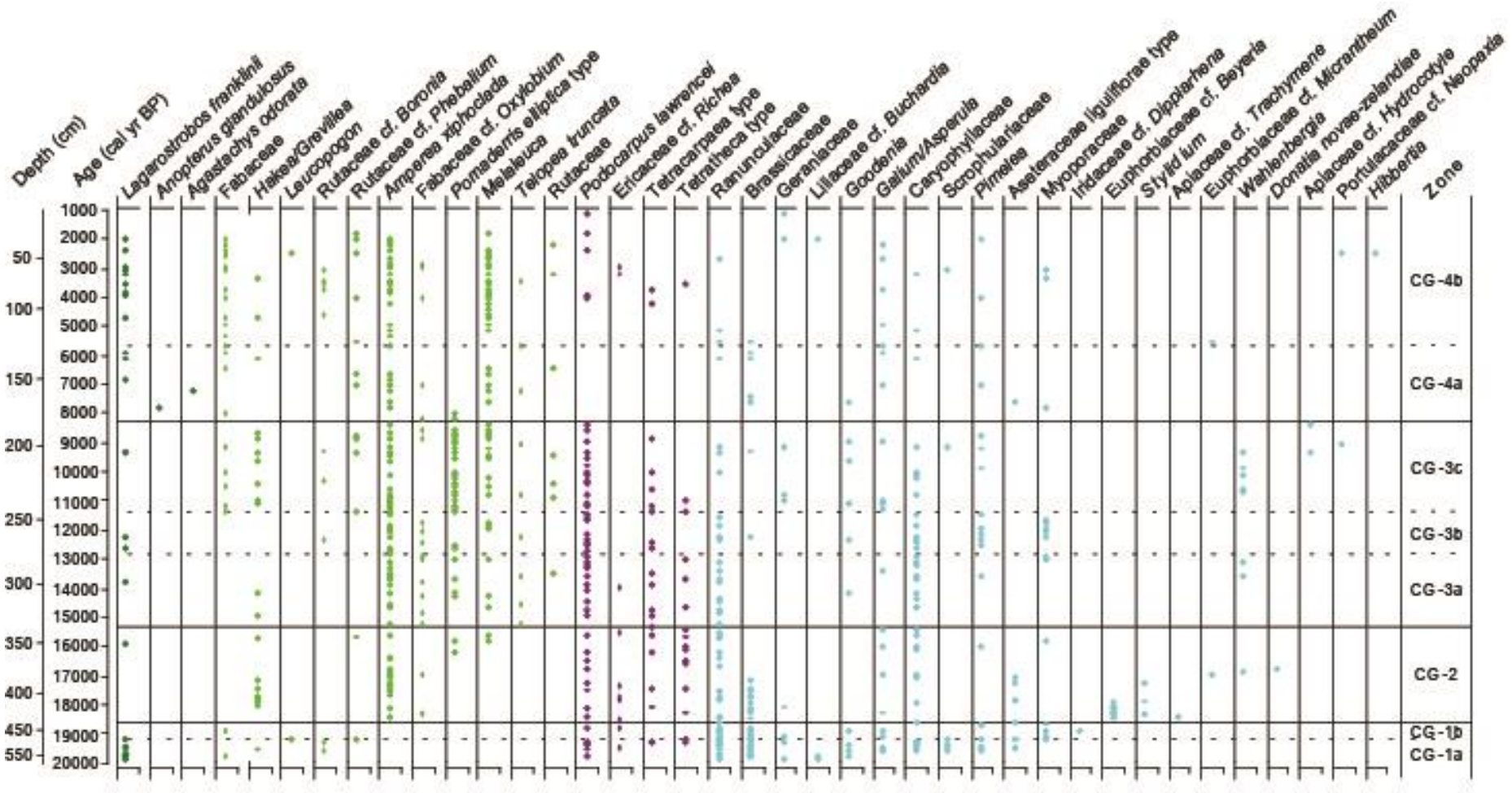

Figure 5-9 Core CG-LC rare pollen taxa

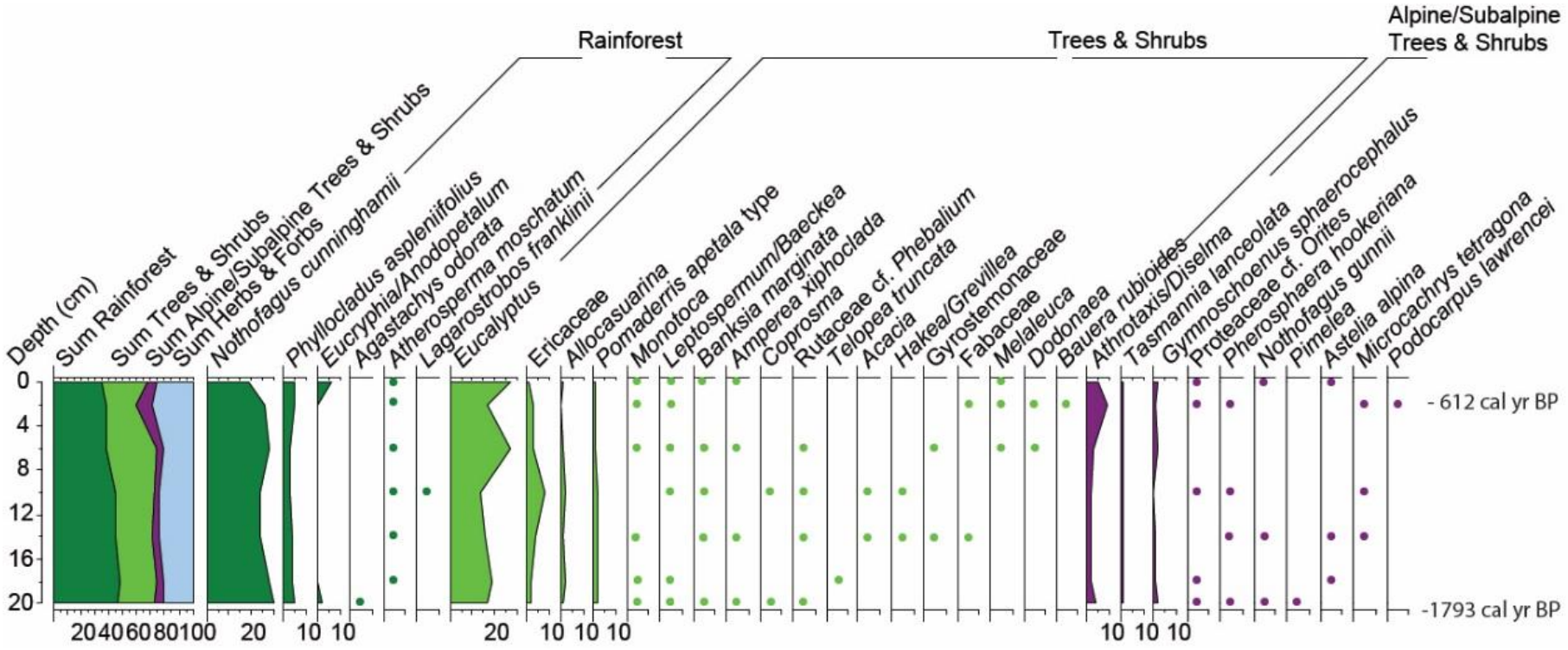

Figure 5-10 Percentage pollen diagram for short core CG (part 1)

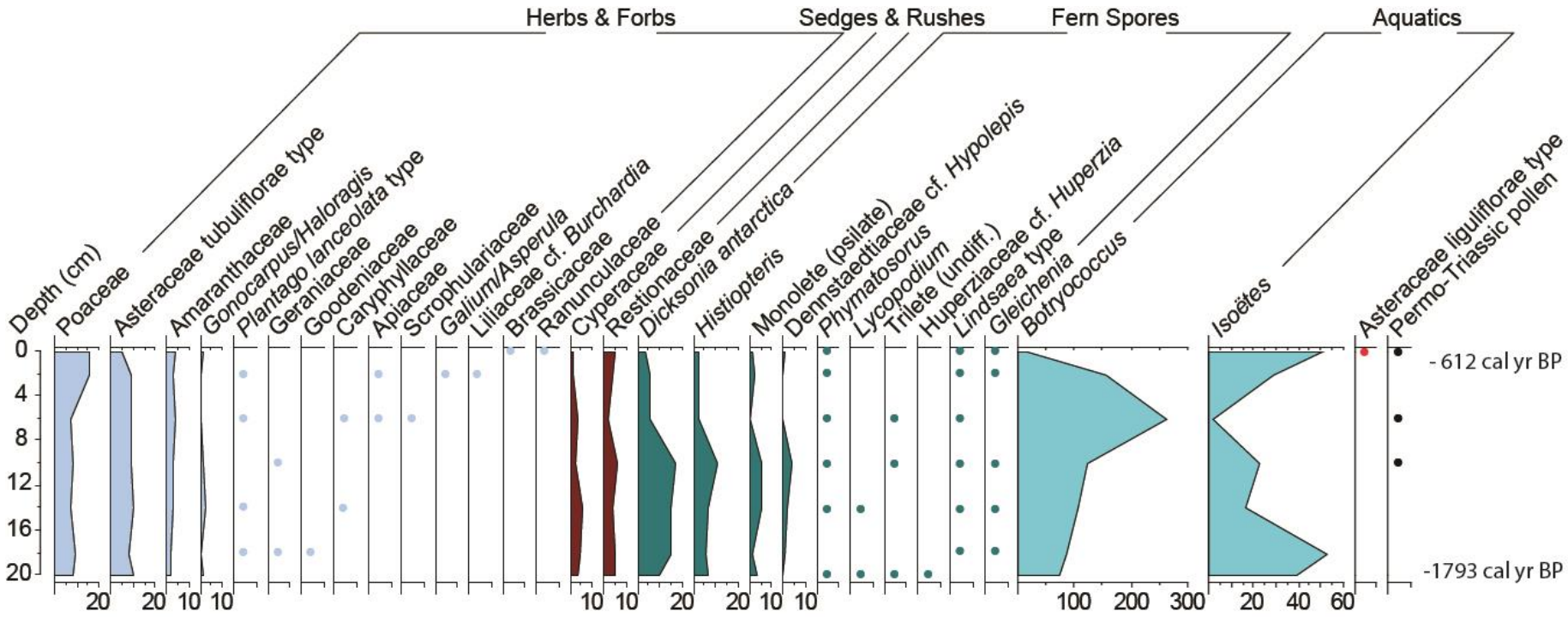

Figure 5-11 Percentage pollen diagram for short core CG (part 2)

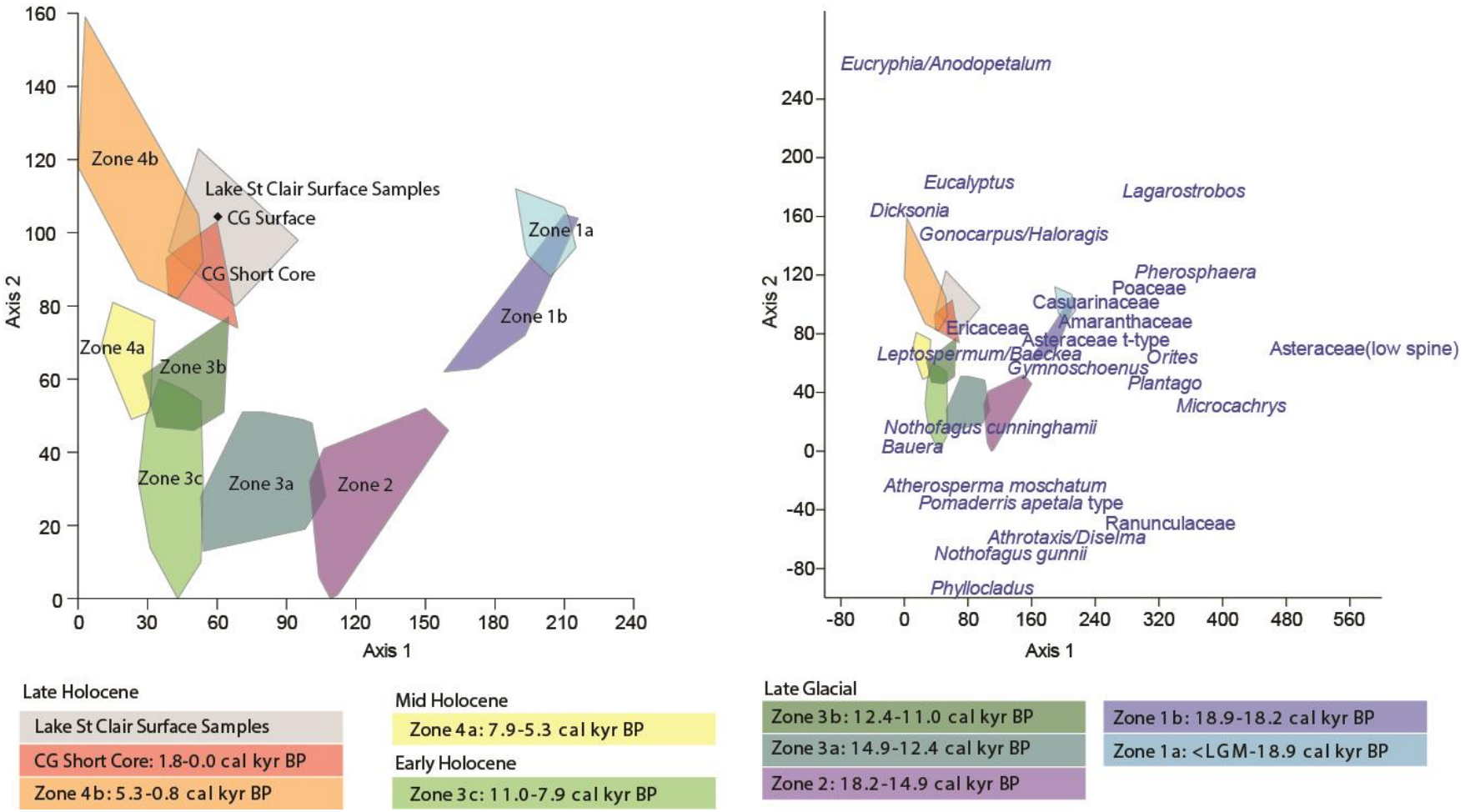

Figure 5-12 DCA biplot of the terrestrial pollen dataset for cores CG-LC and CG-SC plotted together with the Lake St Clair surface (mud-water interface) samples

5.3.3 Pollen Zone Descriptions and Interpretation of Vegetation Types

Subzone 1a: 548-446 cm, post LGM – 18.2 cal kyr BP

Subzone 1a is dominated by Poaceae (29-57%), Amaranthaceae (2-29%) and Asteraceae subf. Asteroideae (5-22%) with *Eucalyptus* (3-15%) and *Athrotaxis*/*Diselma* (1-11%) also important. The rainforest taxa *Nothofagus cunninghamii*, *Phyllocladus asplenniifolius* and *Lagarostrobos franklinii* are only present at trace levels. *Phaerosphaera hookeriana* (0-9%), Casuarinaceae (0-7%), *Gymnoschoenus sphaerocephalus* (0-5%), *Plantago lanceolata* type (0-5%), *Lagarostrobos franklinii* (0-5%), Asteraceae (low spine) (0-3%) and *Gunnera* (0-2%) are notably present at their highest levels for the record during this subzone. The sedges Cyperaceae (1-11%) and Restionaceae (0-16%) are both present at their highest levels towards the top part of subzone 1a. Fern spores are low throughout this subzone

Subzone 1b: 446-419 cm, ca. 18.9-18.2 cal kyr BP

The subzone is distinguished from the basal sediments by a marked increase in *Athrotaxis*/*Diselma* (2-23%) and the alpine/subalpine taxa Proteaceae cf. *Orites* (1-4%), *Microcachrys tetragona* (0-5%) and Ericaceae (0-3%). The aquatic taxon *Botryococcus* (0-80%) shows a marked increase from 464 cm (~19.0 cal kyr BP) reaching peak levels during subzone 1b and *Isoëtes* (0-41%) follows with a sharp increase towards the top of the subzone. Poaceae remains dominant (25-57%) during this subzone, however, exhibits a decreasing trend. The rainforest taxa *Nothofagus cunninghamii* and *Phyllocladus aspleniifolius* are still present at trace levels, although the latter begins to increase at the very top of the subzone reaching 5%.

Zone 2: 419-325 cm, ca. 18.2-14.9 cal kyr BP

This zone is dominated by *Athrotaxis*/*Diselma* (17-50%) with a pronounced peak occurring between 380-350 cm (ca. 16.9-15.9 cal kyr BP). Poaceae (7-29%) decreases strongly towards the middle of zone 2. Asteraceae subf. Asteroideae (10-19%) and Amaranthaceae (3-9%) are present at significant levels. *Phyllocladus aspleniifolius* (5-18%) shows a marked increase together with *Eucalyptus* (2-13%). *Nothofagus cunninghamii* (1-7%) and *Pomaderris apetala* type (0-4%) also begin to increase but are present at more reduced levels. *Gymnoschoenus sphaerocephalus* (0-7%) continues at its highest levels for the record at start of zone 2 and then decreases. *Botryococcus* (13-60%) levels decrease strongly towards the middle of the zone and increase again towards the top, whereas *Isoëtes* (19-46%) maintains more consistent levels. Fern spores slightly increased presence from Zone 1 but levels are still low (1-5%).

Subzone 3a: 325-267 cm, ca. 14.9-12.4 cal kyr BP

This subzone is dominated by *Athrotaxis*/*Diselma* (5-30%), *Phyllocladus aspleniifolius* (10-27%), *Nothofagus cuninghamii* (8-26%), Poaceae (6-20%), Asteraceae subf. Asteroideae (6-20%) and

Eucalyptus (7-14%) with Amaranthaceae (2-8%), *Pomaderris apetala* type (2-7%) (slightly increased levels), *Leptospermum-Baeckea* type (0-6%), *Gymnoschoenus sphaerocephalus* (0-4%), Ericaceae (0-3%) and Ranunculaceae (0-3%) as minor components. Fern spores begin to increase towards the top of the subzone. Notable for this subzone are the peak levels reached by *Phyllocladus aspleniffolius* and the marked increase in *Nothofagus cunninghamii* which is now present at comparable levels to the former.

Subzone 3b: 267-239 cm, ca. 12.4-11.0 cal kyr BP

Subzone 3b is marked by the sharp drop in *Phyllocladus* (2-6%) and strong increase in *Nothofagus cunninghamii* (20-38%). Poaceae (3-12%) is present at increased levels at the start of the subzone as *Athrotaxis*/*Diselma* (6-18%) levels exhibit a pronounced decrease but are still an important component of the pollen assemblage together with *Eucalyptus* (8-17%) and Asteraceae (6-17%). *Leptospermum-Baeckea* type (1-9%), *Pomaderris apetala* type (3-8%), Amaranthaceae (2-7%), *Phyllocladus* (2-6%) and *Eucryphia* (0-6%) are present as minor components. Fern spores peak at some of their highest levels in the record with monolete fern spores, *Dicksonia Antarctica* and *Phymatosorus* most important. Of note is the presence of *Atherosperma moschatum* at its highest levels for record (albeit trace levels, significant for this severely under-represented taxon).

Subzone 3c: 239-174 cm, ca. 11.0-7.9 cal kyr BP

This subzone is dominated by *Nothofagus cunninghamii* (23-40%), *Athrotaxis*/*Diselma* (8-23%) and *Phyllocladus* (4-21%) which increases strongly after its very low levels during the previous subzone. *Eucalyptus* (3-9%) is present at its lowest levels for the record. Poaceae (3-10%), Asteraceae (1-9%), *Eucryphia* (0-7%), *Pomaderris apetala* type (1-6%) and *Leptospermum-Baeckea* type (1-6%) are also important. Ferns spores peak at highest levels at the start of the subzone, predominantly *Dicksonia Antarctica* and *Phymatosorus* and then decrease towards the top of the subzone.

Subzone 4a: 174-118 cm, ca. 7.9-5.3 cal kyr BP

Nothofagus cunninghamii (26-37%) remains dominant during this subzone which is marked by a strong increase in *Eucryphia-Anodopetalum* type (3-17%). *Eucalyptus* (6-14%) levels also increase whilst *Phyllocladus aspleniifolius* (5-15%) and *Athrotaxis*/*Diselma* (1-13%) exhibit decreasing trends.

Asteraceae subf. Asteroideae (1-9%), *Leptospermum-Baeckea* type (1-8%), Poaceae (4-6%), Amaranthaceae (1-5%) and *Pomaderris apetala* type (0-5%) are also important. *Botryococcus* (10-65%) levels increase significantly whereas Isoëtes (2-27%) is present at its lowest levels apart from in the most basal sediments.

Subzone 4b: 118-8 cm, ca. 5.3-0.8 cal kyr BP

Nothofagus cunninghamii (10-38%) remains the overall dominant taxon yet its presence is variable in relation to *Eucryphia-Anodopetalum* type (2-36%) which reaches its highest levels for the record. *Eucalyptus* (12-23%) continues to increase along with Poaceae (4-12%) and Asteraceae subf. Asteroideae (3-13%). *Leptospermum-Baeckea* type (0-13%), Amaranthaceae (1-9%), *Phyllocladus aspleniifolius* (1-8%), *Athrotaxis*/*Diselma* (0-8%) and *Pomaderris apetala* type (0-6%) are also important during this subzone. Of note is the disappearance of *Nothofagus gunnii* pollen from the record during this subzone.

Short Core: 22-0 cm, ca. 1.9 cal kyr – present

Like subzone 4 b, *Nothofagus cunninghamii* (19-30%) dominates with *Eucalyptus* (14-27%) continuing the rising trend along with Poaceae (7-16%). *Eucryphia-Anodopetalum* (0-5.8%) is present in reduced amounts relative to subzone 4b. *Botryococcus* peaks at 6 cm, when Isoëtes values decline and is followed by declining fern spores and increasing, *Eucalyptus,* Poaceae and *Athrotaxis-Diselma* (1-8%) at the top of the core.

5.4 New data for Core CB

5.4.1 Dating and Age Model

One new radiocarbon date was obtained for Core CB at 247 cm (see Table 5.3). A new age model was produced using Bacon and is presented in Figure 5.13. Bacon excluded the date at 260 cm as an outlier.

Table 5-3 Radiocarbon dates for Core CB

Pollen zone	Sample depth (cm)	Material dated	Date (yr BP)	Laboratory number	Sedimentation rate (mm yr-1)	Date (cal yr BP)
LSC2a/2b	55	Organic mud	4290 ± 70	OZD693	0.13	4706
LSC2a	115	Organic mud	6420 ± 50	Beta-108148	0.28	7321
LSC2a	155	Organic mud	8000 ± 60	OZD694	0.25	8854
LSC1b/2a	228-230	Organic mud	11210 ± 50	Beta-106999	0.23	12995
LSC 1b	247	Glacial sediment	11790 ± 50	ANU 9907		13277
LSC1a	260	Charcoal fragments in grey clay	18450 ± 100	OZD695		22068 ± 321

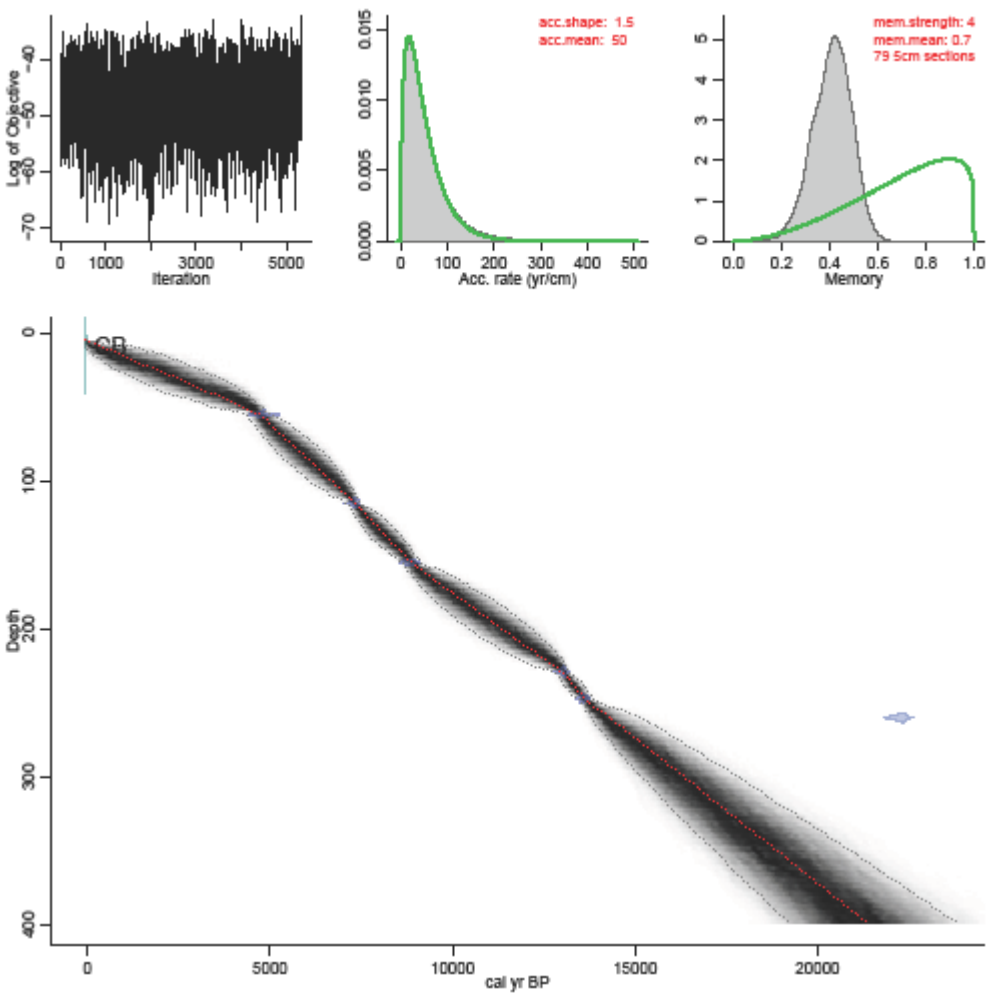

Figure 5-13 Bacon age model for core CB

5.4.2 Updated Pollen Diagram

Hopf et al (2000) published a late Glacial and Holocene pollen record from Cynthia Bay, Lake St. Clair (core CB). The late glacial portion of the record illustrated the herbaceous assemblage Poaceae, Asteraceae and Amaranthaceae, typical of late Glacial Tasmanian pollen records. A more unique feature of the late Glacial record was the dominance by *Podocarpus lawrencii* suggesting a strong alpine coniferous heath component.

This record has since been revisited and the identification of *Podocarpus lawrencii* reviewed. It was suspected that these grains may have been reworked pollen due to the medium brown colour of the grains which contrasted with the typical golden brown colour of younger acetolysed pollen grains typical of the Quaternary. Dr Mike Macphail confirmed the grains to be reworked and identified the grains as Permo-Triassic bisaccates. Figures 5.14-5.17 illustrates an updated version of the Core CB pollen record.

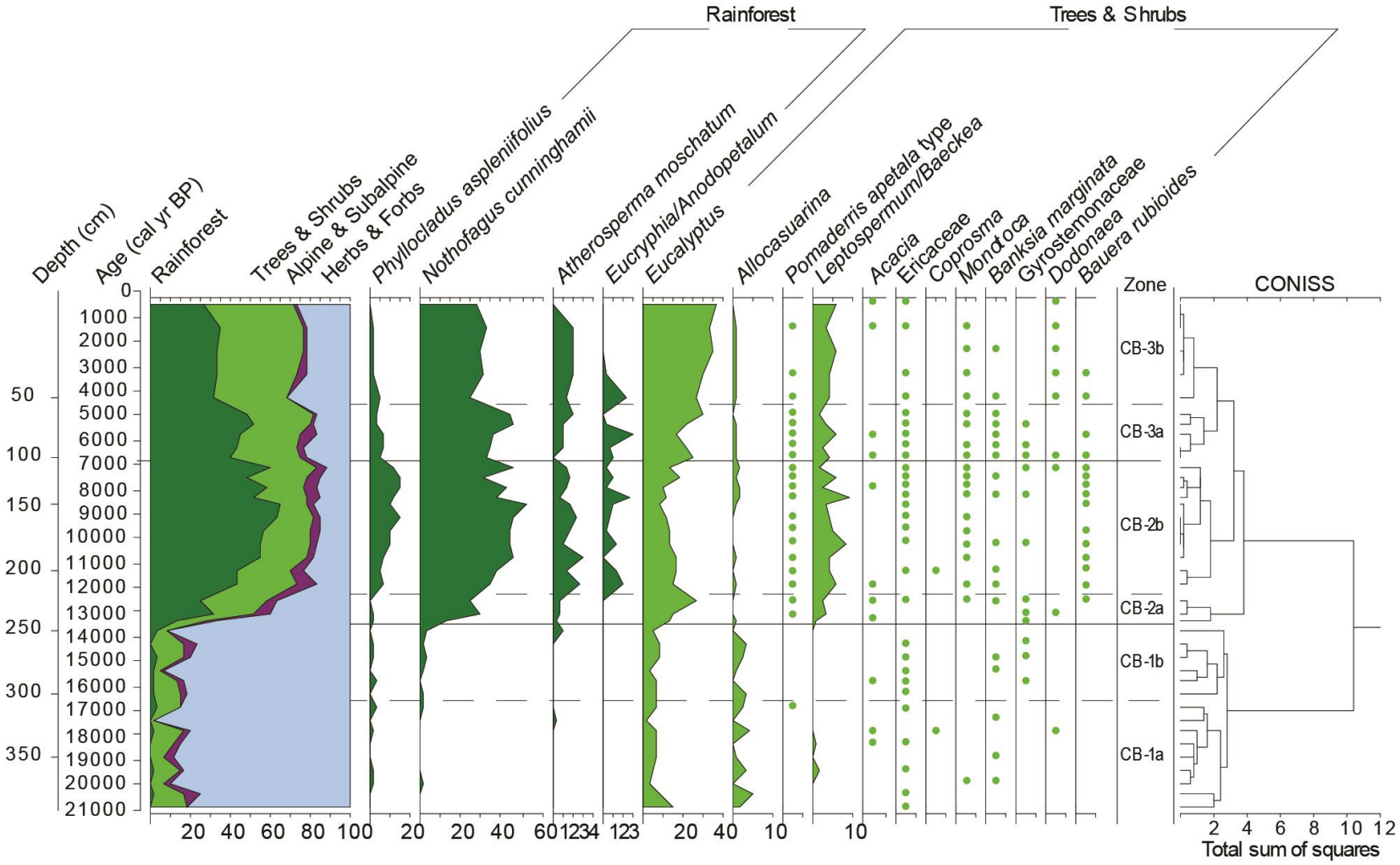

Figure 5-14 Core CB percentage pollen diagram (part 1)

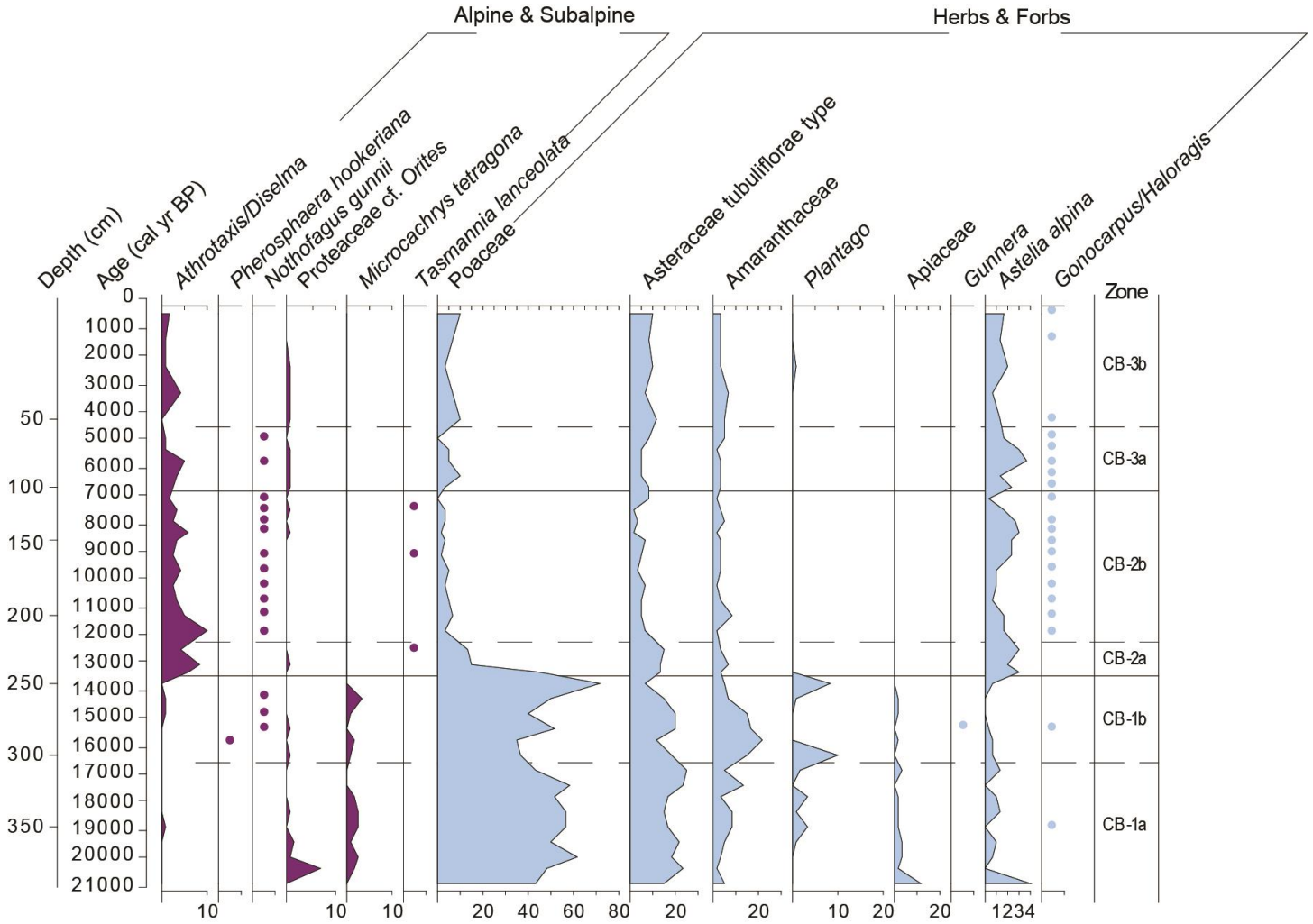

Figure 5-15 Core CB percentage pollen diagram (part 2)

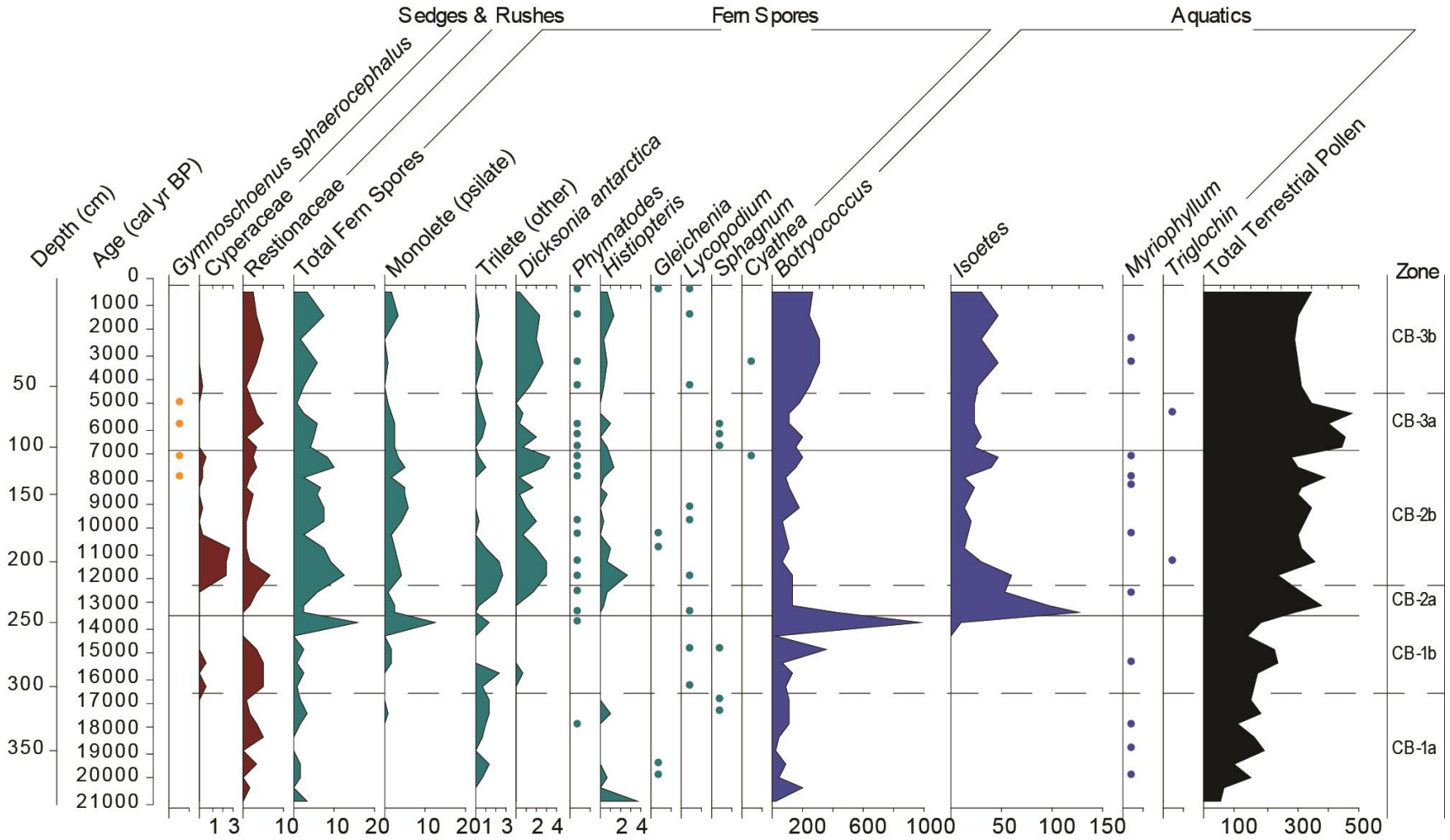

Figure 5-16 Core CB pollen diagram (part 3)

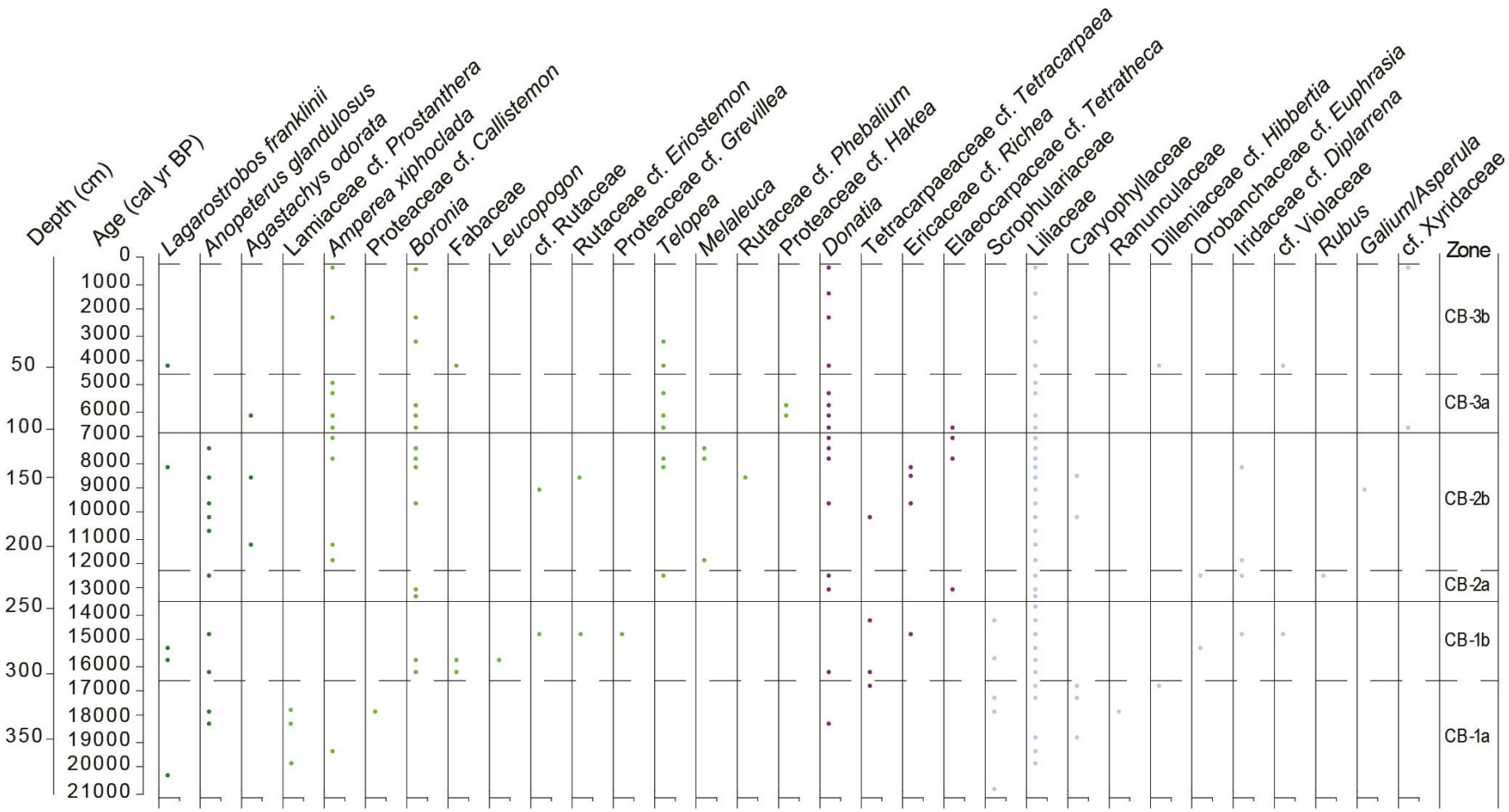

Figure 5-17 Core CB rare pollen taxa

5.4.3 Comparison of CG and CB record

Cores CB and CG show similar overall stratigraphy with a basal sequence of glacial sands, silts and clays overlain by lacustrine sediments, however, Core CB is shorter by 150 cm (figure 5.18). Core CG has a much more extensive sequence of lacustrine sediments, almost 200 cm more than core CB, and core CB a slightly longer sequence of glacial sediments of 164 cm, compared with 111 cm for core CG. Magnetic susceptibility and total organic (%) values (figure 5.18) follow similar trends at both sites, the most notable difference being that values decrease/increase much more abruptly across the glacial/lacustrine sediment boundary in the CB record when compared with the CG record which appears to have a period of transitional values which is of considerable length.

Timing of the glacial/lacustrine sediment boundary differs considerably between the sites. Lake sediments had begun depositing by c. 18.8 cal kyr BP at the northern end of the lake (core CG), but not until c. 13.0 cal kyr BP at the southern end of the lake. The Derwent Glacier is thought to have retreated in clear stages from south to north (Kiernen, 1992). Assuming the glacial sediments were deposited relatively rapidly at a similar time, and if the northern end of Lake St Clair was ice free by c.18.8 cal kyr BP, it appears that the record between 18.8-13.0 cal kyr BP is missing at the southern of the lake.

Further support for this section of record missing from the CB location can be found when comparing the pollen records. The glacial sediments exhibit the same pollen assemblage dominated by Poaceae with Asteraceae and Amaranthaceae (figure 5.19). Some other key taxa are plotted in Figures 5.20 and 5.21 (for lake sediments only) and show that *Nothofagus cunninghamii*, *Phyllocladus aspleniifolius*, *Eucalyptus*, Cupressaceae, Poaceae and *Nothofagus gunnii* all show the same broad trends after c. 13.0 cal kyr BP. What is noticable is that core CB does not capture the period of the *Phyllocladus* bulge (c. 14.5-12.5 cal kyr BP) or the pronounced Cupressaceae peak prior to this (c. 16.9-15.9 cal kyr BP). This is additional support that this period of time is missing from the core CB record.

Core CB only has a single date for the glacial sediments (c. 22 cal kyr BP). At the time it was interpreted that Lake St. Clair was deglaciated very early based on this date (Hopf et al. 2000). Based on the discussion of the core CG chronology in section 5.2.3, it is likely that this age is based on older in-washed carbon and is unlikely to be a true age of the glacial sediments. However, the interpretation that deglaciation occurred early at the site still holds as it seems to have been complete by c. 18.8 cal kyr BP at the northern end of the lake.

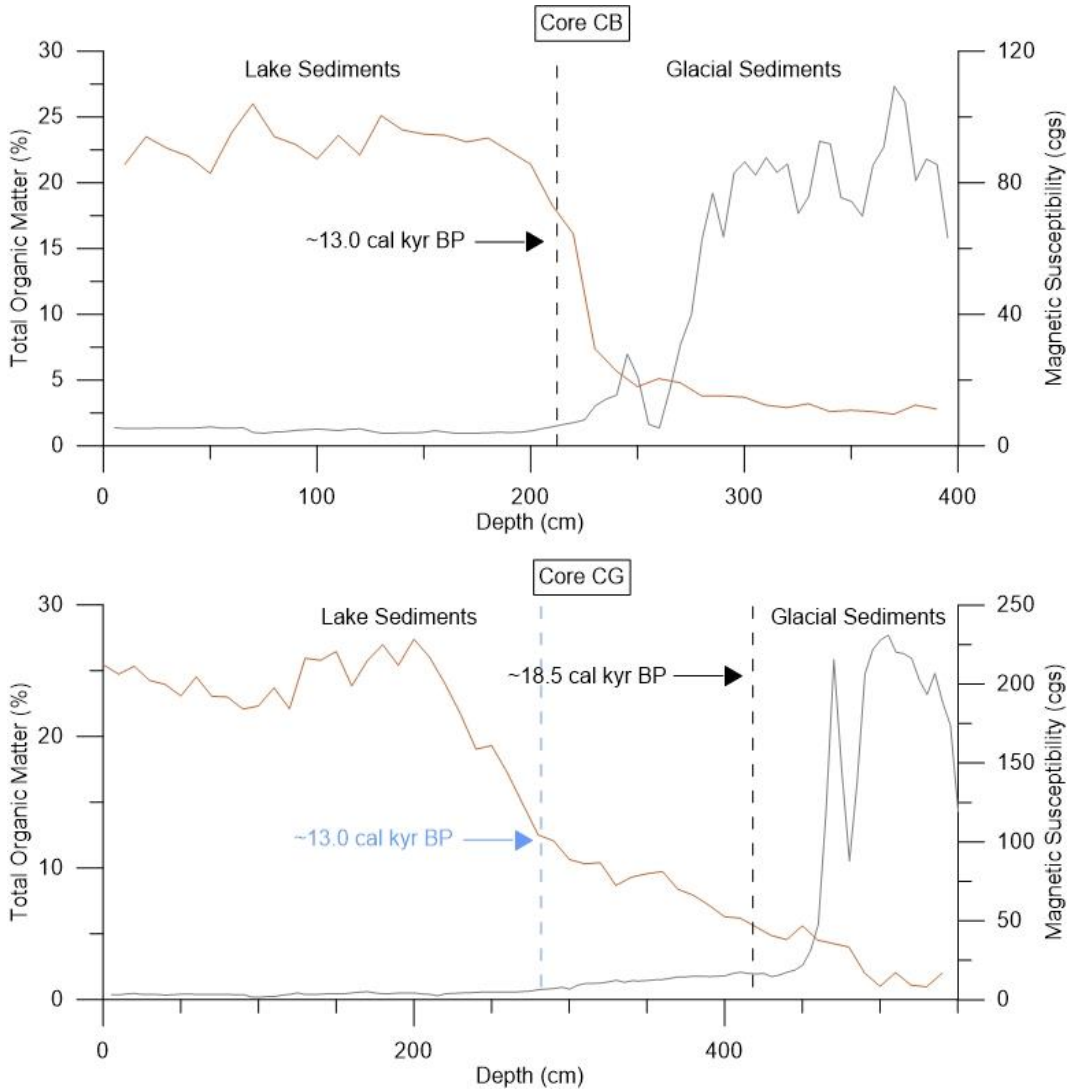

Figure 5-18 Comparison of sediment properties of cores CB and CG

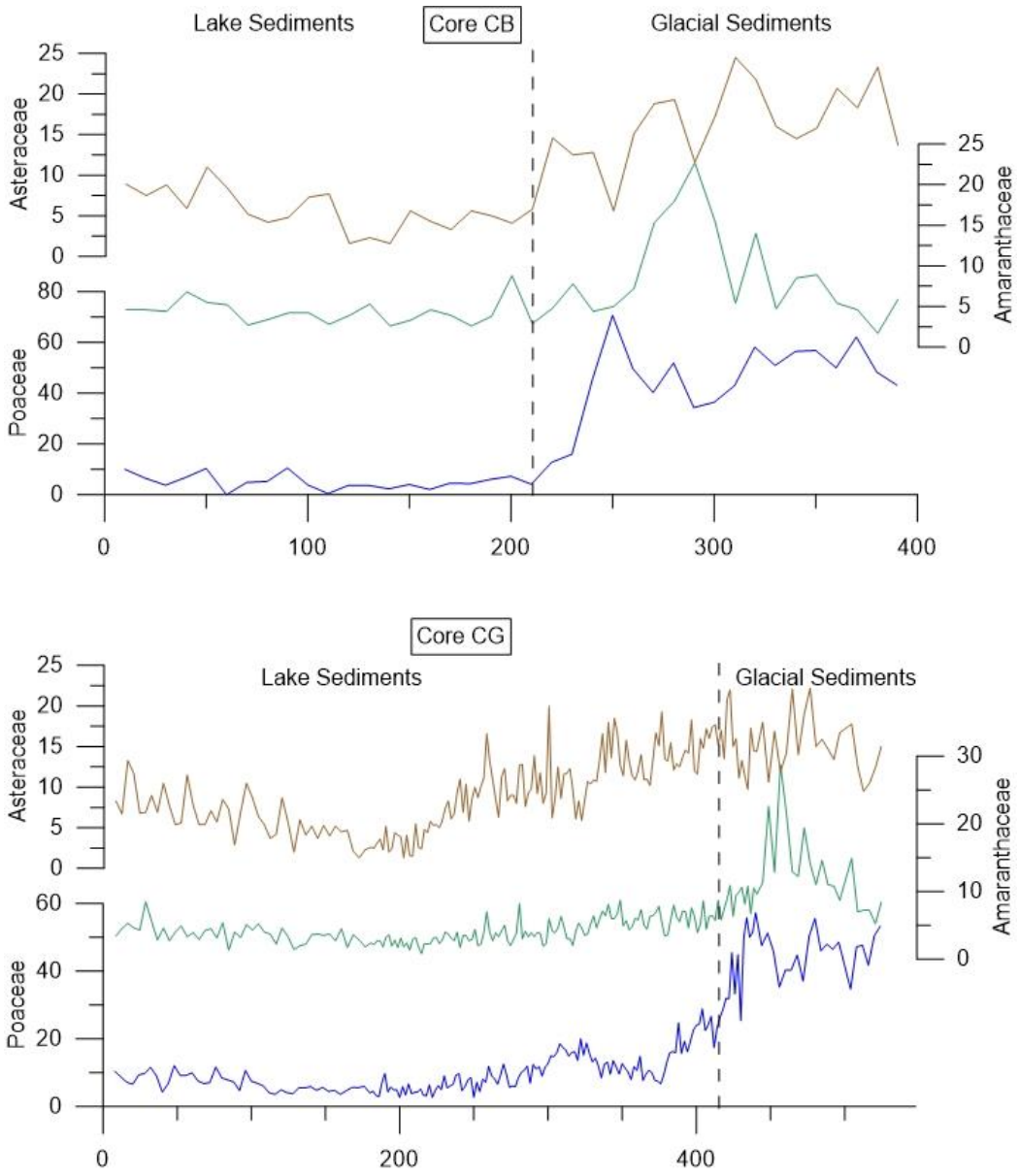

Figure 5-19 Comparison of key taxa of the late Glacial period including Poaceae, Asteraceae and Amaranthaceae

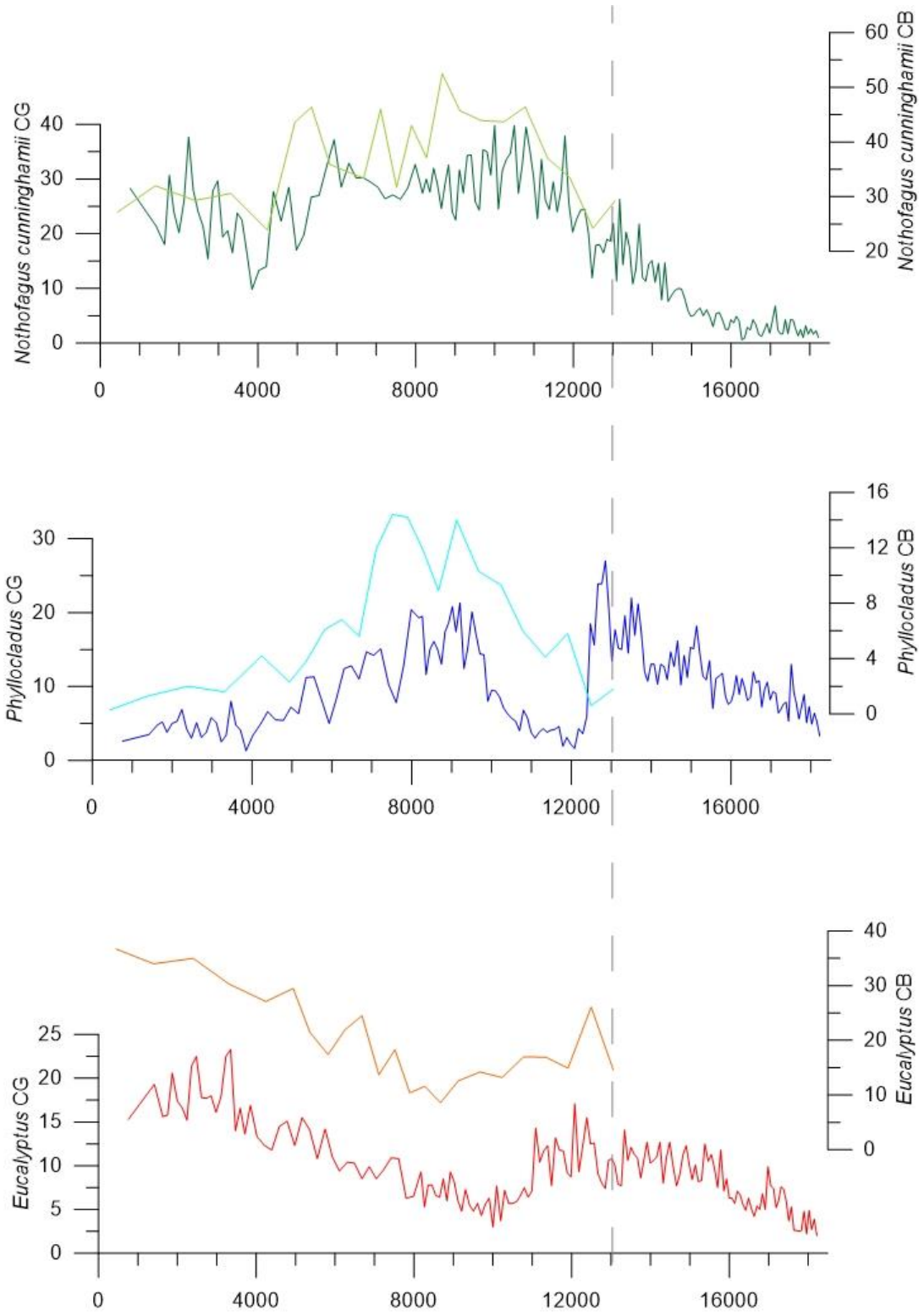

Figure 5-20 Comparison of key forest taxa for cores CB and CG including *Nothofagus cunninghamii*, *Phyllocladus aspleniifolius* and *Eucalyptus*

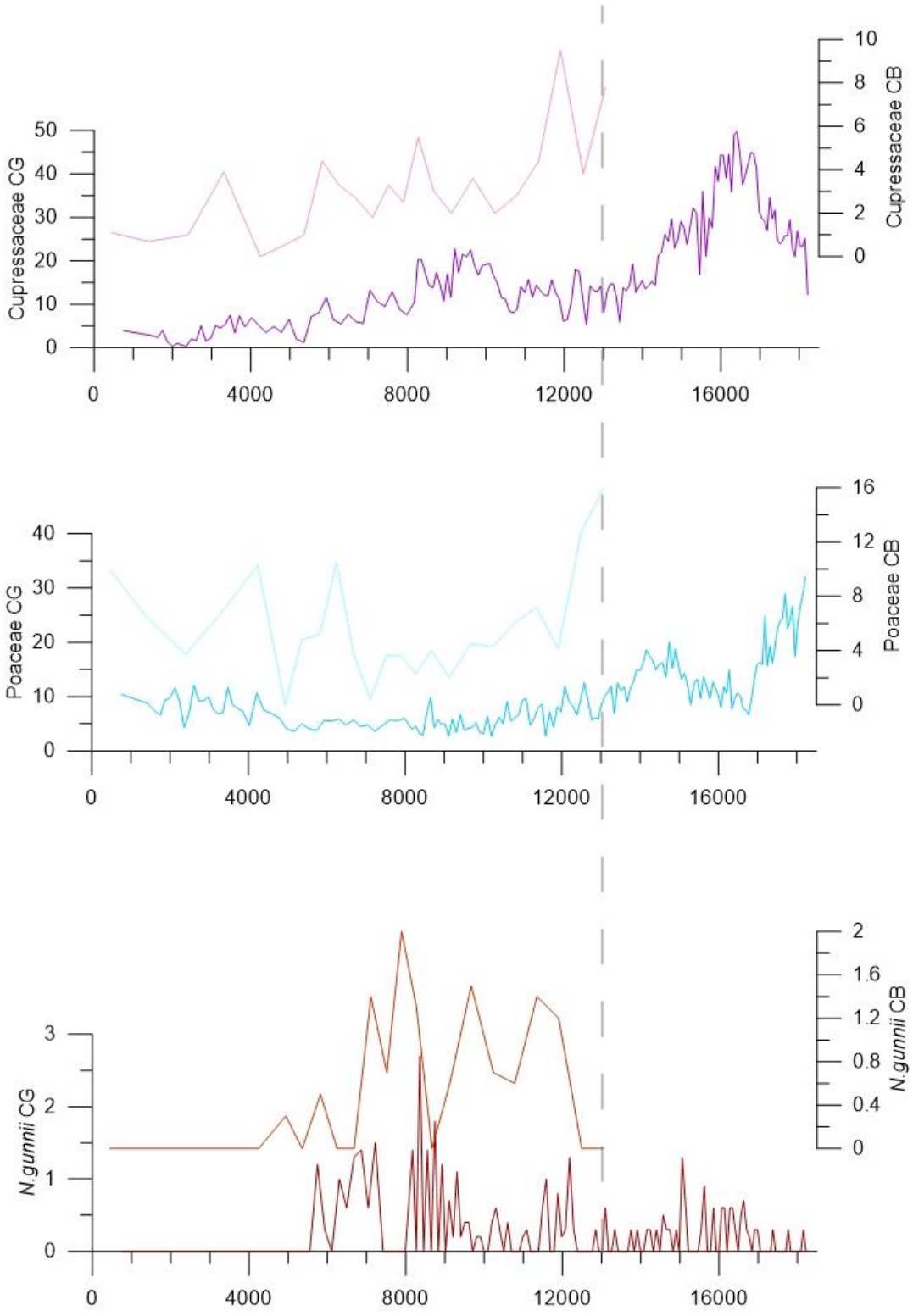

Figure 5-21 Comparison of Cupressaceae, Poaceae and *Nothofagus gunnii* records for cores CB and CG

Chapter 6 Other Sites in the Lake St Clair Region

6.1 Introduction

Few pollen records extend beyond the late Last Glacial in Tasmania. Pre-LGM sites are focused in three areas: the West Coast Range, the north-western plains and in the lowlands of south-eastern Tasmania, with no records available for Central Tasmania (Colhoun and Shimeld, 2012). The secondary aim of this thesis is to extend the record of vegetation change in Central Tasmania beyond the late Last Glacial by targeting sites lying outside the ice limits of the Last Glaciation. Cores taken from Clarence Lagoon and Excalibur Bog produced records pre-dating the LGM and the results are presented in this chapter. Cores taken from Skullbone Plains Bog and Clarence Bog produced full Holocene and Late Holocene records respectively and the results are also presented in this chapter and provide details of local vegetation changes during these periods to supplement the regional vegetation changes captured in the Lake St Clair sediments. The pollen of the Skullbone Plains Bog core was analysed by the author as part of a project with the Tasmanian Land Conservancy led by Em. Prof. Geoffrey Hope at the ANU in collaboration with researchers at University of Tasmania, ANSTO and ANU (Hope et al., 2017).

6.2 Site Descriptions

The Excalibur Bog site (42.1125°S, 146.2865°E, 785 m altitude) is located approximately 8 km east of Lake St Clair and 4 km southwest of Clarence Lagoon (figure 6.1). The closest climate station is at Lake St Clair which receives a mean annual rainfall of 1895.7 mm and records a mean annual temperature of 8.2°C (Bureau of Meteorology, 2018b). The next closest climate station is at Bronte Park, approximately 18 km to the east, which receives considerably less rainfall (934.4 mm per year, mean annual temperature 8.7°C) as a result of the strong west-east precipitation gradient. The geology of the site is classified as Quaternary swamp, marsh and alluvium and is underlain by Tertiary basalt (Tasmania Department of Mines, 1963, "St Clair"). The site is located on a *Gymnoschoenus sphaerocephalus* and Restionaceae dominated bog which is surrounded by dry eucalypt forest with wet eucalypt forest, rainforest and *Leptospermum* scrub growing on the hillslopes to the north. The site lies well beyond the limits of the Last Glaciation, the Cynthia Bay Glaciation, being positioned just outside the ice limits of the much earlier Beehive glaciation (figure 6.2) (Kiernan, 1991).

Clarence Lagoon (146º19'E 42º05'S) lies at an altitude of 960 m on the southwestern edge of the Lower Plateau surface (Banks et al., 1977) of the Central Plateau. The lake is very shallow (< 2 m) and approximately 1.25 km in length. It is fed by various small creeks from the surrounding plains and is the source of the Clarence River, which drains the lake at its

southwestern corner. Clarence Lagoon is surrounded by Jurassic dolerite rock ridges (1000 m – 1100 m) to the east and west supporting dry eucalypt forests and Quaternary glacial outwash plains to the north covered by highland grassy sedgeland, *Sphagnum* peatland and eastern buttongrass moorland which also extend around the western and eastern sides of the lake. The steep slopes to the south of Clarence Lagoon, which descend almost 200 m to the Excalibur Bog surface, are covered in wet and dry eucalypt forest as well as patches of *Athrotaxis cupressoides-Nothofagus gunnii* short rainforest and *Nothofagus cunninghamii* dominated rainforest. An end moraine about 15 m high runs transversely across the valley and the outlet of the Clarence River lies at the eastern end of the moraine. The position and shallowness of the lake (< 2 m) led Jennings and Ahmad (1957) to conclude that the moraine most likely initiated the formation of the lake, hence they classified Clarence Lagoon as a moraine barrage lake.

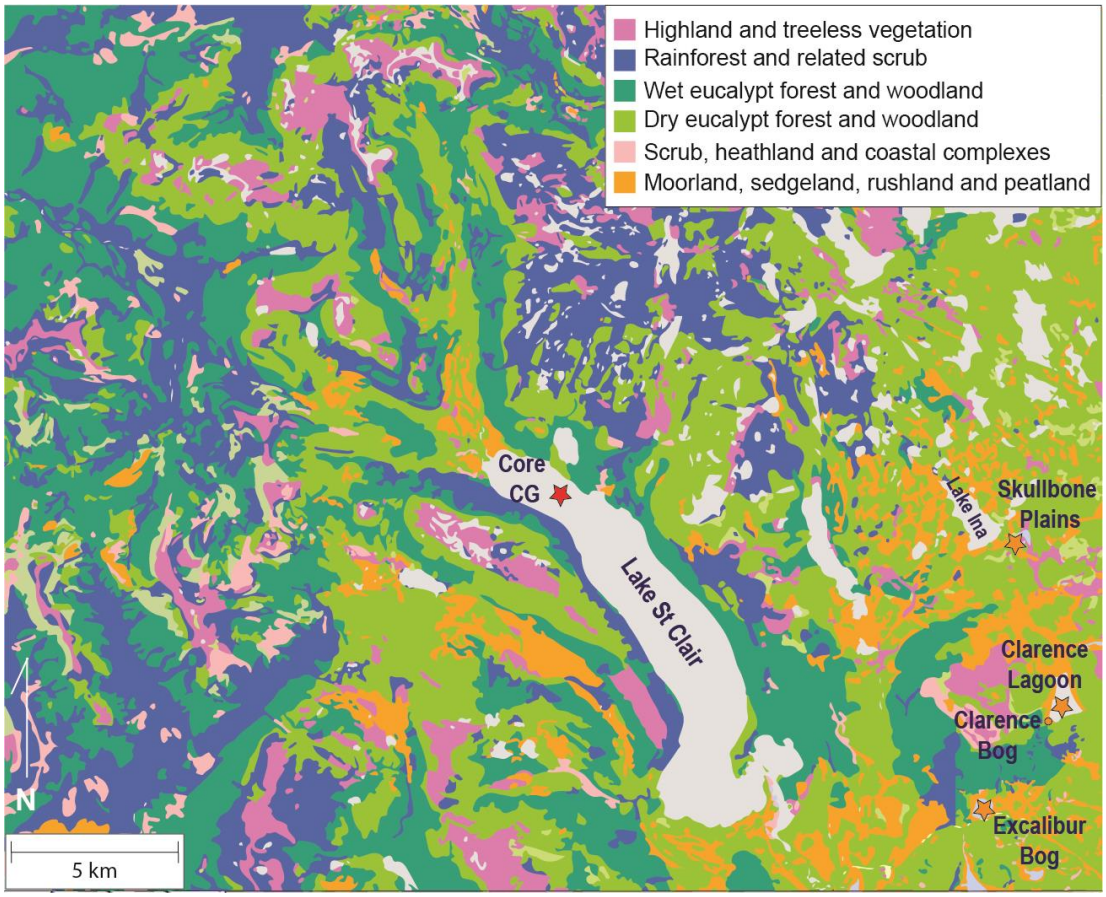

Figure 6-1 Locations of sites in relation to key vegetation types in the Lake St Clair region. Source: vegetation data base map *(Department of Primary Industries, Parks, Water and Environment, 2013)*

The Skullbone Plains bog core site (42°02'03.17 S, 146°17'54.40 E) is located within the Five Rivers Tasmanian Land Conservancy Reserve near Lake Ina on the Central Plateau, at an altitude of 1026 m approximately 11.5 km east of Lake St Clair and 5.2 km north of Clarence Lagoon. The core site lies at the north-western corner of a large *Sphagnum* peatland (~45 ha) which occurs across an interfluve on Skullbone Plains (Hope et al., 2017). The vegetation is

dominated by *Sphagnum* moss hummocks approximately 40 cm in height, which are overtopped by ericaceous and myrtaceous shrubs around 80 cm tall and dominated by *Richea scoparia*, *Sprengelia incarnata, Baeckea gunniana* and *Baloskian australe.* Other plants present include *Epacris serpyllifolia, Oreobolus pumilio, Rubus gunnianus, Gleichenia alpine, Empodisma minus, Richea sprengelioides, Celmisia asteliifolia and Ourisia integrifolia.* The moss hummocks and shrubs are aligned WSW-ENE forming a patterned surface on the bog which can be attributed to wind resonance (Morgan et al. 2010; Hope et al., 2017). The vegetation surrounding the peatland consists of a mosaic of alpine sedgeland and heathland, highland grassy sedgeland and *Poa* grassland, with dry eucalypt forest and woodland widespread, in particular on the Jurassic dolerite hills.

Small moraines at the southern end of Lake Ina are interpreted by Kiernan (1985, 1991, 1999) as marking the southern extent of glaciation during the Last Glacial Maximum (LGM) (figure 6.2). A series of minor moraine ridges and outwash plains occurs between Lake Ina and Clarence Lagoon which become more prominent c.1 km north of Clarence Lagoon. Kiernan (1999) suggests that Clarence Lagoon did not receive any glaciofluvial sediment at this time as meltwater would have been discharged into the Travellers Rest River to the southwest and the Little Nive Rivulet to the northeast. The contrast between the fresh topography at Lake Ina and the degradation of the moraine slopes and significantly advanced pedogenisis at Clarence Lagoon suggests that the Clarence Lagoon end moraine (plate 6.1) is significantly older than those near Lake Ina and the result of a much more extensive glacier (Kiernan 1999). Based on the thickness of subsurface dolerite weathering rinds, Kiernan (1999) proposes four or five periods of glaciation possibly indicating separate Glacial Climate Stages for glacial sediments south of the plateau. He suggests that the phases of glaciation represented by the drifts outside the LGM limits all predate the Last Interglacial Stage. Thus, the Clarence Lagoon end moraine is at least as old as the penultimate glaciation. An ice limit between Clarence Lagoon and Lake Ina raises the possibility that an even older glaciation produced the end moraine at Clarence Lagoon. Ice limits of the locally termed Cynthia Bay Glaciation, equivalent to the Last Glaciation, as well as the Beehive and Powers Creek ice limits from earlier glaciation are illustrated in relation to the core sites in figure 6.2.

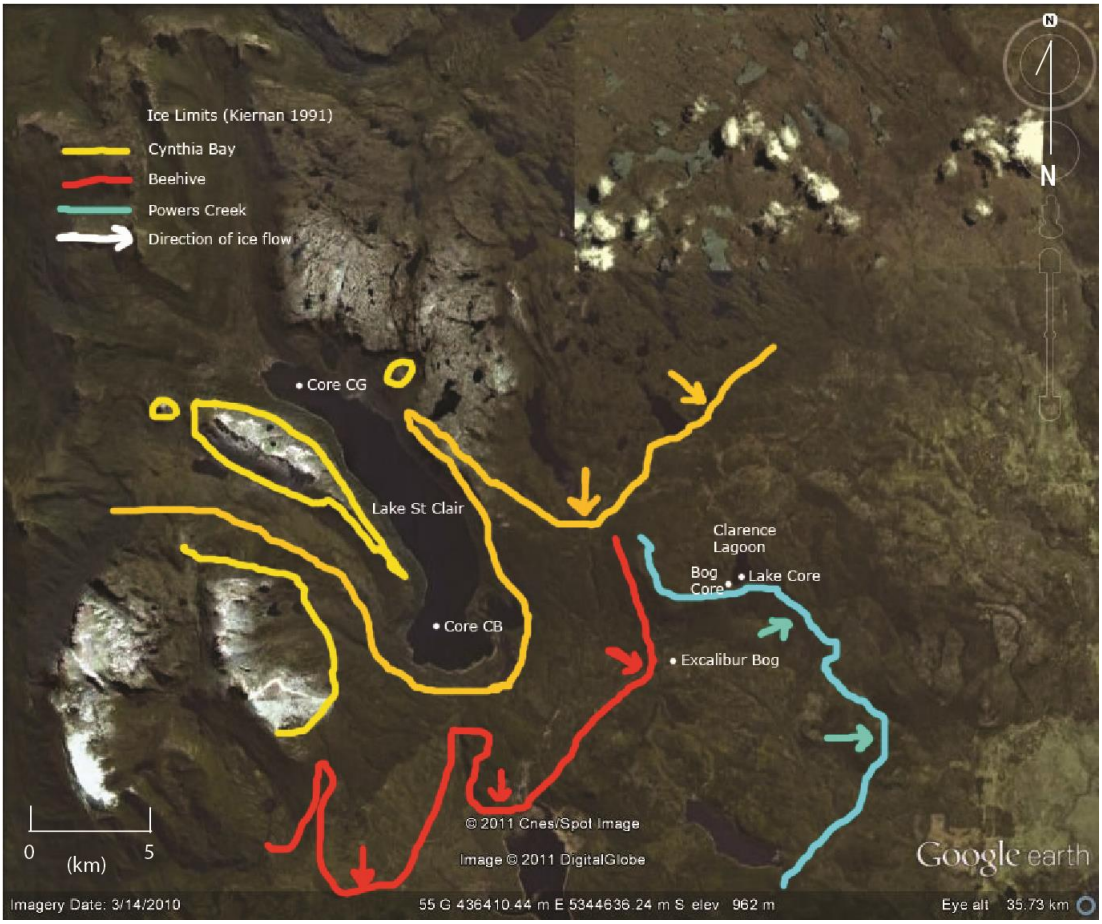

Figure 6-2 Locations of sites in relation to ice limits according to Kiernan (1991). The Cynthia Bay ice limit is the most recent LGM ice limit. The Beehive and Powers Creek ice limits are from earlier, more extensive glaciations. Source: background satellite image, Google Earth.

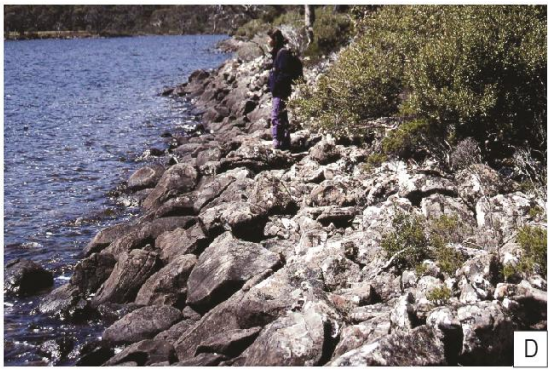

Plate 6-1 A) Clarence Lagoon B) *Sphagnum* hilltop overlooking burnt hillslope and core locations marked in yellow: Clarence Lagoon (left) and Clarence Bog (right) C) Excalibur Bog D) Clarence Lagoon end moraine E) Skullbone Plains, photo credit: Tasmanian Land Conservancy F) *Richea scoparia* growing on *Sphagnum* mounds with *Astelia* and *Eucalyptus* woodland in background at Skullbone Plains, photo credit: Grant Dixon, Tasmanian Land Conservancy G) Coring Clarence Bog

6.3 Excalibur Bog

6.3.1 Modern vegetation and pollen

To explore the degree of representation of moorland and eucalypt woodland by pollen at the Excalibur Bog site as well as the nature of pollen transport across the moorland, two transects were undertaken across the bog and centred on the core site. One transect was positioned approximately E-W, the other N-S, and the vegetation cover was described and a surface sample collected at each site resulting in a total of 17 moorland and 7 eucalypt woodland samples which were analysed (figure 6.3).

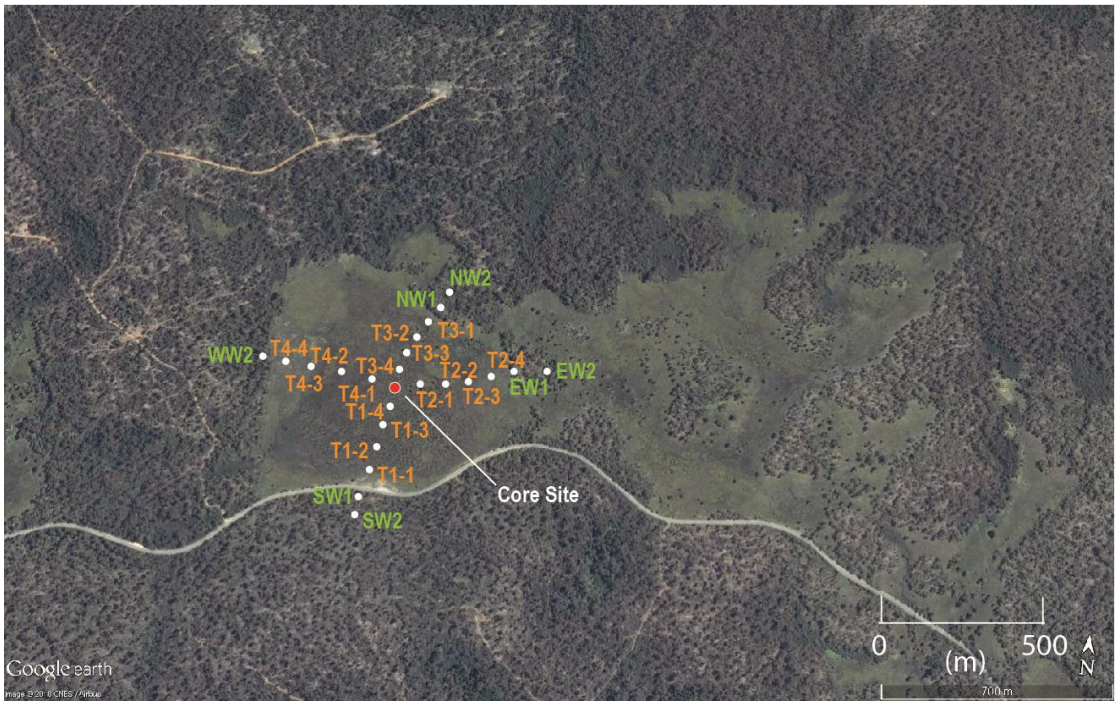

Figure 6-3 Location of transects and sample locations across Excalibur Bog. The sample locations in green are in dry eucalypt woodland and the samples in orange in buttongrass moorland. Source: background satellite image, Google Earth.

The vegetation at the site is summarised as box plots in figure 6.4. The moorland sites are dominated by *Gymnoschoenus sphaerocephalus* and Restionaceae. Some shrubs (Ericaceae, *Melaleuca* and Asteraceae), herbs (*Drosera*, *Utricularia*, Poaceae, Apiaceae and *Astelia*) and mosses are also present. The woodland sites all have a *Eucalyptus* overstorey. The understorey typically contains Poaceae along with *Cyathodes* and other Ericaceous shrubs at some sites and Restionaceae at other sites. Other shrubs (*Hakea*, *Leptospermum*, *Acacia*, *Lomatia*, *Callistemon*, *Tasmannia*, *Leucopogon*, *Orites*, Fabaceae, *Coprosma*, *Banksia*, *Leptomeria*, *Melaleuca*, *Ozothamnus*) herbs (*Astelia*, Ranunculaceae, *Stylidium*, *Microseris*, *Craspedia*, *Acaena*, *Centaurium*, *Wahlenbergia*, *Helichrysum*, *Rubus*) ferns (*Sphagnum*, *Gleichenia*, *Pteridium* and *Blechnum*) and mosses are also present.

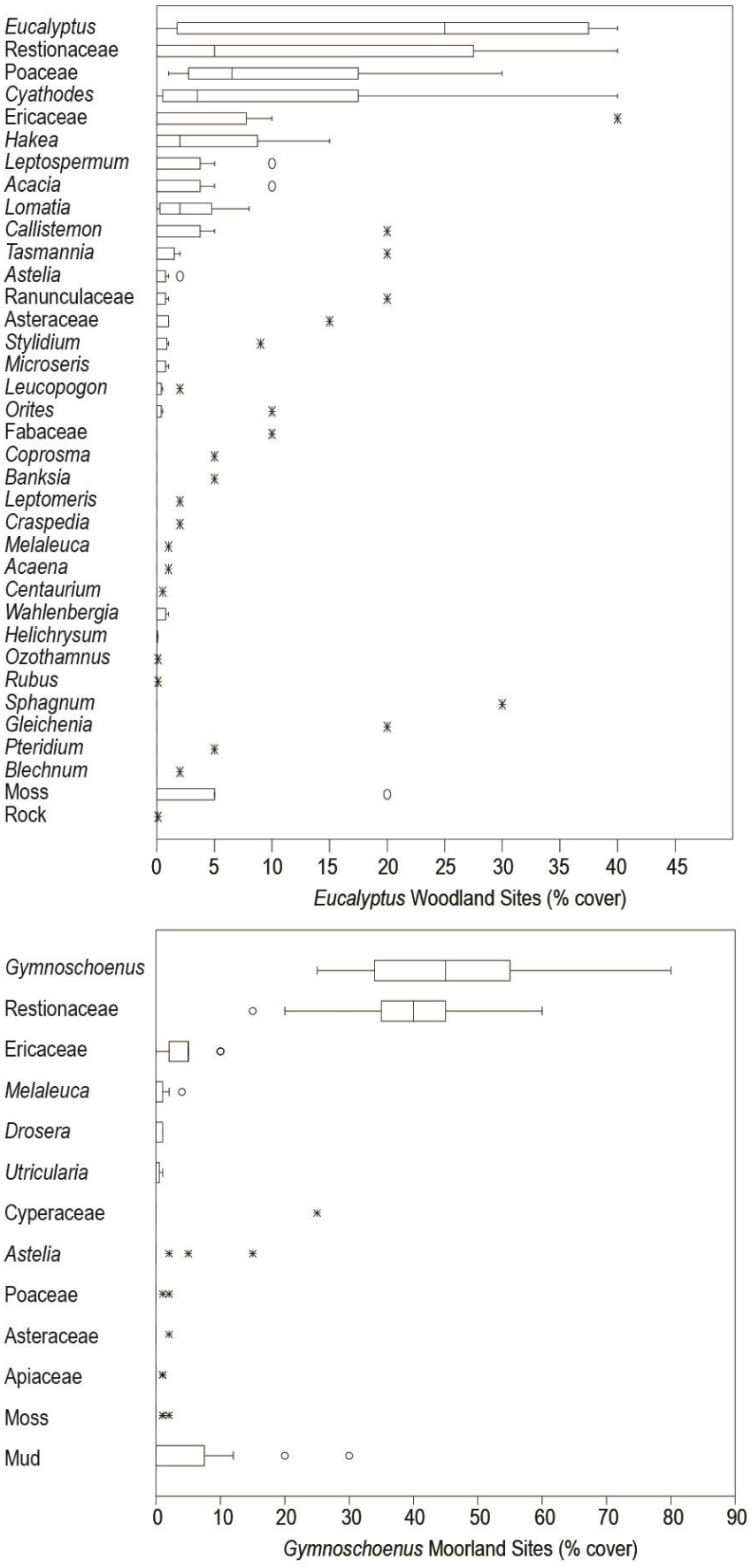

Figure 6-4 Box Plots of vegetation cover (%) a) Eucalyptus woodland sites b) Gymnoschoenus moorland sites

The DCA biplot (figure 6.5) of the modern pollen transect dataset separates the samples into two clear groups corresponding with the vegetation associations observed in the field, with a slight overlap due to one woodland sample taken close to the edge of the moorland. The moorland samples are distinguished most strongly by *Gymnoschoenus* (r^2=0.7) and Ericaceae (r^2=0.5) and the woodland samples are distinguished strongly by high values of *Eucalyptus* (r^2=0.9) on DCA axis 1.

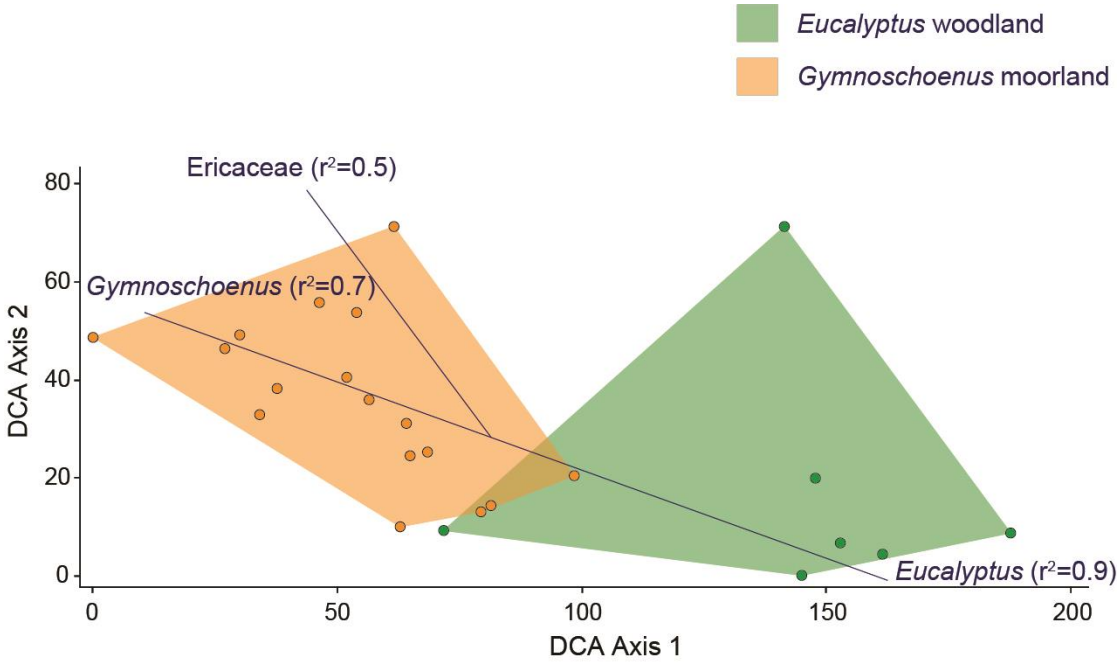

Figure 6-5 DCA biplot of the Excalibur Bog modern pollen transect dataset grouped by vegetation type

The modern pollen transect data is presented as percentage diagrams in figures 6.6-6.9. The taxa have been approximately allocated to the following groups based on comparison with the vegetation data: *Eucalyptus* woodland, *Gymnoschoenus* moorland, long distance transported (LDT) rainforest taxa, LDT subalpine/alpine taxa, LDT other taxa and introduced taxa, however, overlap between groups is bound to occur.

The data indicate that the generally very poorly represented *Gymnoschoenus sphaerocephalus*, although still under-represented by its pollen in this study, is present in good amounts across the bog surface, but rapidly disappears once the *Eucalyptus* woodland boundary is reached, which underpins the poor transport of this taxon. *Eucalyptus* values decrease strongly beyond the woodland boundary, which lies between 300-450 m from the core site, with median values ranging between 61-78% within the woodland and 21-29% on the moorland. Almost 60% of the pollen encountered in the moorland samples is derived from outside the moorland vegetation (figure 10 a, b), even when Restionaceae is included in the pollen sum (figure 10 c, d). The non-local pollen is most likely derived from the adjacent woodland (e.g. *Eucalyptus* and shrub taxa) and by long distance transport from the wider

region (e.g. rainforest and alpine taxa) (figure 10 a, b). Plots of the % presence in the vegetation and pollen sample with fitted regression lines illustrate the relationship for the two key indicator taxa of moorland and woodland (figures 6.11 and 6.12). *Eucalyptus* (figure 6.11) is over-represented in the woodland samples, likely due to the absence of other strong pollen sources within the vegetation. Studies indicating the variability of the representation of *Eucalyptus* from under to well to over were reviewed in Chapter 4. The presence of *Eucalyptus* pollen at 21-29% in the moorland samples, where it is absent in the vegetation, indicates that it is transported at moderate values beyond the source vegetation over a distance of at least 300 m without indicating any distance-related reduction in values. *Gymnoschoenus* (figure 6.12) is under-represented in pollen the local vegetation, however, not severely under-represented as indicated in some cases discussed in Chapter 4 where it is absent from pollen samples even when present in the source vegetation. This suggests that pollen production and/or preservation may be variable. The figure also illustrates that *Gymnoschoenus* pollen does not travel far beyond the source vegetation.

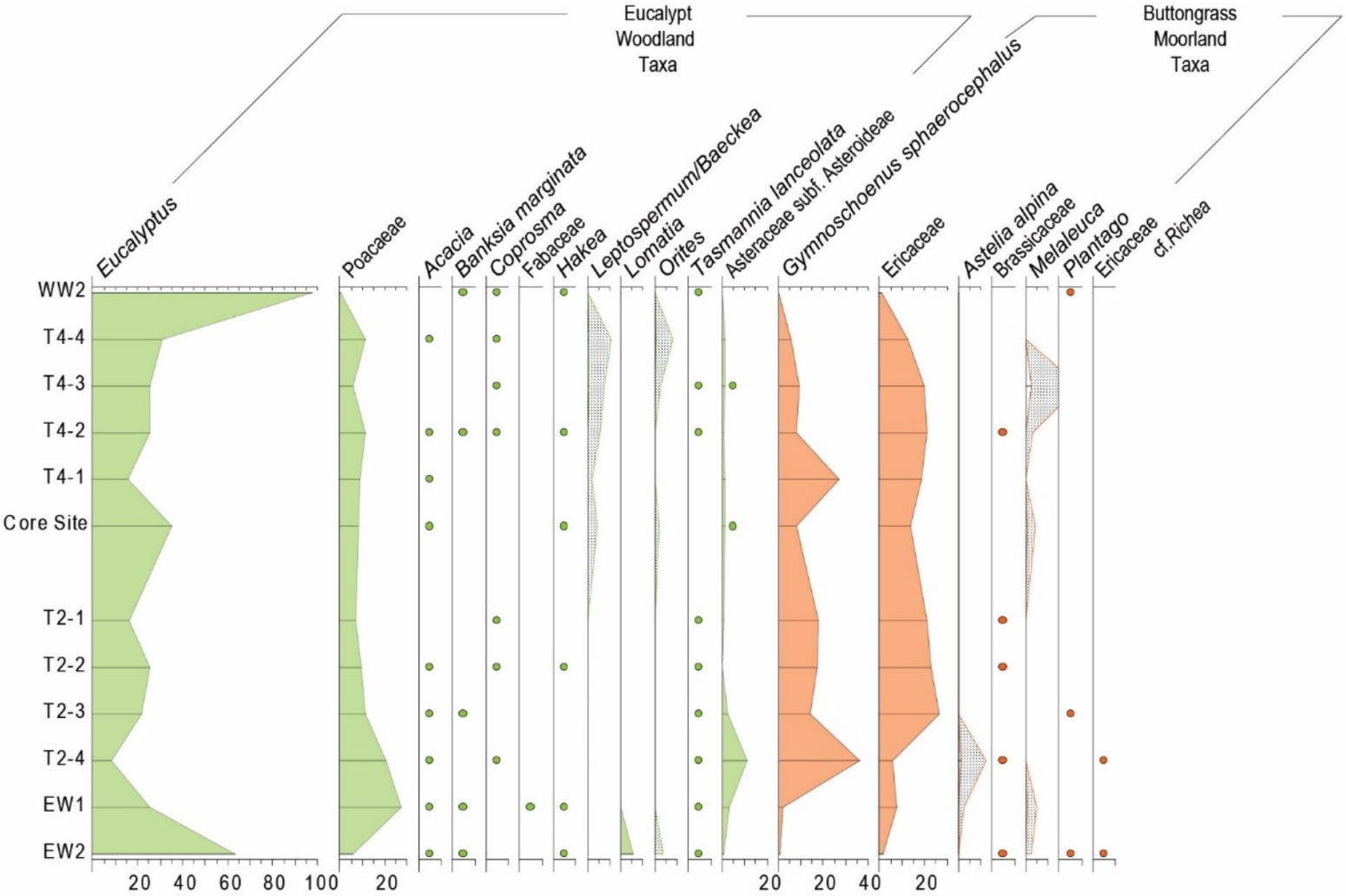

Figure 6-6 Percentage pollen diagram of the Excalibur Bog E-W transect data (part 1)

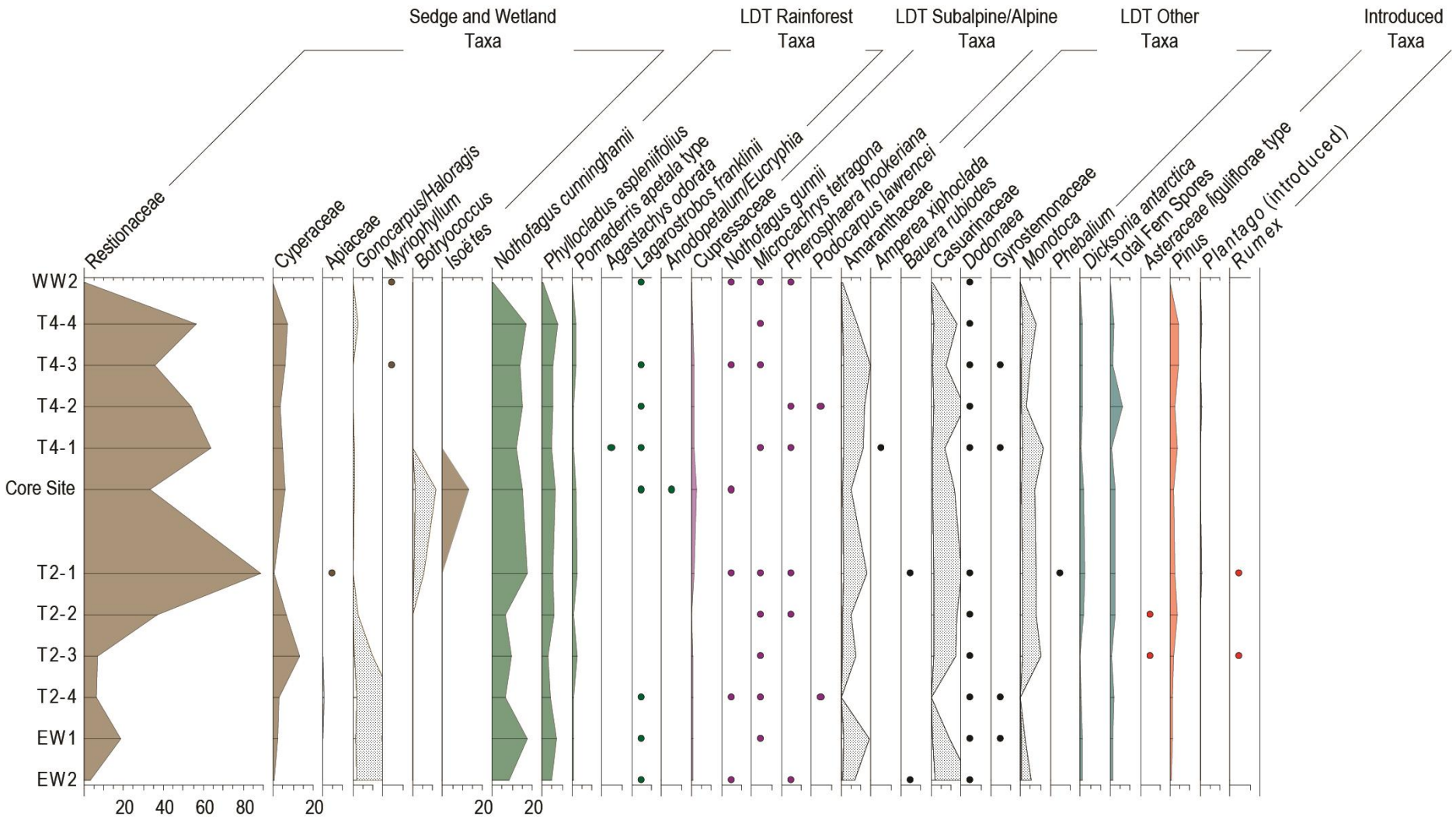

Figure 6-7 Percentage pollen diagram of the Excalibur Bog E-W transect data (part 2)

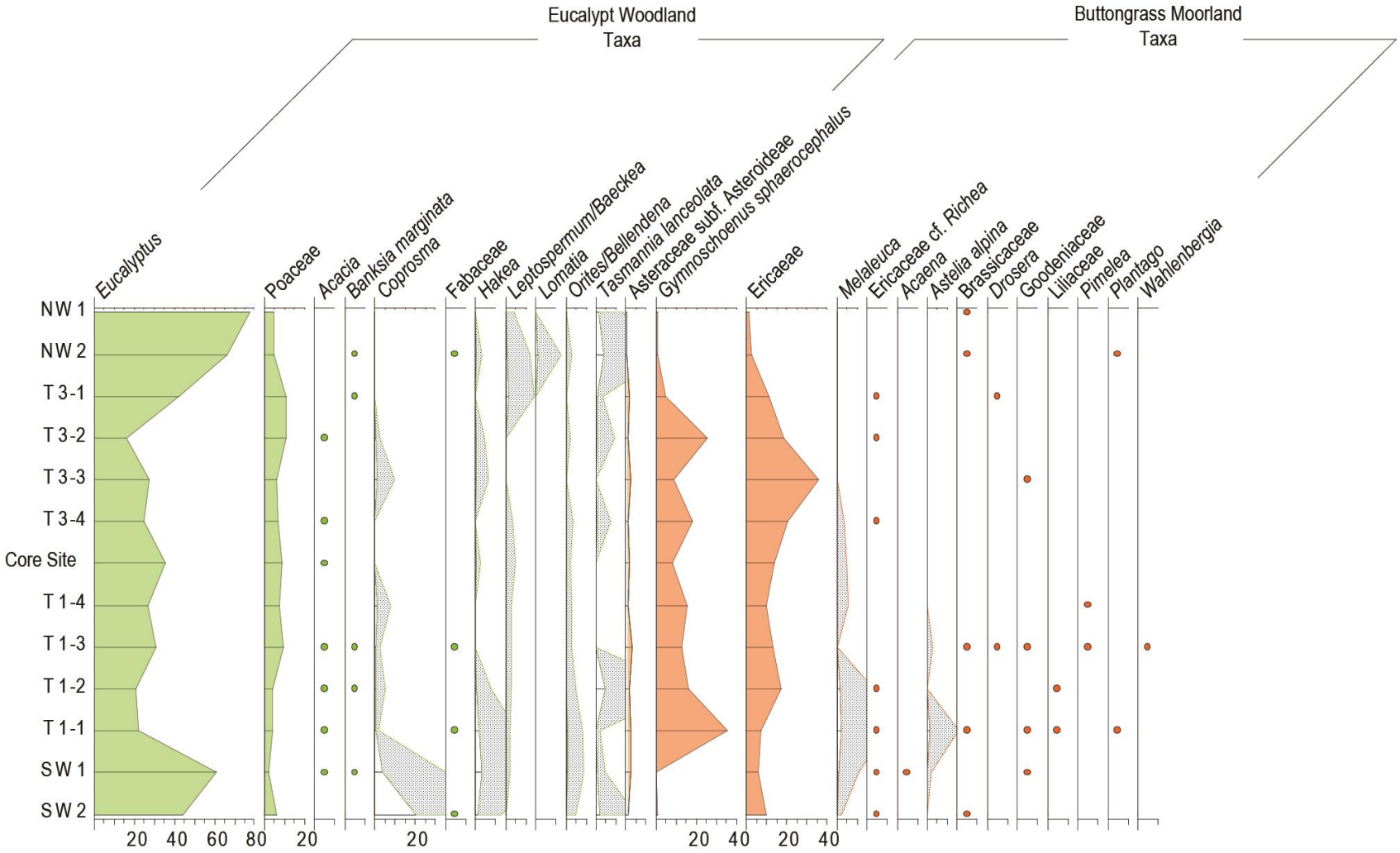

Figure 6-8 Percentage pollen diagram of the Excalibur N-S transect data (part 1)

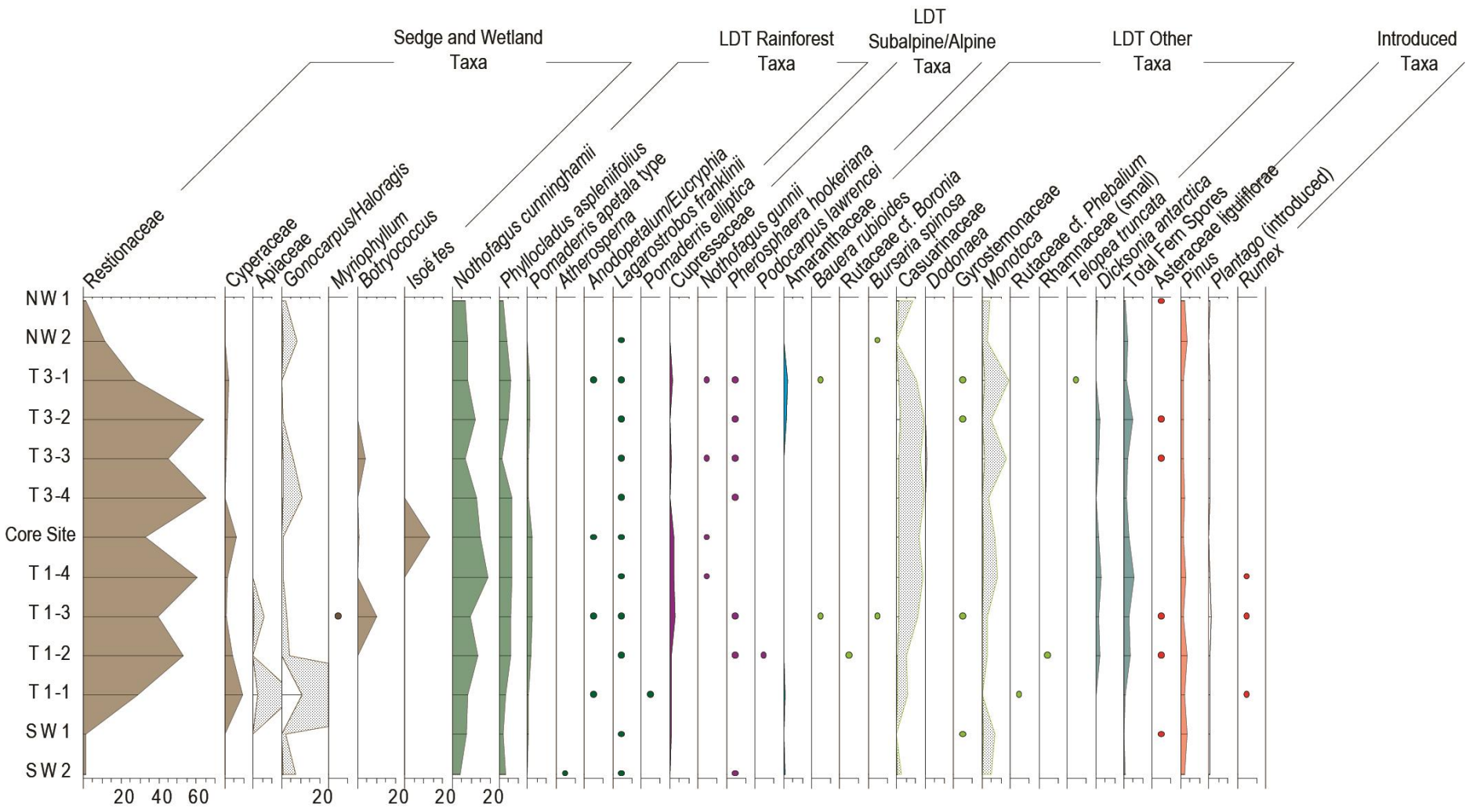

Figure 6-9 Percentage pollen diagram of the Excalibur Bog N-S transect data (part 2)

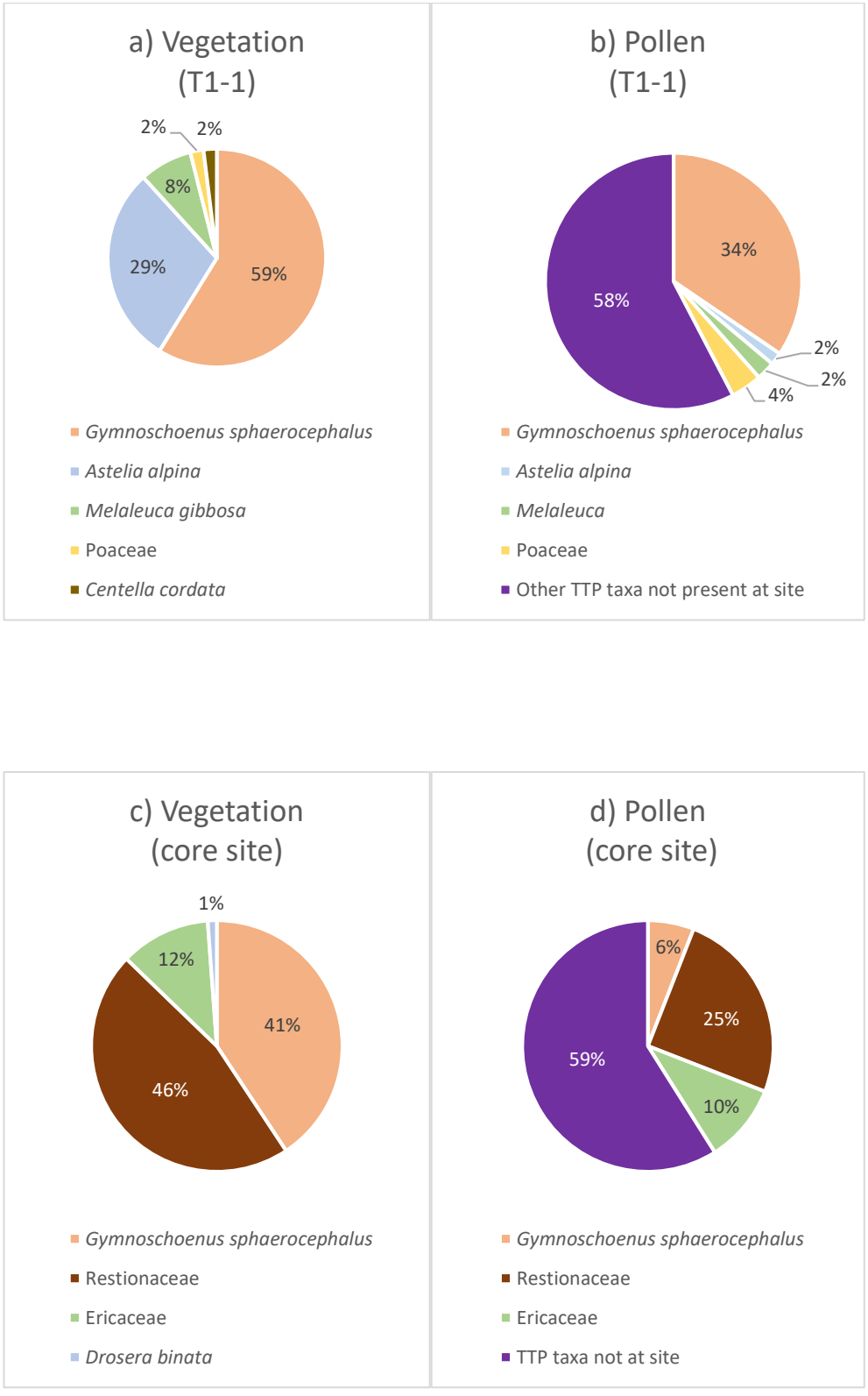

Figure 6-10 a) vegetation (%) cover at site T1-1 b) pollen (%) sample T1-1 c) vegetation (%) core site d) pollen (%) core site

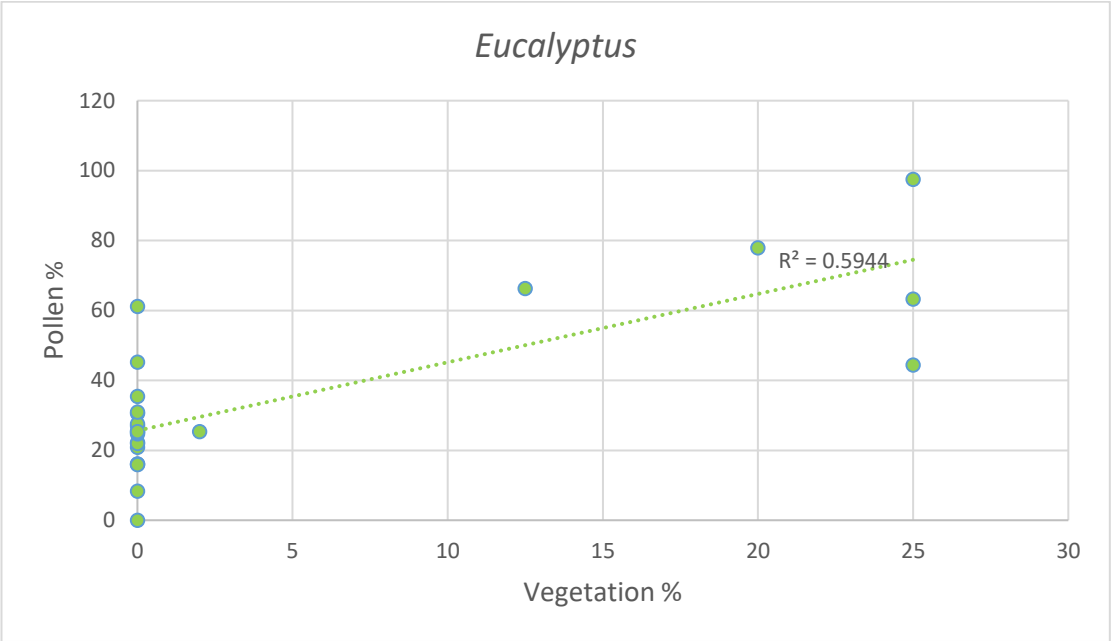

Figure 6-11 Percent pollen versus percent estimated vegetation cover of Eucalyptus linear regression line for all Excalibur Bog sites

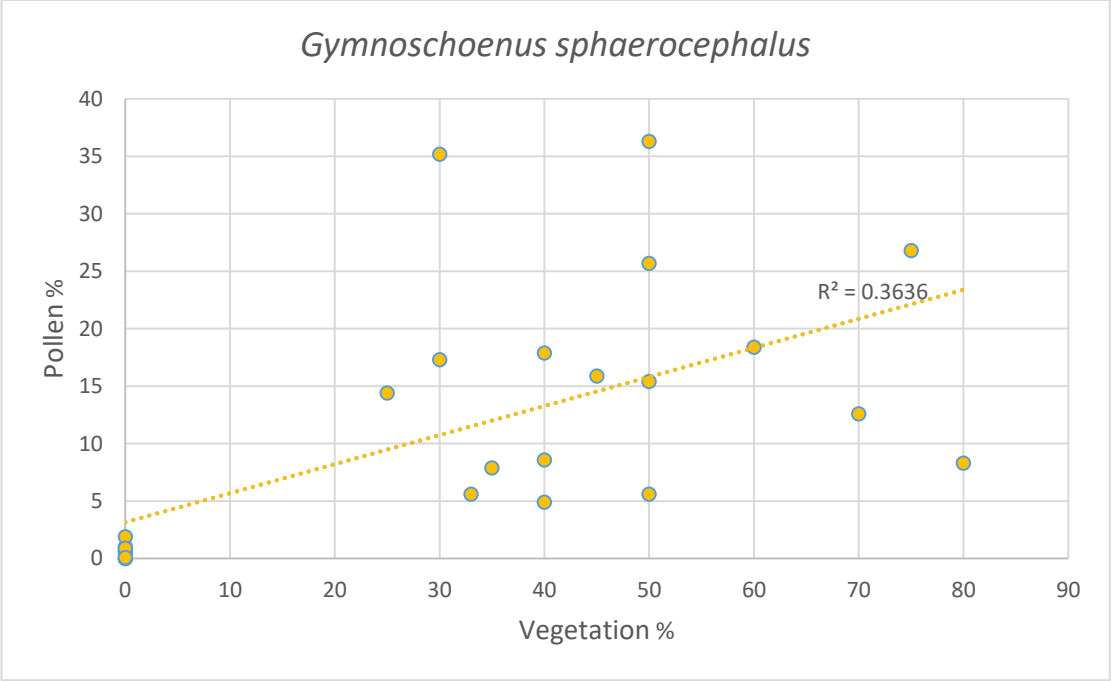

Figure 6-12 Percent pollen versus percent estimated vegetation cover of Gymnoschoenus sphaerocephalus with linear regression line for all Excalibur Bog sites

6.3.2 Excalibur Bog Core

6.3.2.1 Sediments and Dating

The Excalibur Bog core is 185 cm in length and the stratigraphy is presented in figure 6.13, with various properties of the sediment illustrated in figure 6.14. The basal sediments consist of olive clays which are low in carbon and nitrogen. A sharp boundary at 89 cm separates the clays from the overlying mud and peat and is defined by a 5 mm layer of small pebbles (2-3 mm diameter on average, some up to 1.5 cm) overlain by a 21 mm olive grey fine sand layer, also low in carbon and nitrogen. Eight sample depths were radiocarbon dated and the results are listed in table 6.1. For several samples, the humic acid and humin fractions were dated separately. The humin fraction of the sample taken at 60-61 cm failed and the samples for 95-96 cm and 140-141 cm contained no alkali fraction to date.

Table 6-1 Radiocarbon dates for Excalibur Bog. Calibrated ages calculated by CLAM using SHCal13 where applicable, otherwise NHCal13 was used. Ages are followed by probability in brackets. Those dates identified as outliers by BACON (figure 6.15) are coloured in grey and excluded from the age model.

Depth (cm)	Lab Code	Material Dated	Radiocarbon Age (^{14}C yr BP)	Error (^{14}C yr BP)	□^{13}C	Calibrated Age (cal yr BP)
40-41	ANU 31033	Humic acid fraction	2425	45	-32.12	2315-2519 (80.4%), 2636-2698 (10.5%), 2591-2615 (2.9%), 2525-2541 (1.1%)
40-41	ANU 32020	Humin fraction	3400	150	-10.65	3260-3978 (95%)
60-61	ANU 34430	Humic acid fraction	3745	30	-39	3910-4097 (88%), 4117-4146 (6.9%)
60-61	OZF507	Bulk sediment	1140	40		927-1066 (95%)
70-71	OZF506	Bulk sediment	6020	50		6672-6931 (95%)
80-81	ANU 34524	Humic acid fraction	8340	70	-30.29	9087-9463 (93.2%), 9034-9050 (1.7%)
80-81	ANU 34431	Humin fraction	8440	40	-41	9290-9494 (95%)
85-86	OZF505	Bulk sediment	5710	50		6306-6563 (94.7%), 6594-6596 (0.2%)
95-96	ANU 31037	Humin fraction	18590	100	-30.46	21761-22475 (94.6%), 21616-21633 (0.4%)
140-141	ANU 31038	Humin fraction	22100	130	-29.07	26028-27035 (95%)
177.5-178.5	OZF504	Bulk sediment	2810	40		2766-2950 (95%)

0 cm: Sedges growing on surface
0.0-8.0 cm: Dense sedge root and fine, fibrous roots
10YR 3/2 (very dark greyish brown)
8 cm

8.0-69.0 cm: Peat with roots
7.5YR 2.5/1 (black)

69.0 cm (-74.5 cm): Muddy sediment / 10YR 3/2 (very dark greyish brown)

74.5 cm (-84.0 cm): Muddy sediment / 10YR 2/2 (very dark brown)

79.5 cm (-84.0 cm): Muddy sediment / 10YR 2/1 (black)

84.0 cm (-86.5 cm): Muddy, sandy sediment / 5Y 3/2 (dark olive grey)
86.5 cm (-89.0 cm): Fine sand layer / 5Y 4/2 (olive grey)
89.0 cm: Sharp boundary
(5 mm layer of small pebbles (2-3 mm diameter, some upt o 1.5 cm)
and sand)

89.0 - 185.0 cm: clay with roots
5Y 5/3 (olive)
(89.0 - 162.5 cm: crack filled with
5Y 4/2 (olive grey) sand and 5GY 4/1(dark greenish grey) clay)

185.0 cm

Figure 6-13 Excalibur Bog core stratigraphy.

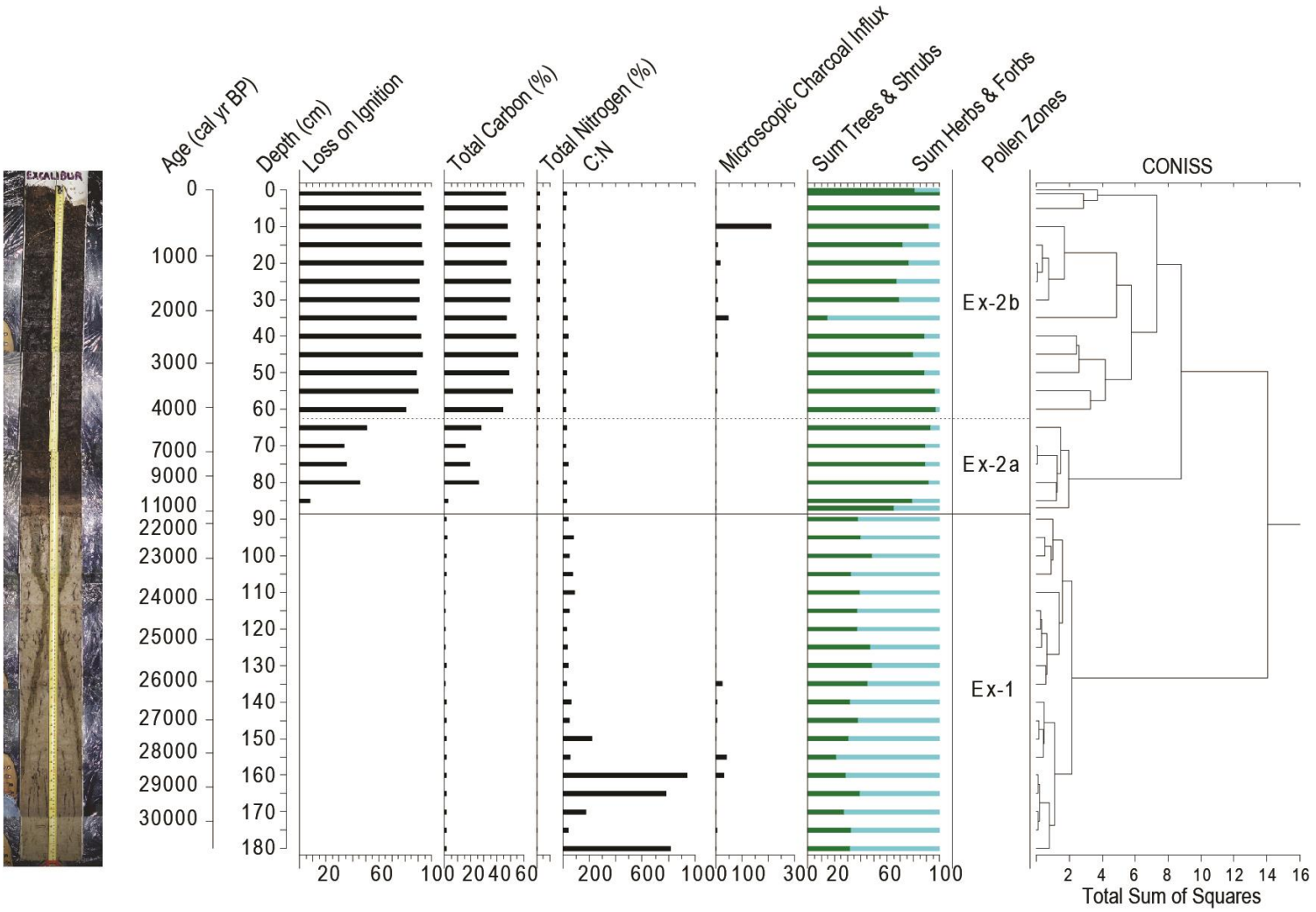

Figure 6-14 Excalibur Bog core sediment properties plotted with summary pollen data and pollen zones derived by CONISS.

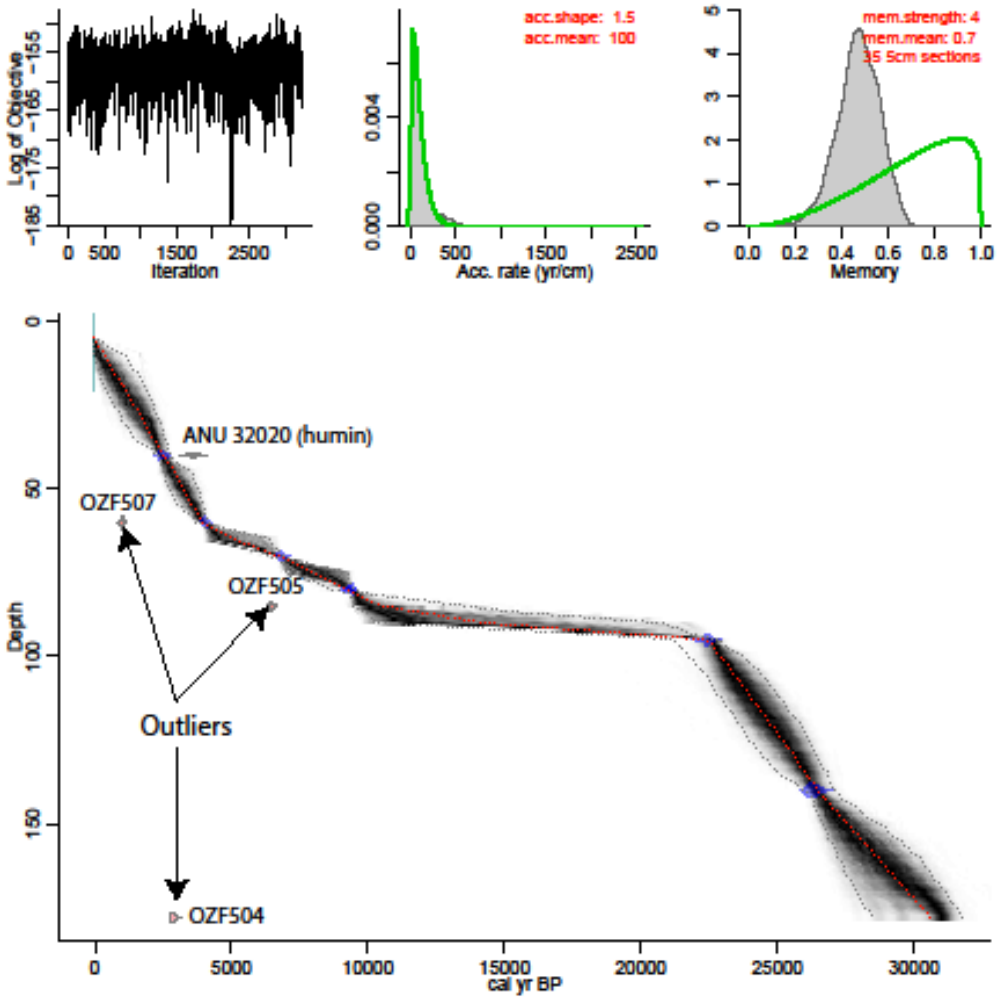

Figure 6-15 Age depth model produced in BACON using SHCal13 calibration curve. BACON identified OZF 504, OZF 505, OZF 507 and ANU 32020 (humin fraction) as outlier

The BACON age model is presented in figure 6.15 and excluded the dates OZF 504, 505 and 507 and ANU 32020 as outliers. The large time gap between the dated samples at 80 cm and 95 cm suggests that there was a hiatus at the stratigraphic boundary at 89 cm. The decision was made to extrapolate dates between 89 and 80 cm using the deposition rate of 231.3 yrs/cm calculated from the sediments above and to extrapolate the dates between 95 and 89 cm using the deposition rate of 103.7 yrs/cm calculated from the sediments below. This was then used as the age scale for the pollen diagram and any other proxies, resulting in an estimated hiatus of c. 9000 years spanning the period between c. 11.3 and c. 21.8 cal kyrs BP at the boundary at 89 cm. Sedimentation was much slower between 60 cm and 80 cm when compared with the remainder of the core. It is possible that this section contains hiatus(es) (e.g. due to burning of peat).

.

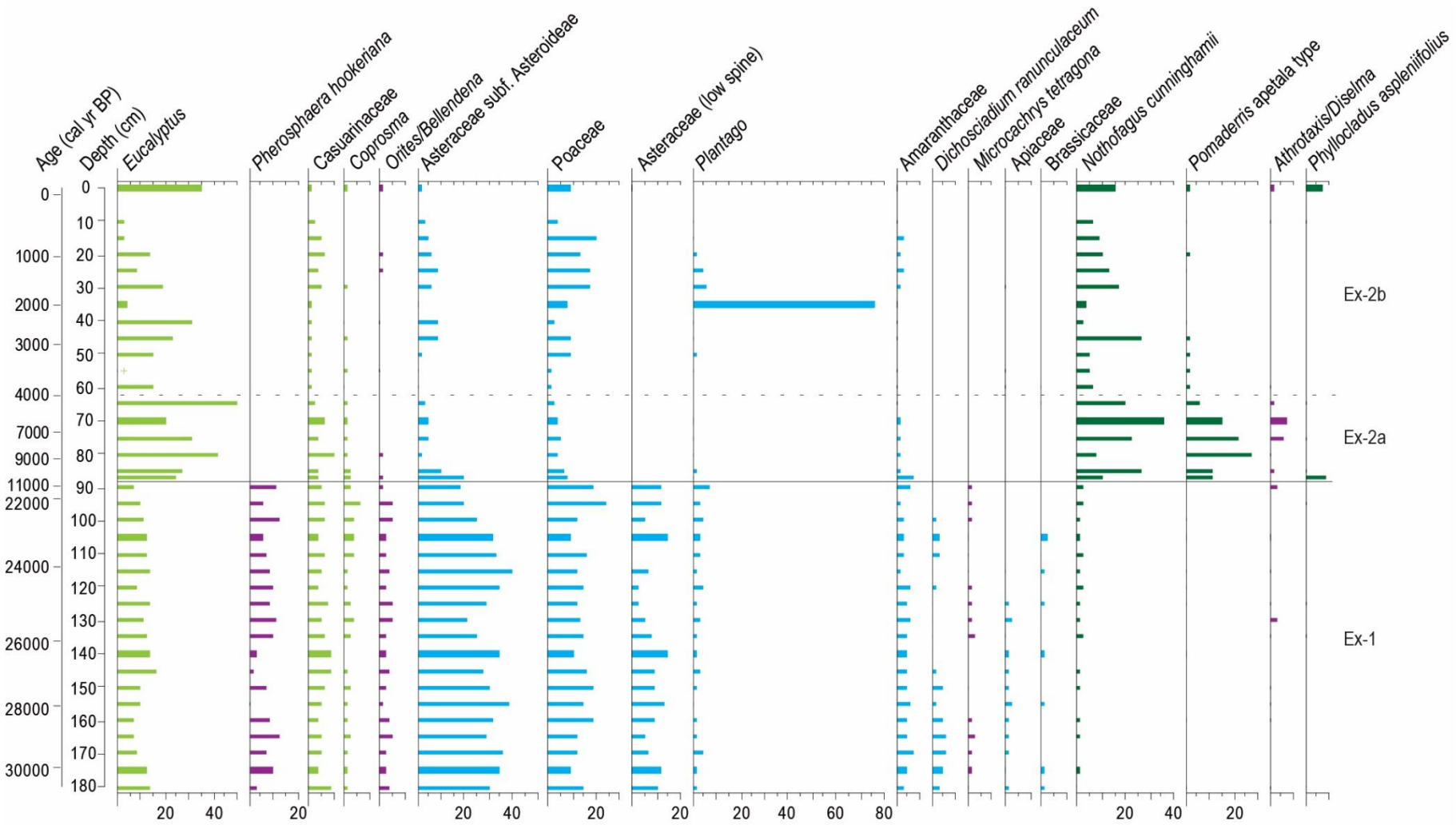

Figure 6-16 Percentage pollen diagram of the Excalibur Bog core (part 1). Note hiatus at 89 cm.

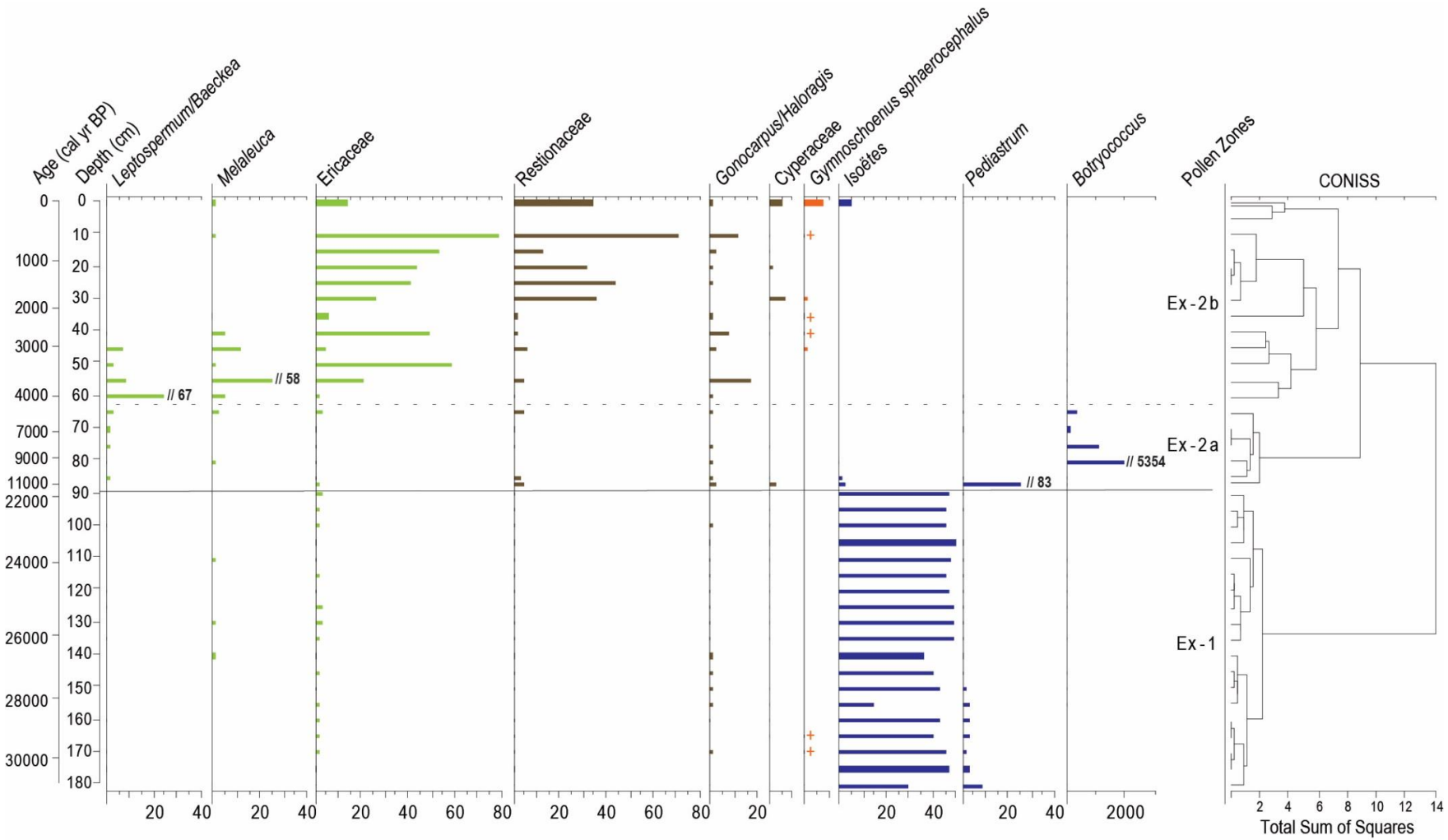

Figure 6-17 Percentage pollen diagram of the Excalibur Bog core (part 2). Note hiatus at 89 cm.

6.3.2.2 Pollen, Spore and Microscopic Charcoal Analysis

CONISS (figure 6.17) clearly separates the basal glacial samples (Ex-1) from the remainder of the core (Ex-2), with zone Ex-2 separated into two subzones: Ex-2a (89-62.5 cm) and Ex-2b (62.5 cm – surface). A percentage pollen diagram of the Excalibur Bog core data is presented in figures 6.16 and 6.17. A DCA biplot (figure 6.18) of the core data grouped by pollen zones illustrates that zone Ex-1 is clearly distinguished as a tight group high on DCA axis 1, driven most strongly by values of Asteraceae (r^2=0.74). Sub-zones 2a and 2b show a small amount of overlap, with samples with large peaks of individual taxa lying as outliers within sub-zone ex-1. Ericaceae (R2=0.7) most strongly distinguishes zone ex-1 from zone ex-2.

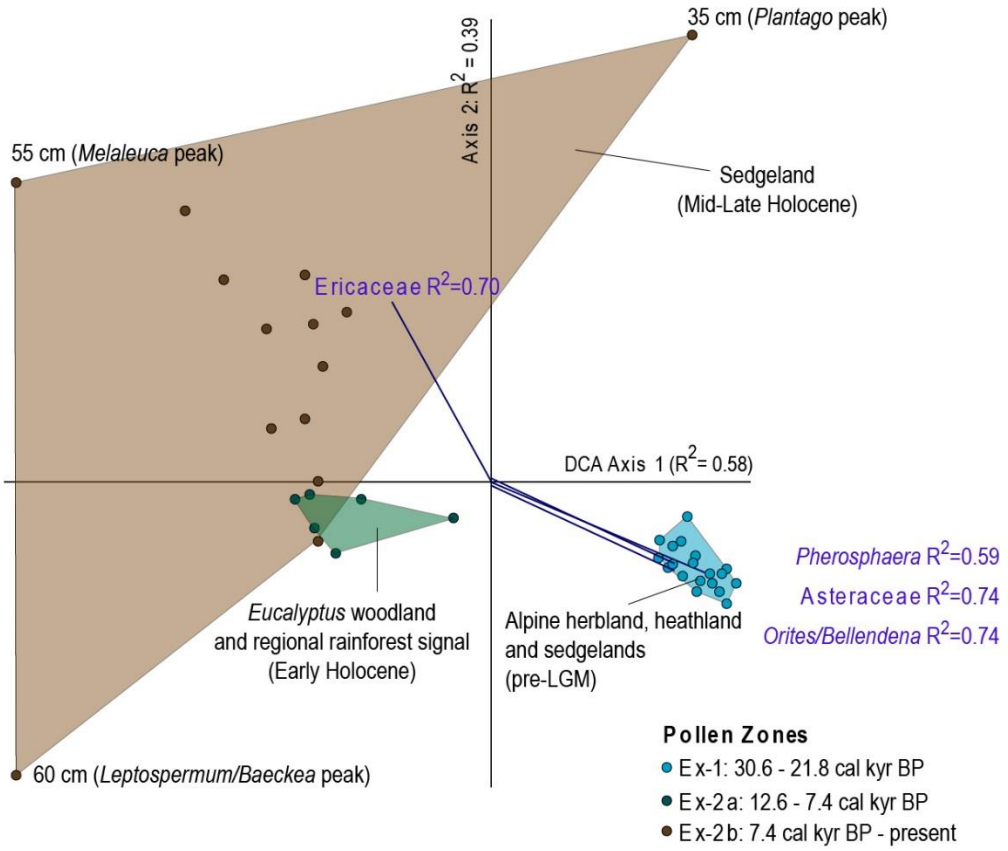

Figure 6-18 DCA biplot of the Excalibur Bog core pollen data grouped by CONISS derived pollen zones.

Zone Ex-1: 185.0-89.0 cm, ca. 30.6-21.8 cal kyr BP

Zone Ex-1 is dominated by herbs, notably Asteraceae subf. Asteroideae (18-40%) and Poaceae (9-24%) with Asteraceae (low spine) (0-14%), *Plantago* (1-7%), Amaranthaceae (1-7%), *Dichosciadium ranunculaceum* (0-6%) and Apiaceae (0-3%) also present. *Eucalyptus* (7-16%) is the only tree taxon present in significant quantities, with Casuarinaceae recorded at 3-9% and only small amounts of *Nothofagus cunninghamii* (0-3%) and Cupressaceae (0-3%). Key shrub taxa include *Phaerosphaera hookeriana* (1-13%), *Coprosma* (0-6%), Proteaceae cf. *Orites* type (1-5%), Ericaceae (0-3%), *Microcachrys tetragona* (0-3%) and *Tasmannia lanceolata* (0-3%).

Isoëtes (29-98%) is present in large quantities. Microscopic charcoal influx is relatively low throughout the zone, varying between 0-39 with three small peaks at 28.7, 28.1 and 26.0 cal kyr BP.

Zone Ex-2a: 89.0-62.5 cm, ca. 11.3-7.4 cal kyr BP

Sub-zone Ex-2a is dominated by tree taxa, notably *Eucalyptus* (21-50%), *Nothofagus cunninghamii* (8-36%) and *Pomaderris apetala* type (6-27%) with Casuarinaceae (3-10%), *Phyllocladus aspleniifolius* (0-8%) and Cupressaceae (0-7%) also present. Small amounts of shrubs (Ericaceae (0-4%), *Leptospermum*/*Baeckea* (0-3%) occur together with mostly low amounts of herbs: Asteraceae subf. Asteroideae (2-19%), Poaceae (2-8%) and Amaranthaceae (1-7%). Small amounts of *Isoetes* present at the start of the zone along with peak values of *Pediastrum* (0-83%) are followed by peak values of *Botryococcus* (1-5354%).

Zone Ex-2b: 62.5-37.5 cm, ca. 7.4 cal kyr BP – present

Sub-zone Ex-2b contains a series of peaks of single taxa (*Leptospermum/Baeckea* type at 60 cm, *Melaleuca* at 55 cm and *Plantago* at 35 cm), but also shows a general increase in Ericaceae (0-80%) and *Gonocarpus*/*Haloragis* (0-17%). Restionaceae (0-71%) increases notably from 30 cm. Tree taxa *Eucalyptus* (1-36%) and *Nothofagus cunninghamii* (0-27%) are present at variable levels (depending on strength of local signal) with *Phyllocladus aspleniifolius* (0-7%) and Casuarinaceae (0-6%) also present. Other herb taxa present include Poaceae (0-20%), Asteraceae subf. Asteroideae (0-8%), *Gymnoschoenus sphaerocephalus* (0-8%) and Amaranthaceae (0-3%). *Botryococcus* (0-46%) values are reduced relative to the previous sub-zone and *Isoëtes* is present at between 0-14%.

6.3.2.3 Comparison of fossil data with modern pollen data

Figure 6.19 presents a DCA biplot of the core data plotted together with the modern pollen data from the site. The samples from sub-zone Ex-2a plot relatively closely with the modern eucalypt woodland samples. A few of the samples from sub-zone Ex-2b plot plot this zone plot in the rough direction of the modern moorland samples. It is likely that the lack of *Gymnoschoenus* pollen counted in the core samples accounts for this deviation.

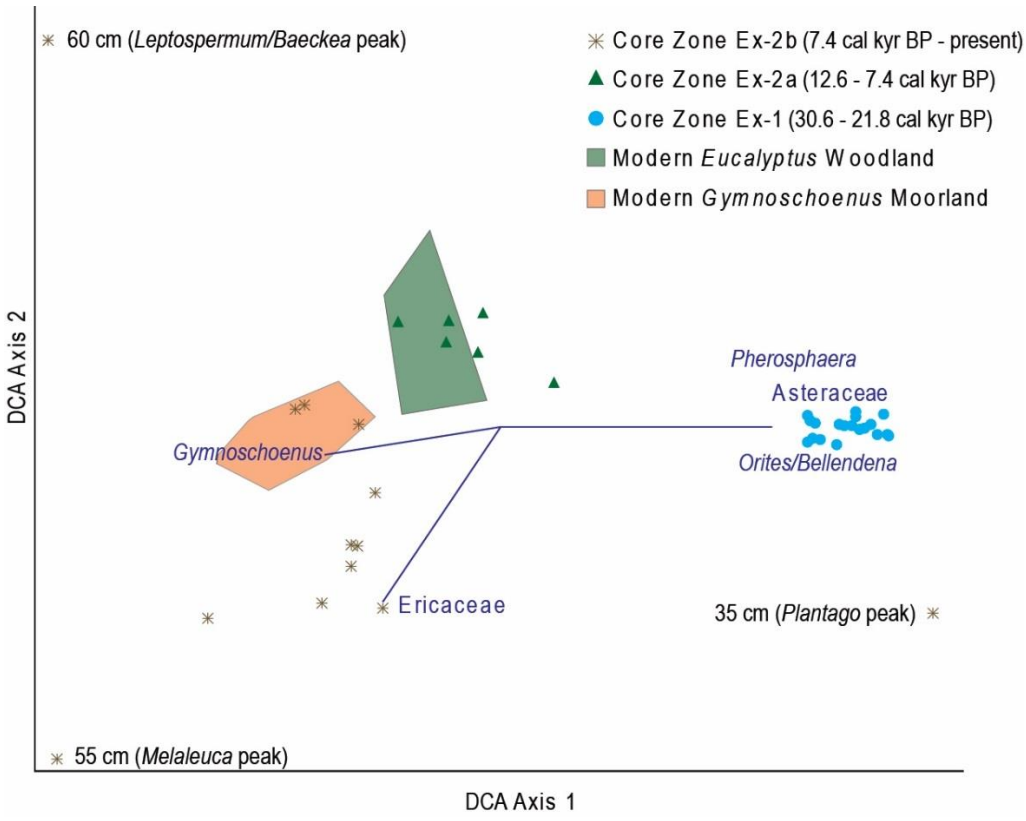

Figure 6-19 DCA biplot of the Excalibur Bog core and modern pollen data.

6.4 Clarence Lagoon

6.4.1 Sediments and Dating

The Clarence Lagoon lake core is 325 cm in length and a simplified stratigraphy, consisting of 288.5 cm of sands, silts and clays overlain by 36.5 cm of hardpan material, is illustrated in figure 6.21 together total organic matter (%) which mostly varies between low values between 5-10%. Four samples were radiocarbon dated and ranged between 42.5-26.3 cal kyr BP in the c. 30 cm below the hardpan (table 6.3). A sample dated at 167.5 cm is of an age beyond radiocarbon dating, suggesting that the record extends well into OIS Stage 3.

Table 6-2 Radiocarbon dates for the Clarence Lagoon lake core.

Depth (cm)	Lab Code	Material Dated	Radiocarbon Age (^{14}C yr BP)	Error (^{14}C yr BP)	Calibrated Age (cal yr BP)
37.7	OZE 282	Bulk sediment	22000	250	26.3 (26.9-25.8)
51.2	OZE 283	Bulk sediment	26750	250	30.9 (31.2-30.6)
64.0	OZE 524	Bulk sediment	38300	550	42.5 (43.2-41.7)
167.5	OZE 284	Bulk sediment	>46000		

6.4.2 Pollen and Spore Analysis

Pollen and spore analysis indicated that a large part of the Clarence Lagoon core contained little or no pollen, resulting in a discontinuous record of vegetation change which is illustrated as a percentage pollen diagram in figures 6.22 and 6.23 with the pollen-rich bands of sediment labelled as zones 1-4.

Zone 1 contains a high percentage of herbaceous taxa, with Poaceae ranging between 33-47 %, Asteraceae between 26-32 % and the long distance transported Amaranthaceae at its highest values (9-11%) for the record. *Pherosphaera* values (5-11%) are notably reduced relative the remainder of the core, with Ericaceae values also reduced and *Orites/Bellendena* absent. Zone 2 sees a reduction in herbaceous taxa and strong increase in *Pherosphaera* values (43-48%). The sample taken at 239 cm from a band of dark sediment (figure 6.20) stands out with significantly elevated values of *Nothofagus cunninghamii* (8%) and other rainforest taxa, including *Phyllocladus aspleniifolius*, *Athrotaxis*/*Diselma* and *Lagarostrobos* also elevated, albeit at lower values, and Poaceae values reduced (5%). Zones 3 and 4 are overall very similar to zone 2 showing a strong dominance of *Pherosphaera* which ranges between 28-40% in zone 3 and between 49-58% in zone 4 when it reaches its highest values for the record. *Eucalyptus* values are mostly below 10%, apart from at 173 cm and 285 cm where it reaches 15 and 16% respectively. Ericaceae (8%) and *Orites*/*Bellendena* (10%) are at their highest at 173 cm when *Pherosphaera* is slightly reduced (28%). The sample at 45 cm just

below the hardpan contains an unusual mix of relatively high values of rainforest taxa together with herbs and alpine/subalpine taxa. It seems likely that this sample was contaminated.

A DCA biplot of the Clarence Lagoon samples plotted together with the basal sediment samples from Excalibur Bog and Lake St Clair is presented in figure 6.20. The plot confirms the clear separation of zone Clg-1 from the other samples in the core, and the close grouping of zones 2 and 4 based on the highest percentages of *Pherosphaera* in these sections of the core. Zone Clg-1 plots close to the Lake St Clair basal samples driven by shared high values of Poaceae. The Excalibur Bog basal samples are separated based on the high percentage of Asteraceae tubuliflorae type and Asteraceae (low spine).

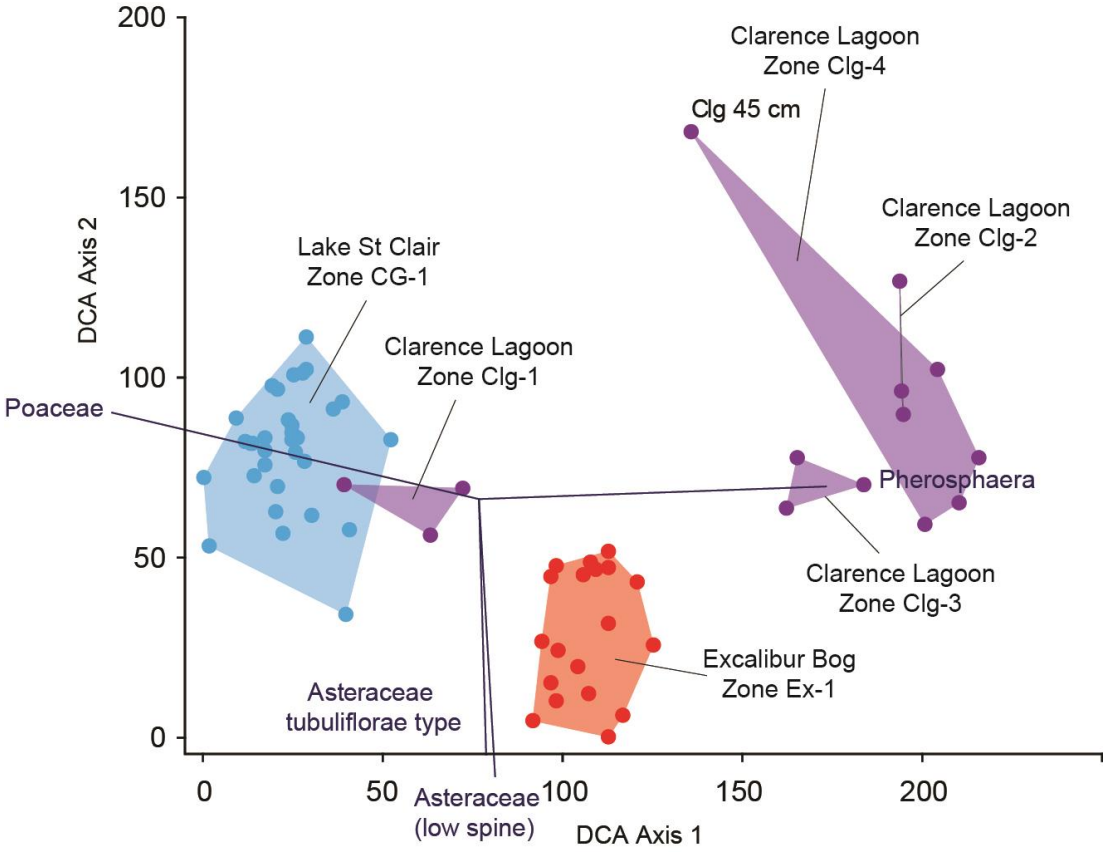

Figure 6-20 DCA biplot of the Clarence Lagoon core pollen data with the Excalibur Bog and Lake St Clair basal pollen samples

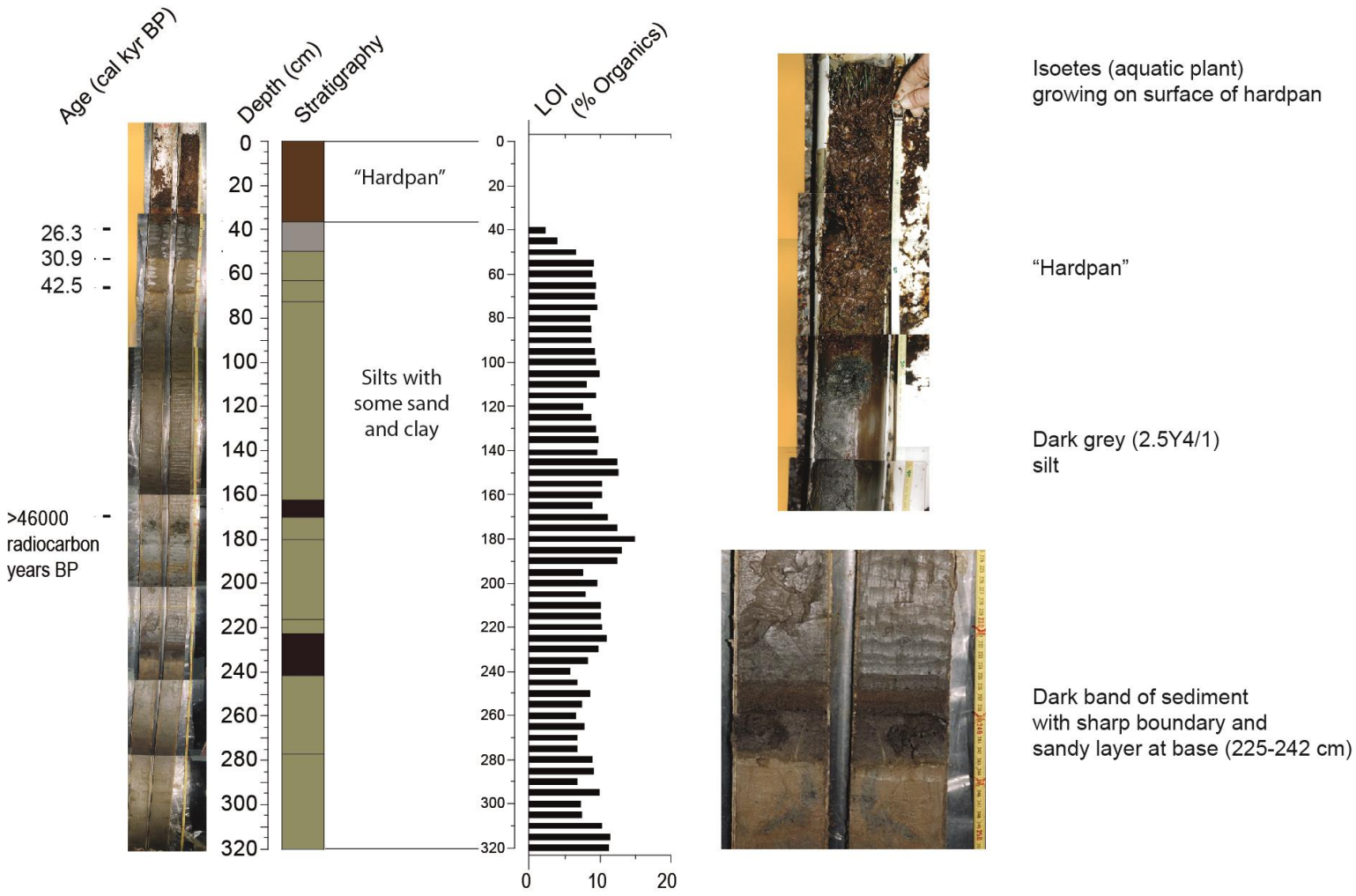

Figure 6-21 Clarence Lagoon core stratigraphy and sediment properties.

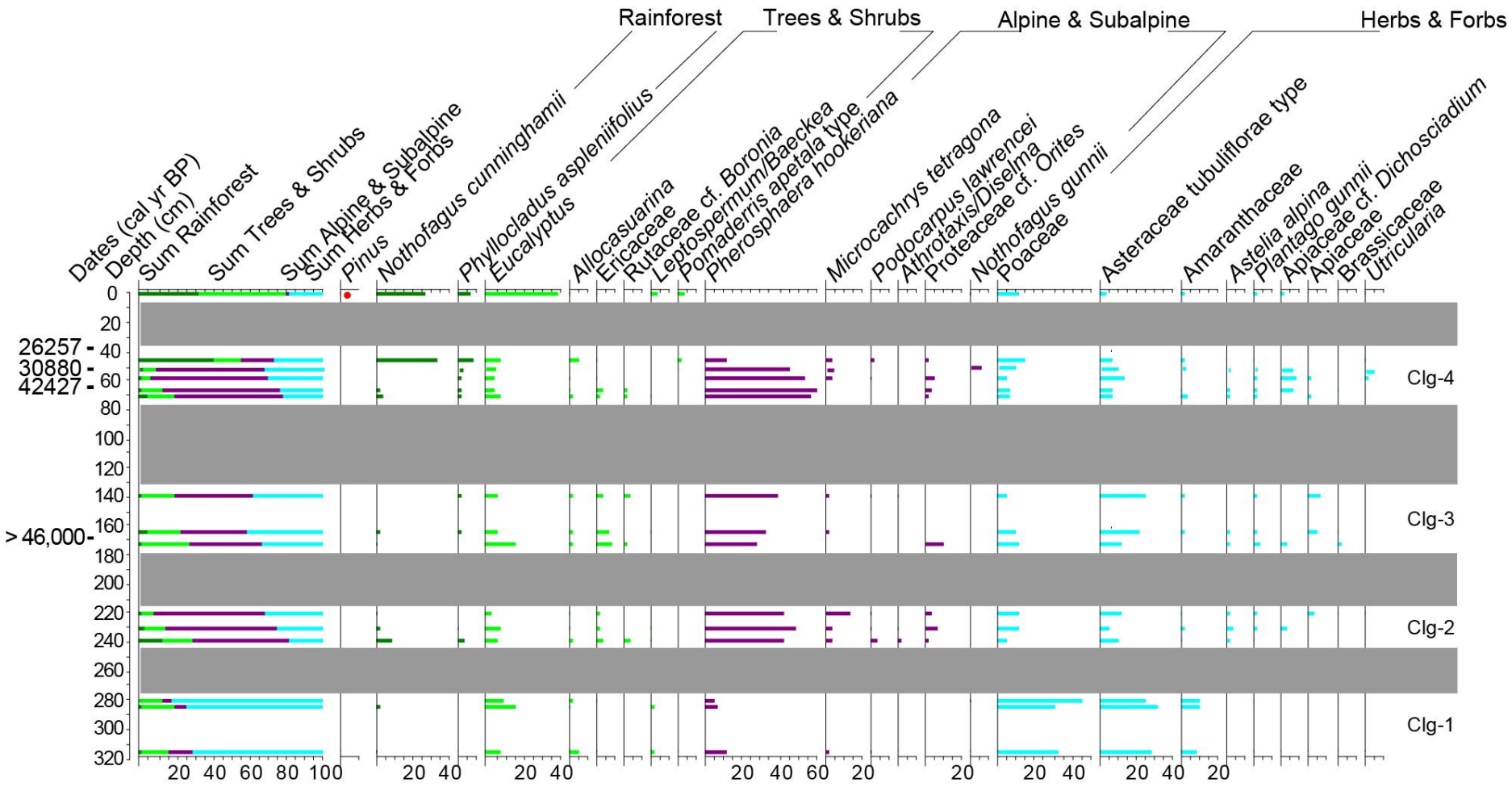

Figure 6-22 Clarence Lagoon percentage pollen diagram (part 1). Grey bands indicate sections of the core with little or no pollen.

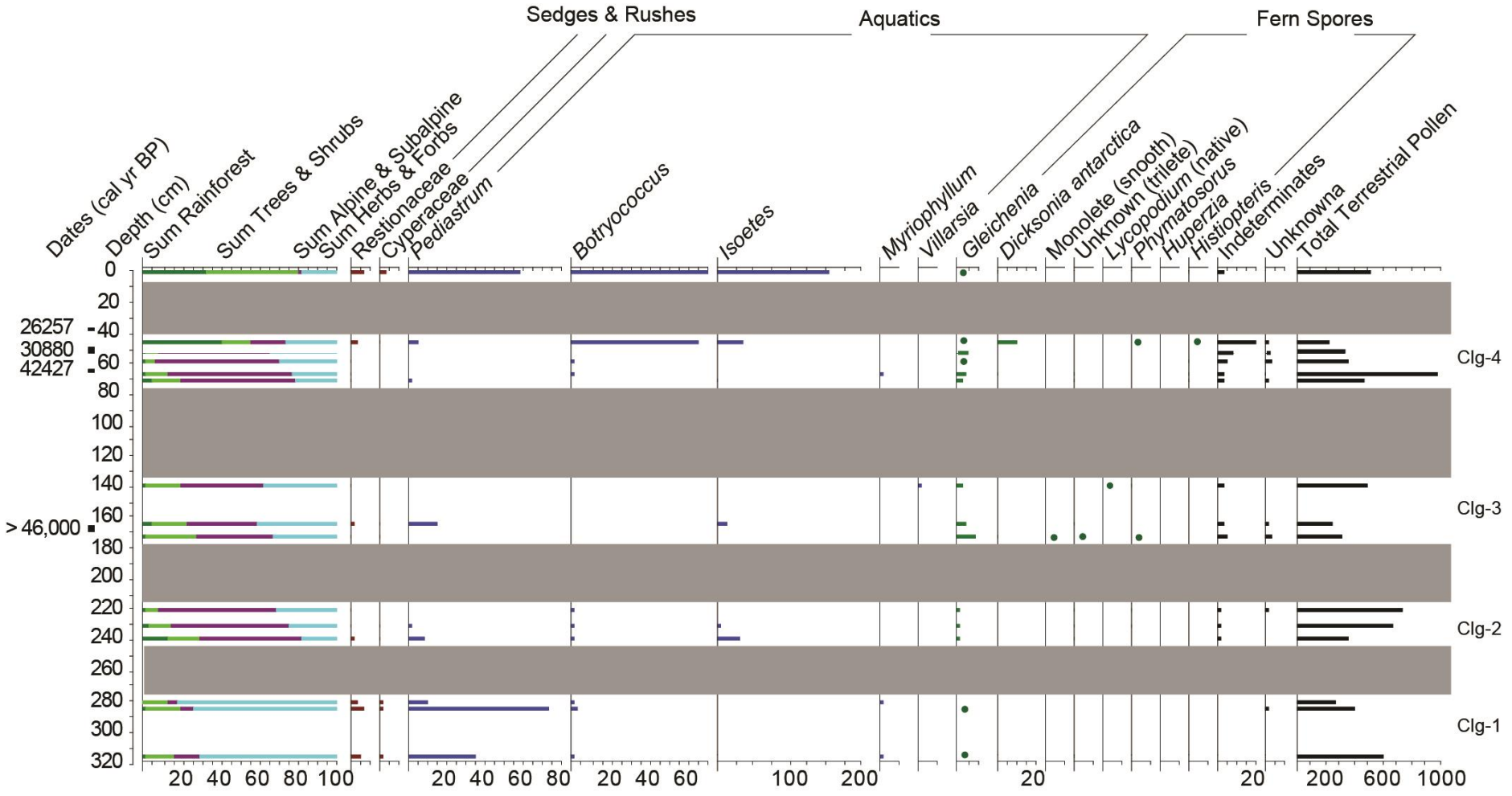

Figure 6-23 Clarence Lagoon percentage pollen diagram (part 2). Grey bands indicate sections of the core with little or no pollen

6.5 Clarence Bog

6.5.1 Sediments and Dating

The Clarence Bog core is 280 cm in length consisting of 90 cm of silts and clays overlain by 112 cm of black peat and 78 cm of dark brown, fibrous peat at the top (figure 6.24). Two samples were dated returning an age of c. 4.8 cal kyr BP just above the gravel layer on the lower boundary of the black peat and c. 1.3 cal kyr BP for the upper boundary (Table 6.4).

Table 6-3 Radiocarbon dates for the Clarence Lagoon bog core.

Depth (cm)	Lab Code	Material Dated	Radiocarbon Age (^{14}C yr BP)	Error (^{14}C yr BP)	Calibrated Age (cal yr BP)
80	OZF508	Bulk sediment	1440	40	1.3 (1.4-1.2)
185	OZF509	Bulk sediment	4280	40	4.8 (4.9-4.6)

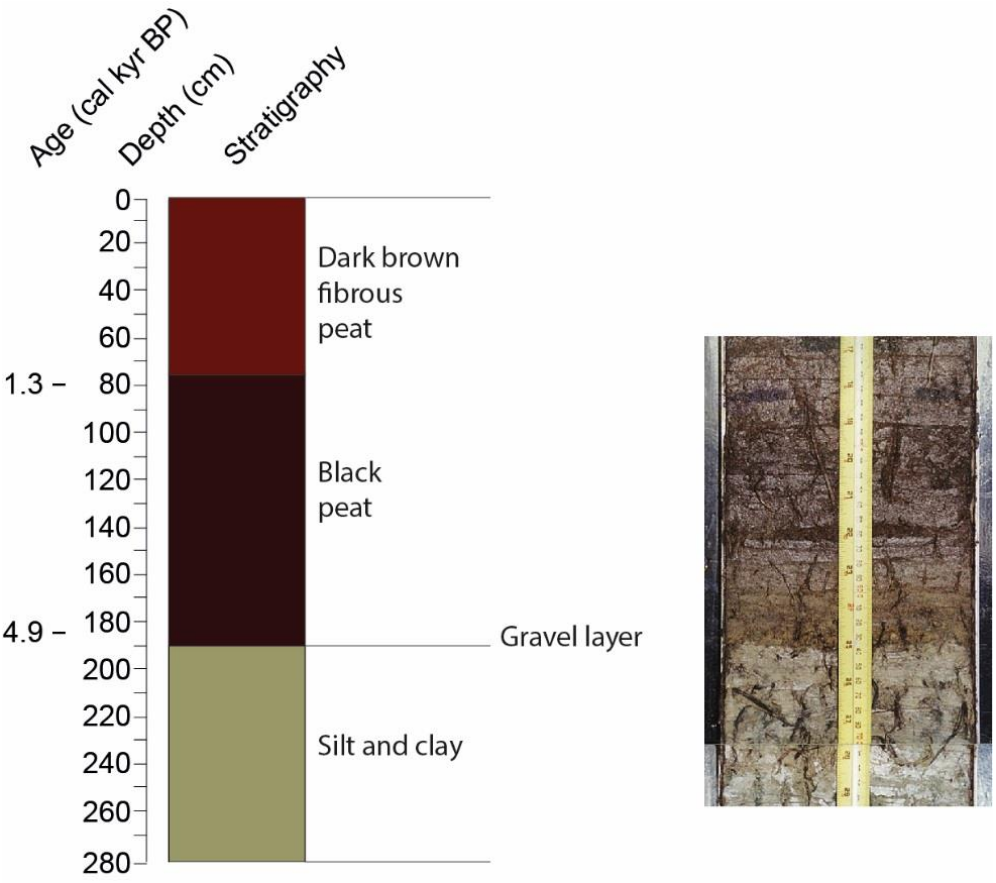

Figure 6-24 Stratigraphy and dates for the Clarence Bog core with detail of gravel layer at the boundary at 190 cm.

6.5.2 Pollen and Spore Analysis

No pollen was observed in the basal silts and clays of the Clarence Bog core and pollen concentrations were relatively low for the peat section of the core. A percentage pollen diagram is presented in figures 6.24 and 6.25 and indicates a shift from a Restionaceae and *Sphagnum* dominated bog during zone 1 to bog dominated more strongly by shrubs (e.g. Eriaceae and *Monotoca*). Values of montane *(Nothofagus cunninghamii* and *Phyllocladus aspleniifolius*) and subalpine (*Athrotaxis*/*Diselma* and *Nothofagus gunnii*) rainforest taxa are higher during zone 1 than zone 2 where *Eucalyptus* values are overall higher.

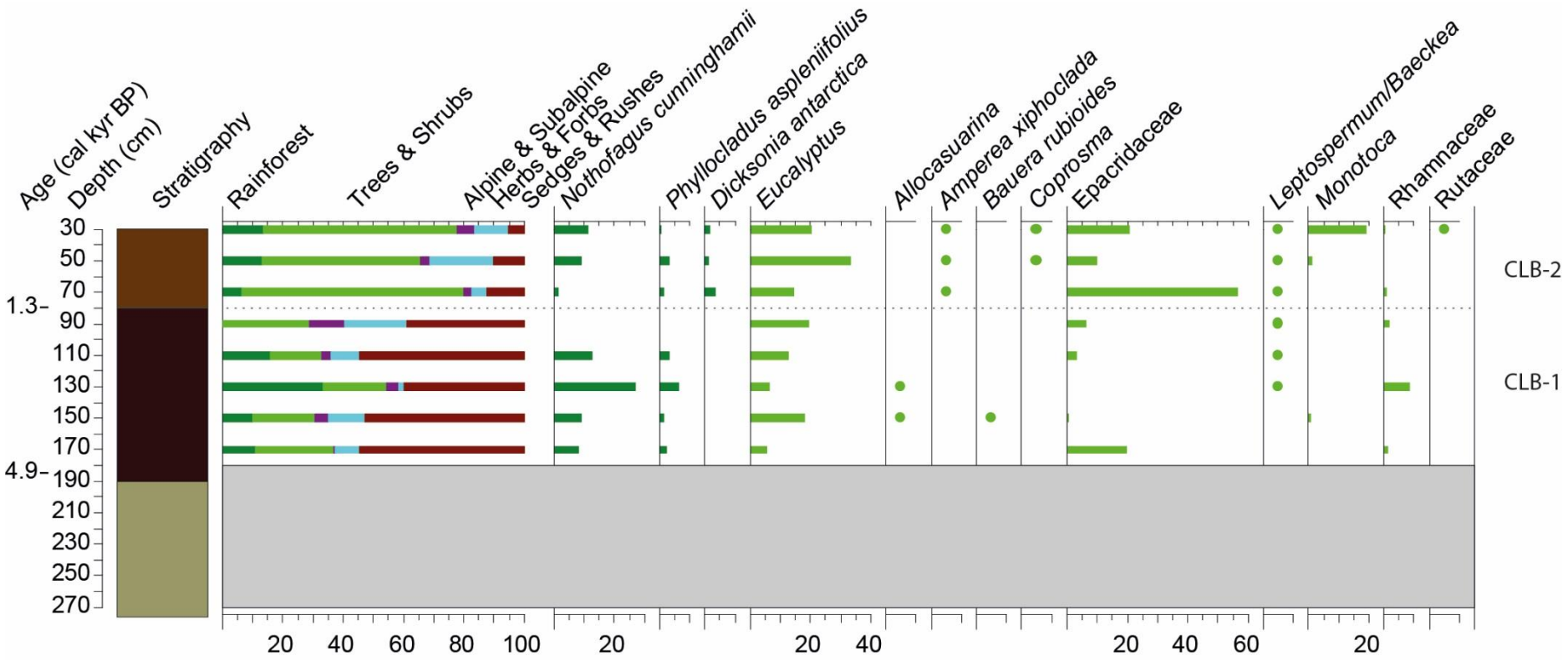

Figure 6-25 Percentage pollen diagram for Clarence Bog core (part 1). The grey band indicates little or no pollen in the sediments.

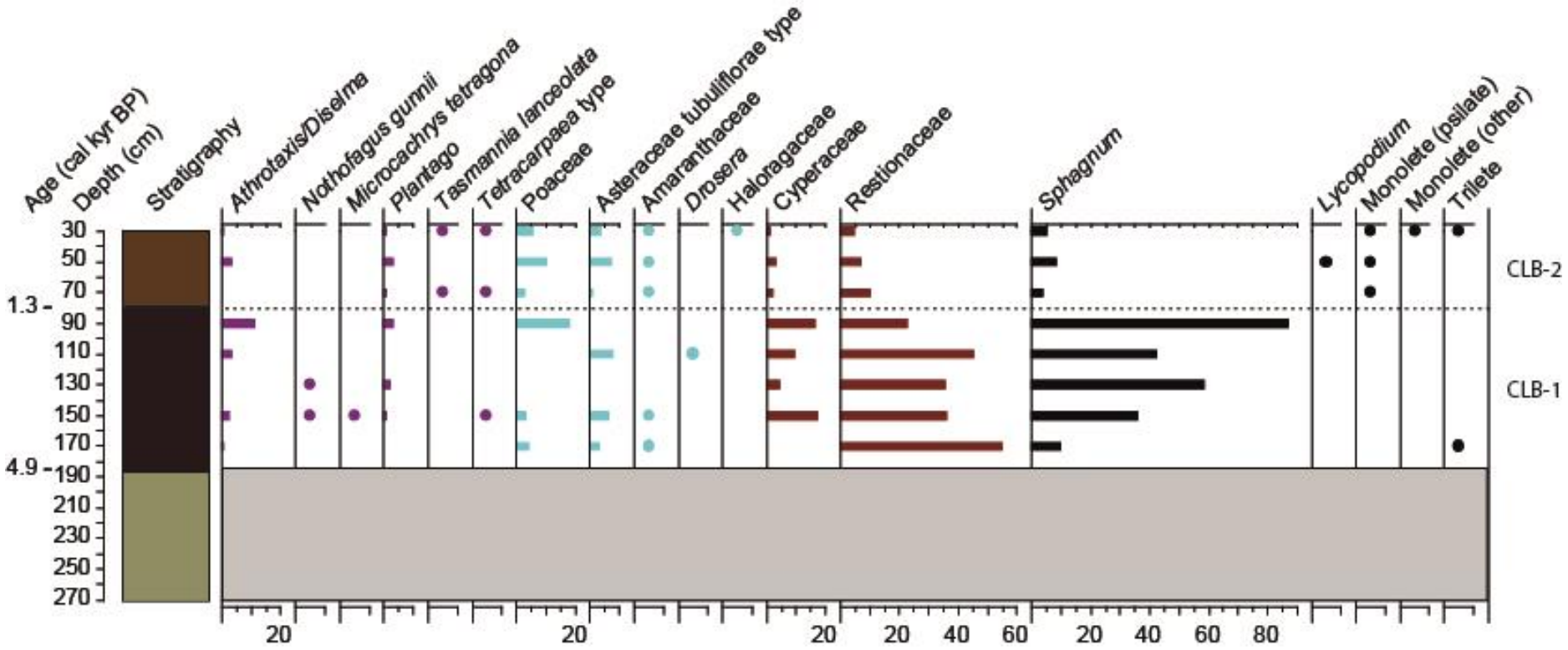

Figure 6-26 Percentage pollen diagram for Clarence Bog core (part 2). The grey band indicates little or no pollen in the sediment

6.6 Skullbone Plains Bog

6.6.1 Sediments and Dating

The SKB-15 core is 380 cm in length and consists of light red-brown *Sphagnum* peat with prominent light and dark bands thought to represent phases of active growth and humification and increasing clay content in the basal 22 cm, but overall high carbon content (40-50%) (Hope et al., 2017). Twelve samples were radiocarbon dated which are reported in Hope et al. (2017) (see Appendix) together with details of other analyses and the age model produced for the record.

Plate 6-2 The SKB-15 core site and core photos illustrating well preserved moss peat. Photo credit: J. Haiblen.

6.6.2 Pollen, Spore and Charcoal Analysis

A percentage pollen diagram of the Skullbone Plains Bog core is presented in figures 6.27-6.29. Figure 6.27 illustrates the changes in the taxa growing locally on the bog. Initially, between c. 10.2-9.0 cal kyr BP sedge taxa (Restionaceae and Cyperaceae) are high together with *Gleichenia* and *Gonocarpus*/*Haloragis*, followed in short by a peak in *Empodisma.* *Gymnoschoenus* increases from c. 9.0 cal kyr BP and between c. 8-7 cal kyr BP *Astelia* peaks together with Restionaceae and Gentianaceae, followed by *Richea.* At c. 6.4 cal kyr BP, Ericaceae, *Sphagnum* and *Leptospermum*/*Baeckea* peak. Two prominent peaks in Retsionaceae and *Richea* occur between c. 5-4 cal kyr BP, the latter joined by *Gleichenia*. The remaining record sees minor peaks of taxa, notably a peak in *Plantago* at c. 1.5 cal kyr BP. Figure 6.28 illustrates the extra-local and regional pollen record which sees highest values of

montane (*Nothofagus cunninghamii* and *Phyllocladus apsleniifolius*) and subalpine (*Athrotaxis*/*Diselma* and *Nothofagus gunnii*) rainforest taxa between c. 10-8 cal kyr BP. *Eucalyptus* values increase steadily through the record reaching peak values between c. 3-2 cal kyr BP, declining slightly towards the present. A pronounced decline in *Eucalyptus* and increase in herbs occurs at c. 4.1-3.9 cal kyr BP, with another pronounced peak in herbs at c. 1.3 cal kyr BP. The macroscopic charcoal record indicates a period of early fire activity until c. 9.5 cal kyr BP which is followed by a period of low fire activity until c. 7 cal kyr BP. Fire activity increases from the mid Holocene and indicates a more variable regime during the late Holocene (Hope et al., 2017).

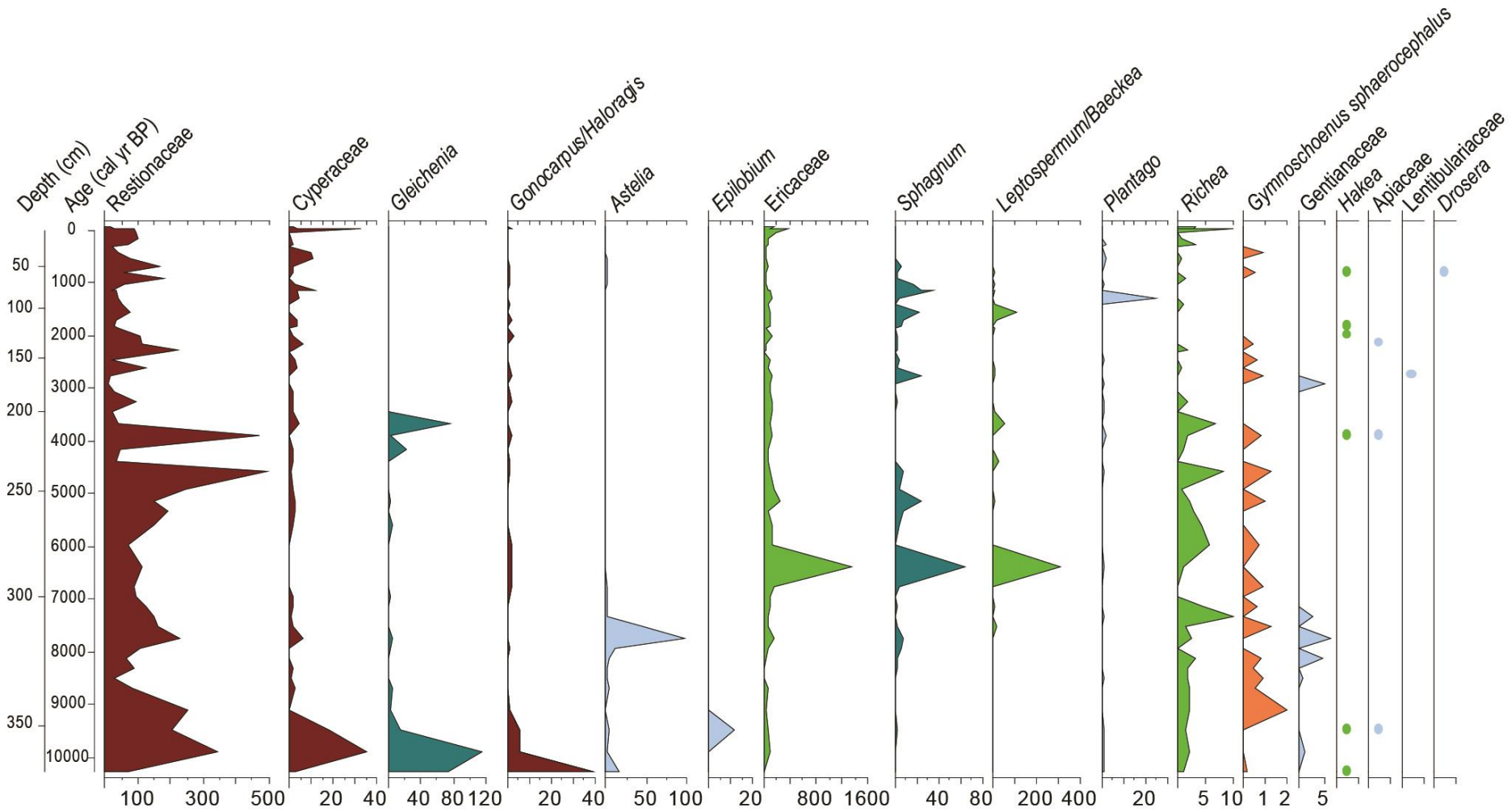

Figure 6-27 Percentage pollen diagram of the Skullbone Plains Bog core (bog taxa).

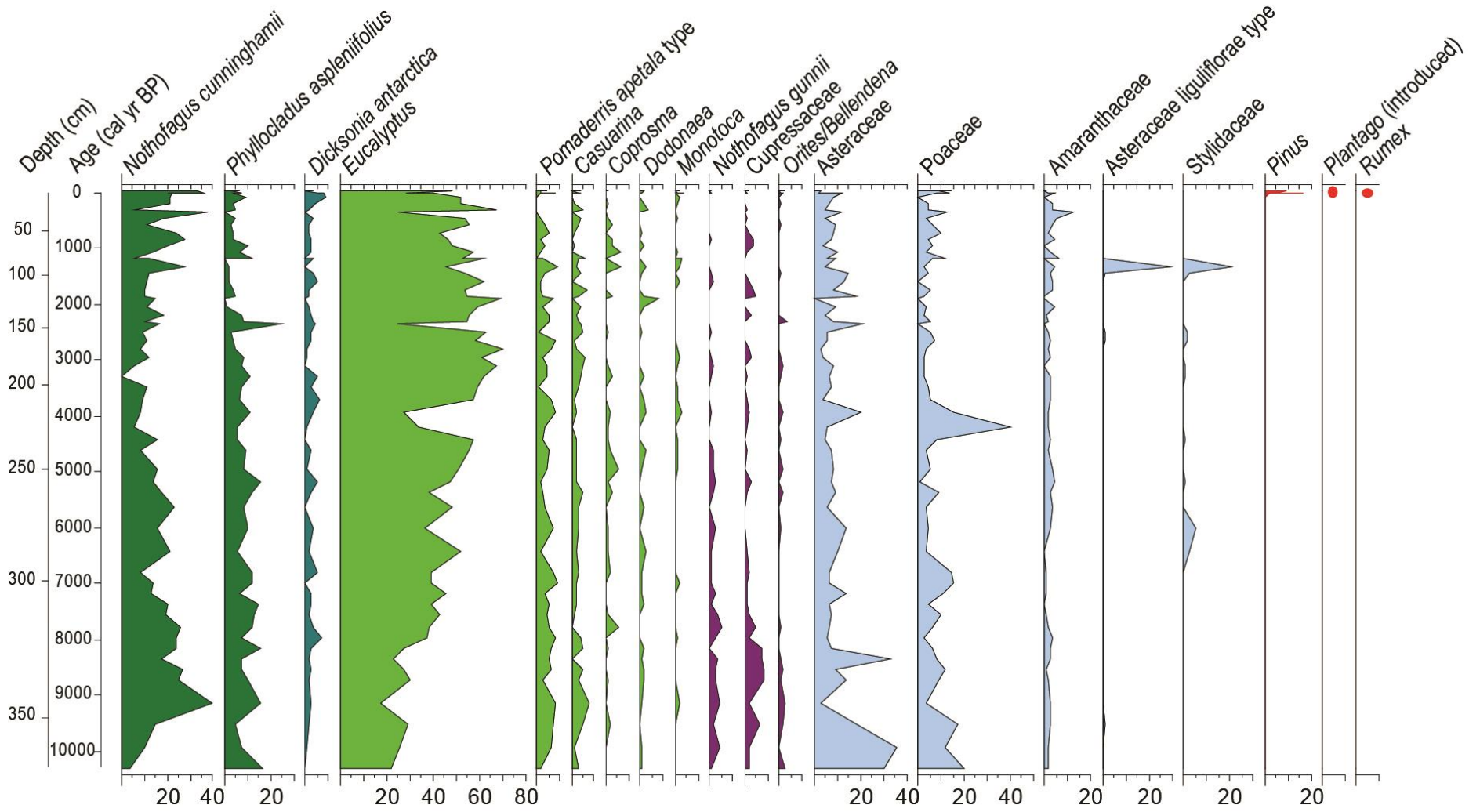

Figure 6-28 Percentage pollen diagram of the Skullbone Plains Bog core (common taxa).

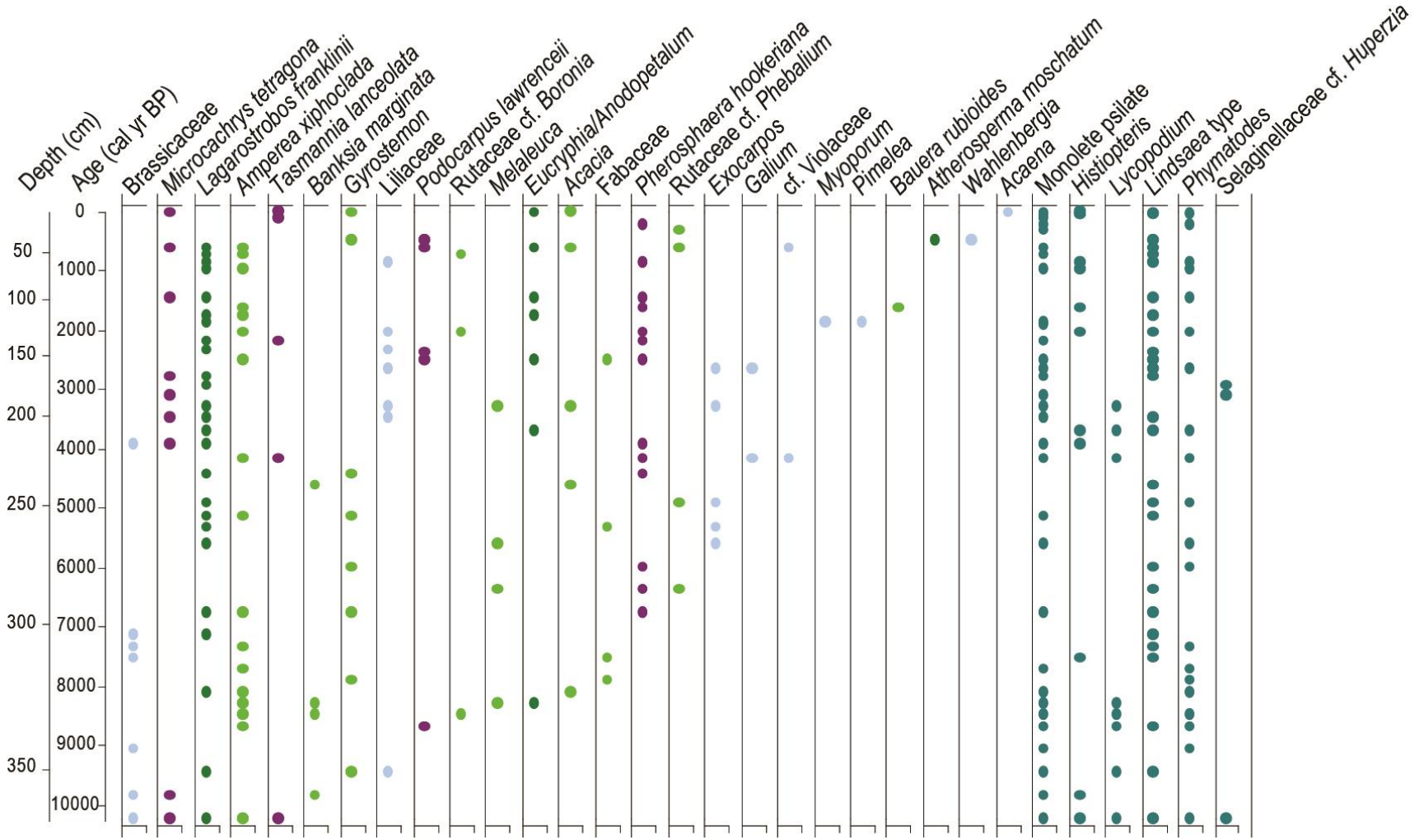

Figure 6-29 Percentage pollen diagram of the Skullbone Plains Bog core (rare taxa).

6.7 Comparisons of Sites

Summary diagrams comparing the key taxa from the Excalibur Bog, Clarence Lagoon and Skullbone Plains Bog records with those from Lake St Clair are illustrated in figures 6.30-6.32. It should be emphasised that the lack of sound chronologies for Excalibur Bog during the Holocene and Clarence Lagoon for a large part of the record means that a comparison of precise timings of vegetation changes can not be compared between records. The intention is to give a visual overview of the directions of vegetation changes within the region likely extending deep into Oxygen Isotope Stage (OIS) 3 through the Clarence Lagoon record. Sedimentation rates calculated between dated samples at 51.2 cm (30.9 cal kyr BP) and 64 cm (42.5 cal kyr BP) are used to estimate the spacing of samples (solid bars) for the base of the record, which are enhanced with an extrapolated step curve. The likely contaminated sample at 45 cm was excluded from the summary plots. This section will focus on the trends of vegetation change observed between the sites, with details of vegetation dynamics being discussed further in the discussion section of this chapter and Chapter 7 which focuses on the Late Glacial and Holocene.

Rainforest and wet eucalypt forest vegetation containing *Nothofagus cunninghamii, Phyllocladus aspleniifolilus* and *Pomaderris apetala* is currently only growing next to Lake St Clair. Sources for these pollen types lie upslope from Excalibur Bog on hillslopes to the north and downslope from Clarence Lagoon, with Skullbone Plains Bog lying most distal from source forests at its position highest on the Central Plateau. All three taxa are prominent components of the regional pollen rain.

Nothofagus cunninghamii reaches highest values during the Early Holocene at Lake St Clair, Skullbone Plains Bog and Excalibur Bog. The later timing within the Early Holocene at Excalibur Bog could well be due to poor chronology. All three records exhibit sharp reductions in *Nothofagus cunninghamii* between c. 5-4 cal kyr BP suggesting the widespread occurrence of a climatic event or disturbance which resulted in the reductions of *Nothofagus cunninghamii* populations at the start of the Late Holocene. The significant peak of *Phyllocladus aspleniifolius* early in the Early Holocene of the Excalibur Bog record possibly reflects the tail end of the *Phyllocladus* buldge seen in the Lake St Clair between c. 13.0-12.4 cal kyr BP, however, despite being very rare throughout the record otherwise, *Phyllocladus* is present at similar levels in the surface sample. At Skullbone Plains, *Phyllcocladus* is overall higher during the early-mid Holocene, with a single peak at c. 2.2 cal kyr BP. Details of late Glacial and Holocene rainforest dynamics are further discussed in the discussion section of this chapter and Chapter 7. Rainforest taxa are mostly present at trace levels in the pre-LGM records from Excalibur Bog and Clarence Lagoon. Of note are the elevated values at 239 cm in the Clarence

Lagoon record, which may indicate a slightly warmer period during OIS 3 when rainforests expanded in the lowlands.

Pomaderris apetala type shows a minor presence in the Skulbone Plains Bog and Lake St Clair records, values being slightly higher during the very late Glacial of the latter indicating early expansion of wet eucalypt forests in the wider region at the time. High values of *Pomaderris apetala* type and *Eucalyptus* during the Early Holocene suggests that wet eucalypt forests were growing proximal to the site, likely in combination with an enhanced regional signal due to expansion of *Pomaderris apetala* rich wet eucalypt forests to the east such as at Tarraleah and Browns Marsh (Macphail, 1979, 1984). *Pomaderris apetala* is only present at trace levels in the pre-LGM Excalibur Bog record and is absent from the Clarence Lagoon record.

Eucalyptus exhibits increasing trends through the mid to Late Holocene in the Skullbone Plains Bog and Lake St Clair records intiating from c. 10 cal kyr BP. In contrast, values decrease during the Late Holocene at Excalibur Bog due to the establishment of a peat bog and the presence of stronger local pollen sources. Moderate values of *Eucalyptus* ranging up to c. 15% persist through OIS 3 in the Clarence Lagoon and Excalibur Bog records until c. 22 cal kyr BP when the Excalibur Bog record exhibits a hiatus. At Lake St Clair, early subalpine *Eucalyptus* woodlands established sometime after c. 16 cal kyr BP.

Variations in the key subalpine/alpine taxa including *Athrotaxis*/*Diselma, Nothofagus gunnii*, *Orites*/*Bellendena* and *Pherosphaera hookeriana* are illustrated in figure 6.31. *Athrotaxis*/*Diselma* is scarce in the early records from Clarence Lagoon and Excalibur Bog, with values only slightly elevated at 239 cm at Clarence Lagoon, when other rainforest taxa increase and temperatures are inferred to have been slightly warmer. The pollen of appears not be as widely as other regional pollen taxa, Although Macphail (1979) suggests *Athrotaxis*/*Diselma* could form part of the regional pollen rain in certain regions, the pollen does not appear to be as widely transported as other regional pollen taxa from the studies as part of this research. The rapid increase of *Athrotaxis*/*Diselma* to very high values in the Lake St Clair record upon initiation of postglacial warming suggests that subalpine populations were not displaced too far from the site during the LGM. However, the Excalibur Bog and Clarence Lagoon records do not support the existence of widespread *Athrotaxis*/*Diselma* populations in the Lake St Clair region during the LGM. The second peak in *Athrotaxis*/*Diselma* at c. 10-8 cal kyr BP in the Lake St Clair region appears to be a widespread expansion of these taxa, with similar peaks observed in both the Skullbone Plains Bog and Excalibur Bog records around this time.

Nothofagus gunnii exhibits similarly low values during the pre-LGM period, apart from a pronounced peak at c. 33 cal kyr BP in the Clarence Lagoon record. The pollen type is poorly

transported and any increases represent local increases in the vegetation. At Skullbone Plains Bog, *Nothofagus gunnii* values are elevated between c. 10-8 cal kyr BP, contemporaneous with the rise in *Athrotaxis*/*Diselma.* This could represent an expansion of *Athrotaxis cupressoides-Nothofagus gunnii* short rainforest, common on the Central Plateau today, suggesting there was a low pressure from fire to reduce its range to fire protected localities as appears to be the case in recent past (Worth et al., 2016). *Orites*/*Bellendena* illustrates a much stronger persistence through the colder, pre-LGM climates with high values, relative to its local pollen representation, through most of the Clarence Lagoon and Excalibur Bog records, apart from the most basal samples in Zone Clg-1 which are inferred to represent the coldest period in the record. The highest values of *Orites*/*Bellendena* occur in the early deglacial sediments of the Lake St Clair record, supporting it as an indicator of cooler climates, although species of *Orites* also grow below the sub-alpine zone in the modern vegetation. Holocene values for *Orites*/*Bellendena* are higher at Skullbone Plains Bog than Lake St Clair, consistent with its location at higher altitude on the Central Plateau with stronger local sources of subalpine communities rich in *Orites/Bellendena* growing nearby.

High values of *Pherosphaera hookeriana*, together with the consistent presence of the pollen of *Microcachrys tetragona* in the Clarence Lagoon and Excalibur Bog (Ex-1) records, suggest that coniferous alpine heath was widespread during the colder climate of OIS 3. The legacy of the much-expanded range of *Pherosphaera* continues into the early postglacial with high values recorded in the deglacial sediments of Lake St Clair, after which the taxon is present only in traces in all records. Taking into account the strong dominance of the Clarence Lagoon record by *Pherosphaera hookeriana*, the values of Poaceae and Asteraceae (figure 6.32) together with other herb taxa indicate that grassland and herbfields were widespread during the colder climates of OIS3, with the coldest period inferred to have occurred during Clg-1 when values of herbs are at their highest and shrub taxa are low relative to the remainder of the record. Asteraceae is more important at Excalibur Bog (Ex-1).

No pollen of *Gymnoschoenus sphaerocephalus* was observed in the Clarence Lagoon record, and only traces in the Excalibur Bog record. The minimal amounts of *Gymnoschoenus spaerocephalus* during the Late Holocene when the peat bog had established are surprising given that percentages over 10 up to over 20 where recorded from samples across the bog. This raises the possibility of poor preservation of this pollen type. The macroscopic charcoal records from Lake St Clair and Skullbone Plains Bog overall highlight the presence of fire events throughout the late Glacial and Holocene, with an intensification indicated for the very Late Holocene in the Skullbone Plains Bog record. The Lake St Clair macroscopic charcoal record only extends to the topmost sample analysed from the long core deposited at c. 1.4 cal kyr BP.

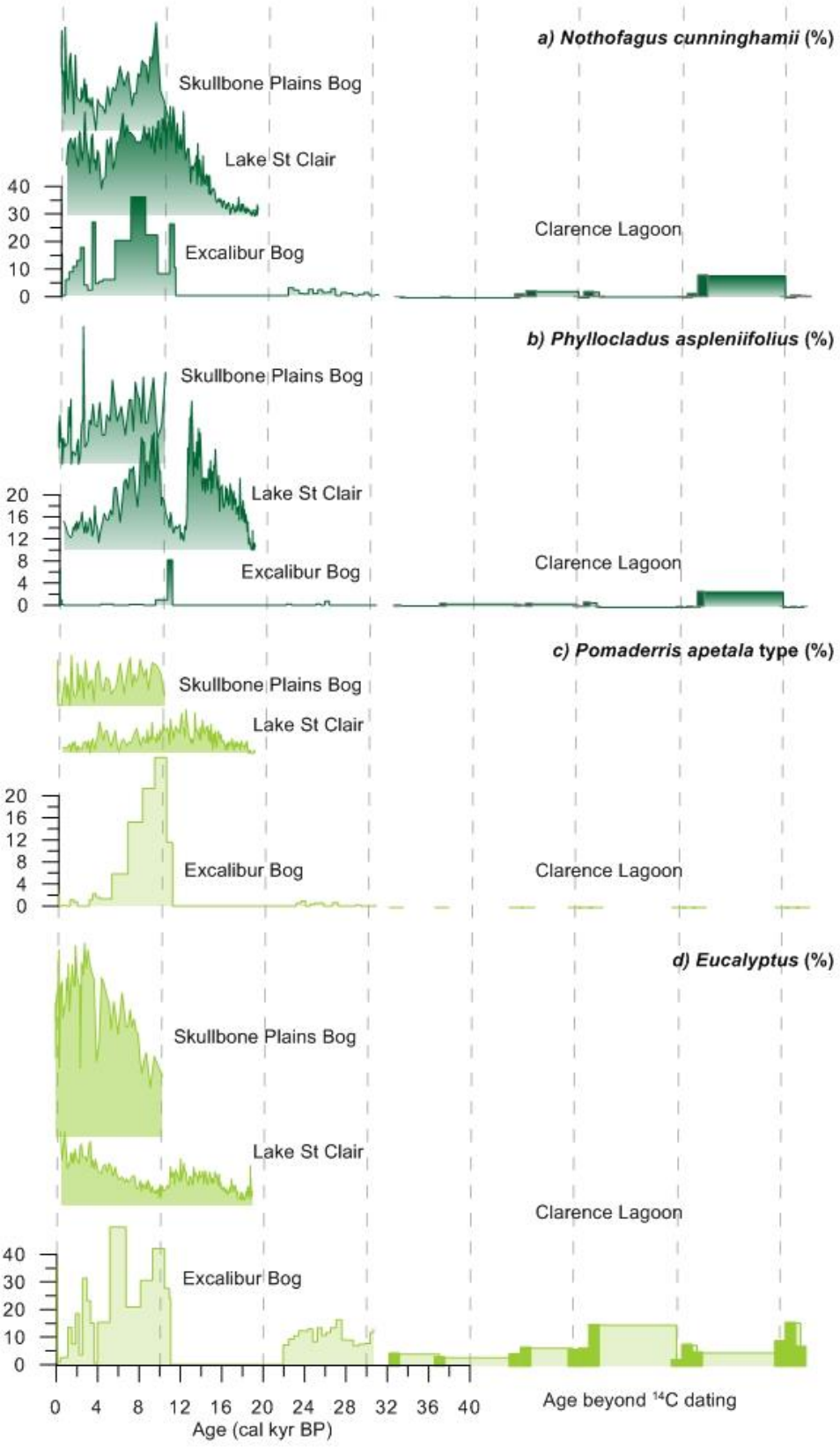

Figure 6-30 Summary diagram of key pollen taxa in the Skullbone Plains Bog, Lake St Clair (Core CG), Excalibur Bog and Clarence Lagoon records: a) *Nothofagus cunninghamii* b) *Phyllocladus aspleniifolius* c) *Pomaderris apetala* type and d) *Eucalyptus*.

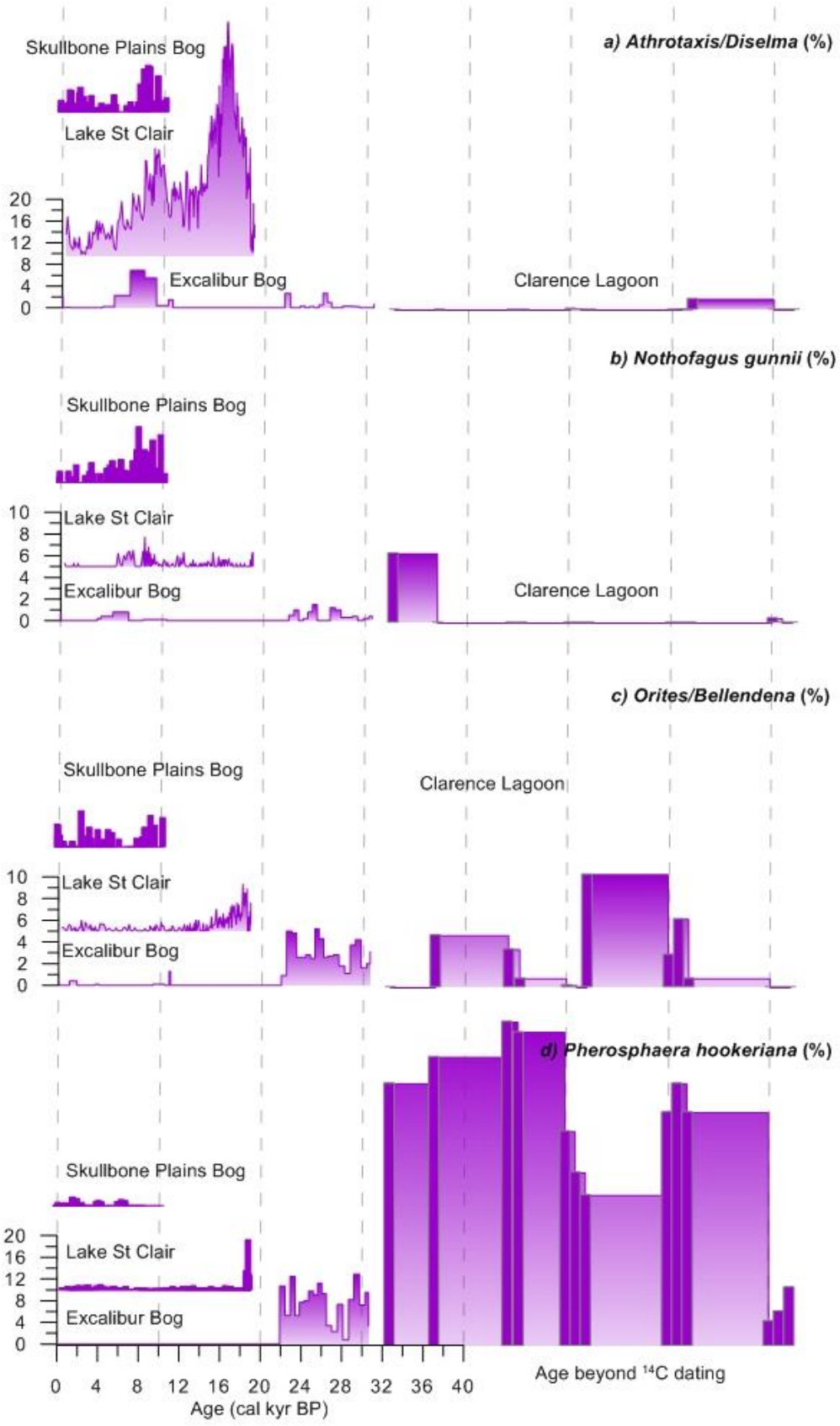

Figure 6-31 Summary diagram of key pollen taxa in the Skullbone Plains Bog, Lake St Clair (Core CG), Excalibur Bog and Clarence Lagoon records: a) *Athrotaxis/Diselma* b) *Nothofagus gunnii* c) *Orites/Bellendena* and d) *Pherosphaera hookeriana*.

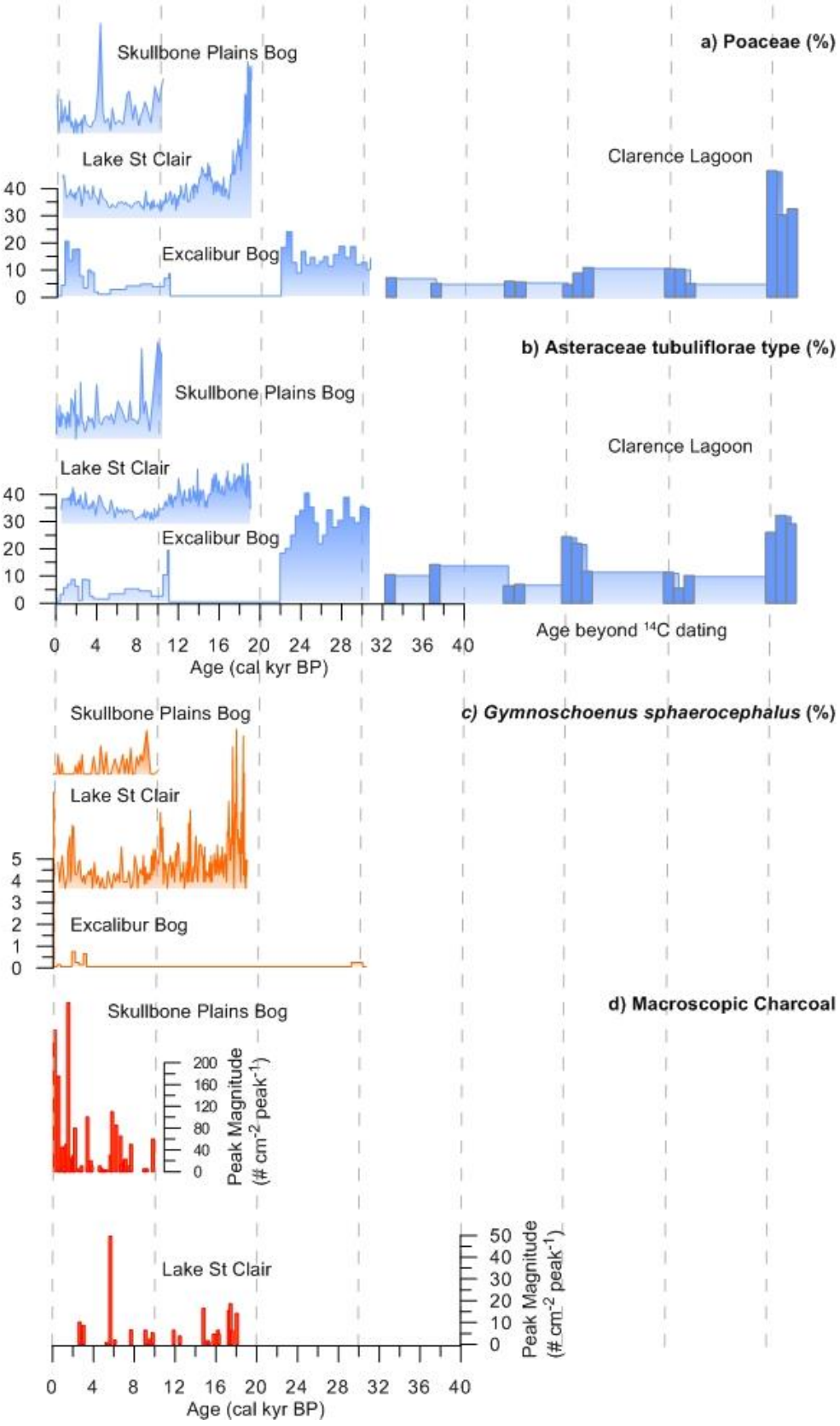

Figure 6-32 Summary diagram of key pollen taxa in the Skullbone Plains Bog, Lake St Clair (Core CG), Excalibur Bog and Clarence Lagoon records: a) Poaceae b) Asteraceae tubuliflorae type c) *Gymnoschoenus sphaerocephalus* and d) macroscopic charcoal

6.8 Discussion

6.8.1 Pre-LGM

Lake Selina, located at an altitude of 516 m in the West Coast Range, contains the most continuous record of vegetation change through to the last interglacial (Colhoun et al., 1999). Prior to the LGM, the vegetation consisted of widespread grasslands and herbfields dominated by Asteraceae, Poaceae and Apiaceae. Significant amounts of *Pherosphaera* (over 10%) indicates that this taxon was also important in western Tasmania and that coniferous heath, including *Microcachrys tetragona*, was growing locally along with, periodically, *Nothofagus gunnii* dominated deciduous heath and Ericaceae, *Leptospermum* and *Melaleuca* as part of alpine heathland. In contrast with the herb dominated vegetation at Lake Selina, Boco Plain (Augustinus et al., 2017), lying at 400 m in the lowlands directly west of the West Coast Range, acted as a refuge for rainforest with abundant pollen of *Lagarostrobos* between c. 42.8-21.2 cal kyr BP together with minor amounts of *Nothofagus cunninghamii* and *Phyllocladus aspleniifolius.* The vegetation was otherwise dominated by *Allocasuarina* and ericaceous shrubs, with notably low amounts of Poaceae and Asteraceae. A spike of *Pherosphaera hookeriana,* which reaches 35%, is suggested to represent peak cooling early in this period (Augustinus et al., 2017). Offshore western Tasmania, the ocean core S036-7SL record reflects the vegetation growing in the coastal areas of central western Tasmania which, prior to the LGM, consisted of a mosaic of *Eucalyptus* woodland, heathland, herbfield and sedgeland growing under a cool and moist climate. The record is dominated by the forest taxa *Allocasuarina, Eucalyptus* and *Phyllocladus aspleniifolius* with alpine/subalpine taxa such as *Athrotaxis/Diselma*, *Pherosphaera hookeriana* and *Astelia alpina* also important (van de Geer et al., 1994; Colhoun and Shimeld, 2012). Dry eucalypt forest dominated in the lowlands in the northwest and southeast, with localised wet sclerophyll forest growing in a gully at Remarkable Cave containing significant amounts of *Pomaderris apetala* type and minor *Nothofagus cunninghamii* and *Phyllocladus aspleniifolius* (Colhoun, 1977; Colhoun and Shimeld, 2012).

The records from Clarence Lagoon and Excalibur Bog extend to the period preceding the LGM. At Clarence Lagoon, the pollen record between ca. 42.5 and 26.3 cal kyr is strongly dominated by *Pherosphaera hookeriana* suggesting that coniferous alpine heath was widespread at this altitude together with alpine herbfields and grasslands. Excalibur Bog was likely a small lake between ca 30.6-21.8 cal kyr BP surrounded by Asteraceae dominated herbfields and grassland with *Pherosphaera hookeriana* coniferous alpine heath also important. At both sites, rainforest taxa occur only at trace values with *Eucalyptus* being the only forest taxon present in significant amounts (up to 16%). Both records are missing the LGM and it is possible that these

shallow lakes dried up under the increasingly cold and dry conditions inferred for the LGM (Petherick et al., 2013a), with the formation of a "hardpan" at Clarence Lagoon and no further sediment accumulation preserved after this time.

Oscillations between wetter and drier periods could explain the discontinuous nature of pollen preservation in the Clarence Lagoon record, where barren sections might represent periods where the shallow lake dried up. The basal samples from Clarence Lagoon contain a higher percentage of herbs and the long distance transported Amaranthaceae and low amounts of subalpine shrubs, which otherwise dominate the record, suggesting that this may have been a colder period. A band of dark sediment between 242-225 cm, although showing no increase in organic matter, may represent slightly warmer phases where rainforest expanded at lower altitudes as indicated by the higher percentages of *Nothofagus cunninghamii.* The layer is underlain by a sharp, sandy boundary suggesting that if the lake had dried up during the barren zone prior to this, that an increase in precipitation initially resulted in the delivery of coarser sediments to in the initial phase of rising lake levels.

Although Excalibur Bog is currently a peat bog, during Zone Ex-1, the high amount of *Isoetes* (29-98%; average 86%) and the lack of Restionaceae and Cyperaceae suggests that the depositional environment may have been a water body of some type. There are 5 species of *Isoetes* in Tasmania, *Isoetes gunnii* being the most widespread and extending into the alpine zone with an altitudinal range of 540-1360 m. *I. elatior* is currently restricted to the lowlands and the other three species only range up to 1020-1180 m just below the current treeline (Garret and Kantvilas, 1992). *Isoetes gunnii* prefers the still waters of lakes and tarns in the alpine and sub-alpine zone of Tasmania where it can be found growing in water depths up to 1-1.5 m. It is less commonly found in running water and only stunted plants in very shallow water are likely to become partly exposed during summer (Garret and Kantvilas, 1992). It seems most likely that the species of *Isoetes* recorded during this zone is *I. gunnii* as the site was above treeline. Although a riverine environment cannot be ruled out, it seems most plausible that there may have been a small, shallow lake at the site. The surface sample at the core site does contain 13.7 % *Isoetes* (and currently there is no permanent water), however, apart from a single spore each found at sites NW1 and T3-2, *Isoetes* was not observed at any other sites on the bog. It is possible that this modern occurrence of *Isoetes* presence could be *I. drummondii* which distinguishes itself from the other species of *Isoetes* in that it does not critically require a permanent covering of water and can be found growing as a non-aquatic amongst grasses and herbs in moist soil (Garret and Kantvilas, 1992).

The vegetation during this zone consists mostly of an Asteraceae dominated alpine herb and shrub assemblage, possibly with some areas of *Astelia* bog and *Plantago* herbfield. At Browns

Marsh (Macphail, 1979) approximately 14 km to the southeast where modern precipitation is reduced, a similar assemblage is observed which is dominated by Poaceae rather than Asteracaeae, which dominates at Excalibur Bog. It is possible that a proportion of the Poaceae recorded at the site is regionally sourced. Notable of the alpine shrubs and herbs are *Phaerosphaera hookeriana*, Asteraceae (low spine) and *Dichosciadium ranunculaceum* which are present in considerable quantities and are indicators of glacial vegetation assemblages as seen also in other Tasmanian records. *Phaerosphaera hookeriana* and Asteraceae (low spine) appear to have much reduced ranges in the modern alpine vegetation.

The most abundant forest taxon during zone Ex-1 is *Eucalyptus* which ranges between 7-16% with *Allocasuarina* at background levels and very little rainforest taxa present. Figure 6.33 below illustrates box plots of the fossil *Eucalyptus* values against modern moorland and woodland values. The *Eucalyptus* values are consistant with the treeline being distal to the site. Modern percentages of *Eucalyptus* range between 8-43% across the moorland with the core site recording 35% *Eucalyptus* at a distance of 300 m to the closest woodland boundary. Shimeld & Colhoun (2001) showed that *Eucalyptus* and LDT rainforest species percentages doubled in lake sediments in transects which led from *Eucalyptus* woodland through moorland into Great Lake. This suggests that if Excalibur Bog was indeed a lake during the Zone Ex-1, then the *Eucalyptus* percentages are likely amplified in comparison with the modern *Eucalyptus* percentages recorded across the moorland and that the *Eucalyptus* treeline may have been even more distal to the site. Microscopic charcoal is low throughout most of the zone with three peaks occurring at 160 cm, 155 cm and 135 cm. The peak at 155 cm coincides with reductions in *Phaerosphaera* and *Microstrobos*, both fire sensitive taxa, however, the other two peaks don't correspond with any apparent local effect on the vegetation.

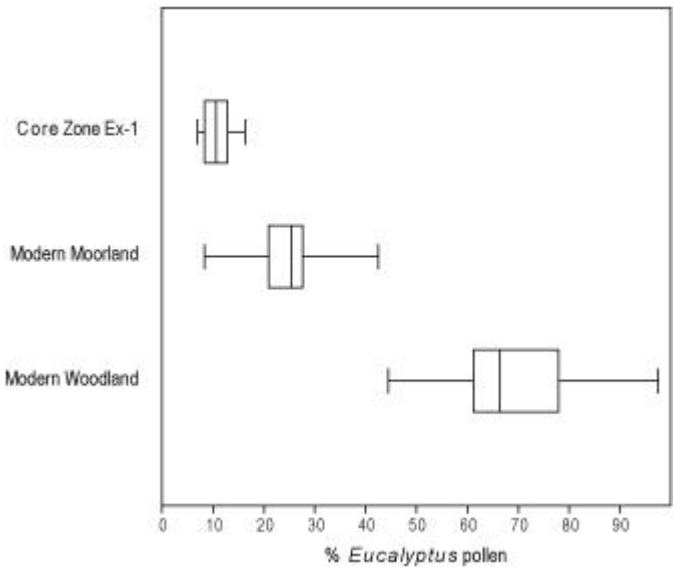

Figure 6-33 Box plots *Eucalyptus* pollen percentages in zone Ex-1 compared with those found in modern moorland and woodland samples at Excalibur Bog.

A hiatus in deposition of c. 10.5 kyr BP appears to have occurred between c. 21.8 and 11.3 cal kyr BP resulting in the absence of a record covering the period of the Last Glacial Maximum and Late Glacial-Holocene transition. It is possible that as temperatures cooled and precipitation decreased after c. 21.9 cal kyr BP leading into the Last Glacial Maximum that the lake at the site dried. The pebble and sand layer at 89 cm marks a high energy event that deposited these sediments, perhaps as a result of increased precipitation in the Early Holocene or an indication that a small river flowed through the site which eroded any sediment deposited between (c. 21.8-11.3 cal kyr BP).

6.8.2 The Holocene

The Excalibur and Skullbone Plains bog records cover most of the Holocene, with only the late Holocene being recorded at the Clarence Bog site. At Excalibur Bog, eucalypt forest dominates the early to mid Holocene and a strong regional pollen signal indicating the expansion of rainforests to the west and wet eucalypt forest to the east is evident. During the late Holocene from c. 4.5 cal kyr BP, a peat bog develops at the site with a switch to a stronger local pollen signal. At Clarence Bog, a peat bog had also developed by at least c. 4.9 cal kyr BP. At Skullbone Plains, establishment of a *Sphagnum*-shrub bog occurred within 1500 years of colonisation of a boulder field by sedges. The record throughout the Holocene is one of remarkable stability, despite the evidence for the recurrence of fire events which appear to have resulted in temporary reductions in the dry eucalypt forests which dominated around the site (Hope et al., 2017).

The early and mid-Holocene record at Excalibur Bog between c. 11.3-4.5 cal kyr BP (zone Ex-2) appears to be very compressed which could be explained by low sedimentation rates or, alternatively, there could have been hiatus(es) in sedimentation during this time period. The depositional environment was likely still a water body of some type, but possibly shallower due to the presence of *Pediastrum* and then *Botryococcus* (with only small amounts of *Isoetes* at the start of the zone) and what seems to be a dominant regional pollen signal of forest taxa including *Eucalyptus*, *Nothofagus cunninghamii* and, in particular, *Pomaderris apetala* type. Values of *Eucalyptus* reach peak levels during this period and are compared with modern *Eucalyptus* percentages from different vegetation types in the modern pollen dataset (figure 6.34). The values range higher than for local modern moorland samples and less than those found in the dry eucalypt forests surrounding the site today. The range of values best match with those found in wet eucalypt forests and, together with the presence of other wet forest taxa as signified by a significant peak in *Pomaderris apetala* type, reaching 27%, at c. 9.3 cal kyr BP, it is plausible that wet eucalypt forest was growing near the site during this time period, which may be in support of a wetter climate than present. At Tarraleah, approximately 35 km

to the southeast, wet sclerophylly forests dominated by *Pomaderris apetala* type occurred between c. 10.2 and 7.8 cal kyr BP, after which *Pomaderris apetala* type decline and dry eucalypt forest association develops (Macphail, 1984). A change from a significant presence of *Atherosperma moschatum* and *Dicksonia Antarctica* in the forest to *Phyllocladus aspleniifolius* is interpreted by (Macphail, 1984) to represent declining soil fertilities as a result of overleaching during a wet early Holocene. Brown Marsh, at a similar altitude (750 m) ~ 27 km to the southeast of Excalibur Bog, records a progression from alpine grassland (with *Astelia* bog and *Plantago* herbfield) to subalpine grassland and by c. 9.5 (9.9-9.1) cal kyr BP establishment of *Eucalyptus* open forest around the site. Macphail (1979) infers an initial shallow lake phase, followed by development of a Cyperaceae-Restionaceae swamp and eventually a Restionaceae-*Spahgnum* peat bog with *Gleichenia* and Ericaceae. The Browns Marsh record also indicates a peak in *Pomaderris apetala* type just after c. 9.5 cal kyr BP, corresponding well with the Excalibur Bog and Tarraleah records. Although there are slightly elevated levels of *Pomaderris apetala* type during the late Glacial in the Lake St Clair record, percentages of the taxon remain mostly below 5%, as is the case for the Skullbone Plains record which indicates very slightly elevated values of the regional signal.

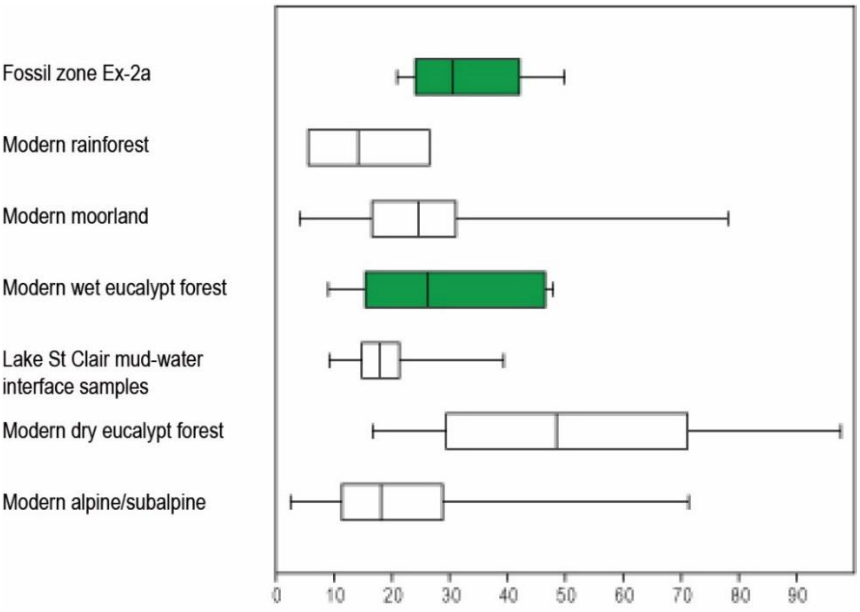

Figure 6-34 Box plots *Eucalyptus* pollen percentages in zone Ex-2a compared with those found in modern samples from various vegetation types in the wider Lake St Clair area.

The small peak of *Phyllocladus aspleniifolius* early in the Early Holocene of the Excalibur Bog record possibly reflects the tail end of the *Phyllocladus* buldge seen in the Lake St Clair between c. 13.0-12.4 cal kyr BP, however, despite being very rare throughout the record otherwise, *Phyllocladus* is present at similar levels in the surface sample. *Nothofagus cunnighamii* initially peaks slightly earlier and then reaches peak levels c. 6.7 cal kyr BP (70

cm). This is likely picking up the peak rainforest development in the wetter west to the site. Similarly, the Skullbone Plains Bog record indicates an increased regional signal of rainforest taxa during the Early Holocene, including *Nothofagus cunninghamii*, *Phyllocladus aspleniifolius* and *Athrotaxis/Diselma,* the latter being elevated approximately contemporaneously with the Lake St Clair record. At Excalibur Bog, elevated levels of *Athrotaxis/Diselma* appear to occur later, however, age control on this section of the core is very poor and dates are merely extrapolated between 80 cm and the boundary with underlying silts and clays at 87 cm. The local signal at the Skullbone Plains Bog between c. 10.7-9.1 cal kyr BP indicates the colonisation of a boulder field by a wet fen dominated by sedges with *Astelia* and *Gleichenia,* with grasslands with scattered shrubs such as *Orites* growing nearby. The period from c. 9.1 cal kyr BP sees the development of a *Sphagnum* bog, with shrubs initially rare until c. 7.1 cal kyr BP when ericaceous and myrtaceous shrubs become dominant. A subalpine eucalypt woodland also established near the site at this time and the vegetation was mostly very stable until present. The fire record indicates a period of early fire activity until c. 9.5 cal kyr BP, when a period of low fire activity followed until c. 7 cal kyr BP. Fire activity increases from the mid Holocene, in line with an onset of ENSO, and becomes more variable during the late Holocene. A pronounced decrease in *Eucalyptus* and increase in herbs between c. 4.1-3.9 cal kyr BP coincides with increased fire activity at this time, both locally and regionally, and may indicate presence of widespread drought at this time (Fletcher et al., 2015; Stahle et al., 2016; Hope et al., 2017; Mariani et al., 2017).

A Late Holocene shift to a widespread increase in burning (Fletcher et al., 2015) and expansion of sclerophyll and herbaceous vegetation (Mariani et al., 2017) occurs along with an increase in fill and scour episodes in montane streams (Cohen and Nanson, 2007) and renewed peat growth (Hope and Nanson, 2015), as supported by the Excalibur and Clarence Bog sites.

Phase of local peat bog development at Excalibur Bog begins sometime between 6.8 (6.9-6.7; 70 cm) and 4.0 (4.2-3.9; 60 cm) cal kyr BP. It is possible that there was a hiatus in deposition between zones Ex-2a and Ex-2b. The stratigraphy changes from mud to peat at around 69 cm and after this a progression of peaks of locally sourced pollen can be observed after a period of more regionally sourced pollen. It is suggested that this marks the initiation of local development of the peat bog. The record during this zone shows a general increase in Ericaceae and *Gonocarpus*, both of which are indicator species of Eastern Moor (Brown, 1999). In the case of Ericacaeae, specifically *Epacris gunnii*, but the pollen of Ericaceae was not identified to generic or species level. *Eucalyptus* reaches peak values of 49.9 % at 65 cm and it is possible that in addition to *Eucalyptus* mixed forest surrounding the site, this could have provided a source of *Eucalyptus* seedlings to migrate onto the actual site accounting for the

high values of *Eucalyptus*. This is followed by peak values (67%) of *Leptospermum/Baeckea* type at 60 cm (= 4.0 cal kyr BP dated sample). *Melaleuca* follows at 55 cm with peak values of 58.3% and then Ericaceae at 50 cm with peak values of 59.1%. Currently see both *Leptospermum* and *Melaleuca* in the woodland surrounding Excalibur Bog, and *Melaleuca* was also observed as occasional component of the bog flora. Ericaceae is a component of both the modern woodland and moorland flora.

The next notable shift occurs after 2.4 (2.7-2.3; 40 cm) cal kyr BP. A peak of *Plantago* (76.3%) at 35 cm suggests a shift from a predominantly shrub cover to herbaceous cover. This is followed by a strong increase to 35.5% of Restionaceae which remains at the site until present where it is present at similar levels in the surface sample (33.7%). This suggests the bog may have been similar to present from this stage on. What is notable though is the rare occurrence of the pollen of *Gymnoschoenus* which could be a preservation issue with this pollen type.

6.9 Conclusions

The pollen records from Clarence Lagoon and Excalibur Bog show that the vegetation prior to the LGM was dominated by herbaceous and alpine and subalpine taxa, in particular *Pherosphaera hookeriana,* and thereby give a glimpse into the evolution of the modern subalpine vegetation. The Clarence Lagoon record, despite the discontinuity of pollen preservation, which could indicate wetting and drying, and the lack of chronological control, suggests that oscilliations in climate are indicated, with evidence for a warmer and a colder period occurring during the generally cool conditions of OIS3. The pollen records from Skullbone Plains Bog, Excalibur Bog and Clarence Bog provide detail of local changes within the Lake St Clair changes to complement the regional record from Lake St Clair.

Chapter 7 Discussion

7.1 Glacial refugia during the LGM

During the Last Glacial Maximum (LGM), the vegetation in Tasmania consisted mostly of alpine grasslands and herbfields with sclerophyll woodlands and savanna fringing the lowlands along the northwest coast and steppe dominating in the eastern coastal areas (Colhoun and Shimeld, 2012). Around 1085 km^2 of Tasmania was covered by ice, most of which took the form of a large ice cap on the Central Plateau with the largest outlet glacier flowing into the upper Derwent Valley and terminating approximately 1 km south of Lake St Clair (Colhoun et al., 2014). Temperatures are estimated to have been c. 6.5°C (Colhoun, 1985) and up to 10°C (Thrush, 2008) colder based on the relationship between altitudes of LGM glacier equilibrium line altitudes (ELAs) and modern mean annual and summer atmospheric freezing levels (Colhoun et al., 2010). The Subtropical Front (STF), which marks the northern boundary of the Southern Ocean and today lies around 45°S (winter) - 47°S (summer) in the region south of Tasmania, was positioned much further north during the LGM, becoming pinned against the Tasmanian landmass with mean annual surface water temperatures 4-5°C colder than today (Sikes et al., 2009; De Deckker et al., 2012). Agreement on the position and strength of the SWW is still lacking based on palaeodata and models, however, the largest proportion of observations point towards an equatorward displacement or strengthening of the SWW during the LGM (Kohfeld et al., 2013).

Two sites, within 10 km of Lake St Clair and lying outside the LGM ice limits, record the vegetation leading up to the LGM. Excalibur Bog (785 m asl; chapter 6) lies at a similar altitude to Lake St Clair and was likely a small lake between ca 30.6-21.8 cal kyr BP surrounded by Asteraceae dominated herbfields and grassland with *Pherosphaera hookeriana* coniferous alpine heath also important. Clarence Lagoon (960 m asl; chapter 6) is a shallow lake lying on the southwestern edge of the Central Plateau. The pollen record between ca. 42.5 and 26.3 cal kyr is strongly dominated by *Pherosphaera hookeriana* suggesting that coniferous alpine heath was widespread at this altitude together with alpine herbfields and grasslands. At both sites, rainforest taxa occur only at trace values with *Eucalyptus* being the only forest taxon present in significant amounts (up to 16%). Both records are missing the LGM and it is possible that these shallow lakes dried up under the increasingly cold and dry conditions inferred for the LGM (Petherick et al., 2013a).

Based on pollen evidence, as well as palaeoclimate modelling, colder and much drier conditions during the LGM, coastal western Tasmania appears to have been the only plausible environment with suitably equable conditions for the survival of rainforest during the LGM.

However, the poor dispersability of many rainforest species makes it difficult to explain the occurrence of rainforest in northeast Tasmania today as the distance is too large to support a model of rapid postglacial migration of rainforest from a single glacial refugium in Western Tasmania (Kirkpatrick and Fowler, 1998; Kiernan et al., 1983; Colhoun, 2000; Worth et al., 2009). DNA-based phylogeographic data for several rainforest taxa (Worth et al., 2009; Worth et al., 2011; Nevill et al., 2010) have shown that rainforest survived in situ in multiple glacial refugia located in western Tasmania, central eastern Victoria, New South Wales and eastern Tasmania, under apparently non-equable conditions in the latter, suggesting that niche changes may have taken place which need to be taken into consideration when applying modern analogues to the past (Worth et al., 2009, 2014).

7.2 Postglacial warming

7.2.1 Timing of Deglaciation

Radiocarbon ages obtained from the basal sediments from Lake St Clair (c. 35-25 cal yr BP) are older than expected and precede the LGM. This is inconsistent with exposure dating of the terminal moraines (24.0 ± 2.0 – 20.7 ± 1.3 cal kyr BP; Barrows et al., 2002) as well as further moraines within the catchment (T. Barrows pers. comm.) which confirm that Lake St Clair was glaciated during the LGM. The basal sediments are very low in organic matter which was likely derived from a mixture of source materials, either entrained by the glacier or washed into the lake from surrounding catchment slopes during deglaciation. Ice wastage or snow in the surrounding uplands is likely to have produced abundant meltwater resulting in rapid sedimentation in the lake during deglaciation (Hopf et al., 2000) which is supported by the low concentration of pollen, charcoal and organics. As a result, the basal sediment zone is inferred to represent no more than a few hundred years. The high magnetic susceptibility of the sediments suggests a high degree of catchment instability. Together these factors make dating the sediments difficult and similar contamination of lake sediments by older carbon has been reported at other sites (e.g. Grimm et al., 2009; Mathewes and Westgate, 1980; Oswald et al., 2005).

The basal sediments also contain a high proportion of reworked Permo-Triassic pollen grains. These are most likely derived from Permo-Triassic sediments from the Parmeneer Supergroup present within the catchment and also inferred to compose the bedrock floor of Lake St Clair (Derbyshire, 1971). The Derwent Glacier would have produced a load of rock flour through the process of grinding which typically generates fresh mineral fragments smaller than 100 microns and could have released some of the P-T pollen (Sugden and John, 1976) from the bedrock lake floor. It is unlikely, however, that this reworked pollen is the source of older carbon resulting in the old radiocarbon ages determined for the glacial sediments.

Sediment from the catchment slopes containing organic matter with ages deriving from the period immediately preceding glaciation (> c. 25.0 – 23.8 cal kyr BP; (Barrows et al., 2002) is the most likely source of older carbon which could produce the older than expected radiocarbon ages (c. 35-25 cal yr BP). When the ice retreated from the catchment during deglaciation, these catchment soils pre-dating the LGM would have been exposed and prone to erosion into the lake. If this was the case, pollen pre-dating the LGM is also likely to have been incorporated into the basal sediments along with contemporary pollen.

The secondary magnetic susceptibility peak can be observed at both the northern and the southern ends of Lake St Clair. This suggests that there may have been a basin wide, high-energy event which deposited a layer of sand during this period. Due to dating issues with the glacial sediments, it is not possible to correlate the timing of this event between sites. This, and the layering observed, does suggest that the glacial sediments, although likely deposited very rapidly, were not deposited en masse without any layering.

Deglaciation was complete at an early stage and by c. 18.3 cal kyr BP lake sediments had begun depositing at the northern end of Lake St Clair. This places a minimum limiting date for deglaciation at 18.3 cal kyr BP. Elsewhere in Tasmania, deglaciation had occurred by 16.5-16.0 cal kyr BP (Mackintosh et al., 2006; Stahle et al., 2016) with some of the highest cirques retaining ice until last (Colhoun, 1996b). These early dates for deglaciation are consistent with those from other Southern Hemisphere mid-latitude environments in New Zealand (Vandergoes et al., 2013; McKellar, 1960 in Barrows et al, 2002) and Patagonia (Moreno Moncada et al., 2015) and is in sync with postglacial warming in Antarctica (WAIS Divide Project Members et al., 2013; WAIS Divide Project Members, 2015).

7.2.2 Early postglacial vegetation

During the initial period of deglaciation (figure 7.1; figure 7.2), the vegetation consisted mostly of herbfields dominated by Poaceae and Asteraceae with expansive chenopod shrublands on the mainland and/or Bass Strait likely contributing a significant LDT component of Amaranthaceae pollen (e.g. Macphail 1979). Low charcoal levels suggest there was little burning (biomass) in the landscape. This herbaceous assemblage is typical of Tasmanian glacial/late glacial pollen records (Macphail, 1979; Colhoun, 1996a; Colhoun and Shimeld, 2012).

Other herbs growing as part of expansive herbfields and within other alpine vegetation types include *Astelia*, *Plantago*, Apiaceae, Asteraceae (low spine), Ranunculaceae, Brassicaceae, Caryophyllaceae, *Galium-Asperula* type, *Gonocarphus-Haloragis*, Scrophulariaceae and *Gunnera*. Small amounts of alpine and subalpine shrub taxa including *Athrotaxis*/*Diselma*,

Phaerosphaera hookeriana, *Microcachrys tetragona*, *Nothofagus gunnii*, Proteaceae cf. *Orites*, *Tasmannia lanceolata*, *Gymnoschoenus sphaerocephalus*, Ericaceae, *Coprosma* and *Monotoca* suggest that a variety of other alpine vegetation types were growing locally including patches of alpine heath, coniferous heath and moorland and wet herbfield (Cyperaceae and Restionaceae), not unlike the mosaic of alpine/subalpine vegetation types growing locally today. Minimal amounts of forest taxa (*Lagarostrobos franklinii*, *Nothofagus cunninghamii*, *Phyllocladus aspleniifolius,* Casuarinaceae, *Eucalyptus*, Cupressaceae) are likely to have been long distance transported from forests at lower altitudes.

The strong reduction in Poaceae and increase in *Athrotaxis*/*Diselma* concurrent with the onset of lake sedimentation at c. 18.3 kyr BP, along with the initial expansion of the forest taxa *Phyllocladus* and *Eucalyptus* at lower altitudes, are indicative of an ameliorating climate. Poaceae levels are still elevated relative to later sections of the record and the herbaceous assemblage Poaceae-Asteraceae-Amaranthaceae prominent in association with smaller amounts of other herbs (e.g. *Plantago*). This indicates that temperatures were still cold, however the notable increase in the alpine/subalpine taxa *Microcachrys*, *Orites*, *Tasmannia* and Ericaceae suggests that a large part of earlier grasslands and herbfields in the catchment had been replaced by shrubs and small trees (*Athrotaxis cupressoides*). The rapid response of *Athrotaxis*/*Diselma* (and other subalpine shrub taxa e.g. *Orites*/*Bellendena* and *Microcachrys tetragona*) to warming suggests that *Athrotaxis* and *Diselma* populations were not displaced too far from the ice during the LGM.

The timing of expansion of *Athrotaxis*/*Diselma* is broadly synchronous with the rapid rise of Antarctic temperatures and CO_2 from c. 18 cal kyr BP, although significant warming had already begun in West Antarctica (WDC) by 20 cal kyr BP with a corresponding decline in sea ice recorded in the southeast Atlantic (Collins et al., 2012; WAIS Divide Project Members et al., 2013). The shift in the ITCZ and westerlies is thought to have played a key role in the termination of the last glaciation through their effect on ocean circulations, Southern Ocean upwelling and venting of CO_2 from the deep ocean driving warming in West and East Antarctica (Anderson et al., 2009; Toggweiler, 2009; Denton et al., 2010; Lee et al., 2011; Ceppi et al., 2013; WAIS Divide Project Members et al., 2013). Global retreat of glaciers also follows between 18-11 cal kyr BP (Shakun et al., 2015).

A poleward shift in the southern westerlies during deglaciation resulted in a southward shift in the oceanic Subtropical Front (STF) (De Deckker et al., 2012). The STF south of Tasmania moved to 47°S in summer, remaining north of 45°S in spring (Sikes et al., 2009). The poleward displacement of the STF allowed warm tropical waters from the Indo Pacific Warm Pool, transported by the Leeuwin Current (LC) along the west coast of Australia, to extend around to

southern Australia (De Deckker et al., 2012). *Globigerinoides ruber*, a subtropical, near-surface dwelling, planktonic foraminifera which is used as an indicator of the presence of the LC south of Australia, increases sharply from c. 18 cal kyr BP in ocean core MD03-2611 offshore southern Australia (figure 7.4), supporting a southward shift of the STF (De Deckker et al., 2012). The rapid increase in sea-surface temperatures (SST) (figure 7.4) signals a concomitant increase in moisture during this period whereby higher SSTs promote evaporation, formation of clouds and precipitation (Calvo et al., 2007).

Buttongrass sedge, *Gymnoschoenus sphaerocephalus,* which is a poor pollen producer/disperser, has elevated levels from c. 18.8 cal kyr BP*,* suggesting that buttongrass moorlands were present locally within the catchment. The peaks in both macroscopic and microscopic charcoal suggest an increase in burning, both locally and in the wider region, and it is likely that moorlands and grasslands were burning during this period. Increasing levels of the fire sensitive *Athrotaxis*/*Diselma* throughout this time and the presence of other fire sensitive taxa such as *Microcachrys* suggest that burning was patchy and mosaics of burnt and unburnt vegetation (pyrogenic and fire sensitive) vegetation existed during the late Glacial as they do in the modern environment.

Of note is the lack of pollen from deciduous beech, *N. gunnii*, also a poor pollen producer/disperser, during this period. This likely reflects a restriction of *N. gunnii* populations in the local catchment due to increased fire activity. Since *N. gunnii* is present in fire protected areas on mountains within the catchment as well as on the Central Plateau in the modern day vegetation, yet little pollen is present in modern mud water interface samples from Lake St Clair, the higher amounts of *N. gunnii* pollen in other sections of the pollen record suggest that *N. gunnii* may have been more expansive at times in the past under milder fire regimes.

7.2.2 Expansion of subalpine coniferous rainforest/woodland

Athrotaxis/*Diselma* reach peak values between c. 16.9-15.8 kyr BP which are accompanied by a strong reduction in macroscopic charcoal and reduced values of *Gymnoschoenus* (figure 7.2). This likely represents an expansion of *Athrotaxis cupressoides* rainforest and/or woodland with *Diselma archeri* also widespread either as a component of the understorey or as part of a mosaic with alpine coniferous heath. Although the ranges of *A. cupressoides* and *A. selaginoides* overlap, *Athrotaxis selaginoides* is less likely to have been growing at this time due to its minor presence in the modern vegetation in the Lake St Clair area, being more widespread in Western Tasmania, as well as its tendency to more commonly grow as a tall forest tree at lower altitudes in contrast with *A. cupressoides* which has a higher tolerance of frost and icy winds and is predominantly found growing above 1000 m (Ogden, 1978; Kitchener and Harris, 2013).

A. cupressoides is most widespread on dolerite substrates in the subalpine zone, in particular on the Central Plateau, where its distribution closely coincides with that of ice during the last glaciation. (Ogden, 1978) notes the importance of abundant soil moisture in the distribution of *A. cupressoides*, with stands often found in locations likely to receive moisture through orographic rain, cloud condensation or prolonged snow lie. It grows in fire protected sites, commonly in rocky areas, block streams, rocky backwalls of cirques, cliffs and scree fields and south facing slopes. When growing at lower altitudes, *A. cupressoides* tends grow in fire protected locations near watercourses and tarns (Ogden, 1978; Kitchener and Harris, 2013).

Athrotaxis cupressoides dominated communities may have ranged from closed rainforest to open woodland, with other rainforest species sometimes becoming co-dominant later in the record as part of rainforest communities and woodland communities growing in association with eucalypts, most likely *Eucalyptus coccifera*. The understorey of modern *A. cupressoides* communities varies according to substrate with coniferous heath and alpine heath predominating on rocky sites, *Sphagnum* and *Richea* (Ericaceae) dominating bog sites and grasses, herbs and scattered shrubs common on mineral soils (Kitchener and Harris, 2013).

The concurrent presence of *Nothofagus gunnii* pollen suggests that *A. cuppressoides-N. gunnii* short rainforest, widespread on the Central Plateau today, but also growing in the Du Cane Range to the north and Mt Olympus and the Cheyne Range to the west, may have been growing in the deglacial landscape around Lake St Clair. This vegetation type can take the form of a closed short *A. cupressoides* forest or scrub with *N. gunnii* forming a dense understorey either alone or with a variety of other shrubs including *Diselma*, *Pherosphaera*, *Microcachrys*, *Orites*, *Richea* and *Tasmannia*, all represented by their pollen in the record during this period. *Phyllocladus* and *Nothofagus cunninghamii* may also be present along with *Astelia*, *Gleichenia* and Restionaceae in small open patches (Kitchener and Harris, 2013).

The preference of *Athrotaxis* for moist environments and the reduction in burning, suggest that the climate had become considerably warmer and wetter during this period of peak expansion of *A. cupressoides* communities. High values of *G. ruber* in core MD03-2611 offshore southern Australia (figure 7.3) indicate a poleward shift of the STF suggesting weaker SWW influence during this period paralleled with increased moisture offshore southern Australia due to increased presence of warm waters.

7.2.3 A variable period leading into the ACR

Athrotaxis/*Diselma* values decline abruptly at c. 15.8 kyr BP (figure 7.2; figure 7.3) and a variable period follows where *Eucalyptus* and *Phyllocladus* begin to increase, the latter peaking at c. 15.1 kyr BP, before declining again as Poaceae values become elevated between 15.1-13.8

kyr BP. During this slight resurgence of grassy vegetation, *Nothofagus cunnighamii* continues to increase, albeit still at lower percentages suggesting it was still more distal to the site. The increased Poaceae values suggests that the climate may have become cooler and/or drier during this period. A significant fire event occurred at c. 14.9 cal kyr BP; the period is otherwise marked by an absence of fire events.

At c. 13.8 kyr BP, sharp increases in *Phyllocladus*, *Nothofagus cunninghamii* and *Athrotaxis*/*Diselma*, accompanied by declining Poaceae values, are consistent with a temperature driven upslope movement of the treeline under warming temperatures and mark the initial establishment of montane rainforest in the region. Subalpine *Athrotaxis cupressoides* forest/woodland is inferred to have moved to higher altitudes at this time.

The period from c. 16 cal kyr is marked by stalling SSTs (figure 7.4) with slight cooling episodes at c. 15.1, 14.0 and 12.8 cal kyr BP before rapidly rising again from ~ 12.0 cal kyr BP. Strengthened SWWs are inferred at c. 15.0 cal kyr BP based on indicators of a well-mixed water column offshore southern Australia (De Deckker et al. 2012). *G. ruber* values decrease sharply from c. 16.3 cal kyr BP, reaching minimum values between c. 14.6-13.8 cal kyr BP before rising again, suggesting that the influence of the Leeuwin Current weakened during the period leading into the ACR as a result of a northward shift of the STF. Minimum *G. ruber* values coincide with increased Poaceae values and their subsequent increase at c. 13.8 cal kyr BP coincides with an increase in rainforest taxa and reduction in Poaceae values. The pattern of vegetation change from 16 cal kyr BP and through the ACR appears to correspond more closely with changing SSTs than Antarctic temperatures, indicating an oceanic influence on climate driven vegetation change.

The pattern of a cooler/drier first half and warmer/wetter second half of the ACR in the Lake St Clair record is similar to the temperature trend indicated by a calculated z score stack of all Southern Ocean and terrestrial temperature records > 40°S (excluding Antarctica) which follows a pattern of stalled temperatures from ~ 15.1 cal kyr BP until c. 13.5 cal kyr BP when temperatures began to rise rapidly again (Pedro et al., 2016). Additional dates through this period could help tighten the chronological control and linking of the observed changes in vegetation with the Antarctic Cold Reversal.

7.2.4 Peak *Phyllocladus* dominated rainforest

Increased values of *Nothofagus cunninghamii* and *Phyllocladus* values from c. 13.8 cal kyr BP (figure 7.2), the later reaching a pronounced peak between c. 13.0-12.4 cal kyr BP, suggests that montane rainforest was expanding in the region as a result of warming temperatures. Initially, both taxa may have been growing as subalpine scrub in association with *Athrotaxis*

communities, but increased values at this time point towards initial establishment of more well-developed forest. Small amounts of *Atherosperma* and *Eucryphia*/*Anodopetalum*, which have poorly dispersed pollen, suggest that other rainforest taxa had also begun to establish locally, with increasing values of *Pomaderris apetala* type suggesting expansion of wet sclerophyll forests to the east.

Although *Phyllocladus* began to increase earlier in the record than *Nothofagus cunninghamii,* by 14.2 cal kyr BP, values of both taxa are consistently above 10% and oscillating to above 20% from c. 13.7 cal kyr BP. In other parts of Tasmania, *Phyllocladus* was more dominant, and *Eucalyptus–Phyllocladus* subalpine woodland associations are inferred to have been widespread in postglacial Southern Tasmania and Lake Vera in the west (Macphail, 1979). Although (Macphail, 1980) put forward that variations in seed dispersability could explain the earlier expansion of *Eucalyptus-Phyllocladus* associations, before the establishment of *Nothofagus cunnighamii* closed forest, by controlling the rate of eastward migration of rainforest taxa from glacial refugia in Western Tasmania, his preferred explanation involved a progressive increase in precipitation from west to east.

The role of *Phyllocladus* as a pioneer rainforest taxon in Tasmania (Colhoun, 1996a) and extending this to include the initial postglacial expansion of subalpine rainforest dominated by *Athrotaxis* and *Diselma*, which are all conifers, is in line with pioneering conifer dominated forests observed in South America and New Zealand (Read and Hill, 1988).

In the Lake St Clair record, *Phyllocladus* appears to respond directly to initial post-glacial warming from c. 18 cal kyr BP and, although values are not consistently above 10% until c. 16 cal kyr BP, lowland *Phyllocladus* populations were clearly expanding at a very early stage. This early expansion of *Phyllocladus* was likely a result of its superior vagility due to having fleshy, bird dispersed seeds, also indicated for the rapid postglacial expansion of podocarps in New Zealand (Moar, 1971). Its tolerance of poor soils likely aided expansion in newly deglaciated terrains (Macphail, 1980) at higher altitudes as it would have taken considerable time for soils to develop in the post glacial landscape.

The hygrophilous nature of *Phyllocladus* is put forward as evidence for cool and moist conditions during the period of increased regional signal of *Phyllocladus* between c. 13.4-12.6 cal kyr BP at Paddy's Lake (northern Tasmania) and between c. 14-12 cal kyr BP at Lake Osbourne (southern Tasmania) (Beck et al., 2017; Fletcher et al., 2018). Fletcher and Moreno (2012) suggest that SWW flow was strong across the Southern Hemisphere between c. 14-12 cal kyr BP resulting in high relative moisture and low fire activity in western Tasmania and low lake levels in eastern Tasmania. Data from core MD03-2611 offshore southern Australia

suggest that the SWWs were strengthened at c. 15 cal kyr BP and 11 cal kyr BP resulting in a well-mixed water column (De Deckker et al. 2012), but increased values of *G. ruber* between c. 14-12 cal kyr BP (De Deckker et al., 2012) suggest that the Leeuwin Current was stronger as a result of a southward shift of the STF, likely as a result of weakening of the SWW.

7.3 The Holocene

7.3.1 Expansion of Callidendrous Rainforest (c. 12.4-10.3 cal kyr BP)

Prior to the beginning of the Holocene at 11.7 cal kyr BP, *Phyllocladus* declines abruptly at c. 12.4 cal kyr BP (figure 7.2) and is present at low levels in the record until c. 11 cal kyr BP when values begin to increase gradually. *N. cunnighamii,* together with the poorly dispersed *Atherosperma*, increase markedly during this period and most likely represent the establishment of a floristically simple, callidendrous type rainforest which predominates until c. 10 cal kyr BP. A marked increase in *Eucalyptus* and other shrubs together with *Pomaderris apetala* type likely reflect expansion of sclerophyll forests both within the catchment and to the east (e.g. Tarraleah; Macphail 1984), where *Acacia* and *Leptospermum* may sometimes also be associated with callidendrous rainforests along with a high diversity of ferns (Jarman et al., 1999). *Athrotaxis*/*Diselma* remain present at moderate values during this period, exhibiting notable decreases at c. 12.1-12.0 cal kyr BP and c. 10.8-10.6 cal kyr BP. It is possible that *Athrotaxis*/*Diselma* pollen represents *A. cupressoides* communities at higher altitudes as well as the establishment of *A. selaginoides* in montane rainforest at lower altitudes. Slight increases in the poorly dispersed *Anodopetalum*/*Eucryphia* suggest that it was growing as a part of local rainforest communities, most locally on poorer soils.

The abrupt decline in *Phyllocladus at c.* 12.4 could be explained by competitive exclusion by *Nothofagus cunninghamii*, made possible by the build-up of nutrients after several millennia of low fire activity and an ameliorating climate with subsequent improvement of soils allowing for the formation of a closed, callidendrous type rainforest. The shade tolerance of *Atherosperma* would have favoured its expansion at the expense of *Phyllocladus* which has high demands for light and moisture for seedling establishment (Barker, 1993). A sharp decline in *Phyllocladus* around this time is a feature of many Tasmanian pollen records (Macphail, 1979; Colhoun, 1996a; Stahle et al., 2016; Beck et al., 2017; Mariani et al., 2017; Fletcher et al., 2018). Macphail (1984, 1979) suggests that more fertile soils during a wet Early Holocene may have been accompanied by rainforests that were richer in *Atherosperma* than the present day as indicated by the Tarraleah and Lake Vera pollen records. At Lake Vera, a similar transition from *Phyllocladus*-dominated vegetation to floristically simple *Nothofagus cunninghamii–Atherosperma* closed forest occurs, whereas closed *Nothofagus* scrub/rainforest established at other sites in western and southern Tasmania (Macphail 1980, Macphail 1979,

Macphail, 1979, 1980; Beck et al., 2017; Fletcher et al., 2018). An early decline of *Phyllocladus* after c. 14 cal kyr BP at Wombat Pool near Cradle Mountain to the north is suggested to have been as a result of competition from expanding woody shrub taxa (e.g. *Leptospermum*/*Baeckea*, *Melaleuca* and Proteaceae) (Stahle et al., 2017).

The dominance and continuous regeneration of *Nothofagus cunnighamii* on optimal sites in cool temperate rainforests in Australia is in contrast with the restriction of *Nothofagus* species to climatically or edaphically suboptimal sites or those subject to infrequent catastrophic disturbance in Chile and New Zealand (Read and Hill, 1988). *Nothofagus cunninghamii* dominates these sites in part due to its faster growth rates on fertile soils, but also as a result of the depauperate Tasmanian rainforest flora which lacks more competitive shade-tolerant taxa (Read and Hill, 1988; Barker, 1993). Callidendrous rainforests are floristically and structurally simple, being dominated by *Nothofagus cunninghamii* and/or *Atherosperma* with a sparse, shady, park-like understorey. A low diversity of woody species is paired with a high diversity of ferns, in particular *Dicksonia Antarctica* and ferns growing as epiphytes on *Dicksonia* (e.g. *Phymatosorus*; Garrett and Council, 1996) (Jarman et al., 1999). Callidendrous rainforests are typically found growing on substrates of higher fertility than thamnic and implicate rainforests which fall on a gradient of increasing diversity and structural complexity in association with decreasing soil fertility (Jackson, 1968; Read and Hill, 1988; Barker, 1993), *Phyllocladus* becoming more abundant with decreasing soil quality and assuming dominance on the poorest sites through its tolerance of extreme site conditions rather than superior a growth rate (Read, 1999).

Like many conifers, *Phyllocladus* is thought to require disturbance in order to regenerate, although if disturbance is too frequent, other species which can regenerate vegetatively may take over as a result of local site extinction of *Phyllocladus* due to reproductive immaturity. *Phyllocladus* rarely regenerates vegetatively and its intolerance of shade and slow growth limit its regeneration success even when gap opportunities emerge in the rainforest due to overtopping and shading by faster growing rainforest species. Its storage of seed in the soil and high vagility, however, means that it is well adapted to regenerate in the face of larger disturbances, yet in the absence of large scale disturbance, *Phyllocladus* is thought to be capable of maintaining its presence throughout its range through smaller scale processes, albeit as reduced populations (Read and Hill, 1988; Barker, 1993, 1995; Barker and Kirkpatrick, 1994). A period of postulated conifer regeneration failure in New Zealand between 1600 and 1800 AD, the “regeneration gap” (Wardle, 1963), was initially explained by changes in climate favouring broadleaved forests (Cockayne, 1921; McKelvey, 1953; Holloway, 1954, 1964; Nicholls, 1956; Robbins, 1962; Wardle, 1963), however, further research developed the idea of

a disturbance based regeneration ecology (Clayton-Greene, 1977; Veblen and Stewart, 1982; Norton, 1983), such as by windthrow and mass movement, for many conifers in New Zealand (Read and Hill, 1988; Stewart and Rose, 1988).

A climate-linked reason for the decline of *Phyllocladus,* based on its hygrophilous nature and suggested tracking of millennial scale trends in hydroclimate (Beck et al. 2017; Mariani et al. 2017), has been proposed where *Phyllocladus* responds to a reduction in regional moisture and/or increased fire activity during this period linked to a hemisphere wide shift to a warmer and drier climate under weakened westerly circulation and increasing seasonality (Fletcher and Moreno, 2012; Beck et al., 2017; Mariani et al., 2017; Fletcher et al., 2018). Barker (1993)'s autecological study of *Phyllocladus* indicates that *Phyllocladus* has a similar climatic range to *Nothofagus cunninghamii*, yet it has a more widespread distribution in wet eucalypt forests (Kirkpatrick et al., 1988). Barker puts forward that the absence of *Nothofagus cunninghamii* from these communities is due to non-climatic factors such as disturbance regimes, migration history and the stability of *Phyllocladus* within the more fire-prone wet eucalypt forests due to factors such as its superior dispersibility and storage of seed in the soil (Barker, 1993). The wider presence of *Phyllocladus aspleniifolius* relative to *Nothofagus cunninghamii* at the arguably drier end of its range in wet eucalypt forests, leaves the question open to what extent *Phyllocladus aspleniifolius* may track moisture changes. However, the similarity in timing of peak expansions of both *Phyllocladus aspleniifolius* and *Athrotaxis*/*Diselma* and peak levels of *G. ruber* offshore southern Australia seems to suggest a climate link driving the expansion of these conifers. The increased presence of warm, tropical waters via the Leeuwin current offshore southern Australia, and a resulting increase in moisture through higher evaporation, formation of clouds and precipitation promoted by higher SSTS (Calvo et al., 2007) during periods of peak presence of *G. ruber* raises the question whether the moister climate inferred for offshore southern Australia may have extended to Tasmania driving the expansion of the conifers.

The proposed shift from *Phyllocladus*-dominated rainforest to *Nothofagus cunninghamii-Atherosperma* rainforest in the Lake St Clair record would have a misleading effect on the total rainforest pollen sum during this period due to the reduction of a strong regional pollen source and the expansion of a local, very weak pollen source (predominantly *Atherosperma*, but also *Anodopetalum*/*Eucryphia*). Although it is likely that *Eucalyptus* forests also expanded at this time, in particular in the wider pollen source area to the east, it seems unlikely that this occurred at the expense of rainforest which appears to have flourished during this period. The large pollen source area of Lake St Clair, which would have been tracking vegetation changes in the wider region both to the west and east as represented by regionally distributed pollen

taxa, and the minimal increase in fire activity observed in the record provides no strong support for a markedly drier climate affecting the region. The decline in *Phyllocladus aspleniifolius* appears to be best explained by out-competition by *Nothofagus cunninghamii* at this time rather than a decline in moisture causing this shift in vegetation, even if the climate may have become drier at this time. The optimal conditions for growth of *Nothofagus cunninghamii,* due to an overall ameliorating climate and improved soil conditions allowed *Nothofagus cunninghamii* to thrive and become strongly competitive.

The decreases in *Athrotaxis*/*Diselma* at c. 12.1-12.0 cal kyr BP and c. 10.8-10.6 cal kyr BP are accompanied by decreased values of *Nothofagus cunnighamii* and coinciding peaks in total fern spores and total herbs, perhaps in response to fire activity, although this can not be concluded from the charcoal record. The latter decrease is followed closely by an increase in *Gymnoschoenus sphaerocephalus* between c. 10.7-10.5 cal kyr BP. Macroscopic and microscopic charcoal values remain low during this period, with a few low magnitude peaks in macroscopic charcoal clustered around c. 12.5-11.9. The period between c. 10.3-7.9 cal kyr BP sees a shift in the rainforest with an expansion of *Phyllocladus* and declining values of *Nothofagus cunninghamii, Atherosperma* and fern spores. *Anodopetalum*/*Eucryphia* remains at low values indicating its presence in the local rainforest. *Nothofagus gunnii* reaches peak values and *Athrotaxis*/*Diselma* increases to moderate values, which could include both *Athrotaxis cupressoides* and *Diselma* in the subalpine zone as well as *A. selaginoides* as part of montane rainforest at lower altitudes. *Eucalyptus* is present at its lowest levels for the Holocene between c. 11.0-7.9 cal kyr BP. Charcoal levels remain low through this period overall, with a cluster of low magnitude fire events identified between c. 9.9-9.2 cal kyr BP, which may have been enough to open up opportunities for *Phyllocladus* to expand, although declining soil fertility would explain a decline in *Nothofagus cunninghamii* and *Atherosperma moschatum* and the shift to expanded conifer-rich rainforest finding more frequent regeneration conditions in potentially more open forests and/or poorer sites. Macphail (1980) puts forward that the shift from *Atherosperma* to *Phyllocladus* at Tarraleah was due to an opening up of the forest as a result of overleaching of soils during a wetter early Holocene.

Fletcher and Moreno (2012) put forward that the period between c. 11-9 cal kyr BP was characterised by hemisphere wide reduced westerly flow expressed as an east-west anti-phased hydroclimatic regime in Tasmania, where eastern Tasmania experienced relatively moist conditions, supported by low fire activity at Stoney and Hazards Lagoon and high lake levels (Harrison and Dodson 1993; Jones et al., 2017; Mackenzie and Moss, 2017), and western Tasmania was affected by drier conditions as indicated by high fire activity and low rainforest cover (Mariani and Fletcher, 2017; Mariani et al., 2017; Fletcher et al., 2018). Macroscopic

charcoal records from Cradle Mountain indicate a mixed signal during this period with records from Wombat Pool, Lake Hanson and Lake Lilla indicating increased fire activity between c. 12-9.5 cal kyr BP and records from Suttons Tarn and Lake Wilks indicating low fire activity, apart from slightly elevated charcoal values prior to c. 11 cal kyr BP, suggested to be due to the topographic protection of these higher altitude sites (Stahle et al., 2017). An increase in woody shrubs, as well as *Gymnoschoenus* at two of the sites, is proposed to have contribute to the increase in biomass burning at the lower altitude sites, whereas contemporaneous high values of *Nothofagus cunninghamii* led Stahle et al. (2017) to suggest the presence of a mosaic of pyrophytic and fire-sensitive vegetation where fires were extinguished at the edge of rainforests.

The particle size record from Lake St Clair shows a marked shift from relatively uniform particle size during the Early Holocene (figure 5.1; figure 7.4), to the delivery of coarser sediments to the lake, initially sand and coarse silt, then medium silt between c. 10.1-7.6 cal kyr BP. Total organic matter increases to its highest levels, whilst charcoal values remain low. C:N ratios over > 20 during this period suggest a terrestrial source for the carbon indicating increased erosion of catchment soil (Meyers, 1994). The transport of coarser sediment is also indicative of higher energy in the fluvial system pointing towards and increase in precipitation and/or storminess during this time. An increase in storminess could also support an increase in disturbance (by e.g. windthrow) leading the shift in rainforest composition to one of more complex floristics.

G. ruber declines to a low between c. 12.0-11.5 cal kyr BP (figure 7.4), before rising sharply again and reaching high values between c.10.7-8.2 cal kyr BP, with a number of minor dips between c. 9.7-9.1 cal kyr BP. This indicates a shift from a weak Leeuwin Current influence to a strong influence as result of a poleward displacement of the STF, most likely due to weakened SWW flow and suggests an overall increase in moisture during this period. This is consistent with the increased precipitation/storminess indicated by the Lake St Clair particle size and C:N record. Enhanced SWW flow is inferred around c. 11 ka based on indicators of a well-mixed water column offshore southern Australia (De Deckker et al. 2012). SSTs increase to their highest levels during this period, reaching modern values by c. 12.2 cal kyr BP, with a period of slightly cooler SSTs between c 9.6-8.5 cal kyr BP.

This agrees well with the findings of Rees et al. (2015) at Lake Dobson where, between 11.5 and 8.3 cal kyr BP, they propose a period of SWW dominance (positive phase of SAM during the summer) based on chironomid and detrital indicators inferring high precipitation during this period. This contrasts with the drier conditions inferred for western Tasmania by Fletcher and Moreno (2012) at this time. Rees et al. (2015) put forward that a southward contraction

of the SWW permitted anomalous, moisture bearing easterlies to develop (Hendon et al., 2007) bringing precipitation to Lake Dobson in the Southern Ranges. The persistence of rainforest at Lake Osborne during this period led Fletcher et al. (2018) to suggest that the Southern Ranges acted as refugium for subalpine rainforest buffered from the drier climatic conditions in the west. They suggest that this is in support of the argument of McGlone et al. (2011) for the persistence of cool, moist conditions between c. 12-9 cal kyr BP in the Southern Alps of New Zealand as a result of increased cloudiness under reduced westerly wind regime.

7.3.2 Mid Holocene switch to an ENSO influenced climate

A major regime shift in the vegetation occurs at c. 7.8 cal kyr BP (figure 7.2; figure 7.5). The shift is marked by a pronounced increase in *Eucryphia*/*Anodopetalum* which is accompanied by both macroscopic and microscopic charcoal peaks and elevated *Pomaderris apetala* type. *Phyllocladus* values are reduced between 7.8-7.4 cal kyr BP and no *Nothofagus gunnii* pollen was recorded between 8.0-7.4 cal kyr BP, while *Athrotaxis*/*Diselma* values reduce significantly after 8 cal kyr BP following a declining trend throughout the late Holocene. A speleothem record from Lynd's Cave, spanning the period between c. 9.2-5.1 cal kyr BP, indicates that temperatures were at their highest between 8.0-7.4 cal kyr BP, accompanied by high evaporation rates and low effective precipitation (Xia et al., 2001). The foraminifera *G. ruber* in ocean core MD03-2611 offshore southern Australia shows a marked decline after c. 8.3 cal kyr BP towards minimum values between 7.7-7.4 cal kyr BP indicating a weaker Leeuwin Current presence offshore southern Australia in response to a northward shift of the STF and strengthening of the SWW and reduced moisture. A warmer and drier climate during this period would have been conducive to an increase in fire activity favouring an increase of *Eucryphia*/*Anodopetalum* and *Pomaderris apetala* type (grows in disturbed areas e.g. after fire) and a reduction in the range of the very fire sensitive *Nothofagus gunnii*.

The pronounced increase in *Eucryphia-Anodopetalum* represents a local signal within the catchment. *Anodopetalum*/*Eucryphia* occurs in relatively few Tasmanian pollen records, likely due to its very local pollen transport. At Lake Vera, *Anodopetalum*/*Eucryphia* increases from c. 7.8 cal kyr BP, but does not become abundant until after c. 5.2 cal kyr BP forming a floristically complex late Holocene rainforest together with *Nothofagus*, *Phyllocladus*, *Atherosperma* and *Lagarostrobos* (Macphail, 1979). At Lake Osborne, *Anodopetalum*/*Eucryphia* increases early at c. 12 cal kyr BP, with a pronounced peak after c. 7.8 cal kyr BP following a significant fire episode accompanied by a reduction in subalpine rainforest (Cupressaceae and *N. gunnii*) (Fletcher et al., 2018).

A high-resolution, multi-proxy record from Lake Pupuke New Zealand (Augustinus et al., 2008) spanning c. 9.5-7.0 cal kyr BP highlights the contrast between the pollen record, which indicates moist and mild conditions suggesting overall stability of the environment during this period, and the records of particle size, diatom palaeoecology, biogenic silica concentrations, sediment elemental and carbon isotope geochemistry reflecting changes in sediment sources and lake conditions, which indicate that this period was actually characterised by considerable environmental variability. They indicate a period of relatively low lake levels and warm, mild conditions between c. 9.5-7.9 ending with a drier period combined with increased storminess between 8.2-7.9 cal kyr BP, approximately coeval, although longer than, the 8.2 cal kyr event recorded in the North Atlantic (Alley et al., 1997). The period of increased dryness and storminess is followed by a period of c. 880 years of milder and moister conditions commensurate with higher lake levels (Augustinus et al., 2008). Although direct teleconnections to the abrupt Northern Hemisphere climate event is not supported by the changes observed in the Lake St Clair record at this time, the marked changes in vegetation and increase in charcoal, together with concurrent reduction in *G. ruber* and SSTs offshore southern Australia, does indicate the possibility of a widespread drought and an increase in fire activity at this time.

Both *Anodopetalum* and *Eucryphia* are relatively short-lived rainforest species with life spans around 200 and 250 years respectively (Barker, 1993; Mallick, 2001) that become more frequent in rainforests with lower soil fertility. *Eucryphia* is represented by a lowland rainforest species, *E. lucida*, which ranges from sea level to 1000 m, and *E. milliganii* which is predominantly restricted to higher altitudes although its range overlaps with *E. lucida* (Curtis, 1975; Mallick, 2001). In contrast with the open, park-like understoreys typical of callidendrous rainforest, *Anodopetalum*, when present, typically forms a thick, tangled mass of stems in the understorey of rainforests as a result of its genetically determined growth habit of its stems which gives it its common name “horizontal scrub”. *Anodopetalum* can dominate rainforest regrowth after disturbance due to its rapid spreading mechanism by layering as well as coppice (Barker and Brown, 1994), for example low intensity fires are thought to promote understorey species like *Anodopetalum* sometimes impeding the ability of other species to regenerate leading to a change in the nature of the rainforest (Read, 1999). *Eucryphia lucida* occurs most frequently in the understorey of thamnic rainforests (intermediate soil fertility), but may also be present in implicate and callidendrous rainforests (Jarman et al., 1999; Mallick, 2001). *Eucryphia lucida* and *Nothofagus cunninghamii* were found to have a greater capacity for regeneration after moderate intensity fires than *Atherosperma* and *Phyllocladus* which failed to regenerate in studies of regeneration on logged coupes in southwest Tasmania (Tanjung,

1993). Members of the Cunoniaceae, the family to which *Anodopetalum* and *Eucryphia* belong, frequently have a disturbance based ecology, with some species such as *Weinmannia racemosa* in New Zealand even requiring disturbance for regeneration (Stewart and Veblen, 1982; Barnes et al., 2001).

There are a number of possible reasons for the increases in *Anodopetalum*/*Eucryphia*. The increases could be explained by the expansion of the short-lived taxa in reponse to an increase in disturbance events affecting the rainforest under an increasingly variable climate. Alternatively, or in combination, an increase in high precipitation, storm and erosion events could have resulted in delivery of "spikes" of sediment to the lake containing pollen from vegetation growing near rivers and streams and via overland flow (Brown, 1985). This would be one mechanism by which the poorly transported pollen types *Anodopetalum*/*Eucryphia* could be incorporated into the lake sediments at enhanced values. The low values of *Anodopetalum*/*Eucryphia* between c. 10.1-7.8 cal kyr BP, when higher precipitation is inferred by the particle size and C:N record and increased delivery of coarser sediments indicates an overall higher energy in the system, points towards actual increases in population ranges of these taxa in response to disturbance rather than a simply enhanced signal in the record due to increased transport of the pollen to the lake. Where higher overall precipitation may not have markedly increased fluvial transport of otherwise poorly transported pollen types, the spikiness in the record does suggest a potentially important role of storm events enhancing pollen transport of these pollen types in pulses of high energy transport. The oscillation between more frequent dry periods and increased fire activity with wetter periods and increased storm activity, would have had the net effect of increased events of post-fire catchment erosion, together with a post-fire depletion of nutrients leading to increased diversity in the rainforest by providing increased niches for various taxa under decreased competition from *Nothofagus cunninghamii.* The depletion of soil nutrients by fire promotes vegetation adapted to lower soil nutrient status, whereby progressive nutrient depletion results as a consequence of feedback mechanism of frequent fires (McIntosh et al., 2005).

The highest magnitude macroscopic charcoal peak occurs at c. 5.7 cal kyr BP and is preceded and followed by two low magnitude peaks at c. 6.2 cal kyr BP and 5.4 cal kyr BP, with accumulation rates indicating a marked shift towards higher accumulation from c. 5.7 cal kyr BP until present relative to the early to mid Holocene. Peaks in organic matter and coarser sediments coincide at c. 5.7 cal kyr BP and indicate increased catchment erosion post fire. *Nothofagus gunnii* is absent from the Core CG pollen record from c. 5.7-1.8 cal kyr BP with the last occurrence of *N. gunnii* in the Core CB record from the southern end of Lake St Clair at c. 5.0 cal kyr BP. The fire sensitive nature of *N. gunnii* suggests that an intensification of the fire

regime during the late Holocene may have strongly reduced its range. Fletcher et al. (2013a) record the local extinction of *Nothofagus gunnii* and Cupressaceae after a succession of fires in the Lake Osborne catchment. *Nothofagus gunnii* disappears from the Lake Osborne record after a high magnitude fire at 5.8 cal yr BP, the timing of which is very comparable to the Lake St Clair record. Fletcher et al (2013a) found that other rainforest taxa such as *N. cunninghamii* and *Eucryphia* recovered within a few centuries of three large fire events during the late Holocene, noting that Cupressaceae exhibit a much slower recovery after fire in the order of 800 years prior to this period until ultimately driven to a reduction in range by consecutive fires. The Lake Gwendolyn and Lake Nancy macroscopic charcoal records also show marked increase in burning on Frenchman's Cap, approximately 37 km to the SW, after c. 5 cal kyr BP along with a switch from multimillennial oscillations in biomass burning to sub millennial (Fletcher et al. 2015)

7.3.3 Late Holocene

The two largest peaks of *Eucryphia* occur at 5.0 cal kyr BP and 3.9 cal kyr BP (figure 7.2; figure 7.5), with the largest peaks in microscopic charcoal occurring at c. 4.6 cal kyr BP and c. 3.9 cal kyr BP, the latter coinciding with the largest peak in *Anodopetalum*/*Eucryphia*. No significant macroscopic charcoal peaks occur at these times, although accumulation rates are high, the only other significant peaks during the late Holocene occurring as a cluster of fire events between c. 3.1-2.7 cal kyr BP with no marked corresponding changes in the vegetation. The Skullbone Plain charcoal record indicates significant fire events at 3.6 and 3.4 cal kyr BP with an observed decrease in *Eucalyptus* and increase in herbs from between c. 4.0-3.6 cal kyr BP. The Cradle Mountain charcoal records indicate a marked increase in fire activity between c. 4.8-3.6 cal kyr BP. A decline in rainforest and subalpine taxa and increase in sclerophyll and herbaceous taxa observed between c. 5.2-4.0 cal kyr BP begins before peak fire activity, but the authors suggest that the vegetation transition was catalysed by fires (Stahle et al., 2017).

The strong reduction in *G. ruber* between c. 5.0-4.3 cal kyr BP points towards a period of drought at this time, which, if extended to Tasmania is supported by increased fire activity at this time. Perner et al. (2018) propose that ENSO was in a predominantly La Niña-like state during the mid Holocene (c. 7.4-3.5 cal kyr BP) producing a strong and warm Leeuwin Current offshore southern Australia as a result of enhanced export of tropical heat from the Indo-Pacific Warm Pool to the Leeuwin Current accompanied by high SSTs. During the Late Holocene (c. 3.5 cal kyr BP to present) ENSO shifts to a predominantly El Niño-like state and becomes more variable, resulting in a weaker Leeuwin Current and cooling SSTs offshore southern Australia. The El Niño like event centred between c. 5.0-4.5 cal kyr BP occurs during an overall La Niña dominant state of ENSO. They identify an apparent synchronicity between

northern hemisphere climatic variability and several distinct millennial-scale phases of El Niño/La Niña development offshore southern Australia supporting ENSO as a potential mediator of coherent interhemispheric climatic and oceanic conditions during the mid to late Holocene.

The Lake St Clair record supports an early onset of ENSO from c. 8 cal kyr BP with an intensification from c. 5 cal kyr BP. A gradual decreasing trend of montane and subalpine rainforest was already underway by 8 cal kyr BP, in particular *Phyllocladus* and *Athrotaxis*/*Diselma*, with *Nothofagus cunninghamii* maintaining a dominant presence until present. *Eucalyptus* and other trees and shrubs, along with herbaceous taxa, begin to increase gradually during this period with pronounced increases during the late Holocene. The vegetation changes during the Holocene, including three phases of rainforest development from floristically simple, closed *Nothofagus cunninghamii – Atherosperma moschatum* callidendrous type rainforest between c. 12.5-11 cal kyr BP, to an expansion of *Phyllocladus* from c. 11-7.9 cal kyr BP to a significant presence of *Anodopetalum/Eucryphia* from c. 7.9 cal kyr BP, point towards declining soil fertility and increasing openness of the vegetation as a result of a more variable climate promoting an increase in disturbance events by both fire and storms. Finally, the Late Holocene increase in herbaceous taxa, in particular Poaceae from c. 5 cal kyr BP, occurs in sync with cooling SSTs offshore southern Australia and supports a cooler climate during this time.

7.3.4 The role of humans

The role of human activity in the vegetation history record of Lake St Clair is unclear in the analysis presented here as the vegetation and fire history reconstructions strongly suggest that climate is the primary driver on vegetation and fire dynamics. Anthropogenic burning was a feature of landscape management (Gammage, 2011), however, the Lake St Clair record, capturing the large scale and regional dynamics of past vegetation is unlikely to be sensitive to human influence on fire regimes and vegetation patterns.

Humans first arrived in Tasmania around 38-39 kyr BP via the Bass Strait land bridge which became exposed sometime after 43 kyr BP (Lambeck and Chappell, 2001; O'Connell & Allen, 2015). The two oldest, dated archaeological sites are located at Warreen Cave (Allen, 1996) in the southwest and Parmerpar Meethaner rockshelter (Cosgrove, 1995) approximately 35 km to the north of Lake St Clair. The highest concentration of Pleistocene sites is focussed in the valleys of southwest Tasmania and Allen et al. (2016) argue that these were a sweet spot for Pleistocene hunters who moved seasonally between lowland and upland sites hunting mostly Bennett's wallabies, but also wombats. Their updated palaeoecological model of subsistence procurement in Pleistocene Tasmania is based on the model of Cosgrove (Cosgrove et al.,

1990; Cosgrove, 1995). The model contrasts a stable ecosystem in southwest Tasmania, where humans focused around patches of moist, grassy microhabits and fertile soils in an otherwise infertile landscape, with a comparably unstable ecosystem in southeast Tasmania, where resources were highly variable and scattered unevenly across the landscape in combination with an unpredictable effective precipitation regime relative to the southwest where precipitation was less variable (O'Connell & Allen, 2015).

No dated archaeological sites exist in the Lake St Clair region, however numerous isolated artefacts, artefact scatters and quarries have been found (DPIPWE, 2017). Dated archaeological sites on the Central Plateau are all located in the east and date to c. 3 cal kyr BP or younger (Thomas, 1993; Cosgrove, 1990). Although it is not possible to distinguish anthropogenic burning from a climate driven increase in fire activity, the increase in charcoal around c. 18.8 cal kyr BP in the immediate post-glacial period of the Lake St Clair record, in combination with significant values of *Gymnoschoenus* and Poaceae pollen, could be an indication of the possible movement of people through the region who may have contributed to burning of moorlands and grasslands once the ice had retreated and the climate ameliorated.

The absence of Holocene archaeological sites in southwest Tasmania has been explained by the expansion of rainforest as the climate became warmer and wetter, which resulted in a displacement of prey animals from their open habitats leading to the movement of humans away from the region under the pressure of a shrinking resource base (Jones and Allen 1984, Jones 1995; Cosgrove et al. 1994; Cosgrove 1999; Porch and Allen, 1995). Others have argued that humans continued to use the region through the Holocene (Thomas, 1993, 1995; Jackson, 1999c), with Fletcher and Thomas (2007a, b 2010a, b) putting forward that open vegetation persisted across western Tasmania throughout the Holocene, in contrast with previous interglacials when humans were absent, and that western Tasmania represents a cultural landscape. This model of landscape evolution is supported by quantitative land-cover estimates for Dove Lake which show that the landscape was dominated by treeless vegetation for the last 12, 000 years (Mariani et al. 2017b). However, Mariani et al. (2017a) suggest that Aboriginal fire management was small scale yet synergistic with millennial-scale climate change through time which exhibits a tight coupling with palaeofire activity in western Tasmania through the Holocene (Mariani and Flecther, 2017).

Two archaeological sites bordering western Tasmania show differing occupation histories. Warragarra Rockshelter, located at an elevation of ~610 m (a.s.l.) in the Mersey Valley to the north of Lake St Clair, was briefly occupied ~ c. 12.9 cal kyr BP, but then abandoned until the Late Holocene (Allen and Porch, 1996; Lourandos, 1983; DPIPWE; 2017), whereas Parmerpar

Meethaner rockshelter, located just 15 km to the north at a lower altitude of ~ 400 m, was occupied throughout the Holocene, although at diminished levels during the mid-Holocene (Cosgrove, 1999). Stahle et al. (2017) conclude that the broad changes observed in the vegetation and charcoal records from the Cradle Mountain area nearby were primarily driven by climate yet likely reinforced by Aboriginal land-use practises. They suggest that when rainforest expanded under wetter conditions and lower fire activity during the mid-Holocene as indicated by the Cradle Mountain records, people may have remained in the area switching to subsistence strategies (Stahle et al. 2017).

After European settlement in 1803, grazing was initially focused in the Tasmanian Midlands, however, expanded to the use of the Central Plateau for summer grazing, which was heaviest between 1840 and 1853, after which stocking levels declined, in part due to the deterioration of natural pastures as a result of sustained grazing pressure and frequent burning to encourage new growth (Shepherd, 1974). Kirkpatrick and Bridle (1999) found that grazing by domestic stock had a greater impact on the vegetation, causing continued deterioration, than by native herbivores and rabbits which mostly affected the abundance of tall herbs but generally permitted regeneration of the vegetation. Holz et al. (2015) reconstructed the fire history of the Central Plateau for the last 250 years using fire scars on *Athrotaxis cupressoides* and found that the frequency of fires was similar during the Aboriginal and European settlement periods until 1960 and consisted of frequent, low-severity, patchy fires which permitted the persistence of *Athrotaxis cupressoides* despite its sensitivity to fire. 1960 saw a series of catastrophic fire events, triggered by routine ignitions by shepherds and trappers to improve pastures, and resulting in 10% mortality of the Central Plateau *Athrotaxis cupressoides* populations, the severity of which Holz et al. (2015) attribute to a possible combination of extreme fire weather, a record dry spring-summer season, and a shift in landscape fuel as a result of overgrazing by domestic stock. The Central Plateau is now conserved as part of the Walls of Jerusalem National Park in the west and the Central Plateau Conservation and Protected Areas in the east.

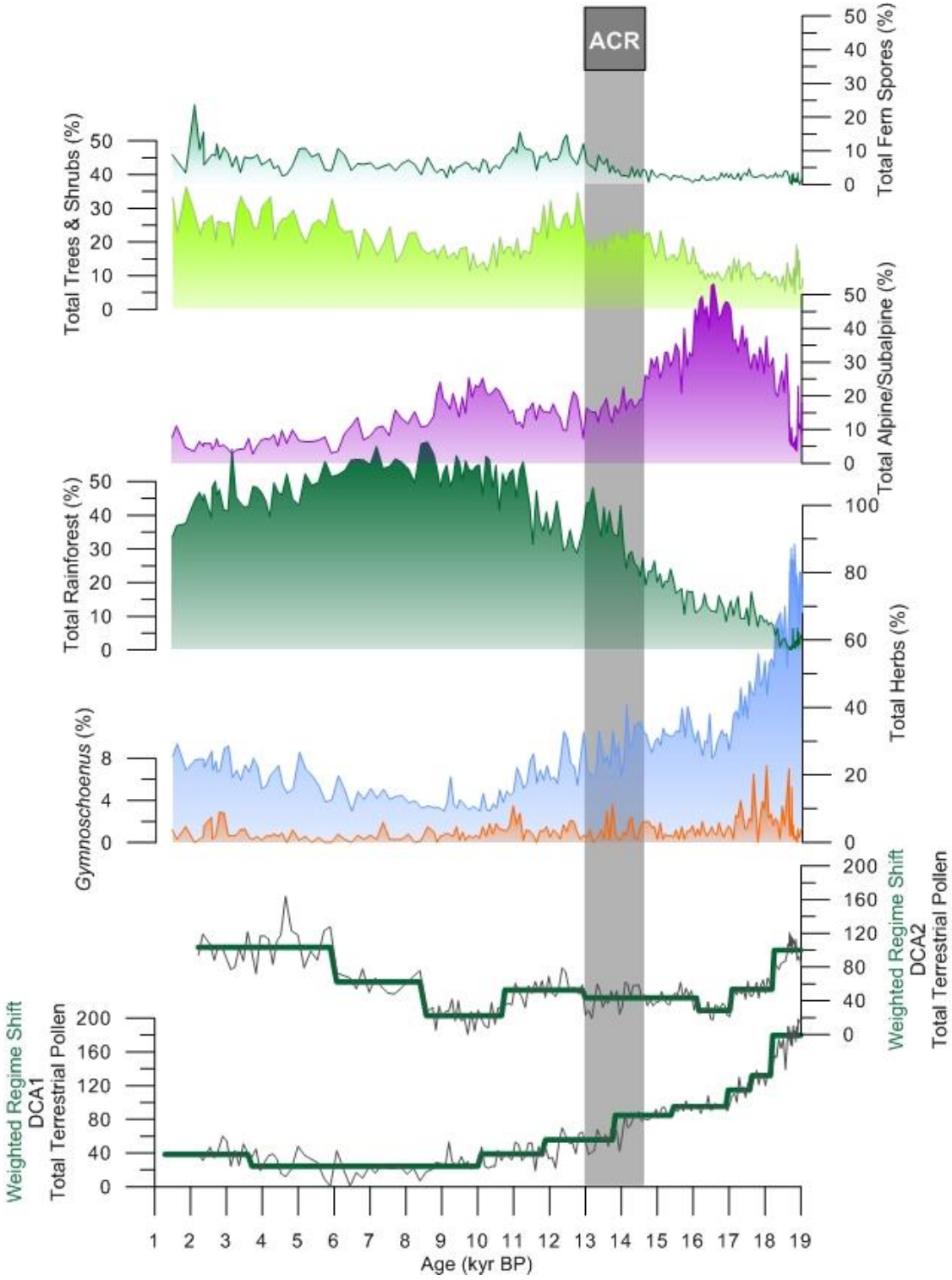

Figure 7-1 Summary pollen diagram of total fern spores (%), total trees & shrubs (%), total alpine/subalpine (%), total rainforest (%), total herbs (%), Gymnoschoenus (%), weighted regime shift for DCA2 of the total terrestrial pollen dataset and DCA1 of the total terrestrial pollen dataset

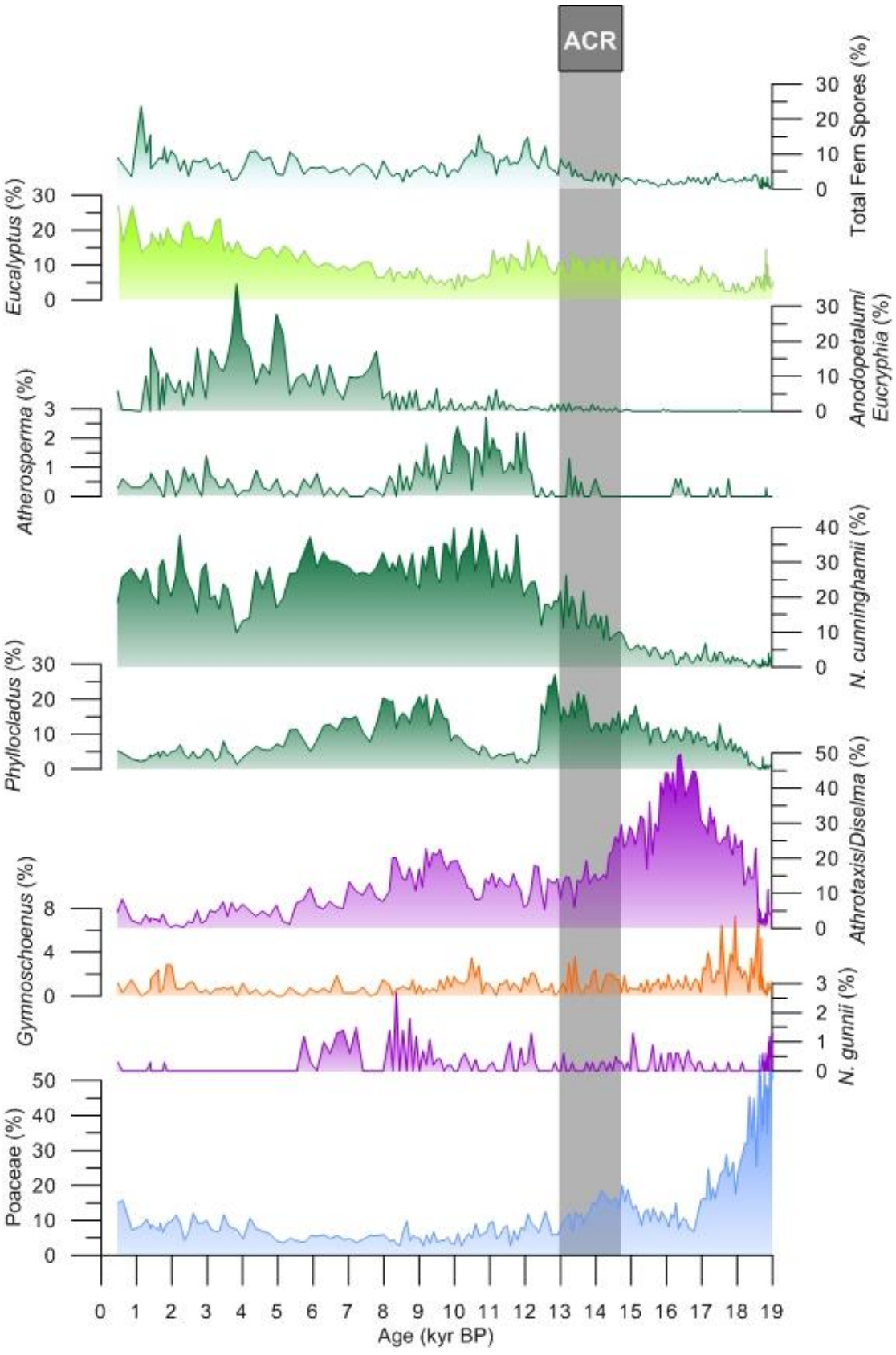

Figure 7-2 Summary diagram of key taxa showing detail of rainforest dynamics: total fern spores (%), *Eucalyptus* (%), *Anodopetalum/Eucaryphia* (%), *Atherosperma* (%), *Nothofogas cunninghamii* (%), *Phyllocladus aspleniifolius* (%), *Athrotaxis/Diselma* (%), *Gymnoschoenus sphaerocephalus* (%), *Nothofagus gunnii* (%) and Poaceae (%)

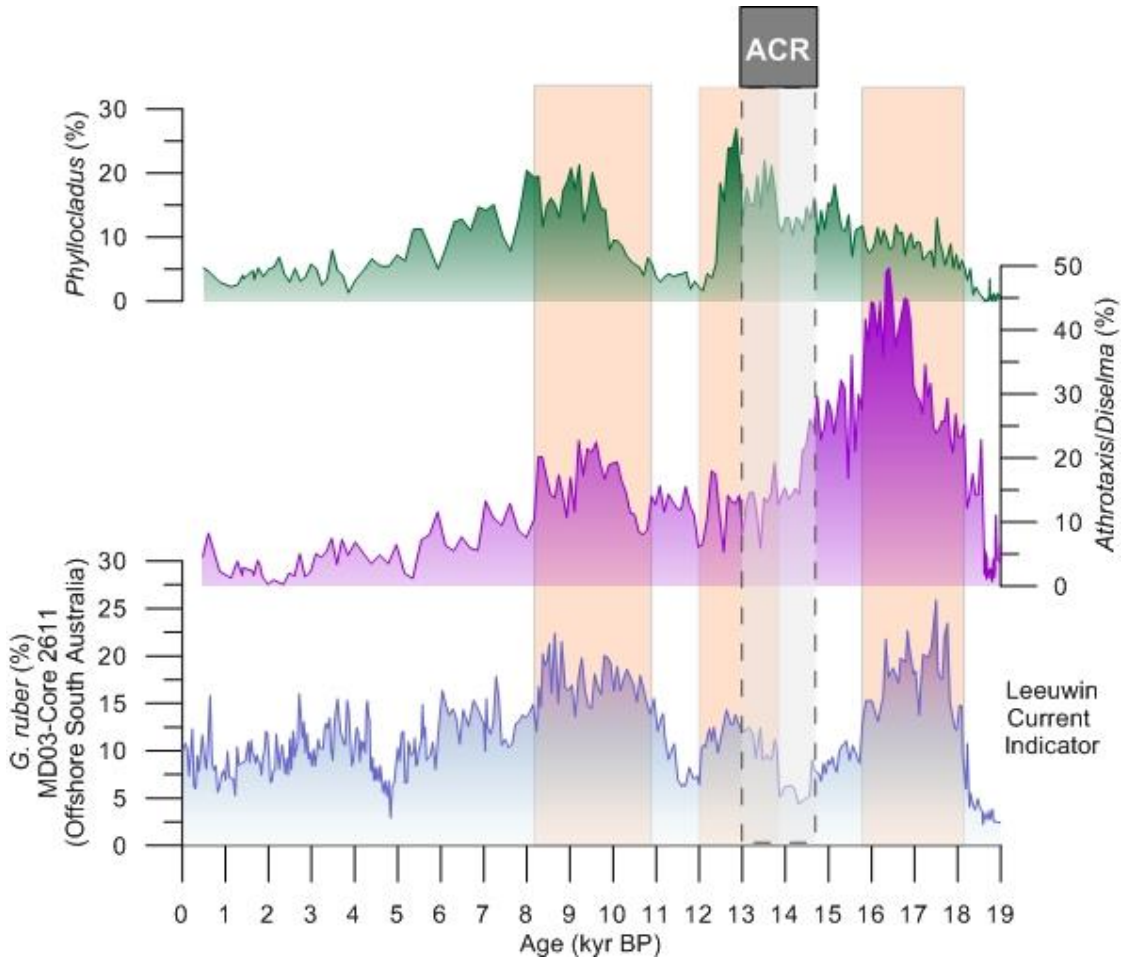

Figure 7-3 Comparison of *Phyllocladus aspleniifolius* (%) and *Athrotaxis*/*Diselma* (%) with *G. ruber* as an indicator of the strength of the Leeuwin Current offshore southern Australia. Higher values indicate the presence of a stronger Leeuwin Current. *G. ruber* data is unpublished data from P. De Deckker (pers. comm.)

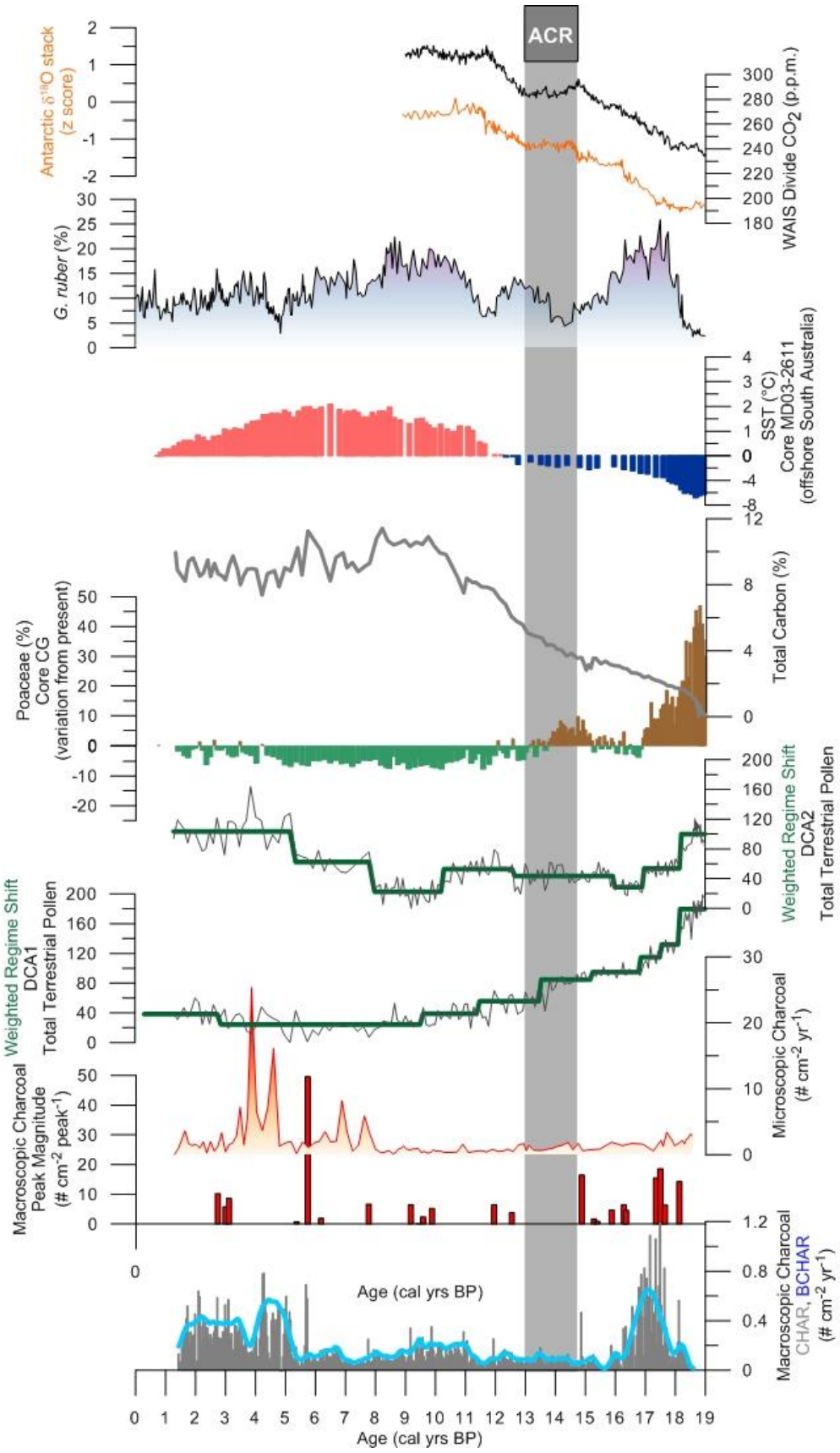

Figure 7-4 Summary diagram comparing select datasets from Core CG, Lake St Clair: macroscopic charcoal (CHAR, BCHAR, peak magnitude), microscopic charcoal, weighted regime shift index for DCA1/2 of the total terrestrial pollen dataset, Poaceae (%) and total carbon (%); with other proxies: SST and *G. ruber* from core MD03-2611 (offshore southern Australia) (unpublished data from P. De Deckker (pers. comm.)), Antarctic temperature proxy and WAIS Divide CO_2 (ppm)

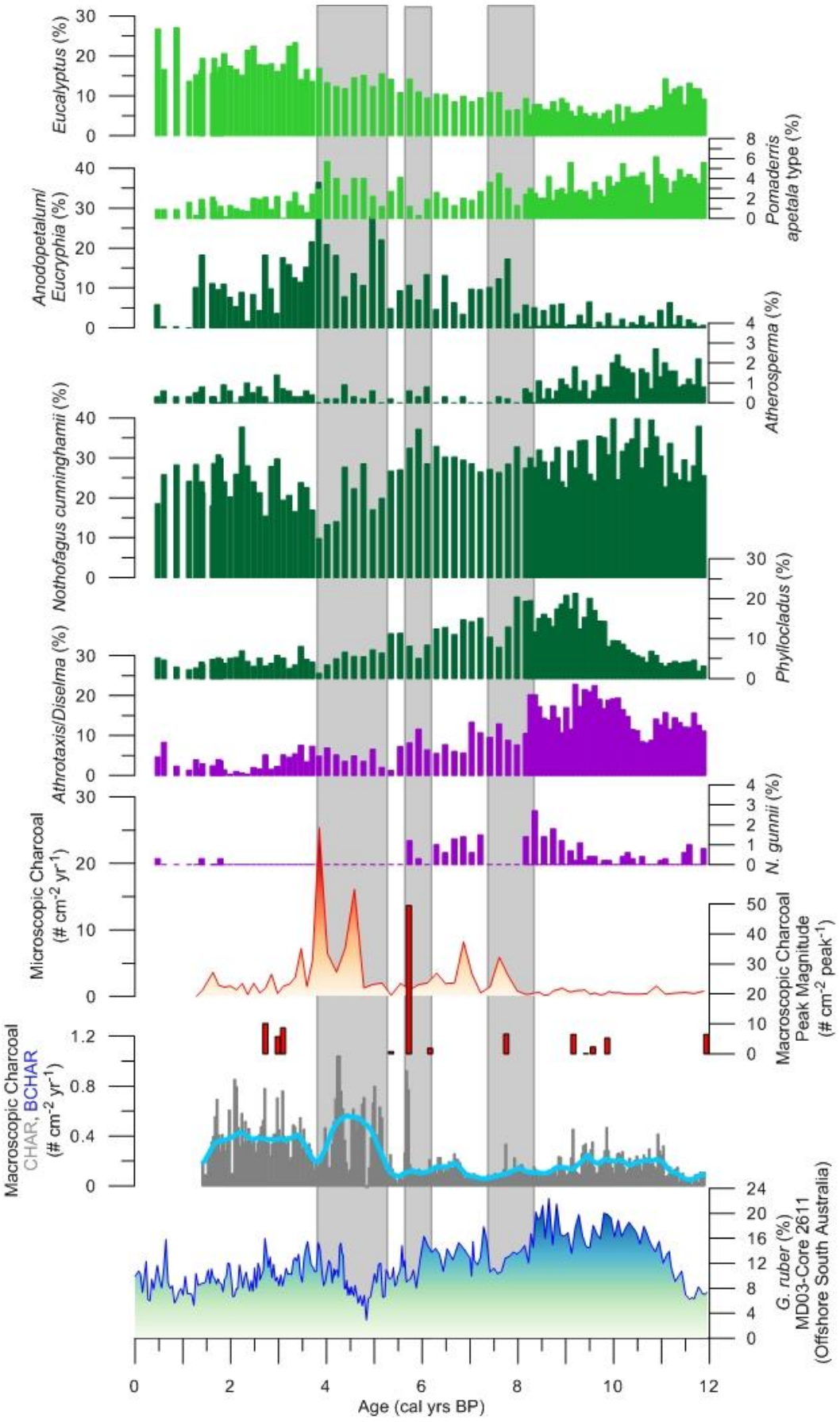

Figure 7-5 Summary diagram with Holocene detail of key pollen taxa, macroscopic and microscopic charcoal and G. ruber (%). The grey bands represent potential periods of drought/increased fire activity with vegetation responses

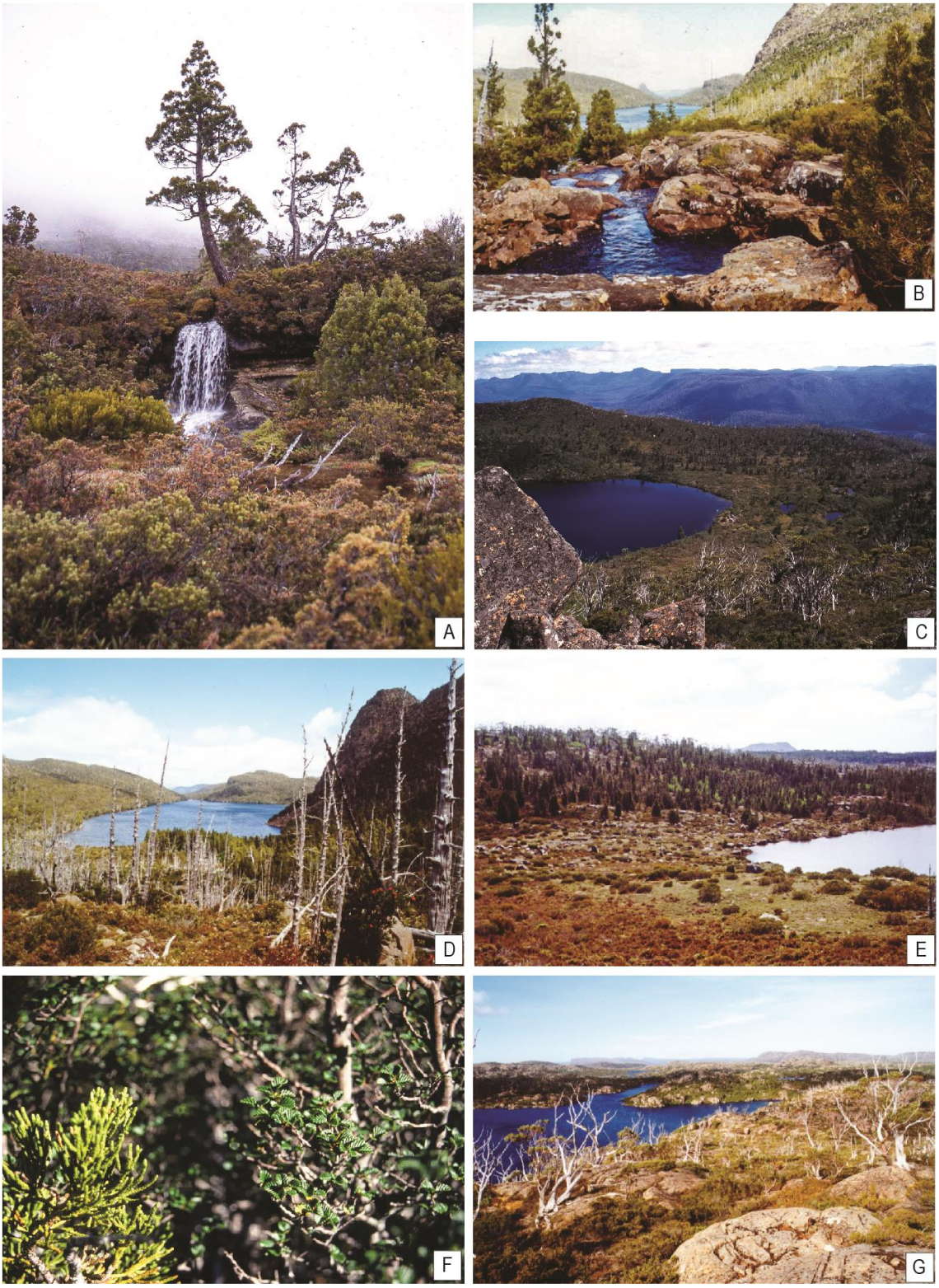

Plate 7-1 Examples of different *Athrotaxis cupressoides* vegetation communities growing in the Lake St Clair region A) *Athrotaxis cupressoides* growing near a tarn and creek at 1200 m altitude on Mt Olympus, B) *Athrotaxis cupressoides* growing along a rocky creek near Lake Riengeena on the Central Plateau (1090 m) C) *Athrotaxis cupressoides* rainforest growing near Lake Oenone (1207 m) on Mt Olympus D) Burnt *Athrotaxis* on hillslope leading down to Lake Riengeena (1065 m), Central Plateau with live forest near the lake edge E) *Athrotaxis cupressoides-Nothofagus gunnii* short rainforest growing near Lake Payana (1130 m) on the Central Plateau. The community can be identified by the bright green colour of *Nothofagus gunnii* (top left of lake) F) Detail of *Athrotaxis cupressoides* (left) and *Nothofagus gunnii* (right) growing together in *Athrotaxis cupressoides-Nothofagus gunnii* short rainforest near Lake Riengeena G) Scattered *Eucalyptus coccifera* woodland on rocky landscape near Lake Pallas (1185 m), Central Plateau with *Athrotaxis cupressoides* growing near lake edge at top of photo

Plate 7-2 A) Athrotaxis cupressoides-Nothofagus gunnii short rainforest growing near Lake Payana (1130 m) on the Central Plateau. The community can be identified by the bright green colour of *Nothofagus gunnii* (top left and top right of the lake). In the foreground alpine heathland and coniferous alpine heath are also found growing B) *Eucalyptus coccifera* woodland and *Athrotaxis cupressoides-Nothofagus gunnii* short rainforest growing at 1160 m altitude on the Labyrinth, just north of Lake St Clair

Chapter 8 Conclusions

This thesis presents a history of regional and local changes in vegetation in the Lake St Clair region, supported by modern vegetation and pollen analyses. The records span into oxygen isotope stage 3, with a focus on the last Glacial Holocene transition and fill a gap in the poorly studied region of Central Tasmania.

An analysis of modern pollen deposition in the large lake system of St Clair indicates a dominant signal of regional vegetation complemented by a suite of pollen types indicating local vegetation types. Supporting charcoal, particle size and carbon/nitrogen analysis, together with analysis of nearby sites with small pollen source areas has allowed the reconstruction of the broad climate driven changes in Tasmania during the last Glacial Holocene period together with detail of local changes within the Lake St Clair region filling a large gap in information of vegetation history of Central Tasmania.

The record of vegetation change from Lake St Clair shows a rapid response to rising temperatures after the LGM which is in sync with Antarctic warming and rising sea surface temperatures. Deglaciation of the lake was complete by 18.3 cal kyr BP when subalpine *Athrotaxis cupressoides* and *Diselma archeri* dominated rainforest and/or woodland rapidly expands replacing the initial mosaic of alpine grasslands, herbfields, heathland and sedgeland. *Phyllocladus aspleniifolius* and *Eucalyptus* also show an early response to warming and are inferred to have begun expansion in the distal lowlands by this time. A brief period of high fire activity together with increased moorland vegetation in the local Lake St Clair catchment precedes peak expansion of *Athrotaxis*/*Diselma* vegetation between c. 16.9-15.8 cal kyr BP when fire activity was reduced. Contemporaneous high presence of the subtropical foraminifera *G. ruber* offshore Southern Australia indicates a strengthened Leeuwin Current as a result of a southward shift of the subtropical front and weakened SWW producing conditions favourable for the expansion of A/D. Today the Leeuwin Current is strongest in winter, in La Nina years, which in Tasmania sees high moisture and low fire activity (Mariani et al., 2016; Perner et al., 2018) and if a similar relationship existed in the past suggests that precipitation was markedly increased in addition to warming temperatures.

A variable period where forest taxa begin to increase is interrupted by a minor re-expansion of grassland for c. 900 years, abruptly ended by strong increases in rainforest taxa. This period of inferred slight cooling/drying begins prior to and leads into the Antarctic Cold Reversal. The pattern of a cooler/drier first half of the ACR and wetter/warmer second half of the ACR is consistent with the general trend of terrestrial and marine records from the Southern Hemisphere mid latitudes (Pedro et al., 2016) possible dating discrepencies of the Lake St Clair

sediments can not be ruled out as cause for a mismatch of precise timing with the Antarctic temperature record. The similar timing of the expansion of grasslands with the sea surface temperature record offshore southern Australia which indicates a stalling of warming and phases of minor cooling from c. 16 cal kyr BP, suggesting the climate in Tasmania showed stronger connections with the ocean rather than Antarctic temperatures.

A peak in *Phyllocladus aspleniifolius* dominated rainforest follows, which declines abruptly at c. 12.4 cal kyr BP when it is succeeded by a floristically simple, closed rainforest dominated by *Nothofagus cunninghamii* and *Atherosperma moschatum* and growing under optimal conditions during the Early Holocene. A return of *Phyllocladus aspleniifolius* to a secondary peak together with *Athrotaxis*/*Diselma* between c. 10-8 cal kyr BP occurs during an inferred period of increased precipitation supported by peaks in deposition of terrestrial sourced organic matter and coarser sediments. The peaks in rainforest taxa at this time are mirrored at Skullbone Plains Bog and Excalibur Bog.

At c. 8 cal kyr BP, a pronounced increase in the rainforest taxon *Anodopetalum*/*Eucryphia* signals a further shift in the rainforest and marks the beginning of an overall decline in rainforest taxa and increase in sclerophyll and herbaceous taxa and fire activity, which intensifies during the late Holocene. Re-occuring spikes of *Anodopetalum*/Eucryphia, coarse sediments and total carbon suggest that frequent disturbance in the form of fires, storms and erosion events were a feature of the mid-late Holocene. Possible periods of extended drought are indicated around c. 8 cal kyr BP and between c. 5-4 cal kyr BP.

An initial period of high fire activity during the early deglacial, is followed by a long period of low fire activity for the remainder of the late Glacial and the bulk of the Holocene until c. 5 cal kyr BP when there is a marked increase through the Late Holocene. The increased fire activity observed between c. 11-9 cal kyr BP (Mariani and Fletcher, 2017; Mariani et al., 2017) only appears as a muted signal in the Lake St Clair record, although it should be noted that the regular occurrence of low magnitude fire events through the record indicates that fire was an important component of the environment throughout the record. Overall, the observed changes during the Holocene are consistent with the onset of ENSO and a more variable climate from c. 8 cal kyr BP and an intensification with cooling temperatures from c. 5 cal kyr BP.

Limitations of the study and future directions

Extending inferences from the vegetation record to changes in climate is limited by the broad climatic envelopes of many of the key taxa that occur frequently in Tasmanian pollen records and the biased representation of certain Tasmanian vegetation types by these taxa. In

addition, the widespread distribution and pollen dispersal of these key taxa makes it difficult to distinguish local from regional sources. Although it was possible to identify local indicator taxa in the large lake record from Lake St Clair, further work is warranted to explore local pollen transport mechanisms to the lake and variations in the local record as indicated by these pollen types. Additional small sites in the region would complement the large lake record from Lake St Clair.

The mid-late Holocene record from Lake St Clair shows a great degree of variability in vegetation change, fire activity and the nature of the sediments delivered to the lake. High resolution analysis of all proxies would allow closer examination of the relationships between and timing of events as indicated by these proxies. The differing sample resolutions for pollen, charcoal and particle size analysis limited the analysis of these relationships. Increasing the resolution of the pollen record to 2 cm intervals in the top, mid-late Holocene section of the core, which was not the focus of this study, would be worthwhile. Matching resolution of particle size analysis would permit more detailed investigation of the delivery of local pollen types to the lake by fluvial transport. Further insight into the environmental changes in the region could be gained by employing additional methods such as high resolution XRF analysis of elements using an ITRAX scanner, diatom and chironomid analysis. Unfortunately, no whole core material remains for Core CG, but numerous whole cores from other locations in the lake are available for further work.

Further dating across the ACR period, to explore the question of whether the timing of the renewed expansion of grassland occurred in sync with the trends in sea surface temperatures before the commencement of the ACR or whether dating discrepencies resulted in a mismatch in timing would be worthwhile. Further dating to explore the degree of a reservoir affect as indicated by the age of the mud-water interface sample from the short core is also warranted. The robustness of the chronology is limited overall by the use of bulk sediment samples.

The discontinuous nature of the longer, local records from the region limited investigation of the LGM time period in the region. Further exploration for sites in the region that may capture detail of the LGM time slice may give more insight into the cause of the apparent hiatuses in the Excalibur Bog and Clarence Lagoon records during this time period. Lake Dixon and Lake Undine would be interesting targets lying at ~ 700 m in Franklin River valleys around 6 km to the southwest of Lake St Clair, between Mt Rufus / Hugel Range and the Cheyne Range.

Chapter 9 References

ALLEN, J. 1996. Wareen cave. In: Allen, J. (Ed.), Report of the Southern Forests Archaeological Project, vol. 1: Site Descriptions, Stratigraphies and Chronologies. Archaeology Publications, School of Archaeology, La Trobe University, Bundoora, pp. 135-167.

ALLEN, J. AND PORCH, N. 1996. Warragarra rockshelter. In: Allen, J. (Ed.), Report of the Southern Forests Archaeological Project, vol. 1: Site Descriptions, Stratigraphies and Chronologies. Archaeology Publications, School of Archaeology, La Trobe University, Bundoora, pp. 135-167.

ALLEY, R.B., MAYEWSKI, P.A., SOWERS, T., STUIVER, M., TAYLOR, K.C., AND CLARK, P.U. 1997. Holocene climatic instability: A prominent, widespread event 8200 yr ago. *Geology* **25**, 483–486.

ALLOWAY, B.V., LOWE, D.J., BARRELL, D.J.A., NEWNHAM, R.M., ALMOND, P.C., AUGUSTINUS, P.C., BERTLER, N.A.N., CARTER, L., LITCHFIELD, N.J., MCGLONE, M.S., ET AL. 2007. Towards a climate event stratigraphy for New Zealand over the past 30 000 years (NZ-INTIMATE project). *Journal of Quaternary Science* **22**, 9–35.

AMPEL, L., BIGLER, C., WOHLFARTH, B., RISBERG, J., LOTTER, A.F., AND VERES, D. 2010. Modest summer temperature variability during DO cycles in western Europe. *Quaternary Science Reviews* **29**, 1322–1327.

ANDERSON, R.F., ALI, S., BRADTMILLER, L.I., NIELSEN, S.H.H., FLEISHER, M.Q., ANDERSON, B.E., AND BURCKLE, L.H. 2009. Wind-Driven Upwelling in the Southern Ocean and the Deglacial Rise in Atmospheric CO2. *Science* **323**, 1443–1448.

ANDERSON, S.T. 1970. The relative pollen productivity and pollen representation of North European trees: And correction factors for tree pollen spectra. Survey of Denmark. 2. series, no. 96 (C. A. Reitzel).

APSA MEMBERS 2007. The Australasian Pollen and Spore Atlas V1.0. (Canberra: Australian National University).

AUGUSTINUS, P., BLEAKLEY, N., DENG, Y., SHANE, P., AND COCHRAN, U. 2008. Rapid change in early Holocene environments inferred from Lake Pupuke, Auckland City, New Zealand. *Journal of Quaternary Science* **23**, 435–447.

AUGUSTINUS, P., FINK, D., FLETCHER, M.-S., AND THOMAS, I. 2017. Re-assessment of the mid to late Quaternary glacial and environmental history of the Boco Plain, western Tasmania. *Quaternary Science Reviews* **160**, 31–44.

BANKS, M.R. 1973. General Geology. In The Lake Country of Tasmania, (Hobart: Royal Society of Tasmania), pp. 25–34.

BANKS, M.R., COLHOUN, E.A., AND CHICK, N.K. 1977. A reconnaissance of the geomorphology of central western Tasmania. In Landscape and Man: The Interaction between Man and Environment in Western Tasmania, p.

BARBANTE, C., BARNOLA, J.-M., BECAGLI, S., BEER, J., BIGLER, M., BOUTRON, C., BLUNIER, T., CASTELLANO, E., CATTANI, O., CHAPPELLAZ, J., ET AL. 2006. One-to-one coupling of glacial climate variability in Greenland and Antarctica. *Nature* **444**, 195–198.

BARKER, P., AND KIRKPATRICK, J. 1994. Phyllocladus aspleniifolius: Variability in the Population Structure, the Regeneration Niche and Dispersion Patterns in Tasmanian Forests. *Australian Journal of Botany* **42**, 163–190.

BARKER, P.C.J. 1993. Phyllocladus aspleniifolius (Labill.) Hook. f. and Anodopetalum biglandulosum (A. Cunn.) ex Endl. : a comparative autecology of coexisting wet forest trees in Tasmania. phd. University of Tasmania.

BARKER, P.C.J. 1995. Phyllocladus aspleniifolius: Phenology, germination, and seedling survival. *New Zealand Journal of Botany* **33**, 325–337.

BARKER, P.C.J., AND BROWN, M.J. 1994. Anodopetalum biglandulosum: Growth form and abundance in Tasmanian rainforest. *Australian Journal of Ecology* **19**, 435–443.

BARKER, S., CHEN, J., GONG, X., JONKERS, L., KNORR, G., AND THORNALLEY, D. 2015. Icebergs not the trigger for North Atlantic cold events. *Nature* **520**, 333–336.

BARKER, S., DIZ, P., VAUTRAVERS, M.J., PIKE, J., KNORR, G., HALL, I.R., AND BROECKER, W.S. 2009. Interhemispheric Atlantic seesaw response during the last deglaciation. *Nature* **457**, 1097–1102.

BARNES, R.W., HILL, R.S., AND BRADFORD, J.C. 2001. The history of Cunoniaceae in Australia from macrofossil evidence. *Australian Journal of Botany* **49**, 301–320.

BARRELL, . J. A., ALMOND, P.C., VANDERGOES, M.J., LOWE, D.J., AND NEWNHAM, R.M. 2013. A composite pollen-based stratotype for inter-regional evaluation of climatic events in New Zealand over the past 30,000 years (NZ-INTIMATE project). *Quaternary Science Reviews* **74**, 4–20.

BARRELL, D.J.A., ALLOWAY, B.V., SHULMEISTER, J., AND NEWNHAM, R.M. 2005. Towards a climate event stratigraphy for New Zealand over the past 30,000 years. 1–12.

BARROWS, T.T., STONE, J.O., FIFIELD, L.K., AND CRESSWELL, R.G. 2002. The timing of the Last Glacial Maximum in Australia. *Quaternary Science Reviews* **21**, 159–173.

BEADLE, N.C.W., AND COSTIN, A.B. 1952. Ecological classification and nomenclature. *Proc. Linn. Soc. N.S.W.* **77**, 61–82.

BECK, K.K., FLETCHER, M.-S., GADD, P.S., HEIJNIS, H., AND JACOBSEN, G.E. 2017. An early onset of ENSO influence in the extra-tropics of the southwest Pacific inferred from a 14, 600 year high resolution multi-proxy record from Paddy's Lake, northwest Tasmania. *Quaternary Science Reviews* **157**, 164–175.

BENNETT, K.D. 1990. Milankovitch Cycles and Their Effects on Species in Ecological and Evolutionary Time. *Paleobiology* **16**, 11–21.

BERGLUND, B.E. 1973. Pollen dispersal and deposition in an area of southeastern Sweden - some preliminary results. In Quaternary Plant Ecology, (Oxford ? Blackwell Scientific Publications), pp. 117–129.

BINDER, R.M. 1978. Stratigraphy and pollen analysis of a peat deposit, Bunyip Bog, Mt Buffalo, Victoria. *Monash Publications in Geography* **19**, 51.

BIRKS, H.J.B. 1993. Quaternary palaeoecology and vegetation science— current contributions and possible future developments. *Review of Palaeobotany and Palynology* **79**, 153–177.

BLAAUW, M. 2010. Methods and code for 'classical' age-modelling of radiocarbon sequences. *Quaternary Geochronology* **5**, 512–518.

BLAAUW, M., AND CHRISTEN, J.A. 2011. Flexible paleoclimate age-depth models using an autoregressive gamma process. *Bayesian Analysis* **6**, 457–474.

BLUNIER, T., CHAPPELLAZ, J., SCHWANDER, J., DÄLLENBACH, A., STAUFFER, B., STOCKER, T.F., RAYNAUD, D., JOUZEL, J., CLAUSEN, H.B., HAMMER, C.U., ET AL. 1998. Asynchrony of Antarctic and Greenland climate change during the last glacial period. *Nature* **394**, 739–743.

BLUNIER, T., SCHWANDER, J., STAUFFER, B., STOCKER, T., DÄLLENBACH, A., INDERMÜHLE, A., TSCHUMI, J., CHAPPELLAZ, J., RAYNAUD, D., AND BARNOLA, J.-M. 1997. Timing of the Antarctic cold reversal and the atmospheric CO2 increase with respect to the Younger Dryas Event. *Geophysical Research Letters* **24**, 2683–2686.

BOND, G., HEINRICH, H., BROECKER, W., LABEYRIE, L., MCMANUS, J., ANDREWS, J., HUON, S., JANTSCHIK, R., CLASEN, S., SIMET, C., ET AL. 1992. Evidence for massive discharges of icebergs into the North Atlantic ocean during the last glacial period. *, Published Online: 19 November 1992; | Doi:10.1038/360245a0* **360**, 245–249.

BONNY, A. P. 1976. Recruitment of pollen to the seston and sediment of some Lake District lakes. *Journal of Ecology* **64**, 859-887.

BONNY, A. P. 1978. The effect of pollen recruitment processes on pollen distribution over the sediment surface of a small lake in Cumbria. *Journal of Ecology* **66**, 385-416.

BOSTOCK, H.C., BARROWS, T.T., CARTER, L., CHASE, Z., CORTESE, G., DUNBAR, G.B., ELLWOOD, M., HAYWARD, B., HOWARD, W., NEIL, H.L., ET AL. 2013. A review of the Australian–New Zealand sector of the Southern Ocean over the last 30 ka (Aus-INTIMATE project). *Quaternary Science Reviews* **74**, 35–57.

BOWMAN, D.M.J.S., WOOD, S.W., NEYLAND, D., SANDERS, G.J., AND PRIOR, L.D. 2013. Contracting Tasmanian montane grasslands within a forest matrix is consistent with cessation of Aboriginal fire management. *Austral Ecology* **38**, 627–638.

BRADSHAW, R.H.W., AND WEBB, T. 1985. Relationships between Contemporary Pollen and Vegetation Data from Wisconsin and Michigan, USA. *Ecology* **66**, 721–737.

BROECKER, W.S. 1998. Paleocean circulation during the Last Deglaciation: A bipolar seesaw? *Paleoceanography* **13**, 119–121.

BROECKER, W.S., DENTON, G.H., EDWARDS, R.L., CHENG, H., ALLEY, R.B., AND PUTNAM, A.E. 2010. Putting the Younger Dryas cold event into context. *Quaternary Science Reviews* **29**, 1078–1081.

BROWN, A.G. 1985. The potential use of pollen in the identification of suspended sediment sources. *Earth Surface Processes and Landforms* **10**, 27–32.

BROWN, M.J. 1999. Buttongrass Moorlands. In The Vegetation of Tasmania, (Hobart: Australian Biological Resources Study), pp. 286–303.

BROWN, M.J., BALMER, J., AND PODGER, F.D. 2002. Vegetation change over 20 years at Bathurst Harbour, Tasmania. *Australian Journal of Botany* **50**, 499–510.

BROWN, A. G., CARPENTER, R. G. AND WALLING, D. E. 2007. Monitoring fluvial pollen transport, its relationship to catchment vegetation and implications for palaeoenvironmental studies. *Review of Palaeobotany and Palynology* **147**, 60-76.

BROWN, M.J., AND PODGER, F.D. 1982. Floristics and fire regimes of a vegetation sequence from sedgeland-heath to rainforest at Bathurst Harbor, Tasmania. *Australian Journal of Botany* **30**, 659–676.

BRYAN, K., MANABE, S., AND PACANOWSKI, R.C. 1975. A Global Ocean-Atmosphere Climate Model. Part II. The Oceanic Circulation. *Journal of Physical Oceanography* **5**, 30–46.

BUIZERT, V.G. 2014. Greenland temperature response to climate forcing during the last deglaciation. *Science* **345**, 1177–1180.

BUIZERT, C., AND SCHMITTNER, A. 2015. Southern Ocean control of glacial AMOC stability and Dansgaard-Oeschger interstadial duration. *Paleoceanography* **30**, 2015PA002795.

BUREAU OF METEOROLOGY, 2018a *Australian Climate Influences*, Bureau of Meteorology, accessed 7 June 2018, < http://www.bom.gov.au/climate/about/>

BUREAU OF METEOROLOGY, 2018b *Climate statistics for Australian locations*, Bureau of Meteorology, accessed 7 June 2018, < http://www.bom.gov.au/climate/averages/tables/cw_031108.shtml>

CALCOTE, R. 1995. Pollen source area and pollen productivity: evidence from forest hollows. *Journal of Ecology* **83**, 591–602.

CALVO, E., PELEJERO, C., DE DECKKER, P., AND LOGAN, G.A. 2007. Antarctic deglacial pattern in a 30 kyr record of sea surface temperature offshore South Australia. *Geophysical Research Letters* **34**, L13707.

CARLSON, A.E., AND WINSOR, K. 2012. Northern Hemisphere ice-sheet responses to past climate warming. *Nature Geoscience* **5**, 607–613.

CARVALHO, L.M.V., JONES, C., AND AMBRIZZI, T. 2005. Opposite Phases of the Antarctic Oscillation and Relationships with Intraseasonal to Interannual Activity in the Tropics during the Austral Summer. *Journal of Climate* **18**, 702–718.

CEPPI, P., HWANG, Y.-T., LIU, X., FRIERSON, D.M.W., AND HARTMANN, D.L. 2013. The relationship between the ITCZ and the Southern Hemispheric eddy-driven jet. *Journal of Geophysical Research: Atmospheres* **118**, 5136–5146.

CLARK, P.U., DYKE, A.S., SHAKUN, J.D., CARLSON, A.E., CLARK, J., WOHLFARTH, B., MITROVICA, J.X., HOSTETLER, S.W., AND MCCABE, A.M. 2009. The Last Glacial Maximum. *Science* **325**, 710–714.

CLAYTON-GREENE, K.A. 1977. Structure and origin of Libocedrus bidwillii stands in the Waikato district. *New Zealand Journal of Botany* **15**, 19–28.

CLEMENT, A.C., AND PETERSON, L.C. 2008. Mechanisms of abrupt climate change of the last glacial period. *Reviews of Geophysics* **46**, RG4002.

COCKAYNE, L. 1921. The vegetation of New Zealand (Leipzig, W. Engelmann; New York, G. E. Stechert & co.).

COHEN, T.J., AND NANSON, G. 2007. Mind the gap: an absence of valley-fill deposits identifying the Holocene hypsithermal period of enhanced flow regime in south-eastern Austrlia. *The Holocene* **17**, 411–419.

COLHOUN, E.A. 1977. The Remarkable Cave, southeastern Tasmania: its geomorphological development and environmental history. *Papers and Proceedings of the Royal Society of Tasmania* **111**, 29–39.

COLHOUN, E.A. 1980. Quaternary Fluviatile Deposits from the Pieman Dam Site, Western Tasmania. *Proceedings of the Royal Society of London. Series B. Biological Sciences* **207**, 355–384.

COLHOUN, E.A. 1985. Glaciations of the West Coast Range, Tasmania. *Quaternary Research* **24**, 39–59.

COLHOUN, E.A. 1992. Late glacial and Holocene vegetation history at Poets hill lake, western Tasmania. *Australian Geographer* **23**, 11.

COLHOUN, E.A. 1996a. Application of Iversen's glacial-interglacial cycle to interpretation of the late last glacial and holocene vegetation history of western Tasmania. *Quaternary Science Reviews* **15**, 557–580.

COLHOUN, E.A. 1996b. Late Wisconsin glaciation of Tasmania. *Papers and Proceedings of the Royal Society of Tasmania* **130**, 33–45.

COLHOUN, E.A. 1998. Pollen analysis of 0-20 m at Darwin Crater, Western Tasmania, Australia. *International Project on Palaeolimnology and Late Cenozoic Climate Newsletter No. 11, Horie S (Eds).*

COLHOUN, E.A. 2000. Vegetation and climate change during the Last Interglacial-Glacial cycle in western, Tasmania, Australia. *Palaeogeography, Palaeoclimatology, Palaeoecology* **155**, 195-209.

COLHOUN, E.A., VAN DE GEER, G., AND FITZSIMONS, S.J. 1991. Late glacial and Holocene vegetation history at Governor Bog, King Valley, western Tasmania, Australia. *Journal of Quaternary Science* **6**, 55–66.

COLHOUN, E.A., GEER, G. VAN DE, AND FITZSIMONS, S.J. 1992. Late Quaternary Organic Deposits at Smelter Creek and Vegetation History of the Middle King Valley, Western Tasmania. *Journal of Biogeography* **19**, 217–227.

COLHOUN, E.A., AND GEER, G.V.D. 1986. Holocene to Middle Last Glaciation Vegetation History at Tullabardine Dam, Western Tasmania. *Proceedings of the Royal Society of London. Series B. Biological Sciences* **229**, 177–207.

COLHOUN, E.A., AND GOEDE, A. 1979. The Late Quaternary Deposits of Blakes Opening and the Middle Huon Valley, Tasmania. *Philosophical Transactions of the Royal Society of London. Series B, Biological Sciences* **286**, 371–395.

COLHOUN, E.A., HARRIS, P.T., HEAP, A., BOTTRILL, R.S., BACON, C.A., AND DUNCAN, D.M. 2014. The Quaternary in Tasmania. In Geological Evolution of Tasmania, (Geological Society of Australia (Tasmania Division)), p. 639.

COLHOUN, E.A., KIERNAN, K., BARROWS, T.T., AND GOEDE, A. 2010. Advances in Quaternary studies in Tasmania. *Geological Society, London, Special Publications* **346**, 165–183.

COLHOUN, E.A., POLA, J.S., BARTON, C.E., AND HEIJNIS, H. 1999. Late Pleistocene vegetation and climate history of Lake Selina, western Tasmania. *Quaternary International* **57–58**, 5–23.

COLHOUN, E.A., AND SHIMELD, P.W. 2012. Late-Quaternary vegetation history of Tasmania from pollen records. In Peopled Landscapes : Archaeological and Biogeographic Approaches to Landscapes / Edited b y Simon G. Haberle & Bruno David., (ANU E Press), pp. 297–328.

COLLINS, L.G., PIKE, J., ALLEN, C.S., AND HODGSON, D.A. 2012. High-resolution reconstruction of southwest Atlantic sea-ice and its role in the carbon cycle during marine isotope stages 3 and 2. *Paleoceanography* **27**, PA3217.

COOK, J., NUCCITELLI, D., GREEN, S.A., RICHARDSON, M., WINKLER, B., PAINTING, R., WAY, R., PETER JACOBS, AND SKUCE, A. 2013. Quantifying the consensus on anthropogenic global warming in the scientific literature. *Environmental Research Letters* **8**, 024024.

COSGROVE, R. 1995. Late Pleistocene behavioural variation and time trends: the case from Tasmania. *Archaeology in Oceania* **408**, 184–187.

COSGROVE, R. 1999. Forty-two degrees south: the archaeology of Late Pleistocene Tasmania. *Journal of World Prehistory* **13**, 357–402.

COSGROVE, R., ALLEN, J. AND MARSHALL, B. 1990. Palaeoecology and Pleistocene human occupation in south central Tasmania. *Antiquity* **64**, 59–78.

COSGROVE, R., ALLEN, J. AND MARSHALL, B. 1994. Late Pleistocene human occupation in Tasmania: a reply to Thomas. *Australian Archaeology* **38**, 28-35.

COX, P.M., BETTS, R.A., JONES, C.D., SPALL, S.A., AND TOTTERDELL, I.J. 2000. Acceleration of global warming due to carbon-cycle feedbacks in a coupled climate model. *Nature* **408**, 184–187.

CRAMER, W., BONDEAU, A., WOODWARD, F.I., PRENTICE, I.C., BETTS, R.A., BROVKIN, V., COX, P.M., FISHER, V., FOLEY, J.A., FRIEND, A.D., ET AL. 2001. Global response of terrestrial ecosystem structure and function to CO2 and climate change: results from six dynamic global vegetation models. *Global Change Biology* **7**, 357–373.

CROWDEN, R.K. 1999. Alpine Vegetation. In The Vegetation of Tasmania, (Hobart: Australian Biological Resources Study), pp. 333–356.

CROWDER, A. A. AND CUDDY, D. G. 1973. Pollen in a small river basin: Wilton Creek, Ontario. In H.J.B. Birks, R.G. West (Eds.), Quaternary Plant Ecology, Blackwell, Oxford (1973), pp. 61-77.

CROWLEY, T.J. 1992. North Atlantic Deep Water cools the southern hemisphere. *Paleoceanography* **7**, 489–497.

CURTIS, W.M. 1975. The student's flora of Tasmania (Hobart, Tasmania: L. G. Shea, Govt. Printer).

DANSGAARD, W., JOHNSEN, S. J., CLAUSEN, H. B., DAHL-JENSEN, D., GUNDESTRUP, N., HAMMER, C. U., AND OESCHGER, H. 1984. North Atlantic Climatic Oscillations Revealed by Deep Greenland Ice Cores. In Climate Processes and Climate Sensitivity, J.E. Hansen, and T. Takahashi, eds. (American Geophysical Union), pp. 288–298.

DANSGAARD, W., JOHNSEN, S.J., CLAUSEN, H.B., DAHL-JENSEN, D., GUNDESTRUP, N.S., HAMMER, C.U., HVIDBERG, C.S., STEFFENSEN, J.P., SVEINBJÖRNSDOTTIR, A.E., JOUZEL, J., ET AL. 1993. Evidence for general instability of past climate from a 250-kyr ice-core record. *Nature* **364**, 218–220.

DAVID, C., AND ROBERTS, N. 1990. Vegetation change and pollen recruitment in a lowland lake catchment: Groby Pool, Leics (England). *SpringerLink* 305–310.

DAVIES, J.L. 1959. High level erosion surfaces and landscape development in Tasmania. *Australian Geographer* **7**, 193–203.

DAVIES, J.L. 1965. Landforms. In Atlas of Tasmania (Ed. J.L. Davies)., (Hobart, Tasmania: The Lands and Surveys Department), pp. 19–25.

DAVIS, M.B. 1963. On the theory of pollen analysis. *American Journal of Science* **261**, 897–912.

DAVIS, M.B. 1967. Pollen accumulation rates at Rogers Lake, Connecticut, during late- and postglacial time. *Review of Palaeobotany and Palynology* **2**, 219–230.

DAVIS, M.B. 2000. Palynology after Y2K—Understanding the Source Area of Pollen in Sediments. *Annual Review of Earth and Planetary Sciences* **28**, 1–18.

DE DECKKER, P., MOROS, M., PERNER, K., AND JANSEN, E. 2012. Influence of the tropics and southern westerlies on glacial interhemispheric asymmetry. *Nature Geoscience* **5**, 266–269.

DEAN, W.E. 1974. Determination of carbonate and organic matter in calcareous sediments and sedimentary rocks by loss on ignition: comparison with other methods . *Journal of Sedimentary Petrology* **44**, 242–248.

DEBUSK JR., G.H. 1997. The distribution of pollen in the surface sediments of Lake Malawˆi, Africa, and the transport of pollen in large lakes. *Review of Palaeobotany and Palynology* **97**, 123–153.

DENG, Y., HORROCKS, M., OGDEN, J., AND ANDERSON, S. 2006. Modern pollen–vegetation relationships along transects on the Whangapoua Estuary, Great Barrier Island, northern New Zealand. *Journal of Biogeography* **33**, 592–608.

DENTON, G.H., ANDERSON, R.F., TOGGWEILER, J.R., EDWARDS, R.L., SCHAEFER, J.M., AND PUTNAM, A.E. 2010. The Last Glacial Termination. *Science* **328**, 1652–1656.

DENTON, G.H., BROECKER, W.S., AND ALLEY, R.B. 2006. The mystery interval 17.5 to 14.5 kyrs ago. *PAGES News* **14**, 14–16.

DEPARTMENT OF PRIMARY INDUSTRIES, PARKS, WATER AND ENVIRONMENT 2013. TASVEG 3.0 (Resource Management and Conservation Division).

DEPARTMENT OF PRIMARY INDUSTRIES, PARKS, WATER AND ENVIRONMENT 2017. Aboriginal Heritage of the Tasmanian Wilderness World Heritage Area (TWWHA): A literature review and synthesis report, March 2017.

DERBYSHIRE, E. 1963. Glaciation of the Lake St. Clair District, west-central Tasmania. *The Australian Geographer* **9**, 97–109?

DERBYSHIRE, E. 1971. The bathymetry of Lake St. Clair, western central Tasmania. *Papers and Proceedings of the Royal Society of Tasmania* **105**, 49–57.

DERBYSHIRE, E. 1972. PLEISTOCENE GLACIATION OF TASMANIA: REVIEW AND SPECULATIONS. *Australian Geographical Studies* **10**, 79–94.

DERRICK, E. 1962. Relative importance of various plants in causation of hay fever and asthma in Australia. *The Medical Journal of Australia* **49(1)**, 972–977.

DERRICK, E. 1966. Airborne pollen and spores in Melbourne. *Aust. J. Bot.* **14**, 49–66.

DODSON, J., AND MYERS, C. 1986. Vegetation and Modern Pollen Rain From the Barrington Tops and Upper Hunter River Regions of New South Wales. *Aust. J. Bot.* **34**, 293–304.

DODSON, J.R. 1977. Late Quaternary palaeoecology of Wyrie Swamp, southeastern South Australia. *Quaternary Research* **8**, 97–114.

DODSON, J.R. 1983. Modern pollen rain in southeastern new South Wales, Australia. *Review of Palaeobotany and Palynology* **38**, 249–268.

DOUGHTY, A.M., ANDERSON, B.M., MACKINTOSH, A.N., KAPLAN, M.R., VANDERGOES, M.J., BARRELL, D.J.A., DENTON, G.H., SCHAEFER, J.M., CHINN, T.J.H., AND PUTNAM, A.E. 2013. Evaluation of Lateglacial temperatures in the Southern Alps of New Zealand based on glacier modelling at Irishman Stream, Ben Ohau Range. *Quaternary Science Reviews* **74**, 160–169.

DUNCAN, F. J. 1999. Dry Sclerophyll Forests and Woodlands. In The Vegetation of Tasmania, (Hobart: Australian Biological Resources Study), pp. 160–197.

FAEGRI, K., AND IVERSEN, J. 2000. Textbook of pollen analysis (Caldwell, N.J.: Blackburn Press).

FELDE, V.A., PEGLAR, S.M., BJUNE, A.E., GRYTNES, J.-A., AND BIRKS, H.J.B. 2014. The relationship between vegetation composition, vegetation zones and modern pollen assemblages in Setesdal, southern Norway. *The Holocene* 0959683614534745.

FITZSIMMONS, K.E., COHEN, T.J., HESSE, P.P., JANSEN, J., NANSON, G.C., MAY, J.-H., BARROWS, T.T., HABERLAH, D., HILGERS, A., KELLY, T., ET AL. 2013. Late Quaternary palaeoenvironmental change in the Australian drylands. *Quaternary Science Reviews* **74**, 78–96.

FLETCHER, M.-S., BENSON, A., HEIJNIS, H., GADD, P.S., CWYNAR, L.C., AND REES, A.B.H. 2015. Changes in biomass burning mark the onset of an ENSO-influenced climate regime at 42°S in southwest Tasmania, Australia. *Quaternary Science Reviews* **122**, 222–232.

FLETCHER, M.-S., BOWMAN, D.M.J.S., WHITLOCK, C., MARIANI, M., AND STAHLE, L. 2018. The changing role of fire in conifer-dominated temperate rainforest through the last 14,000 years. *Quaternary Science Reviews* **182**, 37–47.

FLETCHER, M.-S., AND MORENO, P.I. 2012. Have the Southern Westerlies changed in a zonally symmetric manner over the last 14,000 years? A hemisphere-wide take on a controversial problem. *Quaternary International* **253**, 32–46.

FLETCHER, M.-S., AND THOMAS, I. 2007a. Holocene vegetation and climate change from near Lake Pedder, south-west Tasmania, Australia. *Journal of Biogeography* **34**, 665–677.

FLETCHER, M.-S., AND THOMAS, I. 2007b. Modern pollen-vegetation relationships in western Tasmania, Australia. *Review of Palaeobotany and Palynology* **146**, 146–168.

FLETCHER, M.-S., AND THOMAS, I. 2010a. A quantitative Late Quaternary temperature reconstruction from western Tasmania, Australia. *Quaternary Science Reviews* **29**, 2351–2361.

FLETCHER, M.-S., AND THOMAS, I. 2010b. The origin and temporal development of an ancient cultural landscape. *Journal of Biogeography* no-no.

FLETCHER, M.-S., WOLFE, B.B., WHITLOCK, C., POMPEANI, D.P., HEIJNIS, H., HABERLE, S.G., GADD, P.S., AND BOWMAN, D.M.J.S. 2013a. The legacy of mid-Holocene fire on a Tasmanian montane landscape. *Journal of Biogeography* 476–488.

FLETCHER, M.-S., WOOD, S.W., AND HABERLE, S.G. 2013b. A fire driven shift from forest to non-forest: evidence for alternative stable states? *Ecology*.

FRIEDLINGSTEIN, P., BOPP, L., CIAIS, P., DUFRESNE, J.-L., FAIRHEAD, L., LETREUT, H., MONFRAY, P., AND ORR, J. 2001. Positive feedback between future climate change and the carbon cycle. *Geophysical Research Letters* **28**, 1543–1546.

FRIEDLINGSTEIN, P., COX, P., BETTS, R., BOPP, L., VON BLOH, W., BROVKIN, V., CADULE, P., DONEY, S., EBY, M., FUNG, I., ET AL. 2006. Climate–Carbon Cycle Feedback Analysis: Results from the C4MIP Model Intercomparison. *Journal of Climate* **19**, 3337–3353.

GAMMAGE, B. 2011. The Biggest Estate on Earth: How Aborigines Made Australia (Sydney, Melbourne, Auckland and London: Allen and Unwin).

GARCÍA, J.L., KAPLAN, M.R., HALL, B.L., SCHAEFER, J.M., VEGA, R.M., SCHWARTZ, R., AND FINKEL, R. 2012. Glacier expansion in southern Patagonia throughout the Antarctic cold reversal. *Geology* **40**, 859–862.

GARRETT, M., AND COUNCIL, T.F.R. 1996. The ferns of Tasmania : their ecology and distribution (Hobart, Tas. : Tasmanian Forest Research Council).

VAN DE GEER, G., FITZSIMONS, S.J., AND COLHOUN, E.A. 1989. Holocene to Middle Last Glaciation Vegetation History at Newall Creek, Western Tasmania. *New Phytologist* **111**, 549–558.

VAN DE GEER, G., HEUSSER, L.E., LYNCH-STIEGLITZ, J., AND CHARLES, C.D. 1994. Paleoenvironments of Tasmania Inferred from a 5-75 ka Marine Pollen Record. *Palynology* **18**, 33–40.

GARRETT, M. AND KANTVILLAS, G. 1992. Morphology, ecology and distribution of Isoetes L. in Tasmania. *Papers and Proceedings of the Royal Society of Tasmania* **126**, 115-122.

GIESECKE, T., AND FONTANA, S.L. 2008. Revisiting pollen accumulation rates from Swedish lake sediments. *The Holocene* **18**, 293–305.

GILBERT, J.M. 1959. Forest succession in the Florentine Valley, Tasmania. *Papers and Proceedings of the Royal Society of Tasmania* **93**, 129–151.

GLASSER, N.F., JANSSON, K.N., GOODFELLOW, B.W., DE ANGELIS, H., RODNIGHT, H., AND ROOD, D.H. 2011. Cosmogenic nuclide exposure ages for moraines in the Lago San Martin Valley, Argentina. *Quaternary Research* **75**, 636–646.

GLEW, J.R., SMOL, J.P., AND LAST, W.M. 2001. Sediment core collection and extrusion. In Last, W.M. and Smol, J.P. [Editors] Tracking Environmental Change Using Lake Sediments. Vol 1: Basin Analysis, Coring, and Chronological Techniques., (Dordrecht: Kluwer Academic Publishers), pp. 73–105.

GONG, D., AND WANG, S. 1999. Definition of Antarctic Oscillation index. *Geophysical Research Letters* **26**, 459–462.

GONZÁLEZ, C., DUPONT, L.M., BEHLING, H., AND WEFER, G. 2008. Neotropical vegetation response to rapid climate changes during the last glacial period: Palynological evidence from the Cariaco Basin. *Quaternary Research* **69**, 217–230.

GRIMM, E.C. 1987. CONISS: A Fortran 77 program for stratigraphically constrained cluster analysis by the method of incremental sum od squares. *Computers and Geosciences* **13**, 13–35.

GRIMM, E.C. 2013. Tilia (Springfield: Illinois State Museum).

GRIMM, E.C., MAHER JR., L.J., AND NELSON, D.M. 2009. The magnitude of error in conventional bulk-sediment radiocarbon dates from central North America. *Quaternary Research* **72**, 301–308.

GROOTES, P.M., STUIVER, M., WHITE, J.W.C., JOHNSEN, S., AND JOUZEL, J. 1993. Comparison of oxygen isotope records from the GISP2 and GRIP Greenland ice cores. *Nature* **366**, 552–554.

GUTJAHR, M., AND LIPPOLD, J. 2011. Early arrival of Southern Source Water in the deep North Atlantic prior to Heinrich event 2. *Paleoceanography* **26**, PA2101.

HARRISON, S.P., AND DODSON, J.P. 1993 Climates of Australia and New Guinea since 18,000 yr B.P. In Global Climates since the Last Glacial Maximum, pp. 265–293.

HE, F., SHAKUN, J.D., CLARK, P.U., CARLSON, A.E., LIU, Z., OTTO-BLIESNER, B.L., AND KUTZBACH, J.E. 2013. Northern Hemisphere forcing of Southern Hemisphere climate during the last deglaciation. *Nature* **494**, 81–85.

HEINRICH, H. 1988. Origin and consequences of cyclic ice rafting in the Northeast Atlantic Ocean during the past 130,000 years. *Quaternary Research* **29**, 142–152.

HELLMAN, S., GAILLARD, M.-J., BROSTRÖM, A., AND SUGITA, S. 2008. The REVEALS model, a new tool to estimate past regional plant abundance from pollen data in large lakes: validation in southern Sweden. *Journal of Quaternary Science* **23**, 21–42.

HEMMING, S.R. 2004. Heinrich events: Massive late Pleistocene detritus layers of the North Atlantic and their global climate imprint. *Reviews of Geophysics* **42**, RG1005.

HENDON, H.H., THOMPSON, D.W.J., AND WHEELER, M.C. 2007. Australian Rainfall and Surface Temperature Variations Associated with the Southern Hemisphere Annular Mode. *Journal of Climate* **20**, 2452–2467.

HIGUERA, P.E., BRUBAKER, L.B., ANDERSON, P.M., HU, F.S., AND BROWN, T.A. 2009. Vegetation mediated the impacts of postglacial climate change on fire regimes in the south-central Brooks Range, Alaska. *Ecological Monographs* **79**, 201–219.

HIGUERA, P.E., GAVIN, D.G., BARTLEIN, P.J., AND HALLETT, D.J. 2010. Peak detection in sediment–charcoal records: impacts of alternative data analysis methods on fire-history interpretations. *International Journal of Wildland Fire* **19**, 996–1014.

HILL, K.J., SANTOSO, A., AND ENGLAND, M.H. 2009. Interannual Tasmanian Rainfall Variability Associated with Large-Scale Climate Modes. *Journal of Climate* **22**, 4383–4397.

HILL, M.O., AND GAUCH, H.G. 1980. Detrended correspondence analysis: An improved ordination technique. *Vegetatio* **42**, 47–58.

HILL, R.., AND ORCHARD, A.E. 1999. Composition and Endemism of Vascular Plants. In Vegetation of Tasmania (Eds. Reid, J. B., Hill, R.B., Brown, M. B. and Hovenden, M. J.), (Hobart, Tasmania: Australian Biological Resources Study), pp. 89–124.

HJELLE, K.L., AND SUGITA, S. 2012. Estimating pollen productivity and relevant source area of pollen using lake sediments in Norway: How does lake size variation affect the estimates? *The Holocene* **22**, 313–324.

HOGG, A.G., HUA, Q., BLACKWELL, P.G., NIU, M., BUCK, C.E., GUILDERSON, T.P., HEATON, T.J., PALMER, J.G., REIMER, P.J., REIMER, R.W., ET AL. 2013. SHCal13 Southern Hemisphere Calibration, 0–50,000 Years cal BP. *Radiocarbon* **55**, 1889–1903.

HOLLOWAY, J.T. 1954. Forests and climates in the South Island of New Zealand. *Transactions and Proceedings of the Royal Society of New Zealand* **82**, 329–410.

HOLLOWAY, J.T. 1964. The forests of the South Island: the status of the climate change hypothesis. *New Zealand Geographer* **20**, 1–9.

HOLZ, A., WOOD, S. W., VEBLEN, T.T. AND BOWMAN, D. M. J. S. 2015. Effects of high-severity fire drove the population collapse of the subalpine Tasmanian endemic conifer *Athrotaxis cupressoides*. *Global Change Biology* **21**, 445-458.

HOLZ, A., AND VEBLEN, T.T. 2011. Variability in the Southern Annular Mode determines wildfire activity in Patagonia. *Geophysical Research Letters* **38**, L14710.

HOPE, G., BURROWS, M., GADD, P., HOPF, F.V.L., KEBLE-WILLIAMS, J., AND WHINAM, J. 2017. The history of the Skullbone Plains Peatland, Central Plateau, Tasmania. Unpublished report to the Tasmanian Land Conservancy, Hobart.

HOPE, G., AND NANSON, R. 2015. Peatland carbon stores and fluxes in the Snowy Mountains, New South Wales, Australia. *Mires and Peat* **15**, 1–23.

HOPE, G.S. 1974. The vegetation history from 6000 B.P. to Present of Wilsons Promontory, Victoria, Australia. *New Phytologist* **73**, 1035–1053.

HOPF, F. 1997. A Late Glacial and Holocene Vegetation History of Lake St. Clair, Tasmania. B. Sc. Honours. Univeristy of Newcastle.

HOPF, F.V.L., COLHOUN, E.A., AND BARTON, C.E. 2000. Late-glacial and Holocene record of vegetation and climate from Cynthia Bay, Lake St Clair, Tasmania. *Journal of Quaternary Science* **15**, 725–732.

HUNTLEY, B. 1990. Dissimilarity Mapping Between Fossil and Contemporary Pollen Spectra in Europe for the Past 13,000 Years. *Quaternary Research* **33**, 360–376.

IVERSEN, J. 1958. The bearing of glacial and interglacial epochs on the formation and extinction of plant taxa. *Uppsala Universiteit Arsskrift* **6**, 210–215.

JACKSON, S.T. 1990. Pollen source area and representation in small lakes of the northeastern United States. *Review of Palaeobotany and Palynology* **63**, 53–76.

JACKSON, S.T., WEBB III, T., PRENTICE, C., AND HANSEN, J.E. 1995. Exploration and calibration of pollen/vegetation relationships: a PC program for the extended R-value models. *Review of Palaeobotany and Palynology* **84**, 365–374.

JACKSON, S.T., AND WILLIAMS, J.W. 2004. MODERN ANALOGS IN QUATERNARY PALEOECOLOGY: Here Today, Gone Yesterday, Gone Tomorrow? *Annual Review of Earth and Planetary Sciences* **32**, 495–537.

JACKSON, S.T., AND WONG, A. 1994. Using forest patchiness to determine pollen source areas of closed-canopy pollen assemblages. *Journal of Ecology* **82**, 89–99.

JACKSON, W.D. 1968. Fire, air, water and earth - and elemental ecology of Tasmania. *Proceedings of the Ecological Society of Australia* **3**, 4–16.

JACKSON, W.D. 1983. Tasmanian Rainforest Ecology. In Tasmania's Rainforests: What Future (Eds R. Blakers and P. Robertson), (Hobart: Australian Conservation Foundation), pp. 9–39.

JACKSON, W.D. 1999a. Chapter 1: Vegetation Types. In: Reid, J. B. (ed.) Vegetation of Tasmania, (Australian Biological Resources Study), pp. 11–38.

JACKSON, W.D. 1999b. Chapter 2: The Tasmanian Environment. In: Reid, J. B. (ed.) Vegetation of Tasmania, (Australian Biological Resources Study), pp. 11–38.

JACKSON, W.D. 1999c. Palaeohistory of vegetation change: the last 2 million years. In: Reid, J. B. (ed.) Vegetation of Tasmania, (Australian Biological Resources Study), pp. 64-88.

JACKSON, W.D. AND BROWN, M. J. 1999. Chapter 16: Pattern and Process in the Vegetation. In Vegetation of Tasmania, (Australian Biological Resources Study), pp. 11–38.

JACOBSON, G.L., AND BRADSHAW, R.H.W. 1981. The selection of sites for paleovegetational studies. *Quaternary Research* **16**, 80–96.

JANSSEN, C.R. 1966. Recent Pollen Spectra from the Deciduous and Coniferous-Deciduous Forests of Northeastern Minnesota: A Study in Pollen Dispersal. *Ecology* **47**, 804–825.

JANSSEN, C.R. 1973. Local and regional pollen deposition. In Quaternary Plant Ecology, (Oxford, London, Edinburgh, Melbourne ??? Blackwell Scientific Publications), pp. 31–42.

JARMAN, S.J., AND BROWN, M.J. 1983. A definition of cool temperate rainforest in Tasmania. *Search* **14**, 81–87.

JARMAN, S.J., AND KANTVILLAS, G. 1994. Lichens and bryophytes of the Tasmanian World Heritage Area II. Three forest sites at Pelion Plains. *Tasforests* **6**, 103–120.

JARMAN, S.J., KANTVILLAS, G., AND BROWN, M.J. 1988. Buttongrass Moorlands in Tasmania. (Hobart).

JARMAN, S.J., KANTVILLAS, G., AND BROWN, M.J. 1999. Floristic Composition of Cool Temperate Rainforest. In The Vegetation of Tasmania, (Hobart: Australian Biological Resources Study), pp. 145–159.

JENNINGS, J. N. AND AHMAD, N. 1957. Legacy of an ice cap. *Australian Geographer* **7**, 62-75.

JOHNSEN, S.J., CLAUSEN, H.B., DANSGAARD, W., FUHRER, K., GUNDESTRUP, N., HAMMER, C.U., IVERSEN, P., JOUZEL, J., STAUFFER, B., AND STEFFENSEN, J.P. 1992. Irregular glacial interstadials recorded in a new Greenland ice core. *Nature* **359**, 311–313.

JOMELLI, V., FAVIER, V., VUILLE, M., BRAUCHER, R., MARTIN, L., BLARD, P.-H., COLOSE, C., BRUNSTEIN, D., HE, F., KHODRI, M., ET AL. 2014. A major advance of tropical Andean glaciers during the Antarctic cold reversal. *Nature* **513**, 224–228.

JONES, P.J., THOMAS, I., AND FLETCHER, M.-S. 2017. Long-term environmental change in eastern Tasmania: Vegetation, climate and fire at Stoney Lagoon. *The Holocene* **27**, 1340–1349.

JONES, R. 1995. Tasmanian archaeology: establishing the sequences. *Annual Review of Anthropology* **24**, 423–446.

JONES, R. AND ALLEN, J. 1984. Archaeological investigations in the Andrew River valley, Acheron River valley and at Precipitous Bluff - southwest Tasmania- February 1984. *Australian Archaeology* **19**, 86–101.

JORDAN, G.J., AND TNG, D.Y.P. 2017. Key To Tasmanian Vascular Plants.

KAPLAN, M.R., SCHAEFER, J.M., DENTON, G.H., BARRELL, D.J.A., CHINN, T.J.H., PUTNAM, A.E., ANDERSEN, B.G., FINKEL, R.C., SCHWARTZ, R., AND DOUGHTY, A.M. 2010. Glacier retreat in New Zealand during the Younger Dryas stadial. *Nature* **467**, 194–197.

KAPLAN, M.R., SCHAEFER, J.M., DENTON, G.H., DOUGHTY, A.M., BARRELL, D.J.A., CHINN, T.J.H., PUTNAM, A.E., ANDERSEN, B.G., MACKINTOSH, A., FINKEL, R.C., ET AL. 2013. The anatomy of long-term warming since 15 ka in New Zealand based on net glacier snowline rise. *Geology* G34288.1.

KELLY, R.F., HIGUERA, P.E., BARRETT, C.M., AND HU, F.S. 2011. A signal-to-noise index to quantify the potential for peak detection in sediment–charcoal records. *Quaternary Research* **75**, 11–17.

KIERNAN, K. 1985. Late Cenozoic glaciation and mountain geomorphology in the Central Highlands of Tasmania. PhD Thesis (unpublished). University of Tasmania, Hobart.

KIERNAN, K. 1991. Glacial history of the upper Derwent Valley, Tasmania. *New Zealand Journal of Geology and Geophysics* **34**, 157.

KIERNAN, K. 1992. Mountain geomorphology and the last glaciation at Lake St Clair.

KIRKPATRICK, J.B. 1982. Phytogeographical Analysis of Tasmanian Alpine Floras. *Journal of Biogeography* **9**, 255-271.

KIRKPATRICK, J.B. 1983. Treeless plant communities of the Tasmanian High Country. *Proc. Ecol. Soc. Aust.* **12**, 61–77.

KIRKPATRICK, J.B. 1986. Tasmanian alpine biogeography and ecology and interpretations of the past. In Flora and Fauna of Alpine Australasia: Ages and Origins, (Melbourne: CSIRO Australia), pp. 229–242.

KIRKPATRICK, J.B. 1999. Grassy Vegetation and Subalpine Eucalypt Communities. In Vegetation of Tasmania, (Hobart, Tasmania: Australian Biological Resources Study), pp. 265–285.

KIRKPATRICK, J.B., DOMBROVSKIS, P., DAVIS, G., EBERHARD, J., AND KIRKPATRICK, J. 1997. Alpine Tasmania : an illustrated guide to the flora and vegetation (Melbourne ; Oxford : Oxford University Press).

KIRKPATRICK, J.B., AND FOWLER, M. 1998. Locating likely glacial forest refugia in Tasmania using palynological and ecological information to test alternative climatic models. *Biological Conservation* **85**, 171–182.

KIRKPATRICK, J.B., PEACOCK, R.J., CULLEN, P.J., AND NEYLAND, M.G. 1988. The Wet Eucalypt Forests of Tasmania. (Hobart: Tasm. Conservation Trust).

KITCHENER, A., AND HARRIS, S. 2013. From Forest to Fjaeldmark: Descriptions of Tasmania's Vegetation. (Department of Primary Industries, Parks, Water and Environment, Tasmania.).

KODELA, P.G. 1990a. Modern pollen rain from forest communities on the Robertson Plateau, New South Wales. *Australian Journal of Botany* **38**, 1–24.

KODELA, P.G. 1990b. Pollen-tree relationships within forests of the Robertson-Mosss Vale region, New South Wales, Australia. *Review of Palaeobotany and Palynology* **62**, 273–279.

KOHFELD, K.E., GRAHAM, R.M., DE BOER, A.M., SIME, L.C., WOLFF, E.W., LE QUÉRÉ, C., AND BOPP, L. 2013. Southern Hemisphere westerly wind changes during the Last Glacial Maximum: paleo-data synthesis. *Quaternary Science Reviews* **68**, 76–95.

LADD, P.G. 1976. Past and present vegetation of the Lancefield area, Victoria. *The Artefact* **1**, 113–127.

LADD, P.G. 1978. Vegetation history at Lake Curlip in Lowland Eastern Victoria, from 5200 B.P. to present. *Australian Journal of Botany* **26**, 393–414.

LADD, P.G. 1979a. A short pollen diagram from rainforest in highland eastern Victoria. *Austral Ecology* **4**, 229–237.

LADD, P.G. 1979b. Past and present vegetation on the Delegate River in the highlands of eastern Victoria. *Australian Journal of Botany* **27**, 185–202.

LAMBECK, K. AND CHAPPELL, J. 2001. Sea level change through the last glacial cycle. *Science* **292**, 679-686.

LAMY, F., KAISER, J., ARZ, H.W., HEBBELN, D., NINNEMANN, U., TIMM, O., TIMMERMANN, A., AND TOGGWEILER, J.R. 2007. Modulation of the bipolar seesaw in the Southeast Pacific during Termination 1. *Earth and Planetary Science Letters* **259**, 400–413.

LANDAIS, A., MASSON-DELMOTTE, V., STENNI, B., SELMO, E., ROCHE, D.M., JOUZEL, J., LAMBERT, F., GUILLEVIC, M., BAZIN, L., ARZEL, O., ET AL. 2015. A review of the bipolar see–saw from synchronized and high resolution ice core water stable isotope records from Greenland and East Antarctica. *Quaternary Science Reviews* **114**, 18–32.

LANGFORD, J. 1965. Weather and climate. In Atlas of Tasmania (Ed. J.L. Davies)., (Hobart: Lands and Surveys Department), pp. 2–11.

LEE, S.-Y., CHIANG, J.C.H., MATSUMOTO, K., AND TOKOS, K.S. 2011. Southern Ocean wind response to North Atlantic cooling and the rise in atmospheric CO2: Modeling perspective and paleoceanographic implications. *Paleoceanography* **26**, PA1214.

LIM, E.-P., HENDON, H.H., AND RASHID, H. 2013. Seasonal Predictability of the Southern Annular Mode due to Its Association with ENSO. *Journal of Climate* **26**, 8037–8054.

LONG, J.A., AND STOY, P.C. 2013. Quantifying the periodicity of Heinrich and Dansgaard–Oeschger events during Marine Oxygen Isotope Stage 3. *Quaternary Research* **79**, 413–423.

LOPES DOS SANTOS, R.A., DE DECKKER, P., HOPMANS, E.C., MAGEE, J.W., METS, A., SINNINGHE DAMSTÉ, J.S., AND SCHOUTEN, S. 2013. Abrupt vegetation change after the Late Quaternary megafaunal extinction in southeastern Australia. *Nature Geoscience* **6**, 627–631.

LOPES DOS SANTOS, R.A., WILKINS, D., DE DECKKER, P., AND SCHOUTEN, S. 2012. Late Quaternary productivity changes from offshore Southeastern Australia: A biomarker approach. *Palaeogeography, Palaeoclimatology, Palaeoecology* **363**–**364**, 48–56.

LOURANDOS, H. 1983. 10,000 years in the Tasmanian highlands. *Australian Archaeology* **16**, 39–47.

LULY, J.G. 1995. Holocene palaeoenvironments at Lake Tyrell - response to Sluiter and Parsons. *Journal of Biogeography* **22**, 149–156.

LULY, J.G. 1997. Modern pollen dynamics and surficial sedimentary processes at Lake Tyrrell, semi-arid northwestern Victoria, Australia. *Review of Palaeobotany and Palynology* **97**, 301–318.

MACKENZIE, L., AND MOSS, P. 2017. A late Quaternary record of vegetation and climate change from Hazards Lagoon, eastern Tasmania. *Quaternary International* **432**, 58–65.

MACKERETH, F. J. H. 1958. A Portable Core Sampler for Lake Deposits. *Limnology and Oceanography* **3**, 181-191.

MACKINTOSH, A.N., BARROWS, T.T., COLHOUN, E.A., AND FIFIELD, L.K. 2006. Exposure dating and glacial reconstruction at Mt. Field, Tasmania, Australia, identifies MIS 3 and MIS 2 glacial advances and climatic variability. *Journal of Quaternary Science* **21**, 363–376.

MACPHAIL, M. 1975. Late Pleistocene Environments in Tasmania. *Search* **6**, 295–300.

MACPHAIL, M. 1976. The History of the Vegetation and Climate in Southern Tasmania since the Late Pleistocene (c. 13,000 - 0 BP). PhD. The University of Tasmania.

MACPHAIL, M. 1980. Regeneration processes in Tasmanian forests: a long-term perspective based on pollen analysis. *Search* **11**, 184–190.

MACPHAIL, M. 2010. The burning question: Claims and counter claims on the origin and extent of buttongrass moorland (blanket moor) in southwest Tasmania during the present glacial-interglacial. In Haberle, S.G., Stevenson, J. and Prebble, M. (Eds.), Altered Ecologies: Fire, Climate and Human Influence on Terrestrial Landscapes, (Canberra Australia: ANU E Press), pp. 323–339.

MACPHAIL, M.K. 1979. Vegetation and climates in southern Tasmania since the last glaciation. *Quaternary Research* **11**, 306–341.

MACPHAIL, M.K. 1984. Small-Scale Dynamics in an Early Holocene Wet Sclerophyll Forest in Tasmania. *New Phytologist* **96**, 131–147.

MACPHAIL, M.K. 1986. 'Over the top': pollen-based reconstructions of past alpine floras and vegetation in Tasmania. In B.A. Barlow (Editor) Flora and Fauna of Alpine Australasia: Ages and Origins, (Melbourne: CSIRO), pp. 173–204.

MACPHAIL, M.K., AND COLHOUN, E.A. 1985. Late Last Glacial vegetation, climates and fire activity in southwest Tasmania. *Search* **16**, 43–45.

MACPHAIL, M.K., PEMBERTON, M., AND JACOBSON, G. 1999. Peat mounds of southwest Tasmania: possible origins. *Australian Journal of Earth Sciences* **46**, 667–677.

MALLICK, S.A. 2001. Pollination ecology of Tasmanian leatherwood (Eucryphia lucida Eucryphiaceae Labill.) and the impacts of hive honeybees. phd. University of Tasmania.

MANABE, S., BRYAN, K., AND SPELMAN, M.J. 1975. A Global Ocean-Atmosphere Climate Model. Part I. The Atmospheric Circulation. *Journal of Physical Oceanography* **5**, 3–29.

MANSILLA, C.A., MCCULLOCH, R.D., AND MORELLO, F. 2016. Palaeoenvironmental change in Southern Patagonia during the Lateglacial and Holocene: Implications for forest refugia and climate reconstructions. *Palaeogeography, Palaeoclimatology, Palaeoecology* **447**, 1–11.

MARCOTT, S.A., CLARK, P.U., PADMAN, L., KLINKHAMMER, G.P., SPRINGER, S.R., LIU, Z., OTTO-BLIESNER, B.L., CARLSON, A.E., UNGERER, A., PADMAN, J., ET AL. 2011. Ice-shelf collapse from subsurface warming as a trigger for Heinrich events. *Proceedings of the National Academy of Sciences* **108**, 13415–13419.

MARGARI, V., SKINNER, L.C., TZEDAKIS, P.C., GANOPOLSKI, A., VAUTRAVERS, M., AND SHACKLETON, N.J. 2010. The nature of millennial-scale climate variability during the past two glacial periods. *Nature Geoscience* **3**, 127–131.

MARIANI, M., AND FLETCHER, M.-S. 2016. The Southern Annular Mode determines inter-annual and centennial-scale fire activity in temperate southwest Tasmania, Australia. *Geophysical Research Letters* 2016GL068082.

MARIANI, M., AND FLETCHER, M.-S. 2017. Long-term climate dynamics in the extra-tropics of the South Pacific revealed from sedimentary charcoal analysis. *Quaternary Science Reviews* **173**, 181–192.

MARIANI, M., FLETCHER, M.-S., DRYSDALE, R.N., SAUNDERS, K.M., HEIJNIS, H., JACOBSEN, G., AND ZAWADZKI, A. 2017a. Coupling of the Intertropical Convergence Zone and Southern Hemisphere mid-latitude climate during the early to mid-Holocene. *Geology* **45**, 1083–1086.

MARIANI, M., CONNOR, S. E., FLETCHER, M.-S., THEUERKAUF, M., KUNES, P., JACOBSEN, G. SAUNDERS, K. M. AND ZAWADZKI, A. 2017b. How old is the Tasmanian cultural landscape? A test of landscape openness using quantitative land-cover reconstructions. *Journal of Biogeography* **44**, 2410-2420.

MARIANI, M., FLETCHER, M.-S., HOLZ, A., AND NYMAN, P. 2016. ENSO controls interannual fire activity in southeast Australia. *Geophysical Research Letters* **43**, 2016GL070572.

MASSAFERRO, J.I., MORENO, P.I., DENTON, G.H., VANDERGOES, M., AND DIEFFENBACHER-KRALL, A. 2009. Chironomid and pollen evidence for climate fluctuations during the Last Glacial Termination in NW Patagonia. *Quaternary Science Reviews* **28**, 517–525.

MATHEWES, R.W., AND WESTGATE, J.A. 1980. Bridge River tephra: revised distribution and significance for detecting old carbon errors in radiocarbon dates of limnic sediments in southern British Columbia. *Canadian Journal of Earth Sciences* **17**, 1454–1461.

MCANDREWS, J.H., AND POWER, D.M. 1973. Palynology of the Great Lakes: The Surface Sediments of Lake Ontario. *Canadian Journal of Earth Sciences* **10**, 777–792.

MCBRIDE, J.L., AND NICHOLLS, N. 1983. Seasonal Relationships between Australian Rainfall and the Southern Oscillation. *Monthly Weather Review* **111**, 1998–2004.

MCCULLOCH, R. D., FOGWILL, C. J., SUGDEN, D. E., BENTLEY, M. J., AND KUBIK, P. W. 2005. Chronology of the Last Glaciation in Central Strait of Magellan and Bahía Inútil, Southernmost South America. *Geografiska Annaler: Series A, Physical Geography* **87**, 289–312.

MCCUNE, B., AND GRACE, J.B. 2002. Part 4. Ordination. In Analysis of Ecological Communities Book, (Oregon, USA: Mjm software), pp. 102–181.

McCune, B., and Metford, M.J. 1999. PC-ORD for Windows. (Gleneden Beach, OR: MjM Software).

McGlone, M.S., and Moar, N.T. 1997. Pollen-vegetation relationships on the subantarctic Auckland Islands, New Zealand. *Review of Palaeobotany and Palynology* **96**, 317–338.

McIntosh, P.D., Laffan, M.D., and Hewitt, A.E. 2005. The role of fire and nutrient loss in the genesis of the forest soils of Tasmania and southern New Zealand. *Forest Ecology and Management* **220**, 185–215.

McKelvey, P.J. 1953. Forest colonization after recent volcanicity at west Taupo. *New Zealand Journal of Forestry* **6**, 435–448.

McKendrick, I.G. 1981. The Gondwana Element. In The Vegetation of Tasmania., (Hobart: Botany Department, University of Tasmania.), pp. 123–129.

Menounos, B., Clague, J.J., Osborn, G., Davis, P.T., Ponce, F., Goehring, B., Maurer, M., Rabassa, J., Coronato, A., and Marr, R. 2013. Latest Pleistocene and Holocene glacier fluctuations in southernmost Tierra del Fuego, Argentina. *Quaternary Science Reviews* **77**, 70–79.

Menviel, L., Timmermann, A., Timm, O.E., and Mouchet, A. 2011. Deconstructing the Last Glacial termination: the role of millennial and orbital-scale forcings. *Quaternary Science Reviews* **30**, 1155–1172.

Meyers, P.A. 1994. Preservation of elemental and isotopic source identification of sedimentary organic matter. *Chemical Geology* **114**, 289–302.

Meyers, P.A. and Teranes, J. L. 2001. Sediment Organic Matter. In Last, W.M. and Smol, J.P. [Editors] Tracking Environmental Change Using Lake Sediments. Volume 2: Physical and Geochemical Methods, (Dordrecht: Kluwer Academic Publishers), pp. 239-270.

Mo, K.C., and Paegle, J.N. 2001. The Pacific–South American modes and their downstream effects. *International Journal of Climatology* **21**, 1211–1229.

Moar, N.T. 1971. Contributions to the Quaternary history of the New Zealand flora 6. Aranuian pollen diagrams from Canterbury, Nelson and North Westland, South Island. *New Zealand Journal of Botany* **9**, 80–145.

Moreno Moncada, P., Denton, G.H., Moreno, H., Lowell, T.V., Putnam, A.E., and Kaplan, M.R. 2015. Radiocarbon chronology of the last glacial maximum and its termination in northwestern Patagonia. *Repositorio Académico - Universidad de Chile*.

Moreno, P.I., Kaplan, M.R., François, J.P., Villa-Martínez, R., Moy, C.M., Stern, C.R., and Kubik, P.W. 2009. Renewed glacial activity during the Antarctic cold reversal and persistence of cold conditions until 11.5 ka in southwestern Patagonia. *Geology* **37**, 375–378.

Morgan, S.W., Kirkpatrick, J.B., and di Folco, M.-B. 2010. Wind-controlled linear patterning and cyclic succession in Tasmanian Sphagnum mires. *Journal of Ecology* **98**, 583–591.

Mount, A.B. 1979. Natural regeneration processes in Tasmanian forests. *Search* **10**, 180–186.

Nevill, P.G., Bossinger, G., and Ades, P.K. 2010. Phylogeography of the world's tallest angiosperm, Eucalyptus regnans: evidence for multiple isolated Quaternary refugia. *Journal of Biogeography* **37**, 179–192.

NEWNHAM, R.M., VANDERGOES, M.J., SIKES, E., CARTER, L., WILMSHURST, J.M., LOWE, D.J., MCGLONE, M.S., AND SANDIFORD, A. 2012. Does the bipolar seesaw extend to the terrestrial southern mid-latitudes? *Quaternary Science Reviews* **36**, 214–222.

NICHOLLS, J.L. 1956. The historical ecology of the indigenous forest of the Taranaki upland. *New Zealand Journal of Forestry* **7**, 17–34.

NICHOLLS, N., AND WONG, K.K. 1990. Dependence of Rainfall Variability on Mean Rainfall, Latitude, and the Southern Oscillation. *Journal of Climate* **3**, 163–170.

NICOLLS, K.D., AND DIMMOCK, G.M. 1965. Soils. In Atlas of Tasmania (Ed. J.L. Davies)., (Hobart: Lands and Surveys Department), pp. 27–29.

NORTON, D.A. 1983. Population dynamics of subalpin Libocedrus bidwillii forests in the Cropp River valler, Westland, New Zealand. *New Zealand Journal of Botany* **21**, 127–134.

NUNEZ, M. AND COLHOUN, E.A. 1986. A note on air temperature lapse rates on Mount Wellington, Tasmania. *Papers and Proceedings of the Royal Sociaty of Tasmania* **120**, 11-15.

O'CONNELL, J. F. AND ALLEN, J. 2015. The process, biotic impact, and global implications of the human colonization of Sahul about 47,000 years ago. *Journal of Archaeological Science* **56**, 73–84.

OGDEN, J. 1978. Investigations of the dendrochronology of the genus Athrotaxis D. Don (Taxodiaceae) in Tasmania. *Tree-Ring Bulletin* **38**, 1–13.

ORESKES, N. 2004. The Scientific Consensus on Climate Change. *Science* **306**, 1686–1686.

OSWALD, W.W., ANDERSON, P.M., BROWN, T.A., BRUBAKER, L.B., HU, F.S., LOZHKIN, A.V., TINNER, W., AND KALTENRIEDER, P. 2005. Effects of sample mass and macrofossil type on radiocarbon dating of arctic and boreal lake sediments. *The Holocene* **15**, 758–767.

OVERPECK, J.T., WEBB III, T., AND PRENTICE, I.C. 1985. Quantitative interpretation of fossil pollen spectra: dissimilarity coefficients and the method of modern analogs. *Quaternary Research* **23**, 87–108.

OVERPECK, J.T., WEBB, R.S., AND WEBB, T. 1992. Mapping eastern North American vegetation change of the past 18 ka: No-analogs and the future. *Geology* **20**, 1071–1074.

PARSONS, R.W., AND PRENTICE, I.C. 1981. Statistical approaches to R-values and the pollen—vegetation relationship. *Review of Palaeobotany and Palynology* **32**, 127–152.

PARSONS, R.W., PRENTICE, I.C., AND SAARNISTO, M. 1980. Statistical studies on pollen representation in Finnish lake sediments in relation to forest inventory data. *Annales Botanici Fennici* **17**, 379–393.

PECK, R. 1972. Efficiency tests on the Tauber trap used as a pollen sampler in turbulent water flow. *New Phytologist* **71**, 187-198.

PECK, R. 1974. Studies of pollen distribution in the Oakdale catchment. Thesis, Univ. Cambridge (1974) (unpubl.)

PEDRO, J.B., BOSTOCK, H.C., BITZ, C.M., HE, F., VANDERGOES, M.J., STEIG, E.J., CHASE, B.M., KRAUSE, C.E., RASMUSSEN, S.O., MARKLE, B.R., ET AL. 2016. The spatial extent and dynamics of the Antarctic Cold Reversal. *Nature Geoscience* **9**, 51–55.

PEDRO, J.B., VAN OMMEN, T.D., RASMUSSEN, S.O., MORGAN, V.I., CHAPPELLAZ, J., MOY, A.D., MASSON-DELMOTTE, V., AND DELMOTTE, M. 2011. The last deglaciation: timing the bipolar seesaw. *Clim. Past* **7**, 671–683.

PEMBERTON, M. 1989. Land Systems Survey of Tasmania Region 7 - Southwest. (Department of Agriculture, Tasmania.).

PENNINGTON, W. 1979. The origin of pollen in lake sediments: an enclosed lake compared with one receiving inflow streams. *New Phytologist* **83**, 189-213.

PERNER, K., MOROS, M., DE DECKKER, P., BLANZ, T., WACKER, L., TELFORD, R., SIEGEL, H., SCHNEIDER, R., AND EYSTEIN, J. 2018. Heat export from the tropics drives mid to late Holocene palaeoceanographic changes offshore southern Australia. *Quaternary Science Reviews* **180**, 96–110.

PETERSEN, S.V., SCHRAG, D.P., AND CLARK, P.U. 2013. A new mechanism for Dansgaard-Oeschger cycles. *Paleoceanography* **28**, 24–30.

PETERSON, L.C., HAUG, G.H., HUGHEN, K.A., AND RÖHL, U. 2000. Rapid Changes in the Hydrologic Cycle of the Tropical Atlantic During the Last Glacial. *Science* **290**, 1947–1951.

PETHERICK, L., BOSTOCK, H., COHEN, T.J., FITZSIMMONS, K., TIBBY, J., FLETCHER, M.-S., MOSS, P., REEVES, J., MOONEY, S., BARROWS, T., ET AL. 2013a. Climatic records over the past 30 ka from temperate Australia – a synthesis from the Oz-INTIMATE workgroup. *Quaternary Science Reviews* **74**, 58–77.

PHILLIPS, M.E. 1941. Studies in atmospheric pollen / by Marie E. Phillips (Sydney : Australian Medical Pub. Co).

PHILLIPS, N.A. 1956. The general circulation of the atmosphere: A numerical experiment. *Quarterly Journal of the Royal Meteorological Society* **82**, 123–164.

PODGER, F.D., BIRD, T., AND BROWN, M.J. 1988. Human activity, fire and change in the forest at Hogsback Plain, southern Tasmania. In Frawley K.J., Semple N.M. (Eds) Australia's Ever Changing Forests., (Canberra: Australian Defence Force Academy), pp. 119–140.

POHL, B., FAUCHEREAU, N., REASON, C.J.C., AND ROUAULT, M. 2010. Relationships between the Antarctic Oscillation, the Madden–Julian Oscillation, and ENSO, and Consequences for Rainfall Analysis. *Journal of Climate* **23**, 238–254.

PORCH, N. AND ALLEN, J. 1995. Tasmania: archaeological and palaeo-ecological perspectives. *Antiquity* **69**, 714-732.

PRENTICE, I.C. 1985. Pollen representation, source area, and basin size: Toward a unified theory of pollen analysis. *Quaternary Research* **23**, 76–86.

PRENTICE, I.C., AND PARSONS, R.W. 1983. Maximum Likelihood Linear Calibration of Pollen Spectra in Terms of Forest Composition. *Biometrics* **39**, 1051–1057.

PUTNAM, A.E., DENTON, G.H., SCHAEFER, J.M., BARRELL, D.J.A., ANDERSEN, B.G., FINKEL, R.C., SCHWARTZ, R., DOUGHTY, A.M., KAPLAN, M.R., AND SCHLÜCHTER, C. 2010. Glacier advance in southern middle-latitudes during the Antarctic Cold Reversal. *Nature Geoscience* **3**, 700–704.

PYRKE, A. AND MARSDEN-SMEDLEY, J. 2005. Fire-attributes categories, fire sensitivity, and flammability of Tasmanian vegetation communities. *Tasforests* **16**, 35-46.

QIN, F., ZHAO, Y., LI, Q., AND CAI, M. 2015. Modern pollen assemblages from surface lake sediments in northwestern China and their importance as indicators of vegetation and climate. *Science China Earth Sciences* **58**, 1643–1655.

QINGHAI, X., YUECONG, L., XIAOLAN, Y., JULE, X., WENDONG, L., AND YANJIA, P. 2005. Source and distribution of pollen in the surface sediment of Daihai Lake, inner Mongolia. *Quaternary International* **136**, 33–45.

RASMUSSEN, S.O., BIGLER, M., BLOCKLEY, S.P., BLUNIER, T., BUCHARDT, S.L., CLAUSEN, H.B., CVIJANOVIC, I., DAHL-JENSEN, D., JOHNSEN, S.J., FISCHER, H., ET AL. 2014. A stratigraphic framework for abrupt climatic changes during the Last Glacial period based on three synchronized Greenland ice-core records: refining and extending the INTIMATE event stratigraphy. *Quaternary Science Reviews* **106**, 14–28.

RASMUSSEN, T.L., THOMSEN, E., AND MOROS, M. 2016. North Atlantic warming during Dansgaard-Oeschger events synchronous with Antarctic warming and out-of-phase with Greenland climate. *Scientific Reports* **6**,.

READ, J. 1999. Rainforest Ecology. In The Vegetation of Tasmania, (Hobart: Australian Biological Resources Study), pp. 160–197.

READ, J., AND HILL, R.S. 1988. The Dynamics of Some Rainforest Associations in Tasmania. *Journal of Ecology* **76**, 558–584.

REES, A.B.H., AND CWYNAR, L.C. 2010. Evidence for early postglacial warming in Mount Field National Park, Tasmania. *Quaternary Science Reviews* **29**, 443–454.

REEVES, J.M., BARROWS, T.T., COHEN, T.J., KIEM, A.S., BOSTOCK, H.C., FITZSIMMONS, K.E., JANSEN, J.D., KEMP, J., KRAUSE, C., PETHERICK, L., ET AL. 2013a. Climate variability over the last 35,000 years recorded in marine and terrestrial archives in the Australian region: an OZ-INTIMATE compilation. *Quaternary Science Reviews* **74**, 21–34.

REEVES, J.M., BOSTOCK, H.C., AYLIFFE, L.K., BARROWS, T.T., DE DECKKER, P., DEVRIENDT, L.S., DUNBAR, G.B., DRYSDALE, R.N., FITZSIMMONS, K.E., GAGAN, M.K., ET AL. 2013b. Palaeoenvironmental change in tropical Australasia over the last 30,000 years – a synthesis by the OZ-INTIMATE group. *Quaternary Science Reviews* **74**, 97–114.

RHODES, A.N. 1998. A method for the preparation and quantification of microscopic charcoal from terrestrial and lacustrine sediment cores. *The Holocene* **8**, 113–117.

RISBEY, J.S., POOK, M.J., MCINTOSH, P.C., WHEELER, M.C., AND HENDON, H.H. 2009. On the Remote Drivers of Rainfall Variability in Australia. *Monthly Weather Review* **137**, 3233–3253.

ROBBINS, R.G. 1962. The podocarp-broadleaf forests of New Zealand. *Transactions and Proceedings of the Royal Society of New Zealand* **1**, 33–75.

ROSENZWEIG, C., KAROLY, D., VICARELLI, M., NEOFOTIS, P., WU, Q., CASASSA, G., MENZEL, A., ROOT, T.L., ESTRELLA, N., SEGUIN, B., ET AL. 2008. Attributing physical and biological impacts to anthropogenic climate change. *Nature* **453**, 353–357.

DE SALAS, M.F., AND BAKER, M.L. 2017. A Census of the Vascular Plants of Tasmania, including Macquarie Island (Hobart: The Tasmanian Herbarium, Tasmanian Museum and Art Gallery).

SÁNCHEZ GOÑI, M.F., LANDAIS, A., FLETCHER, W.J., NAUGHTON, F., DESPRAT, S., AND DUPRAT, J. 2008. Contrasting impacts of Dansgaard–Oeschger events over a western European latitudinal transect modulated by orbital parameters. *Quaternary Science Reviews* **27**, 1136–1151.

SANDS, C.C. 1967. A pollen survey in Canberra. *The Medical Journal of Australia* **1**, 208–210.

SEDDON, A.W.R., MACKAY, A.W., BAKER, A.G., BIRKS, H.J.B., BREMAN, E., BUCK, C.E., ELLIS, E.C., FROYD, C.A., GILL, J.L., GILLSON, L., ET AL. 2014. Looking forward through the past: identification of 50 priority research questions in palaeoecology. *Journal of Ecology* **102**, 256–267.

SHAKUN, J.D., CLARK, P.U., HE, F., LIFTON, N.A., LIU, Z., AND OTTO-BLIESNER, B.L. 2015. Regional and global forcing of glacier retreat during the last deglaciation. *Nature Communications* **6**, 8059.

SHAKUN, J.D., CLARK, P.U., HE, F., MARCOTT, S.A., MIX, A.C., LIU, Z., OTTO-BLIESNER, B., SCHMITTNER, A., AND BARD, E. 2012. Global warming preceded by increasing carbon dioxide concentrations during the last deglaciation. *Nature* **484**, 49–54.

SHIMELD, P.W., AND COLHOUN, E.A. 2001. Eucalyptus spp. pollen transport across Liawenee Moor, on the Central Plateau of Tasmania. *Papers and Proceedings of the Royal Society of Tasmania* **135**, 51–55.

SHEPHERD, R. R. 1974. The Central Plateau of Tasmania: A Resource Survey and Management Plan. Thesis (Master of Science), University of Tasmania, Hobart.

SIKES, E.L., HOWARD, W.R., SAMSON, C.R., MAHAN, T.S., ROBERTSON, L.G., AND VOLKMAN, J.K. 2009. Southern Ocean seasonal temperature and Subtropical Front movement on the South Tasman Rise in the late Quaternary. *Paleoceanography* **24**, PA2201.

SIME, L.C. 2014. Greenland deglaciation puzzles. *Science* **345**, 1116–1117.

SITCH, S., HUNTINGFORD, C., GEDNEY, N., LEVY, P.E., LOMAS, M., PIAO, S.L., BETTS, R., CIAIS, P., COX, P., FRIEDLINGSTEIN, P., ET AL. 2008. Evaluation of the terrestrial carbon cycle, future plant geography and climate-carbon cycle feedbacks using five Dynamic Global Vegetation Models (DGVMs). *Global Change Biology* **14**, 2015–2039.

SMART, I.J., TUDDENHAM, W.G., AND KNOX, R.B. 1979. Aerobiology of grass pollen in the city atmosphere of Melbourne: effect of weather parameters and pollen sources. *Australian Journal of Botany* **27**, 333–342.

SMITH, A.G. 1965. Problems of Inertia and Threshold Related to Post-Glacial Habitat Changes. *Proceedings of the Royal Society of London. Series B, Biological Sciences* **161**, 331–342.

STAHLE, L.N., CHIN, H., HABERLE, S., AND WHITLOCK, C. 2017. Late-glacial and Holocene records of fire and vegetation from Cradle Mountain National Park, Tasmania, Australia. *Quaternary Science Reviews* **177**, 57–77.

STAHLE, L.N., WHITLOCK, C., AND HABERLE, S.G. 2016. A 17,000-Year-Long Record of Vegetation and Fire from Cradle Mountain National Park, Tasmania. *Paleoecology* 82.

STEVENSON, J., AND HABERLE, S.G. 2005. Macro Charcoal Analysis: A modified technique used by the Department of Archaeology and Natural History. (Canberra: Australian National University).

STEWART, G.H., AND ROSE, A.B. 1988. Conifer regeneration failure in New Zealand: dynamics of montane <Emphasis Type="Italic">Libocedrus bidwillii</Emphasis> stands. *Vegetatio* **79**, 41–49.

STEWART, G.H., AND VEBLEN, T.T. 1982. Regeneration patterns in southern rata (Metrosideros umbellata) — kamahi (Weinmannia racemosa) forest in central Westland, New Zealand. *New Zealand Journal of Botany* **20**, 55–72.

STOCKER, T.F., AND JOHNSEN, S.J. 2003. A minimum thermodynamic model for the bipolar seesaw. *Paleoceanography* **18**, 1087.

STOCKMARR, J. 1971. Tablets with spores used in absolute pollen analysis. *Pollen et Spores* **13**, 615–621.

STRELIN, J.A., DENTON, G.H., VANDERGOES, M.J., NINNEMANN, U.S., AND PUTNAM, A.E. 2011. Radiocarbon chronology of the late-glacial Puerto Bandera moraines, Southern Patagonian Icefield, Argentina. *Quaternary Science Reviews* **30**, 2551–2569.

SUGDEN, D.E., AND JOHN, B.S. 1976. Glaciers and Landscape: A Geomorphological Approach (London: Edward Arnold (Publishers) Ltd).

SUGITA, S. 1993. A Model of Pollen Source Area for an Entire Lake Surface. *Quaternary Research* **39**, 239–244.

SUGITA, S. 1994. Pollen Representation of Vegetation in Quaternary Sediments: Theory and Method in Patchy Vegetation. *Journal of Ecology* **82**, 881–897.

SUGITA, S. 2007a. Theory of quantitative reconstruction of vegetation I: pollen from large sites REVEALS regional vegetation composition. *The Holocene* **17**, 229–241.

SUGITA, S. 2007b. Theory of quantitative reconstruction of vegetation II: all you need is LOVE. *The Holocene* **17**, 243–257.

TANJUNG, R.H.R. 1993. A comparison between regeneration patterns of Eucalyptus regnans and mixed forest species, on logged coupes in South West Tasmania. cmaster. University of Tasmania.

TASMANIA DEPARTMENT OF MINES, 1963. "St Clair" (Geological Map). Mineral Resources Tasmania, Department of State Growth, Hobart.

TAUBER, H. 1965. Differential pollen dispersion and the interpretation of pollen diagrams, with a contribution to the interpretation of the elm fall.

TAUBER, H. 1967. Investigations of the mode of pollen transfer in forested areas. *Review of Palaeobotany and Palynology* **3**, 277–286.

TAUBER, H. 1977. Investigations of aerial pollen transport in a forested area [Gribskov, Sealand, Denmark]. *Dansk Botanisk Arkiv (Denmark)*.

THOM, B.G., AND CHAPPELL, J.M.A. 1975. Holocene sea levels relative to Australia. *Search* **6**, 90–93.

THOMAS, A.M., RUPPER, S., AND CHRISTENSEN, W.F. 2011. Characterizing the statistical properties and interhemispheric distribution of Dansgaard-Oeschger events. *Journal of Geophysical Research: Atmospheres* **116**, D03103.

THOMAS, I. 1993. Late Pleistocene environments and Aboriginal settlement patterns in Tasmania. *Australian Archaeology* **36**, 1–11.

THOMAS, I. 1995. Models and prima donnas in southwest Tasmania [Reply to Cosgrove, R., Allen, J. and Marshall, B. Late Pleistocene human occupation in Tasmania; in no.38, June 1994]. *Australian Archaeology* **41**, 21–23.

THOMAS, I., CULLEN, P., AND FLETCHER, M.-S. 2010. Ecological drift or stable fire cycles in Tasmania: A resolution? In Haberle, S.G., Stevenson, J. and Prebble, M. (Eds.), Altered Ecologies: Fire, Climate and Human Influence on Terrestrial Landscapes, (Canberra Australia: ANU E Press), pp. 341–352.

THOMPSON, D.W.J., AND WALLACE, J.M. 2000. Annular Modes in the Extratropical Circulation. Part I: Month-to-Month Variability*. *Journal of Climate* **13**, 1000–1016.

THRUSH, M.N. 2008. The Pleistocene Glaciations of the Cradle Mountain Region, Tasmania. PhD. Univeristy of Newcastle.

TIBBY, J. 2012. The Younger Dryas: Relevant in the Australian region? *Quaternary International* **253**, 47–54.

TOGGWEILER, J.R. 2009. Shifting Westerlies. *Science* **323**, 1434–1435.

TRAVERSE, A. 1992. Organic Fluvial Sediment: Palynomorphs and 'Palynodebris' in the Lower Trinity River, Texas. *Annals of the Missouri Botanical Garden* **79**, 110–125.

TRAVERSE, A. 1994. Sedimentation of land-derived palynomorphs in the Trinity-Galveston Bay area, Texas. In Sedimentation of Organic Particles, (Cambridge: Cambridge University Press), pp. 69–85.

TURNEY, C.S.M., KERSHAW, A.P., LOWE, J.J., VAN DER KAARS, S., JOHNSTON, R., RULE, S., MOSS, P., RADKE, L., TIBBY, J., MCGLONE, M.S., ET AL. 2006. Climatic variability in the southwest Pacific during the Last Termination (20-10 kyr BP). *Quaternary Science Reviews* **25**, 886–903.

TZEDAKIS, P.C., FROGLEY, M.R., LAWSON, I.T., PREECE, R.C., CACHO, I., AND ABREU, L. DE 2004. Ecological thresholds and patterns of millennial-scale climate variability: The response of vegetation in Greece during the last glacial period. *Geology* **32**, 109–112.

VANDERGOES, M.J., DIEFFENBACHER-KRALL, A.C., NEWNHAM, R.M., DENTON, G.H., AND BLAAUW, M. 2008. Cooling and changing seasonality in the Southern Alps, New Zealand during the Antarctic Cold Reversal. *Quaternary Science Reviews* **27**, 589–601.

VANDERGOES, M.J., NEWNHAM, R.M., DENTON, G.H., BLAAUW, M., AND BARRELL, D.J.A. 2013. The anatomy of Last Glacial Maximum climate variations in south Westland, New Zealand, derived from pollen records. *Quaternary Science Reviews* **74**, 215–229.

VEBLEN, T.T., AND STEWART, G.H. 1982. On the conifer regeneration gap in New Zealand: the dynamics of Libocedrus bidwillii stand on South Island. *Journal of Ecology* **70**, 413–436.

VELOZ, S.D., WILLIAMS, J.W., BLOIS, J.L., HE, F., OTTO-BLIESNER, B., AND LIU, Z. 2012. No-analog climates and shifting realized niches during the late quaternary: implications for 21st-century predictions by species distribution models. *Global Change Biology* **18**, 1698–1713.

VOELKER, A.H.L. 2002. Global distribution of centennial-scale records for Marine Isotope Stage (MIS) 3: a database. *Quaternary Science Reviews* **21**, 1185–1212.

WAIS DIVIDE PROJECT MEMBERS 2015. Precise interpolar phasing of abrupt climate change during the last ice age. *Nature* **520**, 661–665.

WAIS DIVIDE PROJECT MEMBERS, FUDGE, T.J., STEIG, E.J., MARKLE, B.R., SCHOENEMANN, S.W., DING, Q., TAYLOR, K.C., MCCONNELL, J.R., BROOK, E.J., SOWERS, T., ET AL. 2013. Onset of deglacial warming in West Antarctica driven by local orbital forcing. *Nature* **500**, 440–444.

WANG, Y., HERZSCHUH, U., SHUMILOVSKIKH, L.S., MISCHKE, S., BIRKS, H.J.B., WISCHNEWSKI, J., BÖHNER, J., SCHLÜTZ, F., LEHMKUHL, F., DIEKMANN, B., ET AL. 2014. Quantitative reconstruction of precipitation changes on the NE Tibetan Plateau since the Last Glacial Maximum – extending the concept of pollen source area to pollen-based climate reconstructions from large lakes. *Clim. Past* **10**, 21–39.

WANG, Y.J., CHENG, H., EDWARDS, R.L., AN, Z.S., WU, J.Y., SHEN, C.-C., AND DORALE, J.A. 2001. A High-Resolution Absolute-Dated Late Pleistocene Monsoon Record from Hulu Cave, China. *Science* **294**, 2345–2348.

WARDLE, P. 1963. The regeneration gap of New Zealand gymnosperms. *New Zealand Journal of Botany* **1**, 301–315.

WELLS, P., AND HICKEY, J. 1999. Wet Sclerophyll, Mixed and Swamp Forest. In The Vegetation of Tasmania, (Hobart: Australian Biological Resources Study), pp. 225–243.

WILLIAMS, J.W., SHUMAN, B.N., WEBB, T., BARTLEIN, P.J., AND LEDUC, P.L. 2004. Late-Quaternary Vegetation Dynamics in North America: Scaling from Taxa to Biomes. *Ecological Monographs* **74**, 309–334.

WILLIAMS, P.W., MCGLONE, M., NEIL, H., AND ZHAO, J.-X. 2015. A review of New Zealand palaeoclimate from the Last Interglacial to the global Last Glacial Maximum. *Quaternary Science Reviews* **110**, 92–106.

WILMSHURST, J.M., AND MCGLONE, M.S. 2005. Origin of pollen and spores in surface lake sediments: Comparison of modern palynomorph assemblages in moss cushions, surface soils and surface lake sediments. *Review of Palaeobotany and Palynology* **136**, 1–15.

WOOD, S.W., AND BOWMAN, D.M.J.S. 2012a. Alternative stable states and the role of fire–vegetation–soil feedbacks in the temperate wilderness of southwest Tasmania. *Landscape Ecology* **27**, 13–28.

WOOD, S.W., AND BOWMAN, D.M.J.S. 2012b. Alternative stable states and the role of fire–vegetation–soil feedbacks in the temperate wilderness of southwest Tasmania. *Landscape Ecology* **27**, 13–28.

WOOD, S.W., HUA, Q., AND BOWMAN, D.M.J.S. 2011a. Fire-patterned vegetation and the development of organic soils in the lowland vegetation mosaics of south-west Tasmania. *Australian Journal of Botany* **59**, 126–136.

WOOD, S.W., MURPHY, B.P., AND BOWMAN, D.M.J.S. 2011b. Firescape ecology: how topography determines the contrasting distribution of fire and rain forest in the south-west of the Tasmanian Wilderness World Heritage Area. *Journal of Biogeography* **38**, 1807–1820.

WORTH, J.R.P., JORDAN, G.J., MCKINNON, G.E., AND VAILLANCOURT, R.E. 2009. The major Australian cool temperate rainforest tree Nothofagus cunninghamii withstood Pleistocene glacial aridity within multiple regions: evidence from the chloroplast. *New Phytologist* **182**, 519–532.

WORTH, J.R.P., MARTHICK, J.R., JORDAN, G.J., AND VAILLANCOURT, R.E. 2011. Low but structured chloroplast diversity in Atherosperma moschatum (Atherospermataceae) suggests bottlenecks in response to the Pleistocene glacials. *Annals of Botany* **108**, 1247–1256.

WORTH, J.R.P., SAKAGUCHI, S., RANN, K.D., BOWMAN, C.J.W., ITO, M., JORDAN, G.J., AND BOWMAN, D.M.J.S. 2016. Gondwanan conifer clones imperilled by bushfire. *Scientific Reports* **6**, 1–6.

WORTH, J.R.P., WILLIAMSON, G.J., SAKAGUCHI, S., NEVILL, P.G., AND JORDAN, G.J. 2014. Environmental niche modelling fails to predict Last Glacial Maximum refugia: niche shifts, microrefugia or incorrect palaeoclimate estimates? *Global Ecology and Biogeography* **23**, 1186–1197.

XIA, Q., ZHAO, J., AND COLLERSON, K.. 2001. Early-Mid Holocene climatic variations in Tasmania, Australia: multi-proxy records in a stalagmite from Lynds Cave. *Earth and Planetary Science Letters* **194**, 177–187.

XU, Q., TIAN, F., BUNTING, M.J., LI, Y., DING, W., CAO, X., AND HE, Z. 2012. Pollen source areas of lakes with inflowing rivers: modern pollen influx data from Lake Baiyangdian, China. *Quaternary Science Reviews* **37**, 81–91.

ZHU, Y., CHEN, F., AND DAVID, M. 2002. The environmental signal of an early Holocene pollen record from the Shiyang River basin lake sediments, NW China. *Chinese Science Bulletin* **47**, 267.

Appendix 1: Site data for modern pollen dataset (Lake St Clair area)

Site No	Site Code	Site Area	Latitude (°S)	Longitude (°E)	Alt. (m)	MAT (°C)	Ppt. (mm)	TasVeg Code	TasVeg 3.0 Vegetation Type (detailed)	TasVeg 3.0 Vegetation Group (simplified)	Sample Type
1	LkDix	Lake Dixon	42.16	146.11	661	8.5	1865	QAQ	Water, sea	Other natural environments	Lake Sediment
2	CLC15	Lake St Clair	42.02	146.11	737	8.0	1865	QAQ	Water, sea	Other natural environments	Lake Sediment
3	CLC18	Lake St Clair	42.02	146.11	737	8.0	1865	QAQ	Water, sea	Other natural environments	Lake Sediment
4	CLC12	Lake St Clair	42.02	146.12	737	8.0	1865	QAQ	Water, sea	Other natural environments	Lake Sediment
5	CLC14	Lake St Clair	42.02	146.11	737	8.0	1865	QAQ	Water, sea	Other natural environments	Lake Sediment
6	CLC13	Lake St Clair	42.03	146.12	737	8.0	1865	QAQ	Water, sea	Other natural environments	Lake Sediment
7	CLC20	Lake St Clair	42.03	146.13	737	8.0	1865	QAQ	Water, sea	Other natural environments	Lake Sediment
8	CLC19	Lake St Clair	42.03	146.14	737	8.0	1865	QAQ	Water, sea	Other natural environments	Lake Sediment
9	CLC21	Lake St Clair	42.05	146.16	737	8.0	1865	QAQ	Water, sea	Other natural environments	Lake Sediment
10	CLC10	Lake St Clair	42.06	146.15	737	8.0	1865	QAQ	Water, sea	Other natural environments	Lake Sediment
11	CLC9	Lake St Clair	42.06	146.17	737	8.0	1865	QAQ	Water, sea	Other natural environments	Lake Sediment
12	CLC7	Lake St Clair	42.07	146.18	737	8.0	1865	QAQ	Water, sea	Other natural environments	Lake Sediment
13	CLC5	Lake St Clair	42.08	146.18	737	8.0	1865	QAQ	Water, sea	Other natural environments	Lake Sediment
14	CLC 3b	Lake St Clair	42.09	146.19	737	8.0	1865	QAQ	Water, sea	Other natural environments	Lake Sediment
15	CLC4	Lake St Clair	42.11	146.17	737	8.0	1865	QAQ	Water, sea	Other natural environments	Lake Sediment
16	CLC17	Lake St Clair	42.11	146.18	737	8.0	1865	QAQ	Water, sea	Other natural environments	Lake Sediment
17	CLC11	Lake St Clair	42.11	146.17	737	8.0	1865	QAQ	Water, sea	Other natural environments	Lake Sediment
18	CLC1	Lake St Clair	42.11	146.20	737	8.0	1865	QAQ	Water, sea	Other natural environments	Lake Sediment
19	CLC16	Lake St Clair	42.10	146.21	737	8.0	1865	QAQ	Water, sea	Other natural environments	Lake Sediment

Site No	Site Code	Site Area	Latitude (°S)	Longitude (°E)	Alt. (m)	Temp. (°C)	Precip. (mm)	TasVeg Code	TasVeg 3.0 Vegetation Type (detailed)	TasVeg 3.0 Vegetation Group (simplified)	Sample Type
20	H16	Lake St Clair	42.12	146.19	740	8.0	1865	MBE	Eastern buttongrass moorland	Moorland, sedgeland, rushland and peatland	Moss Polster
21	H19	Lake St Clair	42.12	146.19	740	8.0	1865	DAD	Eucalyptus amygdalina forest and woodland on dolerite	Dry eucalypt forest and woodland	Moss Polster
22	M129	Narcissus Valley	42.01	146.10	755	7.9	1865	MBS	Buttongrass moorland with ermergent shrubs	Moorland, sedgeland, rushland and peatland	Moss Polster
23	M128	Narcissus Valley	42.01	146.10	741	8.0	1865	DAD	Eucalyptus amygdalina forest and woodland on dolerite	Dry eucalypt forest and woodland	Moss Polster
24	M519	Traveller Range	42.03	146.16	748	7.9	1865	WDL	Eucalyptus delegatensis forest over Leptospermum	Wet eucalypt forest and woodland	Moss Polster
25	H3	Lake St Clair	42.10	146.17	750	7.9	1865	RMT	Nothofagus - Atherosperma rainforest	Rainforest and related scrub	Moss Polster
26	H22	Lake St Clair	42.08	146.20	750	7.9	1865	WDR	Eucalyptus delegatensis forest over rainforest	Wet eucalypt forest and woodland	Moss Polster
27	M520	Traveller Range	42.03	146.16	755	7.9	1865	RMU	Nothofagus rainforest (undifferentiated)	Rainforest and related scrub	Moss Polster
28	M143	Narcissus Valley	42.00	146.10	755	7.9	1865	DPD	Eucalyptus pauciflora forest and woodland on dolerite	Dry eucalypt forest and woodland	Moss Polster
29	H13	Lake St Clair	42.09	146.20	760	7.8	1865	RMT	Nothofagus - Atherosperma rainforest	Rainforest and related scrub	Moss Polster
30	M48	Mt Olympus	42.03	146.11	770	7.8	1865	RMT	Nothofagus - Atherosperma rainforest	Rainforest and related scrub	Moss Polster
31	M126	Narcissus Valley	41.99	146.09	777	7.7	1865	DPD	Eucalyptus pauciflora forest and woodland on dolerite	Dry eucalypt forest and woodland	Moss Polster
32	M125	Narcissus Valley	41.98	146.10	781	7.7	1865	DPD	Eucalyptus pauciflora forest and woodland on dolerite	Dry eucalypt forest and woodland	Moss Polster
33	M140	Narcissus Valley	42.00	146.10	783	7.7	1865	WSU	Eucalyptus subcrenulata forest and woodland	Wet eucalypt forest and woodland	Moss Polster
34	ExBog	Excalibur Bog	42.11	146.29	784	7.7	1865	MRR	Restionaceae rushland	Moorland, sedgeland, rushland and peatland	Moss Polster
35	T4-1	Excalibur Bog	42.11	146.29	784	7.7	1865	MRR	Restionaceae rushland	Moorland, sedgeland, rushland and peatland	Moss Polster
36	T4-2	Excalibur Bog	42.11	146.29	784	7.7	1865	MRR	Restionaceae rushland	Moorland, sedgeland, rushland and peatland	Moss Polster
37	T1-2	Excalibur Bog	42.11	146.29	785	7.7	1865	MRR	Restionaceae rushland	Moorland, sedgeland, rushland and peatland	Moss Polster
38	T1-3	Excalibur Bog	42.11	146.29	785	7.7	1865	MRR	Restionaceae rushland	Moorland, sedgeland, rushland and peatland	Moss Polster

Site No	Site Code	Site Area	Latitude (°S)	Longitude (°E)	Alt. (m)	Temp. (°C)	Precip. (mm)	TasVeg Code	TasVeg 3.0 Vegetation Type (detailed)	TasVeg 3.0 Vegetation Group (simplified)	Sample Type
39	T1-4	Excalibur Bog	42.11	146.29	785	7.7	1865	MRR	Restionaceae rushland	Moorland, sedgeland, rushland and peatland	Moss Polster
40	T2-1	Excalibur Bog	42.11	146.29	785	7.7	1865	MRR	Restionaceae rushland	Moorland, sedgeland, rushland and peatland	Moss Polster
41	T2-2	Excalibur Bog	42.11	146.29	785	7.7	1865	MRR	Restionaceae rushland	Moorland, sedgeland, rushland and peatland	Moss Polster
42	T3-3	Excalibur Bog	42.11	146.29	785	7.7	1865	MRR	Restionaceae rushland	Moorland, sedgeland, rushland and peatland	Moss Polster
43	T3-4	Excalibur Bog	42.11	146.29	785	7.7	1865	MRR	Restionaceae rushland	Moorland, sedgeland, rushland and peatland	Moss Polster
44	T2-3	Excalibur Bog	42.11	146.29	786	7.7	1865	MRR	Restionaceae rushland	Moorland, sedgeland, rushland and peatland	Moss Polster
45	T3-2	Excalibur Bog	42.11	146.29	786	7.7	1865	MRR	Restionaceae rushland	Moorland, sedgeland, rushland and peatland	Moss Polster
46	T4-3	Excalibur Bog	42.11	146.28	786	7.7	1865	MRR	Restionaceae rushland	Moorland, sedgeland, rushland and peatland	Moss Polster
47	T4-4	Excalibur Bog	42.11	146.28	786	7.7	1865	MRR	Restionaceae rushland	Moorland, sedgeland, rushland and peatland	Moss Polster
48	M124	Pine Valley	41.20	146.09	787	7.7	1865	MBE	Eastern buttongrass moorland	Moorland, sedgeland, rushland and peatland	Moss Polster
49	T1-1	Excalibur Bog	42.11	146.29	788	7.7	1865	MRR	Restionaceae rushland	Moorland, sedgeland, rushland and peatland	Moss Polster
50	T2-4	Excalibur Bog	42.11	146.29	790	7.6	1865	MRR	Restionaceae rushland	Moorland, sedgeland, rushland and peatland	Moss Polster
51	EW1	Excalibur Bog	42.11	146.29	793	7.6	1865	DPD	Eucalyptus pauciflora forest and woodland on dolerite	Dry eucalypt forest and woodland	Moss Polster
52	T3-1	Excalibur Bog	42.11	146.29	791	7.6	1865	MRR	Restionaceae rushland	Moorland, sedgeland, rushland and peatland	Moss Polster
53	WW2	Excalibur Bog	42.11	146.28	795	7.6	1865	DDE	Eucalyptus delegatensis dry forest and woodland	Dry eucalypt forest and woodland	Moss Polster
54	SW1	Excalibur Bog	42.12	146.29	797	7.6	1865	DDE	Eucalyptus delegatensis dry forest and woodland	Dry eucalypt forest and woodland	Moss Polster
55	EW2	Excalibur Bog	42.11	146.29	798	7.6	1865	DPD	Eucalyptus pauciflora forest and woodland on dolerite	Dry eucalypt forest and woodland	Moss Polster
56	NW2	Excalibur Bog	42.11	146.29	798	7.6	1865	DPD	Eucalyptus pauciflora forest and woodland on dolerite	Dry eucalypt forest and woodland	Moss Polster
57	NW1	Excalibur Bog	42.11	146.29	800	7.6	1865	DPD	Eucalyptus pauciflora forest and woodland on dolerite	Dry eucalypt forest and woodland	Moss Polster

Site No	Site Code	Site Area	Latitude (°S)	Longitude (°E)	Alt. (m)	Temp. (°C)	Precip. (mm)	TasVeg Code	TasVeg 3.0 Vegetation Type (detailed)	TasVeg 3.0 Vegetation Group (simplified)	Sample Type
58	SW2	Excalibur Bog	42.12	146.29	804	7.6	1865	DDE	Eucalyptus delegatensis dry forest and woodland	Dry eucalypt forest and woodland	Moss Polster
59	H4	Lake St Clair	42.09	146.15	820	7.5	1865	MBE	Eastern buttongrass moorland	Moorland, sedgeland, rushland and peatland	Moss Polster
60	M123	Pine Valley	41.97	146.08	840	7.3	1865	DRO	Eucalyptus rodwayi forest and woodland	Dry eucalypt forest and woodland	Moss Polster
61	M122	Pine Valley	41.96	146.06	855	7.2	1865	RKP	Athrotaxis selaginoides rainforest	Rainforest and related scrub	Moss Polster
62	M121	Pine Valley	41.96	146.06	884	7.1	1865	RKP	Athrotaxis selaginoides rainforest	Rainforest and related scrub	Moss Polster
63	H32	Lake St Clair	42.04	146.13	900	7.0	1865	WDR	Eucalyptus delegatensis forest over rainforest	Wet eucalypt forest and woodland	Moss Polster
64	M523	Traveller Range	42.03	146.17	920	6.8	1865	WDL	Eucalyptus delegatensis forest over Leptospermum	Wet eucalypt forest and woodland	Moss Polster
65	M51	Mt Olympus	42.03	146.11	940	6.7	1865	WDR	Eucalyptus delegatensis forest over rainforest	Wet eucalypt forest and woodland	Moss Polster
66	M91	Traveller Range	42.05	146.24	953	6.6	1865	WSU	Eucalyptus subcrenulata forest and woodland	Wet eucalypt forest and woodland	Moss Polster
67	H10	Lake St Clair	42.10	146.12	960	6.6	1865	DCO	Eucalyptus coccifera forest and woodland	Dry eucalypt forest and woodland	Moss Polster
68	ShadLk	Hugel Range	42.09	146.12	960	6.6	1865	QAQ	Water, sea	Other natural environments	Lake Sediment
69	ClarLg	Clarence Lagoon	42.08	146.32	961	6.6	1865	QAQ	Water, sea	Other natural environments	Lake Sediment
70	M119	Pine Valley	41.96	146.08	967	6.5	1865	WDR	Eucalyptus delegatensis forest over rainforest	Wet eucalypt forest and woodland	Moss Polster
71	M407	Clarence Lagoon	42.08	146.30	993	6.4	1865	DCO	Eucalyptus coccifera forest and woodland	Dry eucalypt forest and woodland	Moss Polster
72	M525	Traveller Range	42.03	146.17	994	6.4	1865	DDE	Eucalyptus delegatensis dry forest and woodland	Dry eucalypt forest and woodland	Moss Polster
73	M118	Pine Valley	41.96	146.05	1022	6.2	1865	DCO	Eucalyptus coccifera forest and woodland	Dry eucalypt forest and woodland	Moss Polster
74	SkullPl	Skullbone Plain	42.04	146.30	1026	6.2	1865	ASF	Freshwater aquatic sedgeland and rushland	Saltmarsh and wetland	Peat Bog
75	M83	Mt Olympus	42.04	146.09	1050	6.0	1865	WSU	Eucalyptus subcrenulata forest and woodland	Wet eucalypt forest and woodland	Moss Polster
76	M106	Clarence Lagoon	42.09	146.30	1053	6.0	1865	DCO	Eucalyptus coccifera forest and woodland	Dry eucalypt forest and woodland	Moss Polster

Site No	Site Code	Site Area	Latitude (°S)	Longitude (°E)	Alt. (m)	Temp. (°C)	Precip. (mm)	TasVeg Code	TasVeg 3.0 Vegetation Type (detailed)	TasVeg 3.0 Vegetation Group (simplified)	Sample Type
77	M133	Traveller Range	41.98	146.18	1068	5.9	1865	RPF	Athrotaxis cupressoides - Nothofagus gunnii short rainforest	Rainforest and related scrub	Moss Polster
78	RienBg	Traveller Range	41.98	146.17	1070	5.9	1865	RPF	Athrotaxis cupressoides - Nothofagus gunnii short rainforest	Rainforest and related scrub	Peat Bog
79	M137	Mt Gould	41.99	146.07	1085	5.8	1865	HHE	Eastern alpine heathland	Highland treeless vegetation	Moss Polster
80	M136	Traveller Range	42.01	146.18	1100	5.7	1865	DCO	Eucalyptus coccifera forest and woodland	Dry eucalypt forest and woodland	Moss Polster
81	M53	Mt Olympus	42.03	146.11	1140	5.4	1865	DCO	Eucalyptus coccifera forest and woodland	Dry eucalypt forest and woodland	Moss Polster
82	M115	The Labyrinth	41.94	146.04	1145	5.4	1865	RPF	Athrotaxis cupressoides - Nothofagus gunnii short rainforest	Rainforest and related scrub	Moss Polster
83	M114	The Labyrinth	41.95	146.05	1147	5.4	1865	RPF	Athrotaxis cupressoides - Nothofagus gunnii short rainforest	Rainforest and related scrub	Moss Polster
84	H29	Lake St Clair	42.11	146.09	1150	5.4	1865	RFS	Nothofagus gunnii rainforest and scrub	Rainforest and related scrub	Moss Polster
85	T32	The Labyrinth	41.94	146.04	1163	5.3	1865	RPF	Athrotaxis cupressoides - Nothofagus gunnii short rainforest	Rainforest and related scrub	Lake Sediment
86	M107	The Labyrinth	41.94	146.04	1163	5.3	1865	RPF	Athrotaxis cupressoides - Nothofagus gunnii short rainforest	Rainforest and related scrub	Moss Polster
87	M54	Mt Olympus	42.04	146.11	1167	5.3	1865	RFS	Nothofagus gunnii rainforest and scrub	Rainforest and related scrub	Moss Polster
88	M526	Traveller Range	42.02	146.18	1169	5.3	1865	DCO	Eucalyptus coccifera forest and woodland	Dry eucalypt forest and woodland	Moss Polster
89	M117	The Labyrinth	41.96	146.05	1170	5.3	1865	DCO	Eucalyptus coccifera forest and woodland	Dry eucalypt forest and woodland	Moss Polster
90	M116	The Labyrinth	41.95	146.05	1182	5.2	1865	DCO	Eucalyptus coccifera forest and woodland	Dry eucalypt forest and woodland	Moss Polster
91	M530	Traveller Range	41.96	146.13	1190	5.1	1865	DCO	Eucalyptus coccifera forest and woodland	Dry eucalypt forest and woodland	Moss Polster
92	T17	Mt Olympus	42.04	146.11	1190	5.1	1865	RPF	Athrotaxis cupressoides - Nothofagus gunnii short rainforest	Rainforest and related scrub	Tarn Sediment
93	T9	Hugel Range	42.09	146.10	1200	5.1	1865	HCH	Alpine coniferous heathland	Highland treeless vegetation	Tarn Sediment
94	M22	Hugel Range	42.09	146.10	1200	5.1	1865	HCH	Alpine coniferous heathland	Highland treeless vegetation	Moss Polster
95	T16	Mt Olympus	42.04	146.11	1202	5.1	1865	RPF	Athrotaxis cupressoides - Nothofagus gunnii short rainforest	Rainforest and related scrub	Tarn Sediment
96	T15	Mt Olympus	42.04	146.11	1204	5.0	1865	RPF	Athrotaxis cupressoides - Nothofagus gunnii short rainforest	Rainforest and related scrub	Tarn Sediment
97	H34	Lake St Clair	42.04	146.11	1210	5.0	1865	RPF	Athrotaxis cupressoides - Nothofagus gunnii short rainforest	Rainforest and related scrub	Moss Polster

Site No	Site Code	Site Area	Latitude (°S)	Longitude (°E)	Alt. (m)	Temp. (°C)	Precip. (mm)	TasVeg Code	TasVeg 3.0 Vegetation Type (detailed)	TasVeg 3.0 Vegetation Group (simplified)	Sample Type
98	M135	Traveller Range	41.96	146.12	1213	5.0	1865	HCH	Alpine coniferous heathland	Highland treeless vegetation	Moss Polster
99	H26	Lake St Clair	42.09	146.09	1240	4.8	1865	HCH	Alpine coniferous heathland	Highland treeless vegetation	Moss Polster
100	HugPIT	Hugel Range	42.09	146.09	1247	4.8	1865	HCH	Alpine coniferous heathland	Highland treeless vegetation	Tarn Sediment
101	T3	Hugel Range	42.09	146.09	1250	4.7	1865	HHE	Eastern alpine heathland	Highland treeless vegetation	Tarn Sediment
102	M8	Hugel Range	42.09	146.09	1250	4.7	1865	HHE	Eastern alpine heathland	Highland treeless vegetation	Moss Polster
103	M77	Mt Olympus	42.04	146.10	1300	4.4	1865	HCH	Alpine coniferous heathland	Highland treeless vegetation	Moss Polster
104	M130	Mt Olympus	42.04	146.11	1350	4.1	1865	HCH	Alpine coniferous heathland	Highland treeless vegetation	Moss Polster
105	M149	Mt Olympus	42.05	146.12	1420	3.7	1865	HCH	Alpine coniferous heathland	Highland treeless vegetation	Moss Polster
106	T19	Mt Olympus	42.04	146.10	1446	3.5	1865	HCH	Alpine coniferous heathland	Highland treeless vegetation	Tarn Sediment